

INTEGRATING DEPOSITIONAL FACIES AND SEQUENCE STRATIGRAPHY IN  
CHARACTERIZING CARBONATE RESERVOIRS: MISSISSIPPIAN LIMESTONE,  
WESTERN KANSAS

by

KEITHAN MARTIN

B.S., Kansas State University, 2014

A THESIS

submitted in partial fulfillment of the requirements for the degree

MASTER OF SCIENCE

Department of Geology  
College of Arts and Sciences

KANSAS STATE UNIVERSITY  
Manhattan, Kansas

2015

Approved by:

Major Professor  
Dr. Matthew Totten

**Copyright**

KEITHAN MARTIN

2015

## ABSTRACT

The Mississippian-aged St. Louis Limestone of Western Kansas is a carbonate resource play that has been producing oil, gas, and natural gas liquids (NGL) for over 50 years. The Mississippian Limestone is made up of heterogeneous limestones with interbedded layers of porous and non-porous units, abrupt facies changes, and diagenetic alterations. These factors combine to characterize the St. Louis Limestone's internal complexity, which complicates hydrocarbon exploration. This study focuses on improving the understanding of the geometry, distribution, and continuity of depositional facies within Kearny County, Kansas. Petrophysical analysis of a suite of geophysical logs integrated with core provided the basis for establishing facies successions, determining vertical stacking patterns within a sequence stratigraphic framework, and correlating areas of high porosity with a respective facies.

The following depositional facies were identified; 1) porous ooid grainstone, 2) highly-cemented ooid grainstone, 3) quartz-carbonate grainstone, 4) peloidal grainstone, 5) micritic mudstone, and the 6) skeletal wackestone/packstone. The porous ooid grainstone is the chief reservoir facies, with log-derived porosity measurements between four and eighteen percent. In areas without available core, depositional facies were predicted and modeled using a neural network analysis tool (Kipling2.xla). Values derived from the evaluated core intervals and their respective geophysical logs served as the framework for the neural network model. This study illustrates the advantages of correlating depositional facies with reservoir quality and correlating those specific facies to geophysical logs, ultimately to create a greater understanding of the reservoir quality and potential within the St. Louis Limestone of western Kansas.

## **ACKNOWLEDGEMENTS**

First and foremost, I would like to thank my thesis advisor, Dr. Matthew Totten, and my committee members, Dr. Sambhudas Chaudhuri, and Dr. Abdelmoneam Raef for their guidance throughout my graduate research and completion of this document. Dr. Matthew Totten's around-the-clock availability contributed to completing various aspect of this research in a timely, efficient manner.

I would like to thank the Kansas Geologic Society for allowing me to borrow over 400 feet of core from their facilities in Lawrence, Kansas for evaluation. The KGS also allowed free access to the Robert. F. Walters Digital Library. The KGS was very flexible and helped tremendously with keeping my research costs at a minimum.

I would also like to thank the Kansas Geologic Foundation for the research grant as well as the academic scholarship for the Spring 2015 semester. Between the research grant and scholarship, all of my personal research expenditures were eliminated.

I would like to give a special thanks to my family members for all of their support throughout my undergraduate and graduate career. Finally, I would like to thank my beautiful fiancé, Kaiti, for her support and for putting her academic career on hold during the completion of my master's degree.

## TABLE OF CONTENTS

LIST OF TABLES .....	vii
TABLE OF FIGURES .....	viii
CHAPTER I: INTRODUCTION.....	1
Summary of the Problem .....	1
Previous Studies .....	2
Objective and Goals .....	3
CHAPTER II: HISTORY OF THE MISSISSIPPIAN PLAY.....	6
CHAPTER III: GEOLOGIC BACKGROUND .....	7
Area of Study .....	7
Geologic Setting and Paleogeography.....	9
Regional Stratigraphy .....	11
CHAPTER IV: DATA AND METHODS .....	14
Core Analysis.....	14
Thin Section Analysis.....	15
Well Log Analysis.....	16
X-Ray Fluorescence Analysis.....	18
Petra®: Geologic Software .....	20
Kipling2.xla: A Facies Prediction Software .....	21
Pitfalls and Limitations.....	23
CAPTER V: LITHOFACIES AND DEPOSITIONAL ENVIRONMENTS .....	25
Lithofacies 1: Porous Ooid Grainstone .....	25
Lithofacies 2: Highly Cemented Ooid Grainstone.....	29
Lithofacies 3: Quartz-Carbonate Grainstone .....	30

Lithofacies 4: Peloidal Packstone .....	32
Lithofacies 5: Clay-Rich Mudstone .....	34
Lithofacies 6: Skeletal Wackestone .....	35
CHAPTER VI: RESERVOIR QUALITY.....	37
CHAPTER VII: FACIES DISTRIBUTION.....	39
Applying the Neural Network Model.....	39
Petra Interpolation: Mapping the Facies Distribution .....	45
CHAPTER VII: DISCUSSION .....	52
Depositional System Evaluation .....	52
Geologic Controls on Production.....	59
Reservoir Considerations.....	64
Future Study.....	65
CHAPTER IX: CONCLUSION .....	66
REFERENCES .....	69
APPENDIX A.....	73
APPENDIX B .....	92

## **LIST OF TABLES**

Table 1: Table of the three wells that core was evaluated from. These wells were used to calibrate all wells throughout the study area. The “Study No.” section refers to Figure 1, illustrating the location of the wells in Kearny County.....	5
Table 2: Drilling permits within Kansas from 2010-2013 (values from the Kansas Corporation Commission).....	7
Table 3: A table illustrating the common shade of color attained from applying alizarin red S, potassium ferricyanide, and a mixture of the two when in contact with different mineral assemblages. Table modified from Workman 2013).....	16

## TABLE OF FIGURES

Figure 1: Illustrates the past study areas by Carr (Big Bow and Sand Arroy fields) and Handford (Damme Field) and their location relative to the current study area in Lakin field.....	3
Figure 2: Location of the study area within Kearny County and the three studied wells. Original image modified from the Kansas Geological KGS.....	9
Figure 3: Late Mississippian subperiod orientation of continents, illustrating the inundated regions of Kansas (outlined in black). Image modified from CPGeosystems.....	10
Figure 4: A paleogeographic map during the Osagean-Meramecian. This map illustrates paleostructures and the placement orientation of the inner shelf, main shelf, and shelf margin. Kearny County is pointed out by the red star. Image recreated from Lane and De Keyser (1989); Lianshuang et al. (2004).....	11
Figure 5: Stratigraphic column of the highlighting the mid-to-upper MLS. The St. Louis limestone has been separated into four zones, A-D. Image modified from Lianshuang et al. (2004) .....	14
Figure 6: Dunham's classification scheme for carbonate rocks. Figure modified from SEPM (2013) .....	16
Figure 7: Type log of GR, NPHI, and DPHI with the St. Genevieve, St. Louis, and St. Louis zones B, C and D tops picked.....	17
Figure 8: Illustrates how XRF data was turned into log curves to aid in picking formation/subformation tops. The following logs and elements were used in this analysis; DELTAT (sonic), DPHI, NPHI, GR, facies predictions, silicon, calcium, iron, potassium, magnesium, and aluminum .....	19

Figure 9: Generalized neural network flow. The input values are the four geophysical logs used  
in this study; GR, Neutron, Density, and Sonic curves. The output value would be the  
probabilities of different facies.....22

Figure 10: Core and thin section taken from study well 15-093-20147. The core slab has been  
stained extensive by liquid hydrocarbons. The thin section has been impregnated with blue  
epoxy to illustrate porosity. Abbreviations: Oo (oolithic), EC (echinoderm), LEC (laminated  
echinoderm). PPL 4X magnification.....26

Figure 11: A) Located long the west margin of the Great Bahama Banks, an aerial view of the  
Cat Cay platform margin sand-shoal complex, illustrating the lenicular geometry of modern  
sand shoals with the white outline. B) Geometry of the ooid shoal within the St. Louis C  
zone (pay zone), strongly resembling the geometry of the Cat Cay sand-shoal complex.28

Figure 12: Core and thin section from study well 15-093-20011. Abbreviations: Oo (oolithic), LEC  
(laminated echinoderm), Qz (detrital quartz grain). PPL 4X magnification.....30

Figure 13: Core and thin section taken from study well 15-093-20147. Blue epoxy has been  
applied to thin section, showing that there is very low to no porosity on this slide.  
Abbreviated: Qz (quartz), Pd (peloid). PPL 4X magnification.....31

Figure 14: Core and thin section taken from study well 15-093-20011. Abbreviation: Qz (detrital  
quartz grain), Pd (peloid). PPL 4X magnification.....33

Figure 15: Core and thin section from study well 15-093-20011. PPL 4X magnification.....35

Figure 16: Core and thin section from study well 15-093-00317. Abbreviation: SF (skeletal  
fragments), MC (micritic matrix). PPL 4X magnification.....36

Figure 17: Cross plot of neutron porosity (%) and density porosity (%). Neutron and density log  
values were taken from the three cored study wells. This cross plot illustrates that Facies 1

(Porous Ooid Grainstone) has the highest porosity values and confirms that it is the chief reservoir facies.....	37
Figure 18: Box plot of (DPHI+NPHI)/2 vs. Lithofacies. The box plot derived by calculating and taking the difference of the minimum, quartile 1, quartile 2 (median), quartile 3, and maximum values.....	38
Figure 19: Four plots of the facies probability, facies prediction, facies prediction modified, and core facies (actual facies) that illustrate the neural networks models facies agreement... ..	41
Figure 20: Predicted facies scorecard for 3 key trained wells with core containing GR, Neutron, Density, and Sonic curves. ....	44
Figure 21: Base map with color coded cross section lines running both NS and EW and a key displaying what each well symbol represents Extensive azimuthal subsurface data was difficult to attain due to the linear trend of the wells in the study area.....	46
Figure 22: Cross sections of A,B,C,D,E ,F, G, and H.....	51
Figure 23: Facies succession and their texture, lithology, log curve responses, and depositional environment and sequence stratigraphic interpretation of the cored well, API: 15-093-20147. ....	53
Figure 24: Seven stages of deposition as result of relative sea level rise and fall. 1) formation of an ooid shoal, 2) relative sea level rise, thickening and subsequent drowning of the ooid shoal, 3) relative sea level fall, landward facies prograde seaward, 4) relative sea level rise, seaward facies retrograde landward, 5) continual sea level rise, deep marine facies blankets the carbonate platform, 6) relative sea level fall, erosional surface due to subaerial exposure, and 7) the carbonate platform is flooded due to a relative sea level rise and supratidal and intertidal facies are deposited. ....	56

Figure 25: Illustration of the depositional environment of the Upper Mississippian. Image modified from (Qi and Carr, 2003) and (Hardford, 1988). ....	58
Figure 26: Illustration of a stratigraphic cross section of the ooid shoals. Image modified from Qi and Carr (2003) and Hardford (1988). ....	59
Figure 27: Isopach of the ooid grainstone facies within the St. Louis C zone with production data from this zone posted. ....	61
Figure 28: Structural map throughout the entire study area. The boreholes are posted with a relative to the wells XY or geographic location. ....	62
Figure 29: Bar graph which illustrates the drilling results south of Lakin NW field (27.1% success rate) and north of Lake NW field (76.7% success rate) showing the number of dry holes, oil wells, gas wells, and unknown per geographic location. ....	64

## **CHAPTER I: INTRODUCTION**

### **Summary of the Problem**

The St. Louis Limestone of western Kansas is a carbonate resource play that has been explored for over 50 years. The Mississippian Limestone was deposited during the Mississippian period, roughly 320-360 million years ago. In Kansas, the Upper Mississippian Series is chiefly composed of thick limestone and dolomite beds with integrated thin beds of shale and sandstones, and minor amounts of chert (Goebel, 1968). The total thickness of the Mississippian Limestone ranges between 300 to 500 feet, deepening towards the Anadarko Basin in southwestern Kansas. For the purposes of this discussion, the Mississippian Limestone will be referred to as “MLS”.

The MLS is made up of heterogeneous limestone beds that have proven to be challenging during exploration. Abrupt facies changes, diagenetic alterations, and karst all contribute to the play’s complexity. Limestone units of high and low porosity are interbedded, which places difficulty on predicting new areas of exploration. High porosity MLS’s are notorious for having low permeability, meaning the pores that are potentially hydrocarbon filled are not well interconnected, hindering the flow of hydrocarbons into the borehole. This complexity and variability of the subsurface has made characterizing smaller regions within the MLS a necessity for future exploration.

Due to the MLS’s internal complexity, in-depth studies over the vertical sequence and lateral facies distribution are vital. Previous studies investigated the facies distributions within Upper Meramecian (Upper Mississippian) in fields straddling the Stanton and Grant County line (Big Bow, Sand Arroyo), which is 36 miles southwest of the current study area in Kearny County (Carr et al., 2004). A similar study was also conducted in Finney County (NW), 20

miles west of this study (Handford, 1988). This type of study within Kearny County has never been reported, which created the opportunity to conduct a unique study on the internal framework of the MLS in Kearny County.

### **Previous Studies**

Two key studies covering the St. Louis limestone in western Kansas have been conducted by Carr and Qi (2007) and Handford (1988). Carr and Qi (2007) conducted a multifaceted study over the St. Louis Limestone in Big Bow and Sand Arroyo fields, which straddle the Stanton-Grant County boarder. Carr and Qi's studies had a strong emphasis on ooid grainstones, due to their reservoir quality characteristics. These studies over the St. Louis Limestone included reservoir characterization, geostatistical three-dimensional modeling of oolite shoals, and recognizing exposure surfaces via gamma ray spectral log. For the geostatistical three-dimensional modeling, Carr and Qi (200) used a neural network model in order to predict lithofacies throughout an extensive study area, ultimately using the lithofacies predictions to map the lithofacies in 3D. Handford (1998) conducted an in-depth study of depositional environments within the St. Louis lithofacies in Damme Field, Finney County, having a strong emphasis on ooid grainstones, as this type of lithofacies acts as the chief pay zone in western Kansas within the St. Louis limestone. Lastly, Ball (1966) focused on the ooid shoal deposits, due to their high porosity characteristic. Ball attempted to predicted effective porosity (or inter-connected porosity) within the shoal deposits to create porosity trends throughout Pleasant Prairie field, primarily through core evaluation and well cutting analysis.

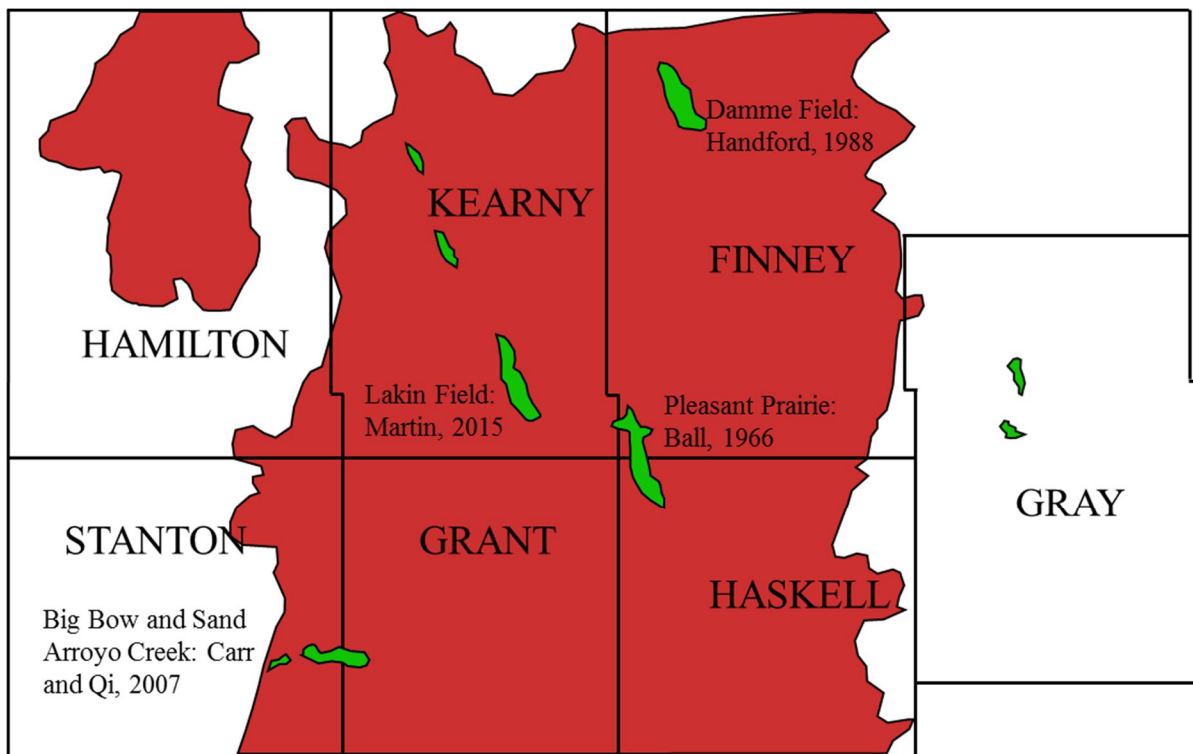


Figure 1: Illustrates the past study areas by Carr and Qi (2007) (Big Bow and Sand Arroyo fields), Handford (1988) (Damme field), and Ball (1966) (Pleasant Prairie field) and their location relative to the current study area in Lakin field. Red represents “gas fields” and green represents “oil fields”.

### **Objective and Goals**

Core from three separate wells targeting the MLS in Kearny County were evaluated in order to establish facies successions, determine vertical stacking patterns within the parameters of the sequence stratigraphic framework, and interpret their respective depositional environments (Table 1). Calibrating the core with the wire-line log data enabled the identification of reservoir quality zones within the study area. This core to wire-line log calibration allowed for the use of facies prediction software, where the key depositional facies were predicted on wells that had only wire-line log data and were statistically mapped throughout the study area.

This study illustrates the advantages of correlating depositional facies with reservoir quality and linking those specific facies with wire-line log signatures to create a greater understanding of the vertical and lateral distribution of reservoir quality facies. This integrated approach will aid in locating new prospective areas or areas that may have been overlooked.

The objectives of this research consist of:

1. Investigating what the environmental setting was during deposition of Upper Mississippian sediments.
2. Determining the depositional facies within the parameters of a sequence stratigraphic framework.
3. Establishing an understanding of the geometry, distribution, and continuity of reservoir quality lithofacies.
4. Determining whether reservoir quality is controlled by depositional facies (stratigraphic), structural properties, or both.
5. Attempting to correlate well log signatures with each respective facies and significant sequence stratigraphic surfaces; in particular, to determine whether wire-line logs are sensitive enough to differentiate lithofacies, specifically reservoir-quality flow units, and to assess whether significant sequence stratigraphic surfaces can be correlated throughout the study area using wire-line log curves.

Study No.	Location	API No.	Lease Name	Well No.	Operator	County	Field Name	Type-Status	KB	Cored Interval in Miss (ft)		
										Top	Btm	Total
#1	T26S R36W, Sec. 4 C NE SW	15-093-20147	LEE 'A'	1	Oil Producers Inc. of Kansas	Kearny	Lakin South	Oil-P&A	3039	4,830	5,009	179
#2	T25S R36W, Sec. 18 C NE NE	15-093-00317	J. K. MOSER	1	Pan American Petroleum Corp	Kearny	Hugoton Gas Area	Oil-D&A	3036	4,858	4,976	118
#3	T24S R36W, Sec. 31 C NW NW	15-093-20011	J. K. MOSER	1	Pan American Petroleum Corp	Kearny	Hugoton Gas Area	Oil-D&A	3163	4,963	5,067	104
										Cumulative Total:	401	

Table 1: Table of the three wells from which core was evaluated. These wells were used to calibrate all wells throughout the study area. The “Study No.” section refers to Figure 1, illustrating the location of the wells in Kearny County.

## **CHAPTER II: HISTORY OF THE MISSISSIPPIAN PLAY**

Industry interest in the MLS is due to the low drilling costs relative to other top plays in North America. The average depth of the MLS, 3,000- 6,000 feet, can be compared to other significant plays such as North Dakota's Bakken, 9,000- 10,000 feet, and Texas' Eagle Ford and Permian, 4,000- 15,000 feet (Cross, 2014). The shallow depths of the MLS results in faster drilling time, lower requisites of drilling rigs, and lower fracturing pressures, which collectively drive down the total cost per well (KIOGA, 2014). While average horizontal MLS wells cost around \$3.0- 3.5 million, deeper, unconventional plays can cost up to two or three times this amount (Cross, 2014).

The MLS is one of the most productive plays in North America, following the Bakken of North Dakota, and the Eagle Ford and Permian of Texas. Throughout the play history of the MLS within Kansas, in excess of 4,000 vertical wells have been drilled, recovering an average of 86,000 boe (barrel of oil equivalent) per well (KIOGA, 2014). Implementation of new technologies—such as 3D seismic, horizontal and directional drilling, and hydraulic fracturing—made previously unrecoverable oil and natural gas within the MLS accessible. It has been estimated that MSL wells that were horizontally drilled recover up to 250,000- 450,000 boe per well, which approaches four times the amount of a traditional vertical well (KIOGA, 2014).

With the success of a horizontal MLS well in 2009, a sharp increase in horizontal drilling began in Kansas (Table 1). By 2013, horizontal wells drilled into the MLS accounted for 7.7% of Kansas' total oil production (KIOGA, 2014). Horizontal and directional drilling revitalized the MLS play in Kansas.

Drilling Permit Information in Kansas		
Year	Total Drilling Permits	MLS Horizontal Well Permits
2010	4,521	11
2011	5,441	57
2012	6,861	251
2013	6,367	251
2010-2013	22,904	570

Table 2: Drilling permits within Kansas from 2010-2013 (values from the Kansas Corporation Commission).

### CHAPTER III: GEOLOGIC BACKGROUND

#### Area of Study

The study area contains three cored wells, oriented SE-NW, through the south central portion of Kearny County, western Kansas (Figure 2). The study area is within the northwestern portion of the Hugoton Embayment, which is a low relief extension of the Anadarko Basin. A structurally high, subsurface uplift northeast of the Hugoton Embayment is referred to as the Central Kansas uplift. This uplift separates the Hugoton embayment from two other significant basins in Central Kansas, the Salina and Sedgwick basins (Goebel, 1968).

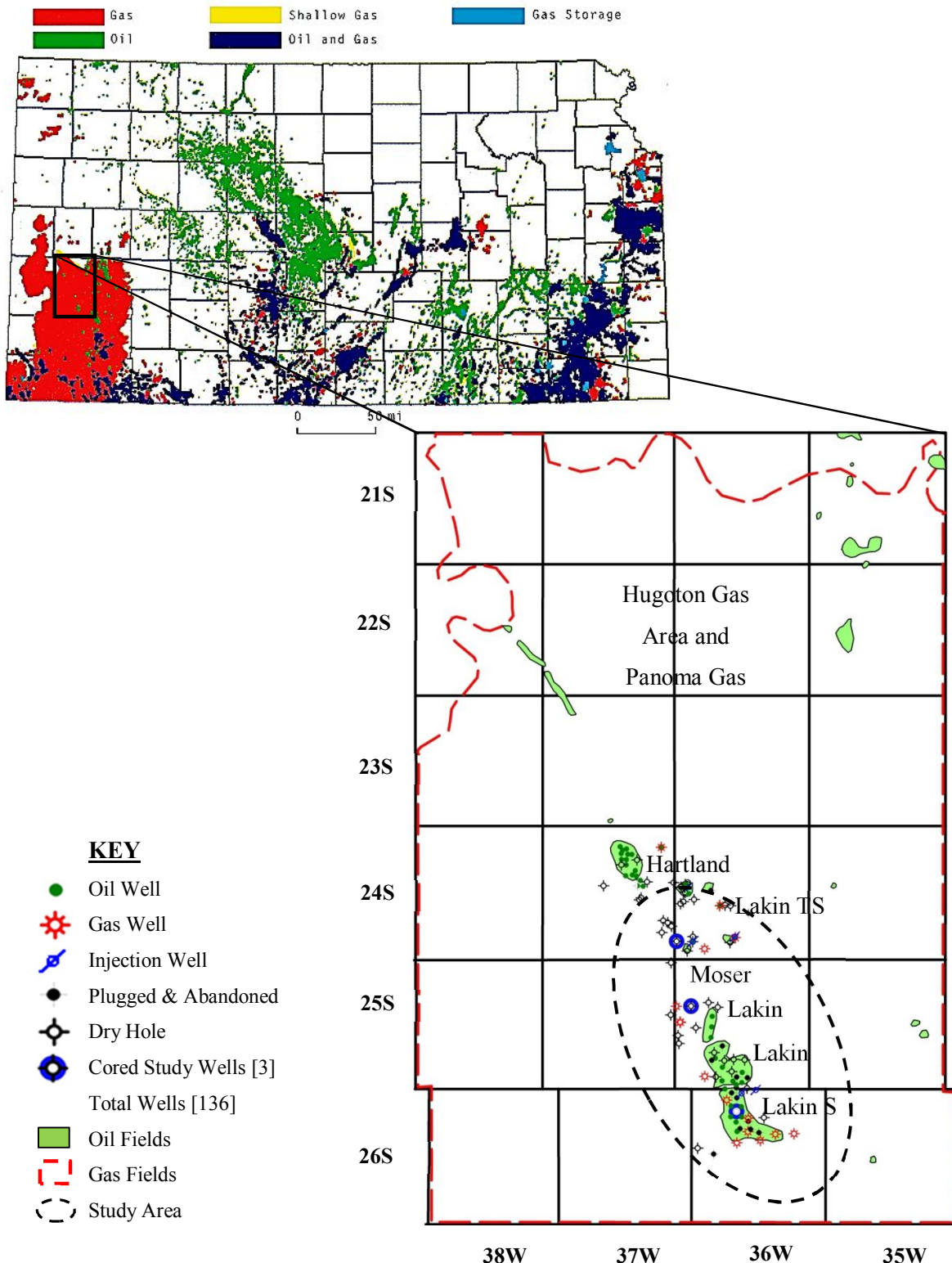


Figure 2: Location of the study area within Kearny County and the three studied wells.

Original image modified from the Kansas Geological KGS (<http://www.kgs.ku.edu/PRS/> county/klm/kearny.html).

### **Geologic Setting and Paleogeography**

During the Late Mississippian subperiod, shallow epicontinental seas covered much of Kansas, namely the western and southern portions (Figure 3). During this time, Mississippian sediments were deposited, creating shallow-marine limestones, cherts, and cherty limestones (Evans and Newell, 2013). The Mississippian is overlain by the regional sub-Pennsylvanian unconformity. As interpreted by Montgomery et al. (2000), the Mississippian's upper surface is an erosional karst terrain.

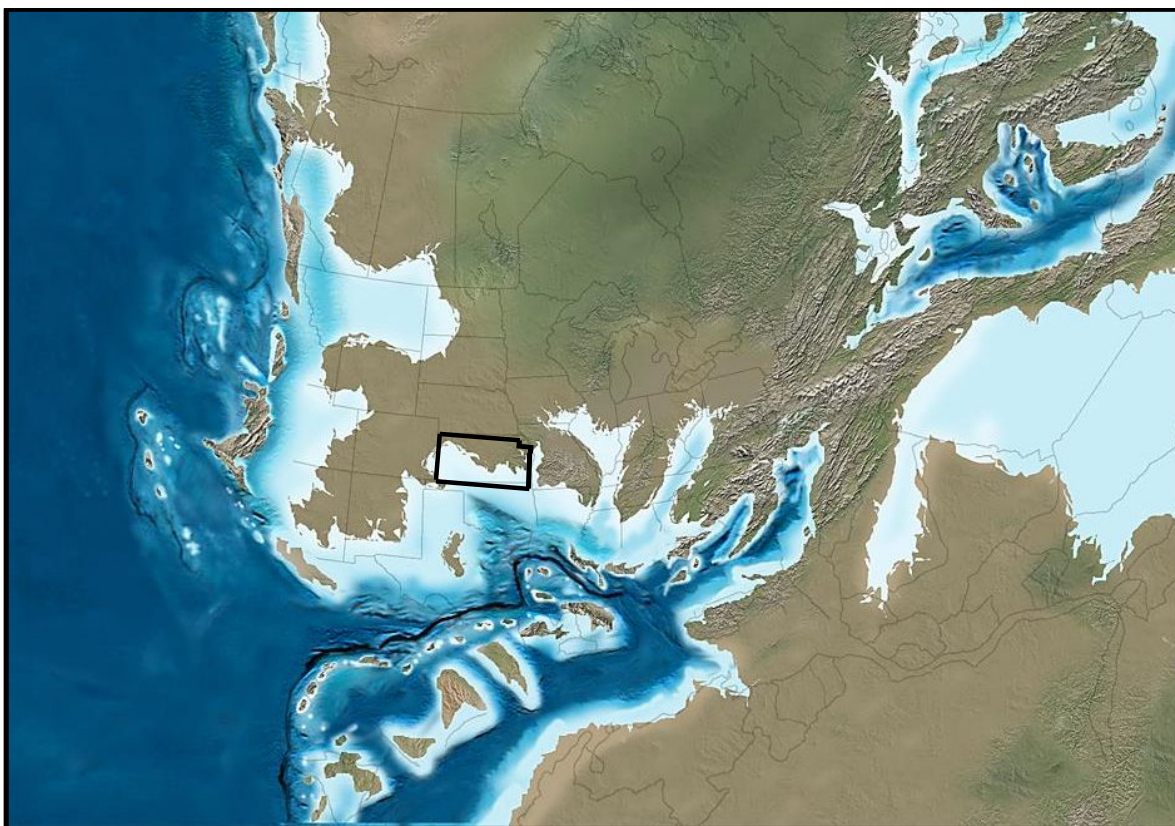


Figure 3: Late Mississippian Subperiod orientation of continents, illustrating the inundated regions of Kansas (outlined in black). Image modified from CPGeosystems (<http://cpgeosystems.com/nam.html>).

Mississippian paleogeography is illustrated in Figure 4, showing the location of the study area with a star. The key features shown are: the Transcontinental Arch, Salina Basin, Central Kansas Uplift, Hugoton Embayment, Sierra Grande Uplift, Anadarko Basin, and the Amarillo-Wichita Arc. Interpretation made from lithology distribution and thickness concludes that the midcontinent is made up of a broad inner shelf, main shelf, and shelf margin combining to make up a large carbonate platform which formed along the southern margin of the Transcontinental Arch (Watney et al., 2008).

Subsurface data have concluded that numerous hydrocarbon fields within southwestern Kansas are made up of oolitic shoals that are NW-SE oriented. During this Mississippian period, a combination of numerous factors such as global paleoclimate, global sea level change, and geochemical influences, along with the best possible regional paleogeographic and tectonic conditions, resulted in extensive deposition of marine oolitic limestones across the continent of North America (Lianshuang et al., 2004).

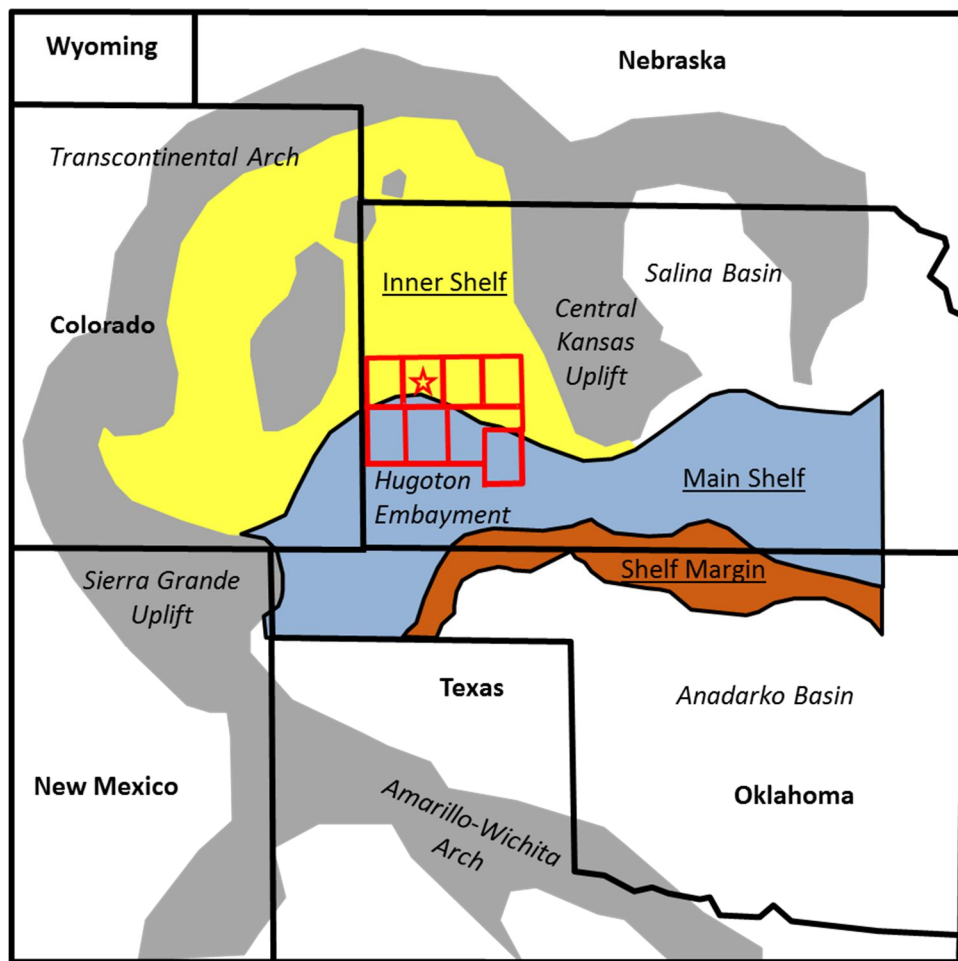


Figure 4: A Paleogeographic map during the Osagean-Meramecian. This map illustrates paleostructures and the locations and orientations of the inner shelf, main shelf, and shelf margin. Kearny County is pointed out by the red star. Imagine recreated from Lane and De Keyser (1989); Lianshuang et al. (2004).

### **Regional Stratigraphy**

#### **Upper Mississippian Series**

In Kansas, the Upper Mississippian Series is chiefly composed of limestone and dolomite beds, with inbedded shale and sandstones, and minor amounts of chert (Goebel, 1968).

### **Meramecian Stage (Upper Mississippian)**

Lying disconformably on the Osagian rocks are rocks of the Meramecian Stage, although the disconformity becomes unrecognizable in northeastern and southwestern Kansas. In the Meramecian Stage, the upper formations consist primarily of granular, sandy, oolitic, and fossiliferous limestone (Goebel, 1968). The lower formations consist chiefly of interbedded dolomite and dolomitic limestone with notable quantities of chert. Rocks from the Meramecian Stage most likely were widespread through Kansas originally. Before Pennsylvanian deposition, erosive forces wore away these rocks in much of the State (Goebel, 1968).

In the Upper Mississippian, the Meramecian series contains four different rock units that are split into the Upper and Lower Meramecian. The Upper Meramecian contains the Ste. Genevieve limestone, St. Louis limestone, and the Lower Meramecian contains the Salem/Spergen limestone, and the Warsaw limestone, which are in stratigraphic order from youngest to oldest. The Upper Meramecian, Ste. Genevieve and St. Louis limestone, will be the focal point of the study

#### **Ste. Genevieve Limestone**

The Ste. Genevieve Limestone is prevalent in the Hugoton Embayment, occurs in the deeper part of the Forest City Basin, and is lacking in Salina Basin. The Ste. Genevieve Limestone resides disconformably beneath the Chesteran rocks, while lying conformably on the St. Louis Limestone (Goebel, 1968). This unit consists mainly of silty and sandy, light gray to white fossiliferous limestone. The light gray to white fossiliferous limestone is found to be interbedded with fine-textured oolitic limestone and calcarenite (Goebel, 1968). Where finely oolitic limestone beds of the Ste. Genevieve overlie finely oolitic limestone beds of St.

Louis Limestone, it is difficult to differentiate between the two beds. In the Hugoton Embayment, the Ste. Genevieve Limestone's thickness is found to be greater than 200 feet and continues at that thickness except where the unit has been beveled by pre-Chesteran or in areas that have been uplifted and eroded away (Goebel, 1968).

### **St. Louis Limestone**

The St. Louis Limestone is considered conformable with lower Meramecian rocks. This unit contains limited amounts of chert within the limestone, although beds of oolitic limestones and calcarenite are extensive throughout. Within the semi-granular limestone, traces of translucent chert occur locally. The St. Louis consists of coarsely crystalline fossiliferous limestone as well as dolomitic limestone in the deeper portions of the Hugoton Embayment (Goebel, 1968). Chert breccias, brecciated limestones, and anhydrite are locally intraformational and well preserved (Goebel, 1968). Overall, the St. Louis limestone is more widespread than the Ste. Genevieve. The St. Louis limestone cannot be distinguished in the Salina basin. In the Forest City Basin, it is relatively thin, 50 feet, whereas it thickens in the Hugoton embayment up to around 200 feet (Goebel, 1968).

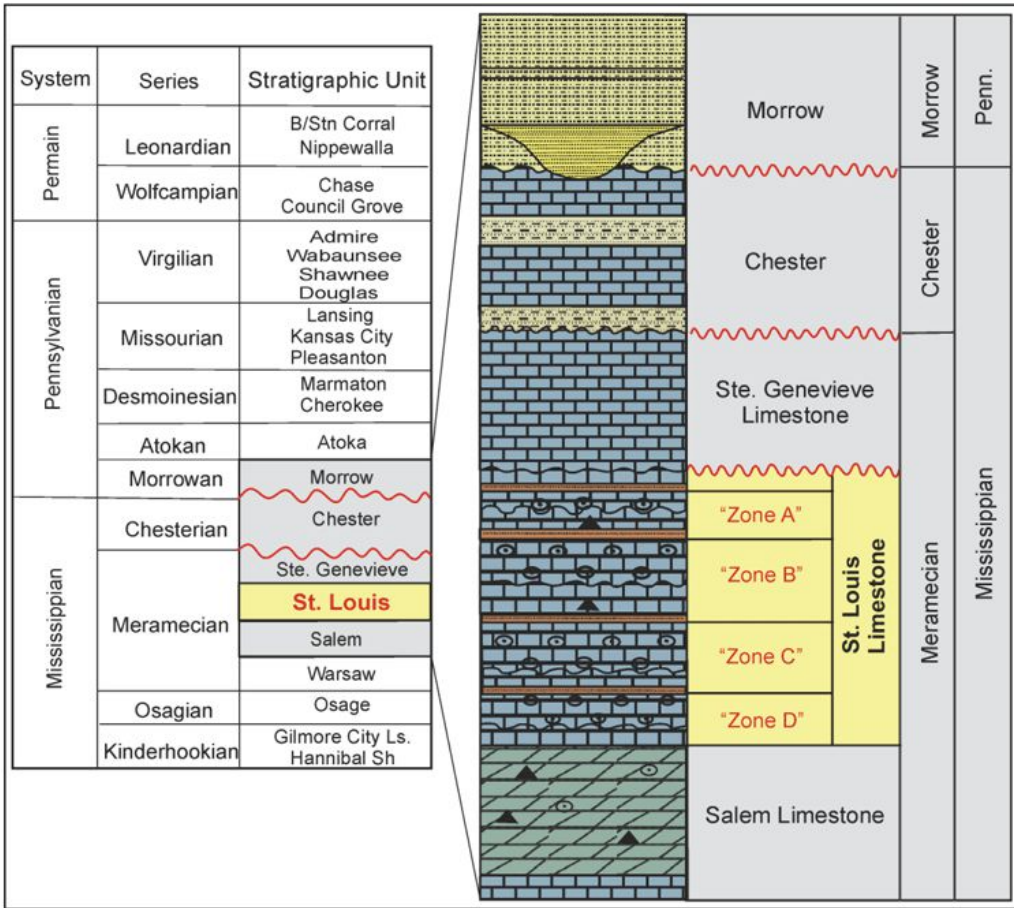


Figure 5: Stratigraphic column of the highlighting the mid-to-upper MLS. The St. Louis limestone has been separated into four zones, A-D. Image modified from Qi et al. (2004).

## CHAPTER IV: DATA AND METHODS

The methods employed for this study included: 1) core evaluation, 2) thin section analysis, 3) well log analysis, 4) X-Ray Fluorescence (XRF) analysis, 5) a neural networking analysis tool (Kipling2.xla), and 6) Petra® (geologic software).

### Core Analysis

Three wells in the Kearny County study area were chosen based on: 1) extensive cored intervals available (>100 ft.), 2) the core was within the Upper Mississippian (Upper Meramecian), and 3) the core intervals were located within a proximal distance relative to

each other to limit variability in the subsurface. Following the guidelines of the AAPG Sample Examination Manual by Swanson (1981), a total of 401 feet of core was described in detail. The core was viewed using a corvascope, which aided in identifying textural changes throughout the intervals. Textural changes were noted and marked, cut into billets, and ultimately made into thin sections. The entirety of the evaluated core where information was sourced was photographed. If the core photographs are sought after, contact keithan@ksu.edu.

### **Thin Section Analysis**

Thin section locations were selected on the following criteria: 1) distinct color changes, 2) changes in grain size, roundness, and degree of sorting, 3) changes in fossil material (high or low concentrations), and 4) distinct variation in the wire-line log signatures. Each thin section was examined using a petrographic microscope, which augmented the original evaluation of the core. The thin sections were classified according to depositional texture and followed Dunham's classification scheme (Figure 6). Thin sections were examined to aid in accurately determining the depositional facies. The thin sections were impregnated with blue epoxy, which provided an effective way to identify porosity of each facies. To help differentiate carbonate mineralogy, one half of each thin section was saturated with alizarin red S and potassium ferricyanide (view Table 3). Thin sections aided with determining depositional environments, fossil identification, and diagenetic history. Refer to appendix A to view all thirty-six thin sections along with their descriptions.

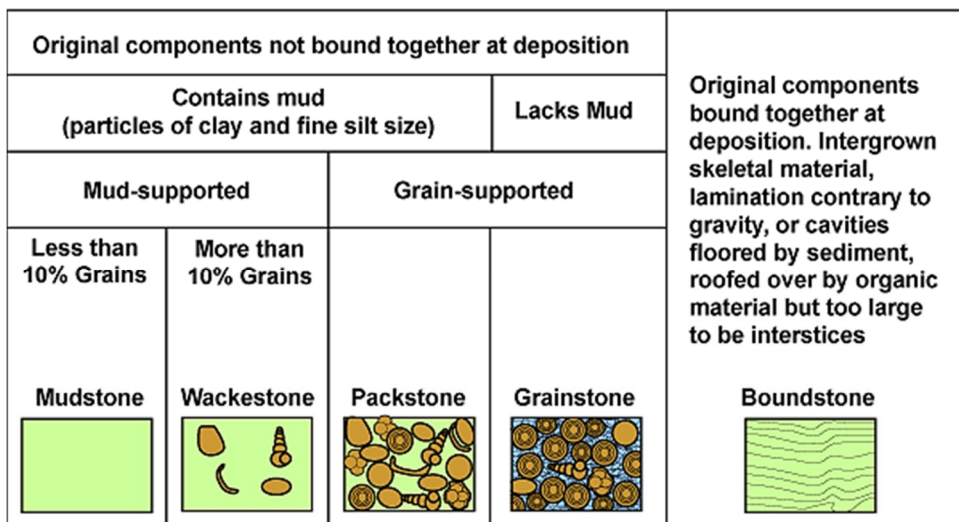


Figure 6: Dunham's classification scheme for carbonate rocks. Figure modified from SEPM (2013).

	Mineral	Typical Color from Staining		Effects of Etching on Relief	Combined Result
		Alizarin Red S	Potassium Ferricyanide		
Calcite	Low-Mg	Colorless			
	High-Mg	Purple			
	Non-Ferroan	Pink to red-brown	None	Considerable	Pink to red-brown
	Ferroan ( $\text{Fe}^{2+}$ )	Pink to red-brown	Pale to deep blue	Considerable	Mauve to blue
Dolomite	Non-Ferroan	None	None	Negligible	Unstained
	Ferroan ( $\text{Fe}^{2+}$ )	None	Very pale blue	Negligible	Very pale blue

Table 3: A table illustrating the common shade of color attained from applying Alizarin Red S, Potassium Ferricyanide, and a mixture of the two when in contact with different mineral assemblages. Table modified from Workman (2013).

### Well Log Analysis

A suite of geophysical well logs (Neutron/Density, Gamma Ray, Sonic, Induction, CMB) was used to aid in locating lithology changes throughout the core intervals. The great majority of well logs taken from the Kansas Geologic Survey were not digitized, and as a result were manually digitized within Petra. Well log analysis was used for the following: 1)

locating formation tops (Ste. Genevieve, St. Louis), 2) locating subformation tops (St. Louis B, C, D), 3) locating St. Louis “pay zones” in both the St. Louis B and C zone, and 4) along with other methods, estimating porosity to aid in finding pay zones. Figure 7 illustrates a type log used for locating the significant formations and zones using wire line log signatures.

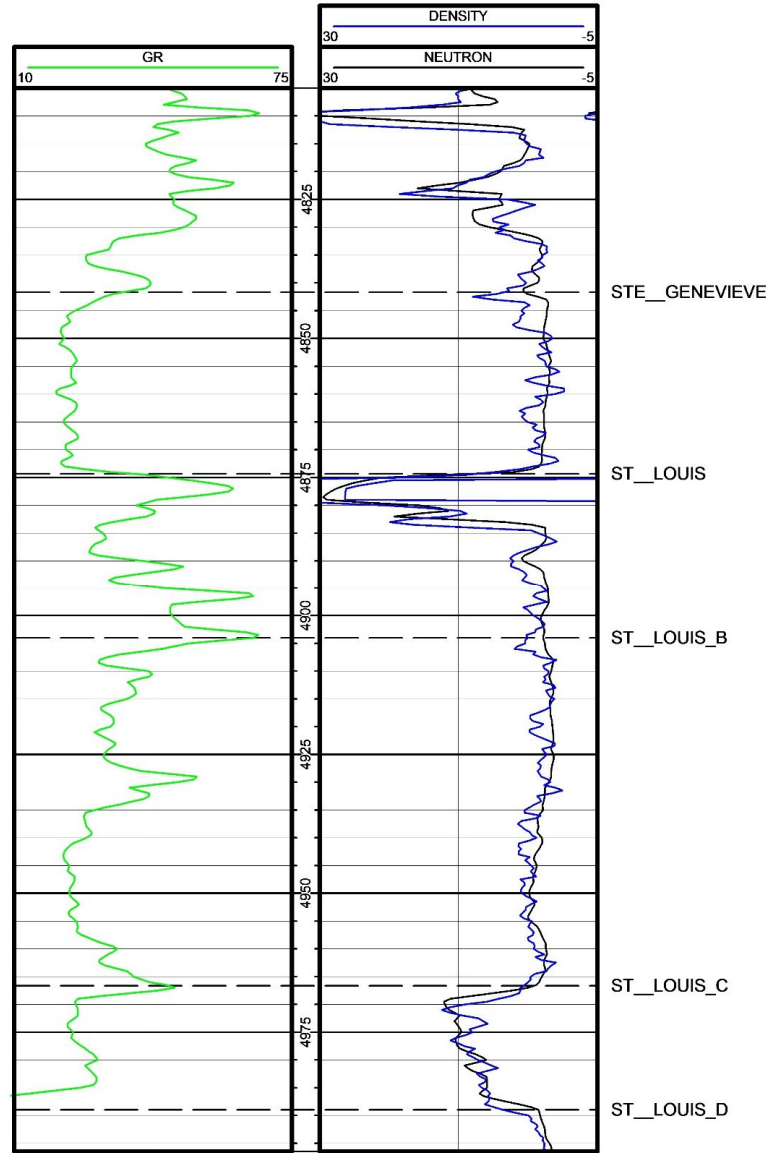


Figure 7: Type log of GR (gamma ray), NPHI (neutron porosity), and DPHI (density porosity) with the St. Genevieve, St. Louis, and St. Louis zones B, C and D tops picked.

## **X-Ray Fluorescence Analysis**

When evaluating the three separate core intervals, an X-Ray Fluorescence analysis was conducted. With a handheld NITON X3 XRF, all three cored intervals were scanned every one to two feet, at lithology changes, at specific points where well logs illustrate a different signature, and where there were textural changes. The elemental analyses were integrated with the core descriptions and well log signatures to augment the differentiation from one key facies to another. The NITON X3 XRF recorded values for the following elements: sodium (Na), magnesium (Mg), aluminum (Al), silicon (Si), phosphorus (P), sulfur (S), potassium (K), calcium (Ca), barium (Ba), titanium (Ti), chromium (Cr), manganese (Mn), iron (Fe), cobalt (Co), nickel (Ni), copper (Cu), and zinc (Zn). Following the XRF data collection, the respective elemental values were plotted against the depth where the scan took place on the core. This created a well log curve that illustrated the elemental concentrations throughout the entire core interval (Figure 8). The elemental values were uploaded into Petra and integrated with the suite of geophysical logs for that respective well.

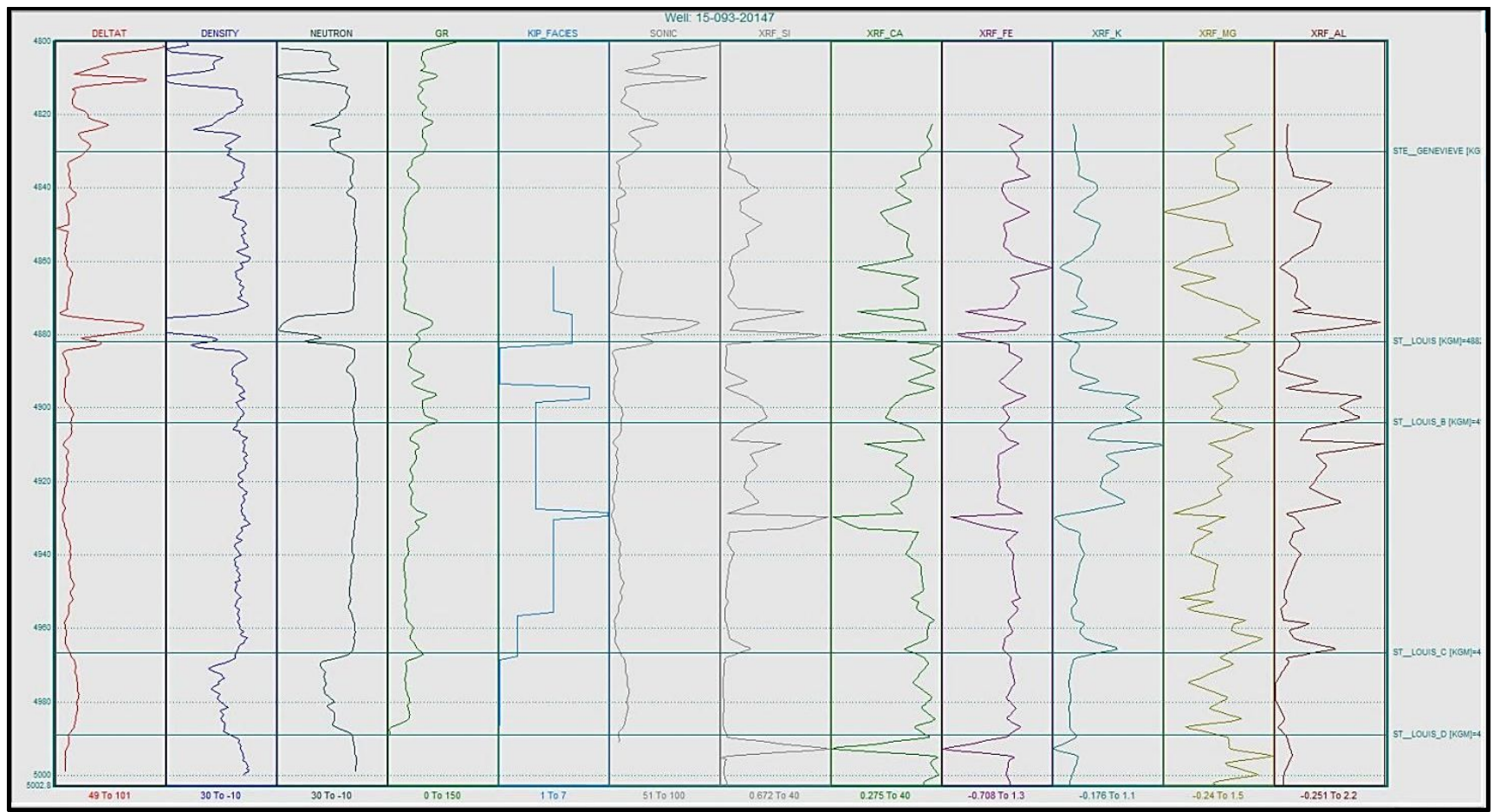


Figure 8: Illustrates how XRF data were turned into log curves to aid in picking formation/subformation tops. The following logs and elements were used in this analysis; DELTAT (sonic), DPHI, NPHI, GR, facies predictions, silicon, calcium, iron, potassium, magnesium, and aluminum.

## Petra®: Geologic Software

Upon creating a project in Petra, 2,948 wells within the study area were taken from the Kansas Geologic Society's database and uploaded into Petra. The key formation and subformation tops defined in this study included the Ste. Genevieve limestone, St. Louis limestone, and St. Louis B, C, and D zones. Formation tops that had been previously defined by various companies were taken into consideration, although each formation top for every well was handpicked to insure consistency throughout the study area. Upon defining the formation and subformation tops, structural, stratigraphic, and isopach thickness subsurface maps were created. Various cross sections were also created on structure and stratigraphic settings to aid in the subsurface analysis.

The MLS occurs 4,000 feet below the surface throughout all of Kearny County. Any well with a total depth less than 4,000 feet was assigned a unique numeric identifier or well sequence number (WSN) and was taken out of the study area, leaving 157 wells that had been drilled through the MLS. Raster logs (scanned paper logs) and digitized logs for all 157 were downloaded from the Kansas Geologic Society and Walter's Digital Library and uploaded into Petra. Each well had an average of four logs that were transferred to Petra, totaling roughly 640 uploads. Raster logs were calibrated within Petra, assigning depth markers and track thickness. In order to derive accurate values in the most efficient manner, the calibrated raster logs were manually digitized in Petra, with a sampling interval of 0.5 ft. This enabled log values to be exported from Petra and placed into Excel to ultimately be inputted into a neural network model.

## **Kipling2.xla: Facies Prediction Software**

Kipling.xla is an Excel add-in that was developed at the Kansas Geological Survey by Dr. Geoffrey C. Bohling. This software can be used for modeling and prediction of both discrete and continuous data. As defined in Bohling (2001), “Kipling can be used for either nonparametric regression or nonparametric discriminant analysis, developing a model for the prediction of either a continuous variable (such as permeability) or a categorical variable (such as facies) based on a set of underlying predictor variables (a set of well logs, for example). It can also be run in both modes simultaneously, developing different regression-type relationships for data from different categories.” Dr. Bohling developed a new version of the original Excel add-in, Kipling2.xla. This study used Kipling2.xla, as it is the most up-to-date version of the software, with useful upgrades and is also compatible with newer Excel workbooks.

Within Kipling2.xla, the neural network was implemented as a single hidden-layer feed-forward network (Figure 9). The hidden layer nodes in network compute a linear combination or weighted sum of the input variables (a suite of geophysical logs) representing variation along a certain direction in the input variable space (Bohling, 2007). The lines linking the input and hidden layer nodes signify the weights within the linear permutation (Figure 9). The weighted sum is passed through a sigmoid transfer function, giving an output ranging from zero to one (Bohling, 2007). As Bohling has summarized, the output layer nodes then compute a linear combination of the sigmoid basis function values computed by the hidden layer nodes and the entire set of linear combinations computed by the output nodes is rescaled to represent a set of probabilities of facies membership. Therefore, on a single pass

forward, a suite of log curve values are transformed within the network into a connected set of probabilities of facies occurrence (Bohling, 2007).

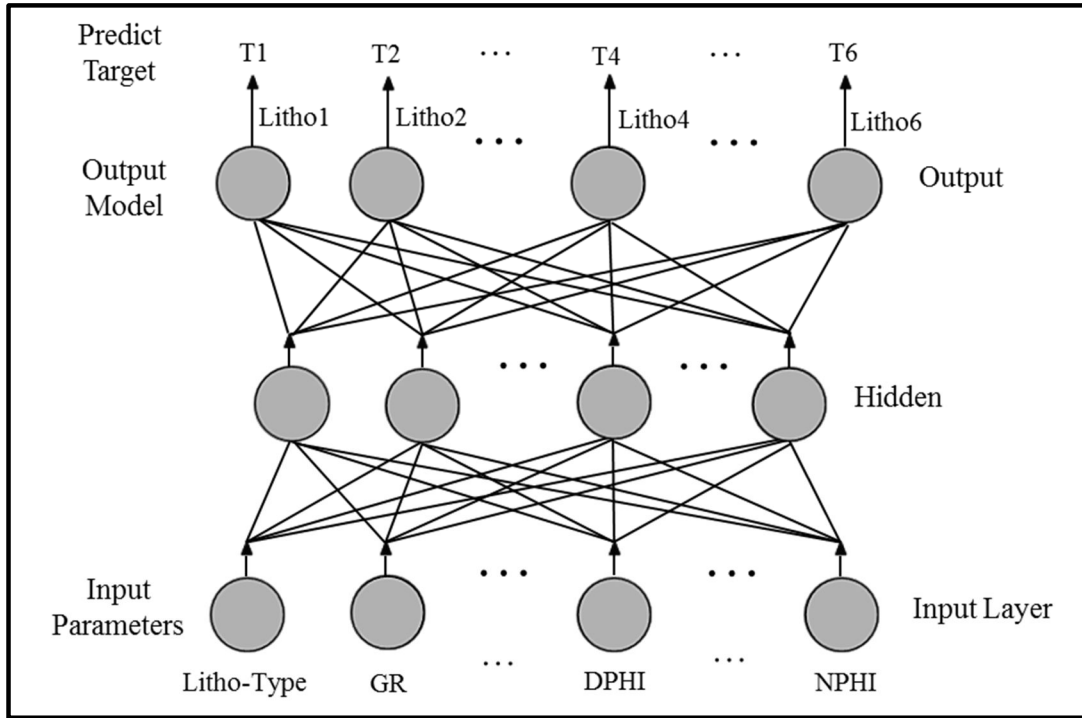


Figure 9: Generalized neural network flow. The input values are the four geophysical logs used in this study; GR, Neutron, Density, and Sonic curves. The output value would be the probabilities of different facies.

The network is “trained”, where predictor variables (log values) and a categorical response variable (core facies) are defined (Bohling, 2007). In this study, four geophysical logs from three different evaluated core intervals were used for the predictor variables: gamma ray, neutron porosity, density porosity, and sonic interval transit time. During the training process, the hidden layer nodes and dampening parameter values were repetitively adjusted (Bohling, 2007). A higher number of hidden layer nodes (larger network), a lower

dampening parameter, and a larger number of iterations all lead to a more complex network. Inversely, a lower number of hidden layer nodes (smaller network) and a higher dampening parameter, and a smaller number of iterations all lead to a smoother, less complex network. The inputted values of these three variables were repetitively adjusted until the predicted facies matched the core facies as closely possible, with a final value of 50 hidden layer nodes, a 0.05 dampening parameter, and 100 iterations. Refer to Appendix B for raw calculation Excel spread sheets of the three cored wells that the neural network models were created on.

### **Pitfalls and Limitations**

#### **Well Data**

The three neural network models created for this study have been shown quantitatively to accurately predict facies in the subsurface in this locality, although there are numerous factors that contribute to the overall accuracy when applying the predictions. When using neural networks for facies prediction, well placement, well frequency, availability of all necessary log curves, and availability of core controls the overall accuracy of the facies predictions. The creation of a neural network model is possible only where core is evaluated and/or the vertical stacking patterns of the facies are known. There is a direct relationship between prediction accuracy and the physical distance a well is from the neural network model. With shorter distances, the predictions are likely to be more accurate, and as distance increases, accuracy diminishes. More wells with core available for evaluation enables the creation of additional neural network models. With additional models and frequent wells with shorter distances away from the models, the facies distribution within the subsurface can be mapped with a higher accuracy.

With only three core intervals within the St. Louis available in the study area, distant facies predictions diminish in accuracy. Well placement and frequency also placed constraints on the facies predictions. The maximum distance between two wells that the neural network model was applied to was 16,353 ft. (3.1 mi.). Especially within the MLS, significant variability in the subsurface can take place over this distance, and caution should be used when creating a cross section over this distance. The range and average distance between wells within the neural network to which the model was applied are 717-16,353 ft. (0.14-3.1 mi.) and 5,324 (1.01 mi.), respectively.

The availability of all necessary log curves per each well also limits the number of wells the neural network model can be applied to. Only 30 wells had the necessary suite of geophysical log curves: sonic, neutron, density, and gamma. A neural network model with fewer log curves could be created, although detailed prediction of facies would be compromised. The more log curves applied in the neural network model, the higher the accuracy of the facies predictions.

### **Petra: Interpolation between Wells**

Although the facies prediction values determined using Kipling2.xla were honored, the interpolation function has limitations and does not provide a geologically reasonable interpretation. Within the parameters of two formation tops, the predicted facies may not be in agreement with adjacent facies, which can be expected with abrupt facies changes or the discontinuation of a facies. In this situation, the interpolation function may extend the facies until it is truncated against the next borehole. Geologically, it is more probable that the facies “pinches” out, but without well control between the two wells, this is the best interpretation the interpolation function can make. In a different scenario, where there is a facies

disagreement, the interpolation function can have a very abrupt, square truncation, which also illustrates the limitations of this function.

## **CHAPTER V: LITHOFACIES AND DEPOSITIONAL ENVIRONMENTS**

### **Lithofacies 1: Porous Ooid Grainstone**

The porous ooid grainstone is the main reservoir facies within the St. Louis Limestone. It is characterized as a very light gray, very well sorted, well rounded, and medium (upper) grain size facies. The porous ooid grainstone is poorly cemented by equant calcite cement with primary-depositional interparticle porosity, and less common intraparticle and fracture porosity. Heavy hydrocarbon staining was found in numerous core samples within the facies intervals. Ooid concentrations varied throughout the interval of the facies, with areas of higher concentrations containing heavier hydrocarbon staining. The individual ooids are concentrically laminated with their radial internal structure remaining, with an average size from 0.3-0.5mm.

Articulated and disarticulated echinoderms, brachiopods, bryozoans, as well as high concentrations of peloids and low amounts of detrital quartz grains combine to make up the remaining constituents of the facies. Varying degrees of micritization were found during analysis, with many grains having thick micritic rims or envelopes. The overwhelming majority of peloids are spherical with all internal structure absent. Peloids in the porous ooid grainstone are interpreted as past ooids that have been biologically degraded or micritized, which abolished any past internal structure within the concentrically laminated ooids. The origin of other peloids in this facies were interpreted as either fecal pellets or unknown. Of the chief fossils identified, echinoderms are the most prevalent. The echinoderm fragments are

relatively large, ranging from 2.0-3.0mm, and some echinoderm fragments have been concentrically laminated along with numerous other grains. Sedimentary structures within the porous ooid grainstone are rare, which could be due to excellent sorting or bioturbation (Handford, 1998). Lithofacies 1 and 2 are both ooid grainstones, although, cementation is variable. As concluded in Cluff (1984), cementation has a relationship with the degree of oolitic coating, where higher degrees of coating results in great porosity. This relationship was also found in this study, and can be viewed by comparing thin section images from Lithofacies 1 and 2 (Figure 10 and 12). Of the three cored intervals evaluated, the thickness of Lithofacies 1 reaches up to roughly 24ft (7m), occupying up to 24% of the St. Louis core intervals.

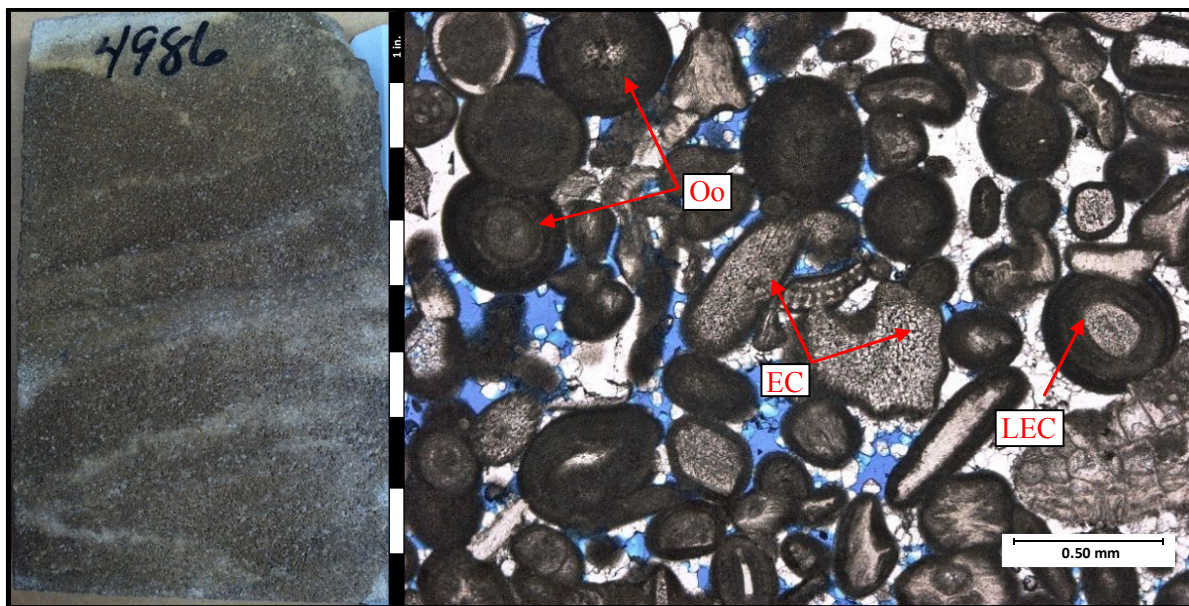


Figure 10: Core and thin section taken from study well 15-093-20147. The core slab has been stained extensively by liquid hydrocarbons. The thin section has been impregnated with blue epoxy to illustrate porosity. Abbreviations: Oo (ooid), EC (echinoderm), LEC (laminated echinoderm). PPL 4X magnification.

## **Depositional Environment: Ooid Shoal**

The porous ooid grainstone and highly-cemented ooid grainstone were deposited in an ooid shoal on a shallow-marine, open shelf. An ooid shoal is defined as a linear landform completely within or extending into a body of water with high concentrations of ooids that may accumulate in carbonate platforms on ramps, shelves, and rimmed shelf edges (Ahr, 1973; Read, 1982). Shelves are characteristically shallow, flat to nearly-flat platforms. Minor sea-floor perturbations, established by local topography, organic build-ups, islands, faults, and various other structural features have the capability of influencing deposition on the platforms (Handford, 1988). Topography created from these features has the capability of having control on local currents and waves, creating a new energy regime, thus different deposition patterns. Ooid shoals can form from high energy currents passing over local topographic highs (e.g. shoals formed on the windward side of a topographic high or between two topographic highs, along shorelines) (Handford, 1998). As stated by Handford (1998), ooid shoals largely form where the sea floor crosses the fair-weather wave base generating a high-energy zone that can be found in the distant offshore or at the shoreline.

Orientation and geometry are key diagnostic features when identifying ooid shoal deposits. Within the St. Louis C zone, Lithofacies 1 and 2 form an outstretched, northwest-southeast oriented, lenticular body roughly 16 miles (6km) long and 2 miles (1km) wide. Similarly to Damme field's shoal geometry by Handford (1988), the ooid shoal within St. Louis B and C zone are oriented with the depositional strike, or perpendicular to the paleoslope (northwest-southeast trending), and is determined to be deposited as a marine sand belt on a carbonate shelf.

Handford (1998) determined the Great Bahama Banks marine sand shoals are analogous with western Kansas' Mississippian shoals. In order to conceptualize the geometry of the ooid shoals, a review of the modern Great Bahama Banks will be compared with the ancient St. Louis ooid shoals. In Figure 11, an isopach of ooid grainstone illustrates the geometry of the St. Louis ooid shoals south of Lakin NW field (7.3 miles (11.7 km)), with a similar, elongate geometry with the Great Bahama Banks shoal (5 mi. (8 km)).

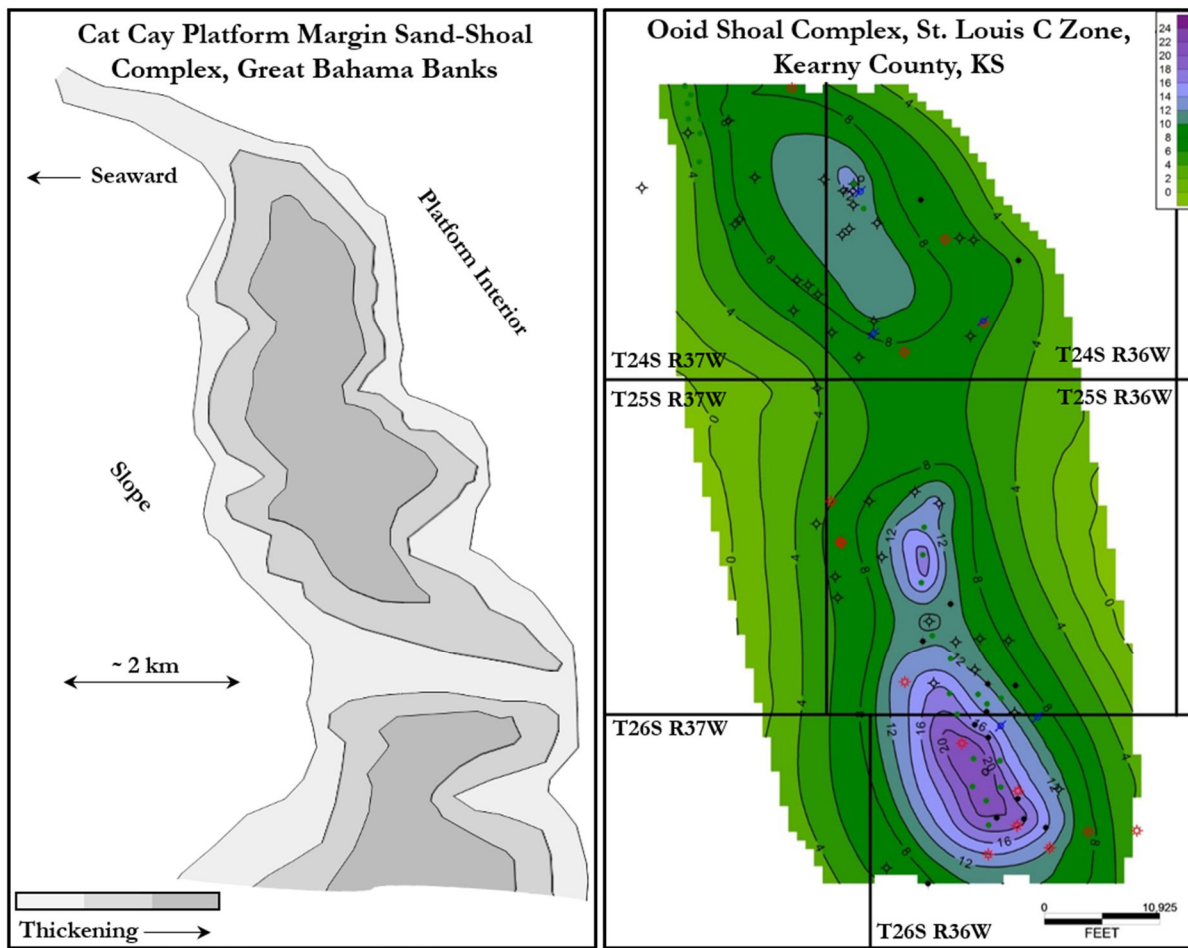


Figure 11: Located along the west margin of the Great Bahama Banks, an aerial view of the Cat Cay platform margin sand-shoal complex, illustrating the lenicular geometry of modern

sand shoals with the white outline. Geometry of the ooid shoal within the St. Louis C zone (pay zone), strongly resembling the geometry of the Cat Cay sand-shoal complex.

### Lithofacies 2: Highly Cemented Ooid Grainstone

The highly cemented ooid grainstone has similar characteristics with the porous ooid grainstone, although the primary porosity in the porous ooid grainstone is replaced with equant calcite cement, abolishing the porosity in the highly cemented ooid grainstone. Majority of ooids have internal structure, although the internal structure of many ooids has been abolished through micritization and are classified as peloids. The fossil concentrations are low, with the most prevalent being gastropods, foraminifera, and crinoids. The highly cemented ooid grainstones contain 1-5% of detrital quartz grains (whole-rock volume). This facies is defined as a non-reservoir flow unit. Of the three cored intervals evaluated, the thickness of Lithofacies 2 ranges between 9-21ft (3-6m), occupying up to 22% of the St. Louis core intervals.

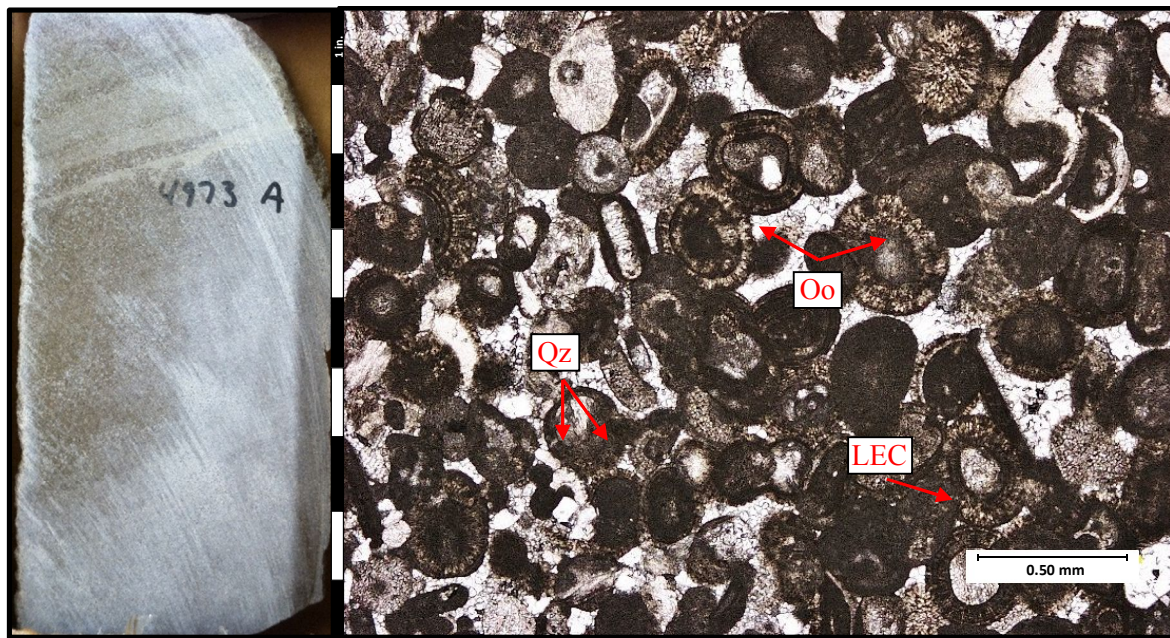


Figure 12: Core and thin section from study well 15-093-20011. Abbreviations: Oo (oolith), LEC (laminated echinoderm), Qz (detrital quartz grain). PPL 4X magnification.

### **Depositional Environment: Ooid Shoal**

Lithofacies 1 and 2 formed in the same depositional environment, with the only difference between the two being porosity variability, due to the highly-cemented characteristic of Lithofacies 2. For environment of deposition interpretation, view the “Lithofacies 1” interpretation.

### **Lithofacies 3: Quartz-Carbonate Grainstone**

The quartz-carbonate grainstone facies is characterized as a very light gray, medium-to-very fine grained, subrounded, well sorted interval with individual laminations being very well sorted. Very few fossil fragments are visible and most are not identifiable. Detrital quartz grain abundances are between 20-36% of the whole rock volume, with an average grain size of 0.227mm. Along with detrital quartz grains, the quartz-carbonate grainstone contains high concentrations of peloids and contains micritic and blocky calcite cement with portions of the facies having a strong peloidal fabric. Very fine (<1mm) dark laminations commonly repeat through significant portions of the intervals, with larger, 3mm dark laminations occurring in other portions. The dark laminations are made up of very fine quartz grains, with the grains ranging between 0.06- 0.1mm in size. Small scale (15mm) fining upward graded bedding cyclically repeats through large portions of the interval. The quartz-carbonate grainstone is declared as a non-reservoir facies, due to compaction and pore filling cementation. Within the three cored intervals evaluated, the thickness of Lithofacies 3 ranges between 10-34ft (3-10m), occupying up to 30% of the St. Louis core intervals.

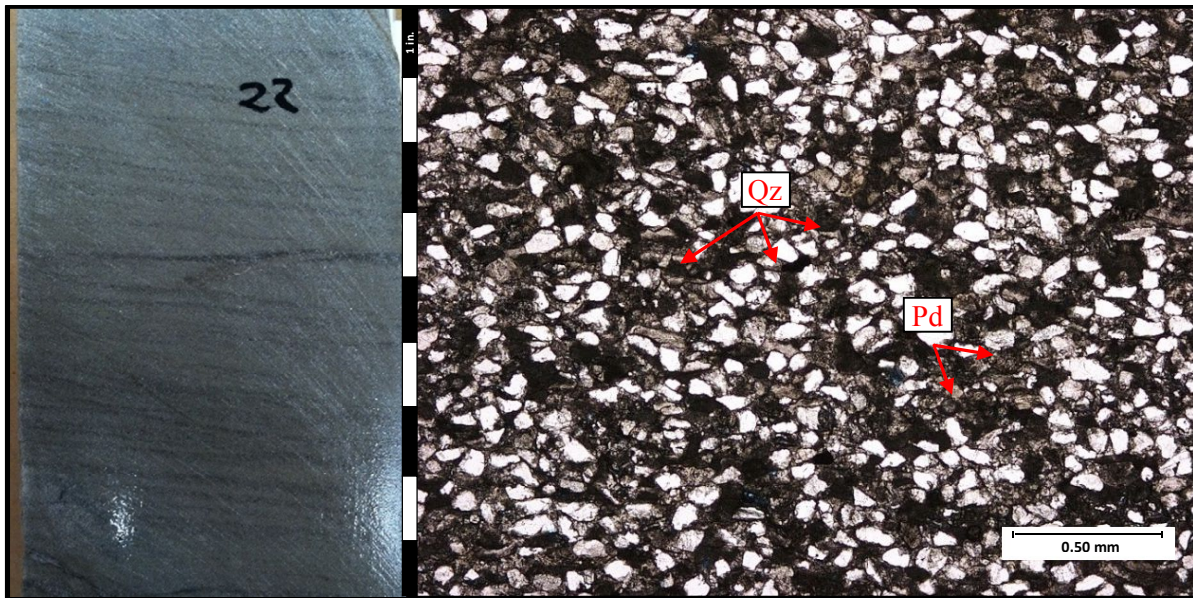


Figure 13: Core and thin section taken from study well 15-093-20147. Blue epoxy has been applied to thin section, showing that there is very low to no porosity on this slide. Abbreviated: Qz (quartz), Pd (peloid). PPL 4X magnification.

### **Depositional Environment: Eolianite Dune**

The quartz-carbonate grainstone is interpreted as a carbonate eolianite dune. A carbonate eolianite is defined as any rock formed by the lithification of sediment deposited by eolian processes and contains >50% CaCO<sub>3</sub> (Fairbridge and Johnson, 1978). As stated by Abegg et al. (2001), “The main factors that promote carbonate eolianite deposition include the following: 1) subaerial exposure, 2) glacioeustatic sea-level changes (promotes widespread deposition of eolian limestones), 3) warm tropical waters, 4) limited siliciclastic input, 5) arid climate, and 6) high-energy windward margin. Limited siliciclastic input and subaerial exposure are the only prerequisites for carbonate eolianite deposition.” The great majority of carbonate eolianites are deposited in warm climates as coastal dunes. Coastal dunes are

notoriously deposited adjacent to high-energy beaches, where a significant amount of calcareous sand accumulates (McKee and Ward, 1983).

The following acted as the key diagnostic features used to identify this facies: 1) intervals that contained over 20% (total rock volume) detrital quartz, 2) having a climbing translatent stratification and indistinctly stratified sedimentary structures, 3) well sorted; medium to fine grained, and cross stratified, and 4) lacking larger marine shells. Reports of this depositional facies from studies within a proximal distance to the Kearny County study area (Damme and Big Bow-Sand Arrow) assisted in solidifying this interpretation.

#### **Lithofacies 4: Peloidal Packstone**

The peloidal packstone is characterized as a very light gray, medium grained, rounded, well sorted interval. Peloids make up the overwhelming majority of the facies and intraparticle shape is filled with sparry calcite cement. Very few ooids have visible internal structure. Many of the peloid are interpreted as past ooids that have been micritized, losing all internal structure, while others are classified as fecal pellets or undeterminable. Dark, quartz-filled laminations appear throughout most intervals as well as stylolites. Detrital quartz grains make up around 2-8% of the rock volume, with an average grain size of 0.09mm. Fossil concentrations are very low, with foraminifera and gastropods being the most prevalent. Lithofacies 4 is the most vertically extensive lithofacies, with thicknesses ranges between 40-60ft (12-18m), occupying up to 55% of the St. Louis core intervals.

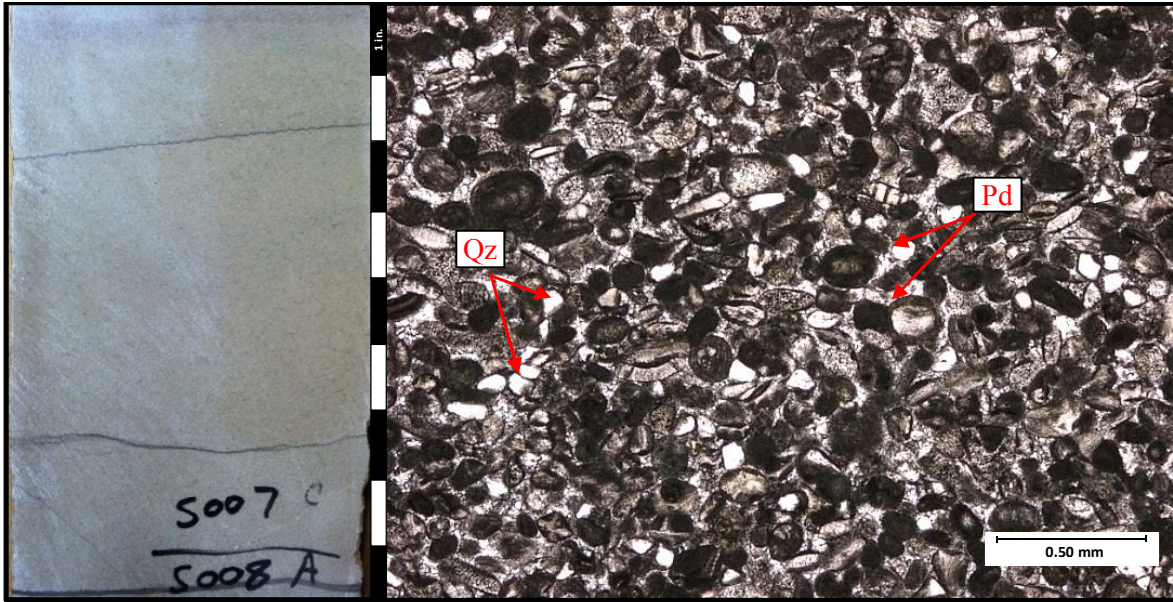


Figure 14: Core and thin section taken from study well 15-093-20011. Abbreviation: Qz (detrital quartz grain), Pd (peloid). PPL 4X magnification.

#### **Depositional Environment: Lagoonal/ tidal flat (back barrier lagoon deposit)**

The peloidal packstone facies is interpreted as being deposited in a lagoonal/tidal shelf environment landward of the ooid shoal. Lagoons are often bodies of water in a completely enclosed, restricted environment with no connection to the sea. A lagoon-type environment is shallow, although they can rarely reach up to several tens of meters deep. This restricted type environment may be created by any type of physical barrier such as reefs, islands, skeletal or oolitic sand shoals (Enos, 1983).

The key diagnostic criterion for restricted shelves or lagoons is vertical sequences and lateral transitions. As previously covered, lagoon-type environments form from the presence of a physical barrier, thus a lateral change into a barrier-type facies assists in the determination of a restricted, lagoon environment. In conjunction with a barrier-type facies, in the opposing direction, a transition into low-energy shoreline facies is characteristic (Enos.

1983). A characteristic vertical sequence is a low-energy shoaling upward cycle (Enos, 1983).

Within the parameters of a sequence stratigraphic framework, the laterally equivalent facies to the peloidal grainstone (lagoon) facies within the study area was the ooid grainstones (shoal) facies. The ooid shoal sand body acted as a “barrier facies”, or immediate cause of restriction, and contributed heavily to the formation of the lagoon. This can be compared to its modern counterpart, the Florida Bay. A semi-restricted, low-energy shelf can be found in the inner part of the south Florida shelf margin (Enos, 1983). This restriction is caused by skeletal sand shoals, which are formed from large amounts of skeletal debris being transported via wave from reefs that have formed further seaward, near the slope break (Enos, 1977; Enos 1983).

### **Lithofacies 5: Clay-Rich Mudstone**

The clay-rich mudstone is characterized as a grayish black, very finely grained, highly micritized interval. Detrital quartz grains make up between 0-3% of the rock volume. Very little fossil content was identified and moderate quantities of highly micritized peloids are present. Some clay-rich mudstone intervals have a strong green tint, which is interpreted as the presence of high amounts of glauconite. The handheld XRF was used to scan all intervals, although the green tinted areas were scanned intensely. Relative to other x-rayed intervals, very high iron (Fe) values, between 10-100 ppm, were recorded from the green tinted areas. The mineral glauconite (chemical formula:  $(K,Na)(Fe^{3+}Al,Mg)^2(Si,Al)^4O^{10}(OH)^2$ ), is an iron potassium phyllosilicate and is a part of the mica group. The high iron (Fe) value from the x-ray fluorescence analysis was also accompanied by a strong green. Of the three cored intervals evaluated, the thickness of Lithofacies 5 ranges between 3-9ft (1-3m), occupying up

to 7% of the St. Louis core intervals. Lithofacies 5 is a non-reservoir flow unit. Many of the clay-rich mudstone core intervals were disarticulated, as seen in the core image below.

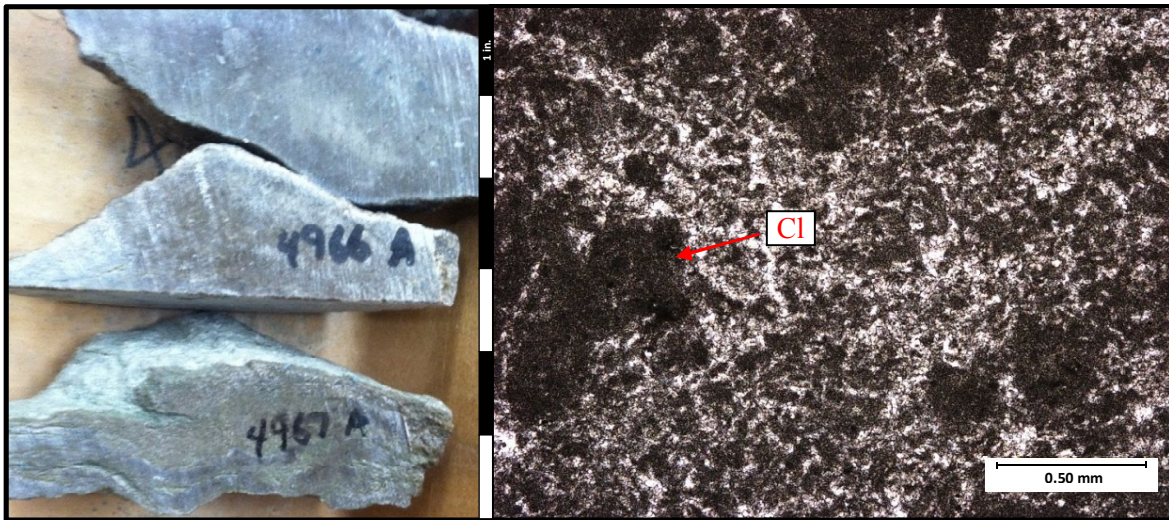


Figure 15: Core and thin section from study well 15-093-20011. Abbreviation: Cl (clay). PPL 4X magnification.

#### **Depositional Environment: Relatively deep marine**

Lithofacies 5 is understood to signify the deepest environment found in the St. Louis limestone, determined to be deposited in a low energy, open-marine shelf environment. Key criteria for this interpretation includes; 1) little-to-no detrital quartz grains, 2) little-to-no skeletal fragments, 3) lacking evidence of subaerial exposure, 4) the matrix is exclusively made up of micrite, and 5) it is a clay-rich facies.

#### **Lithofacies 6: Skeletal Wackestone**

The skeletal wackestone is characterized as a medium light gray, fine grained, poorly sorted, fossil-rich interval. Many of the fossils are fully articulated, and relatively large. Fossils identified in the skeletal mudstone include: echinoderms, crinoids, bryozoans, foraminifera, and tabulate corals. Detrital quartz grains are in very low abundance of the rock volume. Lithofacies 6 is a non-reservoir flow unit. Of the three cored intervals evaluated, the

thickness of Lithofacies 6 ranges between 4-5ft (1-1.5m), occupying up to 4% of the St. Louis core intervals.

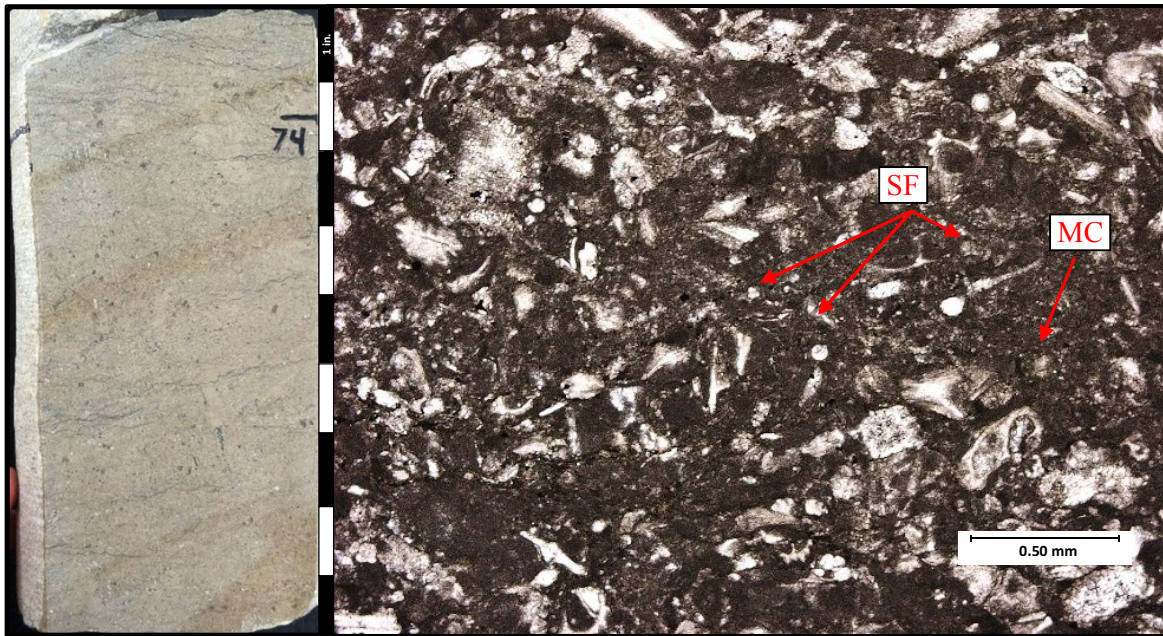


Figure 16: Core and thin section from study well 15-093-00317. Abbreviation: SF (skeletal fragments), MC (micritic matrix). PPL 4X magnification.

#### **Depositional Environment: Low energy, open shelf environment**

The skeletal wackestone/packstone was determined to be deposited in a low energy, open-marine shelf environment. Key criteria for this interpretation include; 1) little-to-no detrital quartz grains, 2) abundant, large, disarticulated skeletal fragments, 3) lacking evidence of subaerial exposure, and 4) the matrix is exclusively made up of micrite. Lithofacies of this nature are thought to be in waters that are between 10-30 m (30-100 ft) deep, located seaward from grainstone shoals, such as the Lithofacies 1 and 2 (Cluff, 1984).

## CHAPTER VI: RESERVOIR QUALITY

Reservoir quality and potential were analyzed on the three main study wells. Porosity estimates were collected for each facies from two sources: 1) thin sections, where the percent of blue epoxy relative to the entire thin section acted as a proxy from porosity, and from 2) neutron (NPHI) and density (DPHI) values from the wells' respective geophysical logs. Drill stem tests were not available to view, which disabled any gathering of permeability values. To illustrate porosity, NPHI was plotted against DPHI, which can be viewed in Figure 17. The porous ooid grainstone is the only facies with reservoir quality porosity (bulk porosity values circled in red). When exploring the St. Louis Limestone, the porous ooid grainstone, located in the St. Louis C zone, is the pay zone within Kearny County. Thin section porosity analysis also indicated the porous ooid grainstone as the only reservoir facies, with thin section derived porosity values between 12-16%.

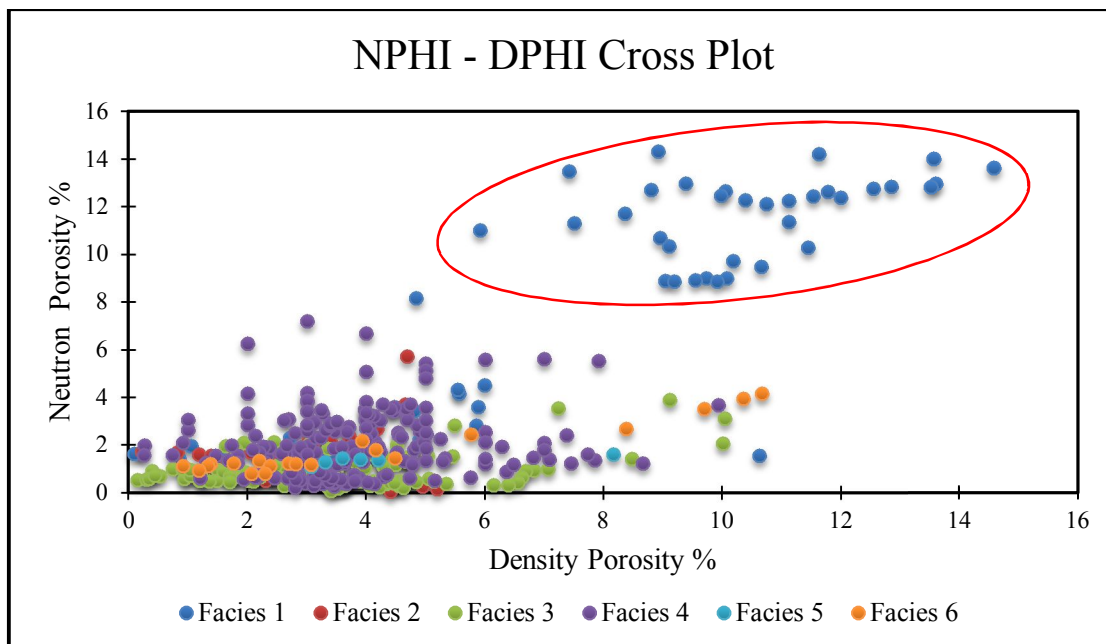


Figure 17: Cross plot of neutron porosity (%) and density porosity (%). Neutron and density log values were taken from the three cored study wells. This cross plot illustrates that Facies 1

(Porous Ooid Grainstone) has the highest porosity values and confirms that it is the chief reservoir facies.

In order to display porosity in a different graphic form, a box plot was created. The box plot was derived by calculating the minimum, quartile 1, quartile 2 (median), quartile 3, and maximum values. The differences in these values were used to create the box plot. The color scheme within the box plot correlates to Figure 18 (cross plot), and further illustrates that Facies 1 (porous ooid grainstone) is the chief reservoir facies.

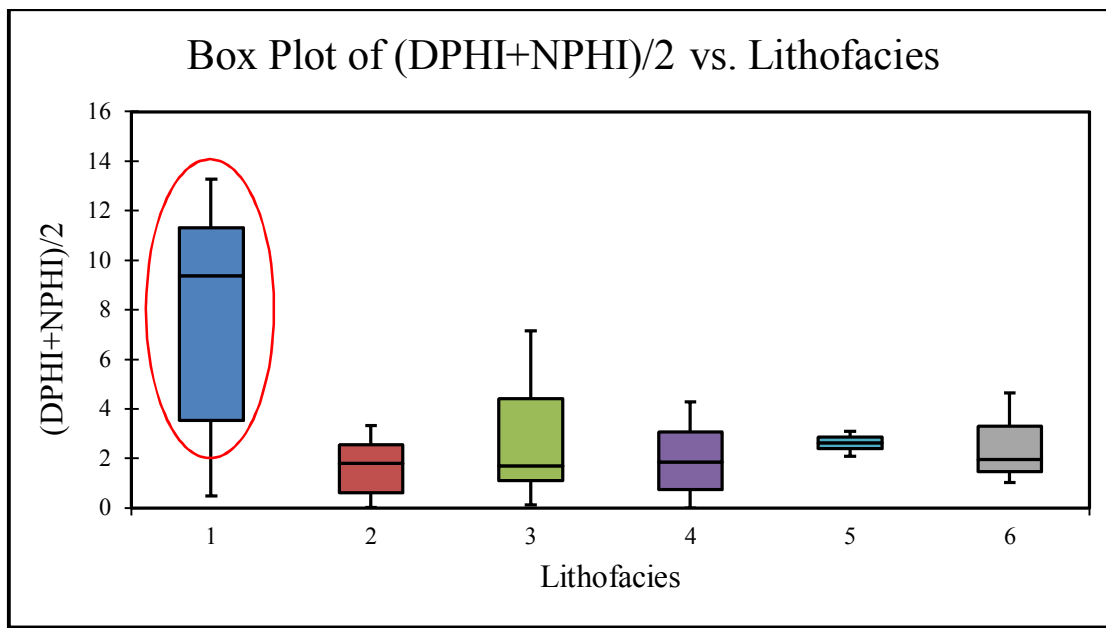


Figure 18: Box plot of  $(DPHI+NPHI)/2$  vs. Lithofacies. The box plot derived by calculating and taking the difference of the minimum, quartile 1, quartile 2 (median), quartile 3, and maximum values.

## CHAPTER VII: FACIES DISTRIBUTION

### Applying the Neural Network Model

Lithofacies identification and transitions via log signatures have proven to be very subtle, and in some cases indistinguishable. With human error, the difficulty of locating lithofacies via log signatures is great. In order to remove bias, a mathematical approach was taken, using Kipling2.xla, a neural network analysis tool. This neural network analysis tool allows for vertical and lateral facies predictions in wells without core throughout the study area.

The result of a neural network model with 50 hidden layers, a damping parameter of 0.05, and 100 iterations from one of the three cored study wells that containing GR, Neutron, Density, and Sonic curves can be seen in Figure 19. This figure illustrates the agreement of facies between the predicted and core facies. Facies Probability, the plot to the farthest left, is equivalent to the “maximum” probability within the neural network. Within the model, the value at a specific point is checked for agreement with each facies, giving a probability or likelihood for each facies. The facies with the highest probability or “maximum” probability will then be the facies that is predicted, which is shown in the second plot in Figure 19.

At this point in the neural network, only the log curve values are taken into consideration for the facies prediction. As seen in Figure 19, relative to the Core Facies (plot 4), the Predicted Facies (Plot 2) includes several thin facies (<2 ft) and illustrates an erratic behavior. Adding geologic significance to the probabilities yields a better overall prediction of the observed core facies (plot 4). Transitions between physically adjacent depositional environments occur more frequently opposed to environments which are significantly distant from each other (Bohling, 2001). To apply this concept to the data, a TPM (Transition

Probability Matrix) was computed and applied. The TPM is derived from the stacking pattern of the core facies, which calculates the probability of one facies underlying or overlying one another. After computing and applying the TPM modification, the very thin ( $<1$  ft) predicted facies were eliminated, which ultimately enhanced the agreement between the Facies Prediction and Core Facies. The result of applying the TPM can be seen in Figure 19, by comparing the “Facies Prediction”. This process was repeated for all three of the main study wells, which created a total of three neural network models.

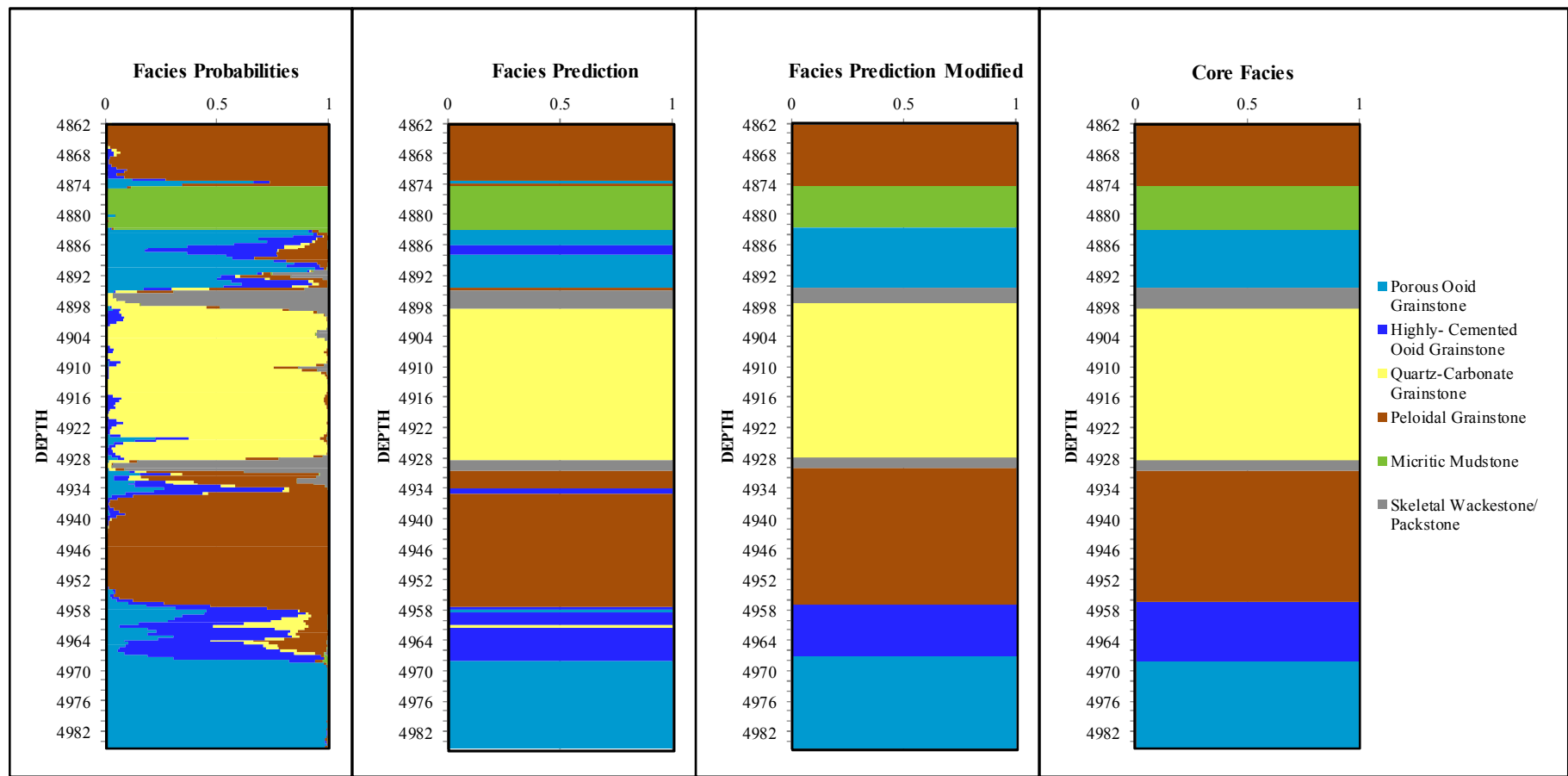


Figure 19: Four plots of the facies probability, facies prediction, facies prediction modified, and core facies (actual facies) that illustrate the neural networks models facies agreement with observed core facies.

In order to quantitatively analyze the accuracy of the neural network models, a facies prediction “scorecard” was created using Excel’s PivotTable, with Core Facies as the row variable, predicted facies as the column variable, and count of predicted facies in the table itself. The Core Facies refers to the “actual” facies that was evaluated from three separate core intervals (Figure 20). During the creation of this scorecard, values were taken from all three of the main study wells. The maximum probability was calculated by summing the maximum probability per facies for the three main study wells combined, and averaging those values per each facies. It is important to note that predicted facies are derived from the maximum facies probability, with the difference being that maximum facies probability is the highest decimal value between zero and one relative to the remaining facies and the predicted facies is a value of either zero or one, with the value one indicating the presence of a facies and zero indicating its absence (predicted facies is the equivalent of taking the decimal value of the maximum facies probability to the nearest whole number, one).

Combining all of the maximum probabilities per each facies and averaging the values gives the average percent of confidence in specific facies. The Maximum Probability Modified was calculated just as the Maximum Probability, with the only difference being that the values taken had the Transitional Probability Matrix applied to them. In order to cross reference the probability or confidence in a facies with the actual facies, an absolute accuracy was calculated. The absolute accuracy was calculated by dividing the predicted facies count by the core facies count. The end result of these calculations gives a quantitative analysis of the neural networking model having two vital components: (1) the maximum facies probability or maximum confidence of a facies, compared with (2) the absolute accuracy or the maximum probability’s agreement with the core facies.

After the training process was completed for each of the three main study wells, the three neural network models were then applied to a total of 30 wells that contained the same input variables (log curves) as the model. For wells that contained all input variable needed (the four main geophysical logs; GR, Neutron, Density, and Sonic) one of the three neural network models was applied. Determining which of the three models to apply to a specific well was controlled by the distance from the well to the three neural network models. The model with the shortest distance to the well was the chosen model to be applied. The model then calculated the most probable facies from the log values and ultimately predicted the facies succession in each of the 30 wells. The predicted facies, which were derived from four log curves at a specific point (depth), were then plotted against their respective depth and generated into LAS files. The LAS files were then uploaded into Petra to create cross sections of the 30 wells throughout the study area.

Core Facies	Predicted Facies							Absolute Accuracy	Maximum Probability	Maximum Probability Modified
	1	2	3	4	5	6	Grand Total			
1	54	4					58	96.43%	88.60%	96.22%
	1	75	2	4			82	90.36%	79.61%	96.08%
		1	143	1	2		147	96.62%	92.78%	98.49%
		1	3	3	313		320	98.12%	94.78%	99.14%
					37		37	94.87%	92.61%	99.01%
				1		19	20	100.00%	90.19%	92.86%
Grand Total	56	83	148	319	39	19	664	Facies Prediction Model Accuracy		
Proportion Percent	96.55%	101.22%	100.68%	99.69%	105.41%	95.00%		Absolute Accuracy	Maximum Probability	Maximum Probability Modified
Difference	2	1	1	1	2	1	8	96.07%	89.76%	96.97%

Figure 20: Predicted facies scorecard for 3 key trained wells with core containing GR, Neutron, Density, and Sonic curves.

#### Table Formulas

- Body of the table: Count of Predicted Facies
- Proportion Percent:  $(\text{Grand Total (x-axis)} / \text{Grand Total (y-axis)}) * 100$
- Difference: Absolute value of Grand Total (x-axis) – Grand Total (y-axis)
- Absolute Accuracy:  $(\text{Count of Predicted Facies} / \text{Grand Total (y-axis)}) * 100$
- Maximum Probability: Average of all maximum probabilities per facies for the three trained wells
- Maximum Probability Modified: Average of all maximum probabilities per facies for the three trained wells with TPM applied
- Facies Prediction Model Accuracy: Average of all facies within the three categories; Absolute Accuracy, Maximum Probability, Maximum Probability Modified

### **Petra Interpolation: Mapping the Facies Distribution**

Upon uploading the LAS files into Petra, which contained the predicted facies for each of the 30 wells, cross sections were created. The 30 wells containing the predicted facies LAS files are distributed throughout the study area, which enabled a detail analysis of the facies vertical and lateral distribution in the study area. Due to the elongate, linear trend of the field, azimuthal subsurface data were very limited. Using Petra's interpretive fill, the facies were interpolated between wells then filled with a specific color assignment per facies. During the interpolation process, major tops were defined for all 30 wells, which included the St. Louis, St. Louis B, C, and D. This trained the interpolation function to interpolate between two tops. This places a sequence stratigraphy framework on the interpolation function, disabling the linkage of two facies that are not genetically related.

Eight cross sections with interpretive color fill activated were created. The cross section lines can be viewed in cross sections A-H (figure 22). Four of the eight cross sections are NW oriented with the remaining four being EW oriented. Cross sections A-H show that the two dominating facies are Lithofacies 3 and 4, Quartz-Carbonate facies and Peloidal facies, respectively. Moving towards the south, Lithofacies 1 (porous ooid grainstone) becomes more prevalent, which corresponds well with production data and isopach maps of the pay zone. Numerous cross sections that connect wells in various directions can be viewed in Appendix B.

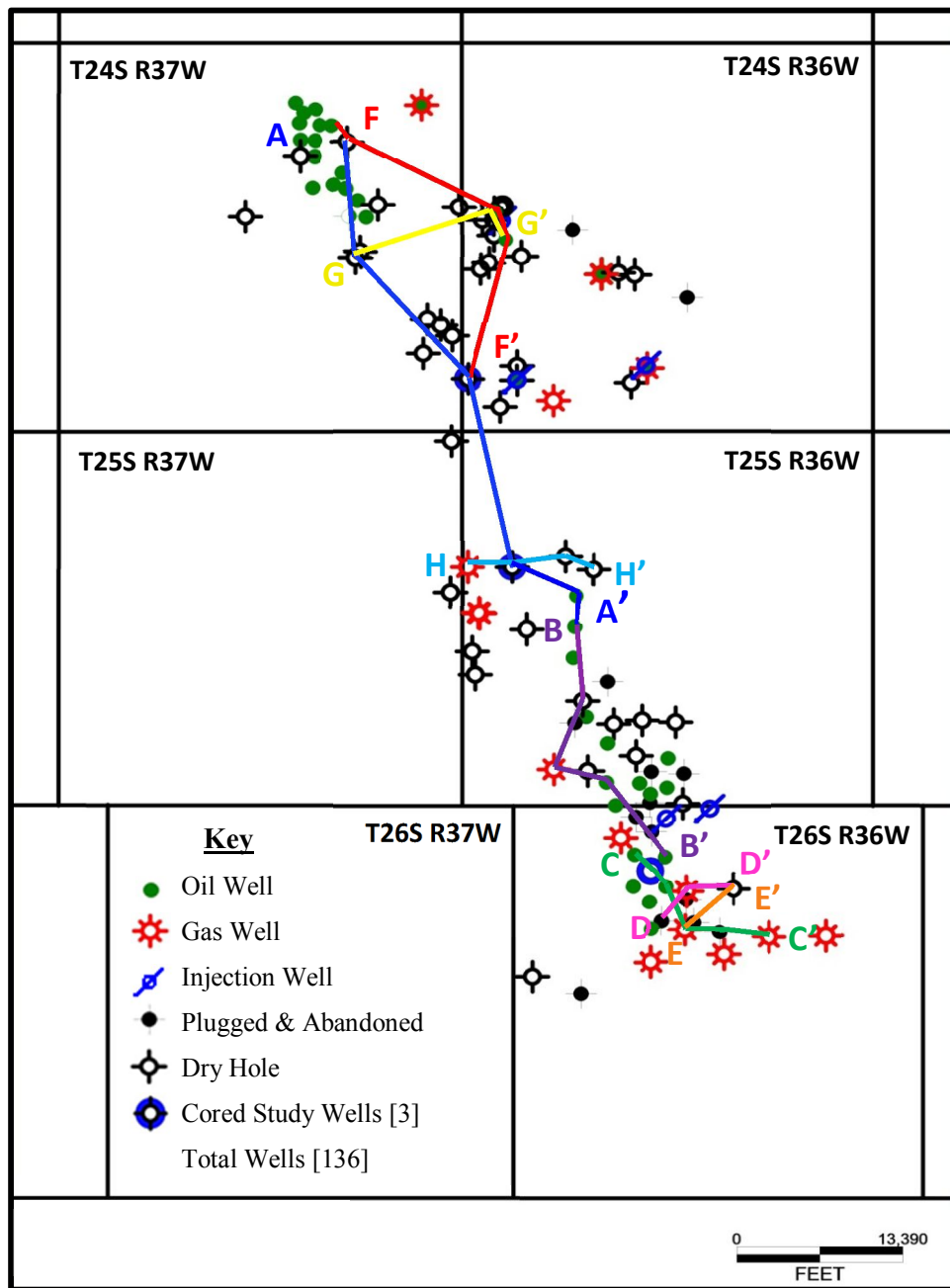
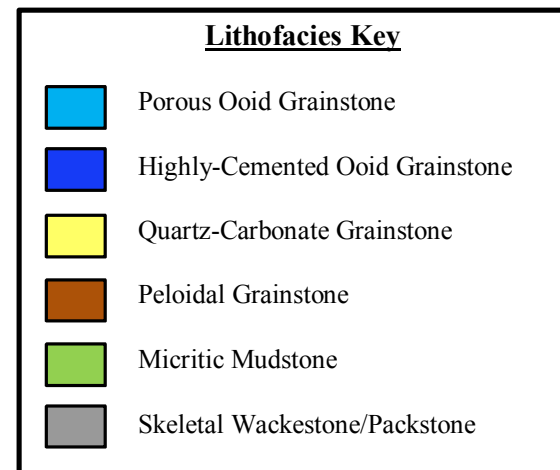
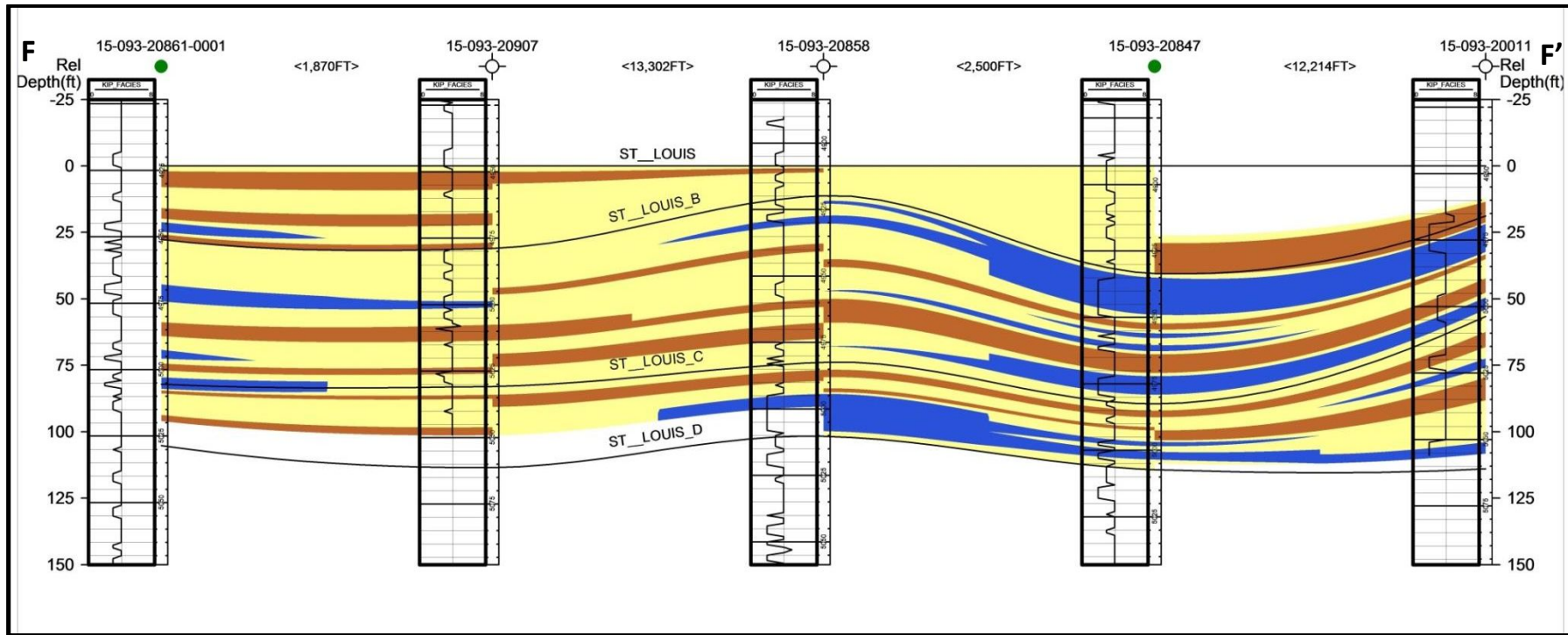
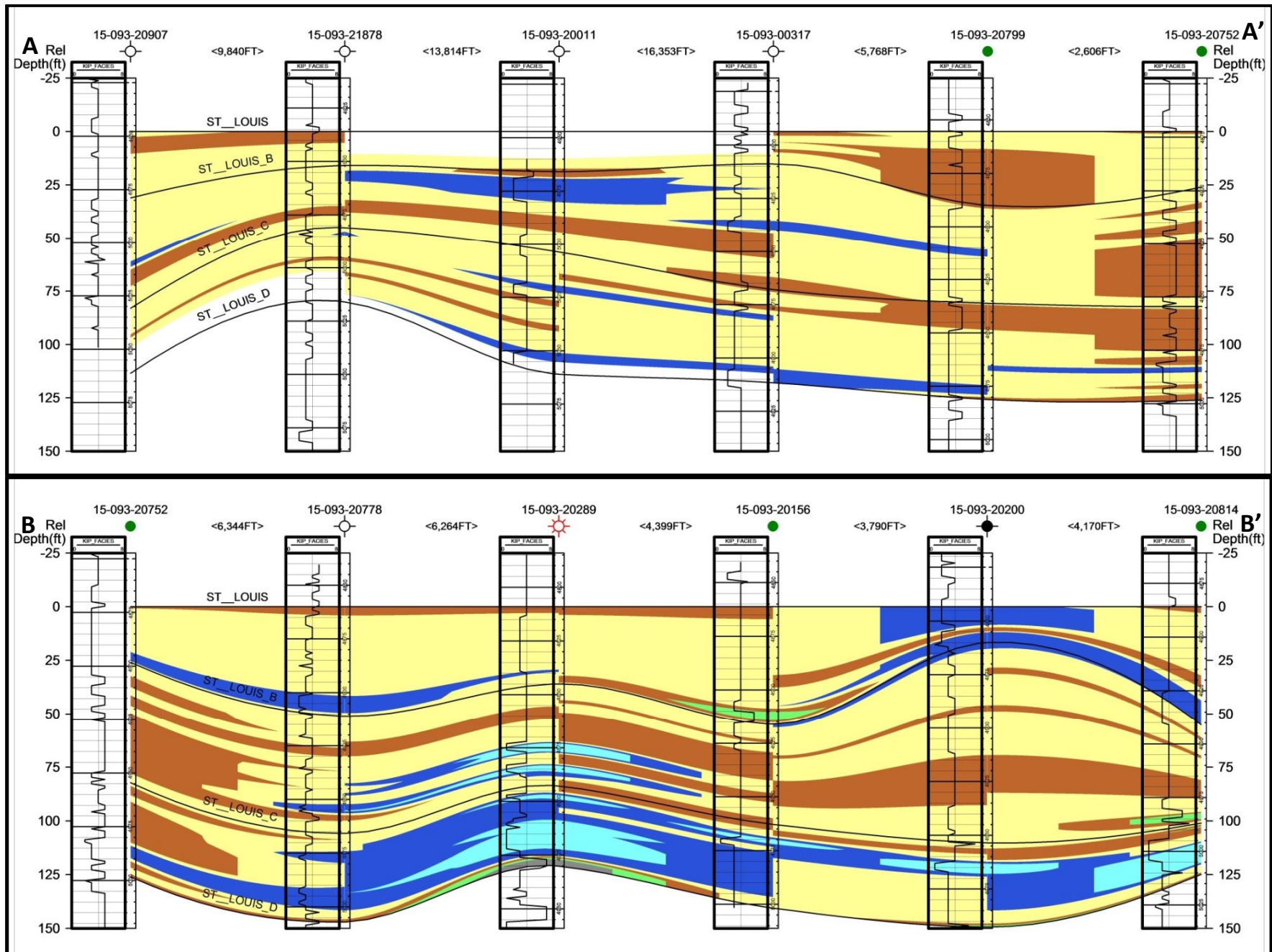
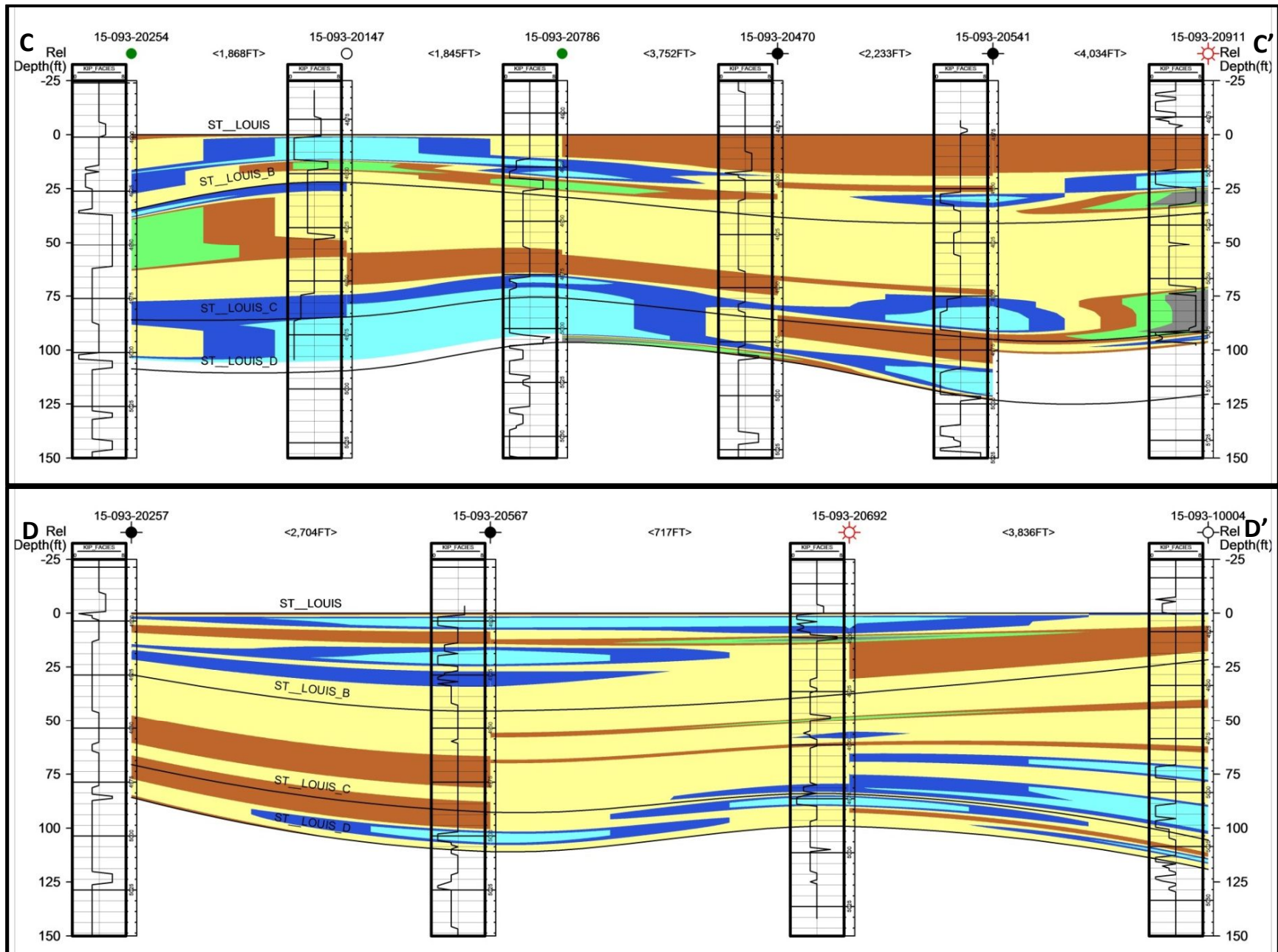
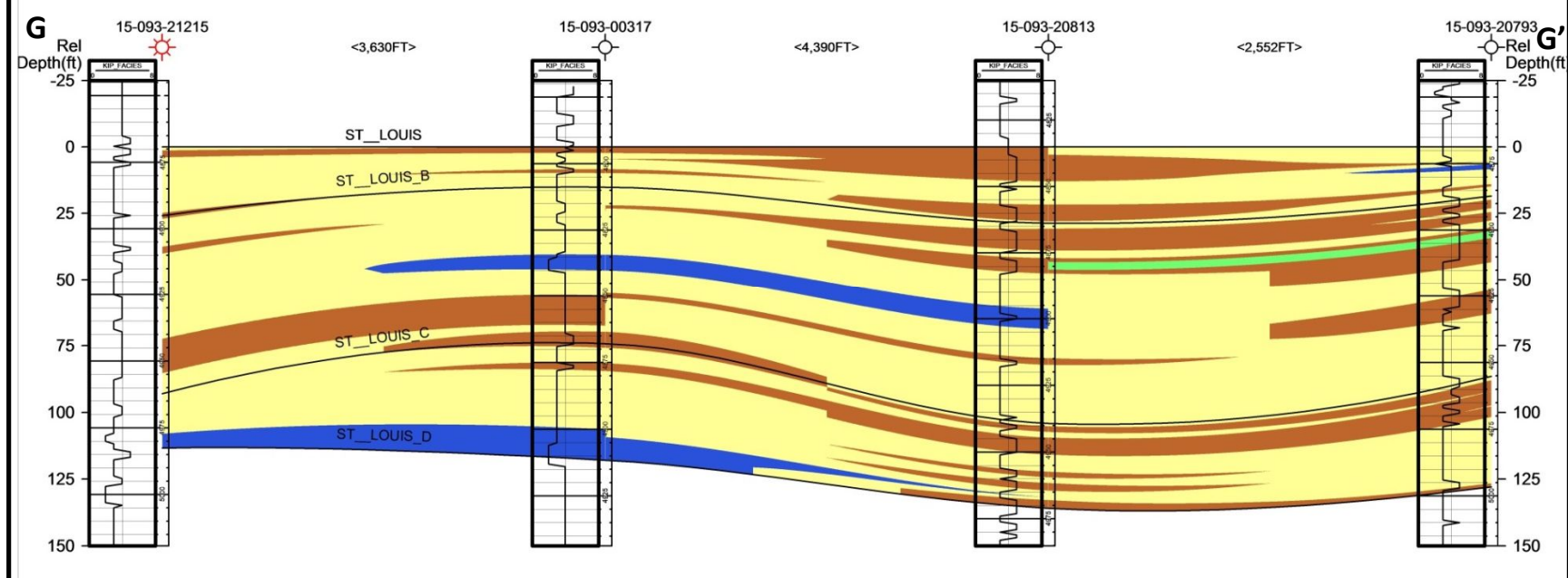
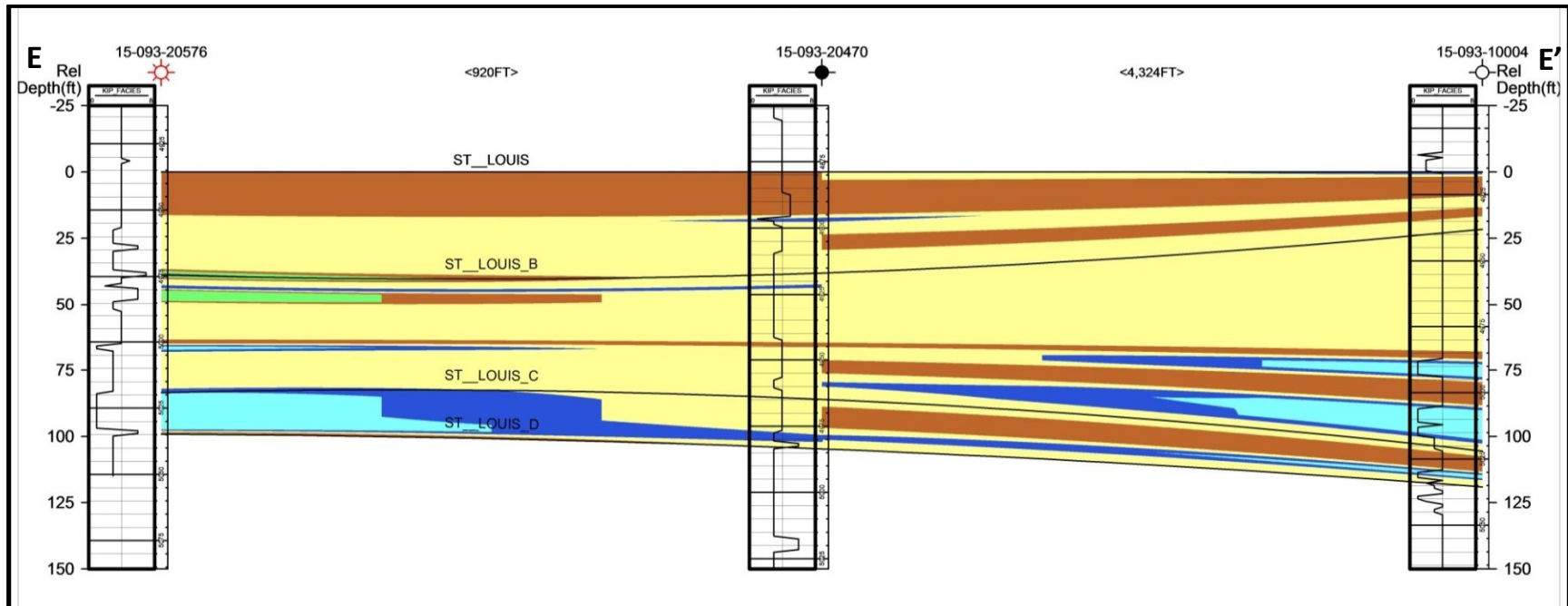


Figure 21: Base map with color coded cross section lines running both NS and EW and a key displaying what each well symbol represents Extensive azimuthal subsurface data was difficult to attain due to the linear trend of the wells in the study area.









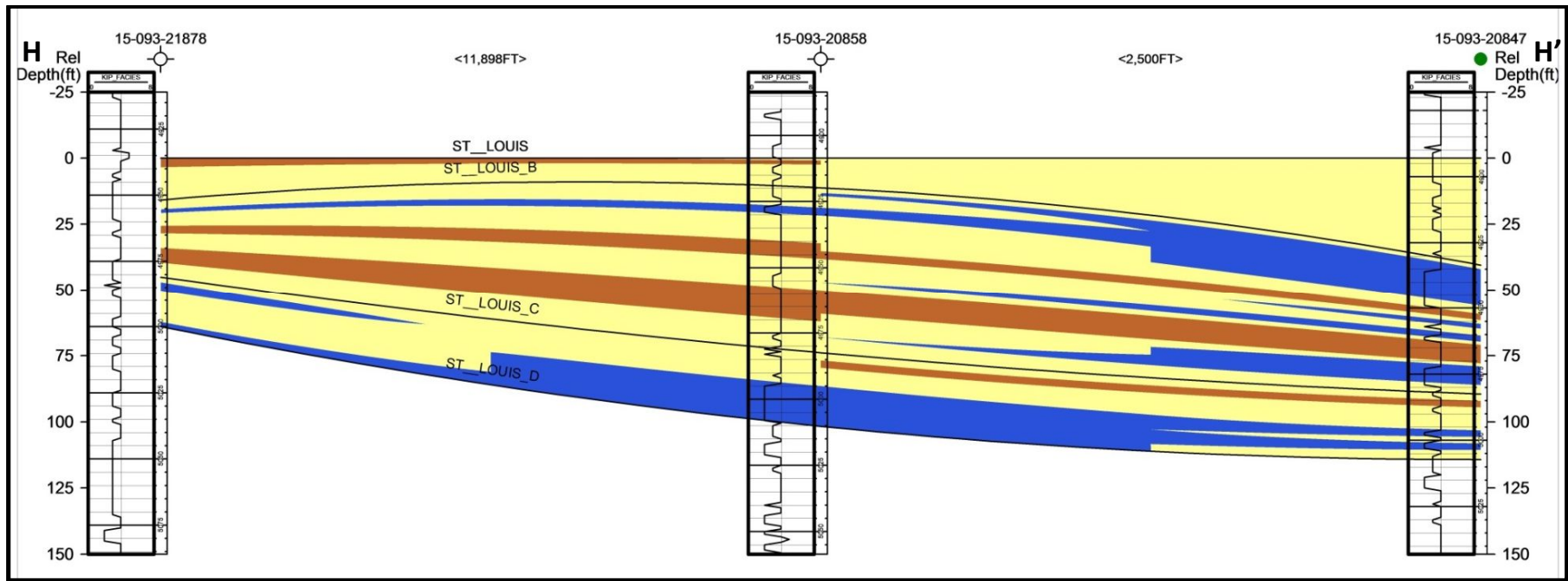


Figure 22: Cross sections of A, B, C, D, E, F, G, and H.

## **CHAPTER VII: DISCUSSION**

### **Depositional System Evaluation**

As documented across the majority of the Mid-Continent region, the Mississippian in western Kansas represents two distinct events; 1) the flooding of a craton by epicontinental shallow seas and deposition of Kinderhookian-Meramecian aged skeletal and oolitic limestone, and 2) a relative sea level fall during the Late Mississippian with associated deposition of interfingered marine and continental sediments (Handford, 1988). Sea level rise and falls throughout the Early Devonian-Late Mississippian is referred to as the Kaskaskia sequence, which is characterized as a second-order cycle, and thus is made up of numerous, third order-cycles (Handford, 1988). The St. Louis- Ste. Genevieve sequence represents a third-order cycle, with duration of less than 5 m.y., and is a result of sea level rise and fall (Handford, 1988).

Of the three cored intervals that were evaluated, the core interval from well 15-093-20147 is the only interval that was cored through the Ste. Genevieve, St. Louis, and St. Louis B and C units. For this reason, this specific interval will be the focal point of the sequence stratigraphic interpretation, as the entire upper Meramecian was available for core evaluation. Figure 22 is an image that shows the facies succession and their texture, lithology, log curve responses, and depositional environment and sequence stratigraphic interpretation.

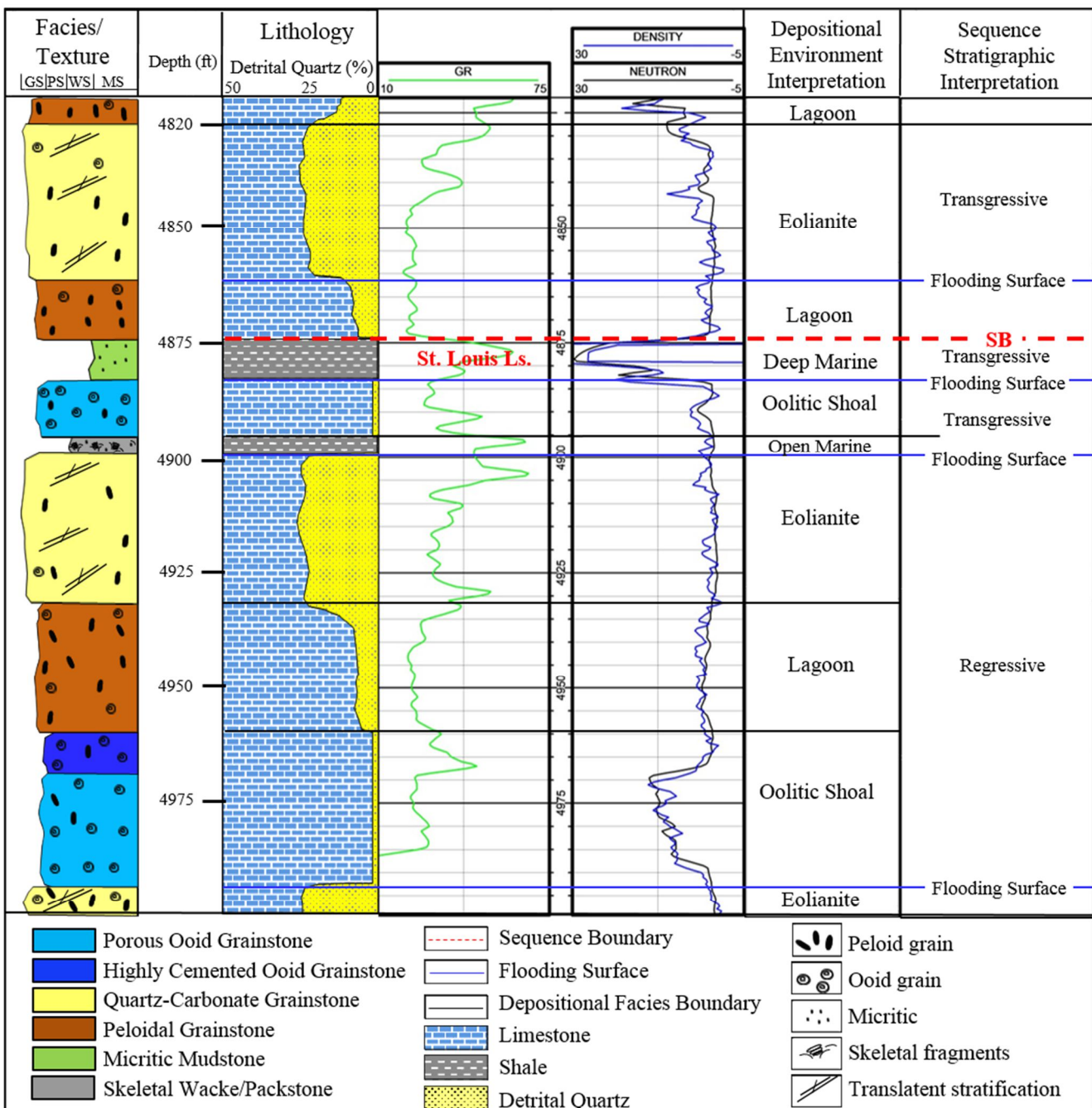
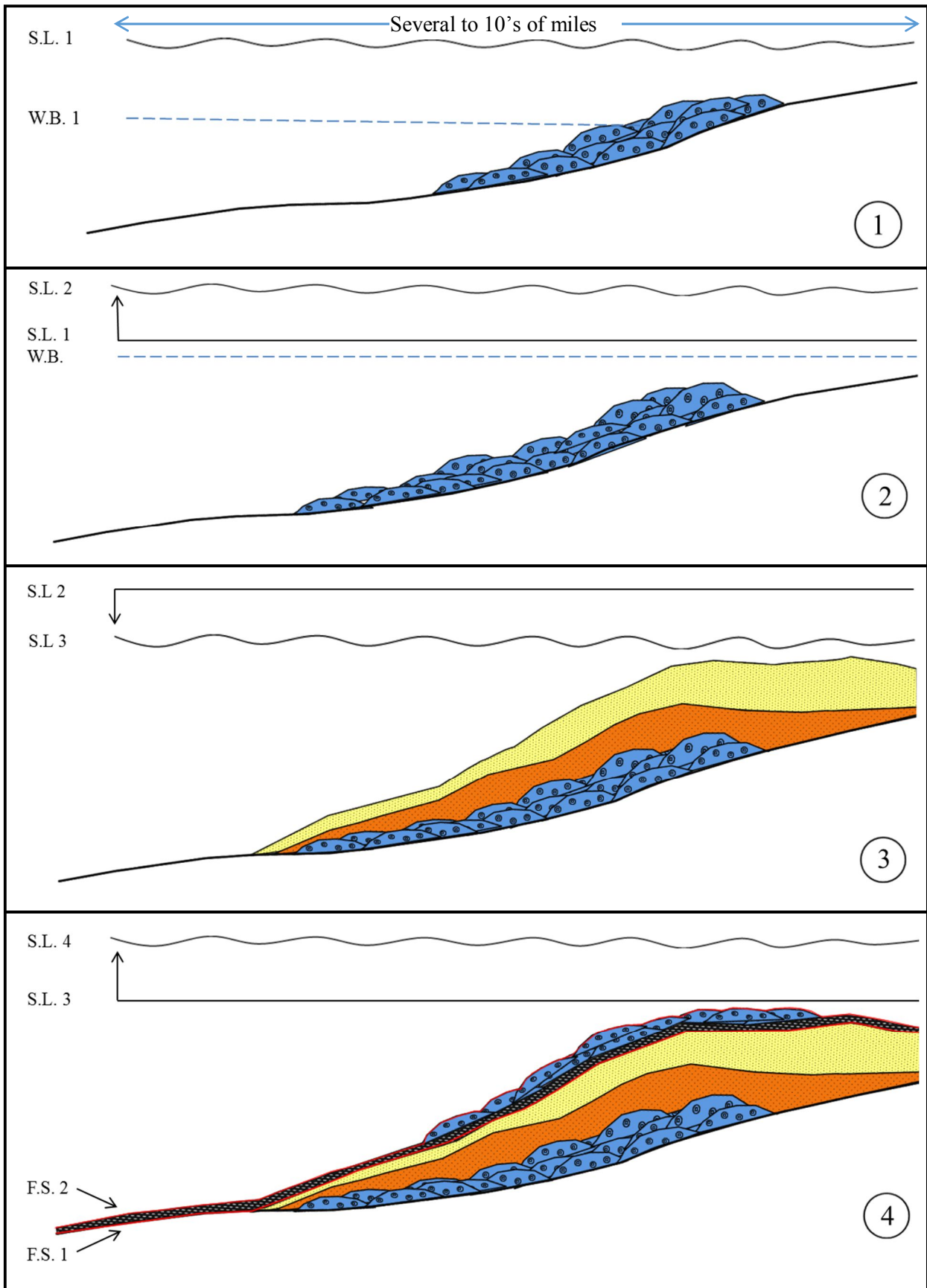


Figure 23: Facies succession and their texture, lithology, log curve responses, and depositional environment and sequence stratigraphic interpretation of the cored well, API: 15-093-20147.

The depositional history and sequence stratigraphic interpretation are shown in seven stages (Figure 24). The initial ooid shoal, within the St. Louis C zone, formed at the intersection of the wave base and the very low angle sea floor. A slight relative sea level increase caused thickening of the ooid shoal (up to 24 ft. (7 m)) until the rising sea level outpaced carbonate production and drowned the shoal. A relative sea level fall initiated the progradation of the lagoonal facies and, with continual sea level fall, further progradation of the carbonate eolianite facies. At the end of the lowstand, relative sea level rise flooded the carbonate platform, causing a landward shift of the successive parasequence, onlapping the open marine facies onto the prograded carbonate eolianite facies. The St. Louis B zone ooid shoal was deposited at the intersection of the wave base, overlying the open marine facies. Relative sea level continued to rise, thickening the St. Louis B zone shoal (up to 14 ft. (4m)), but was ultimately outpaced and drowned, and the deep marine facies onlapped the ooid shoal facies.

The deep marine facies deposit is overlain by the restricted lagoon facies. This is a significant stratigraphic relationship, as it shows a deep marine facies overlain by an intertidal-to-supratidal facies. This depositional facies relationship is indicative of a sequence boundary, where the transitional depositional facies between the deep marine facies and intertidal-to-supratidal facies, which originally overlaid the deep marine micritic mudstone, were subaerially exposed due to relative sea level fall and subsequently were eroded away. As stated, the sequence boundary is capped by a restricted lagoon, which is overlain by the coastal eolianite, which concludes the Upper Mississippian's St. Genevieve/St. Louis limestone sedimentary package.



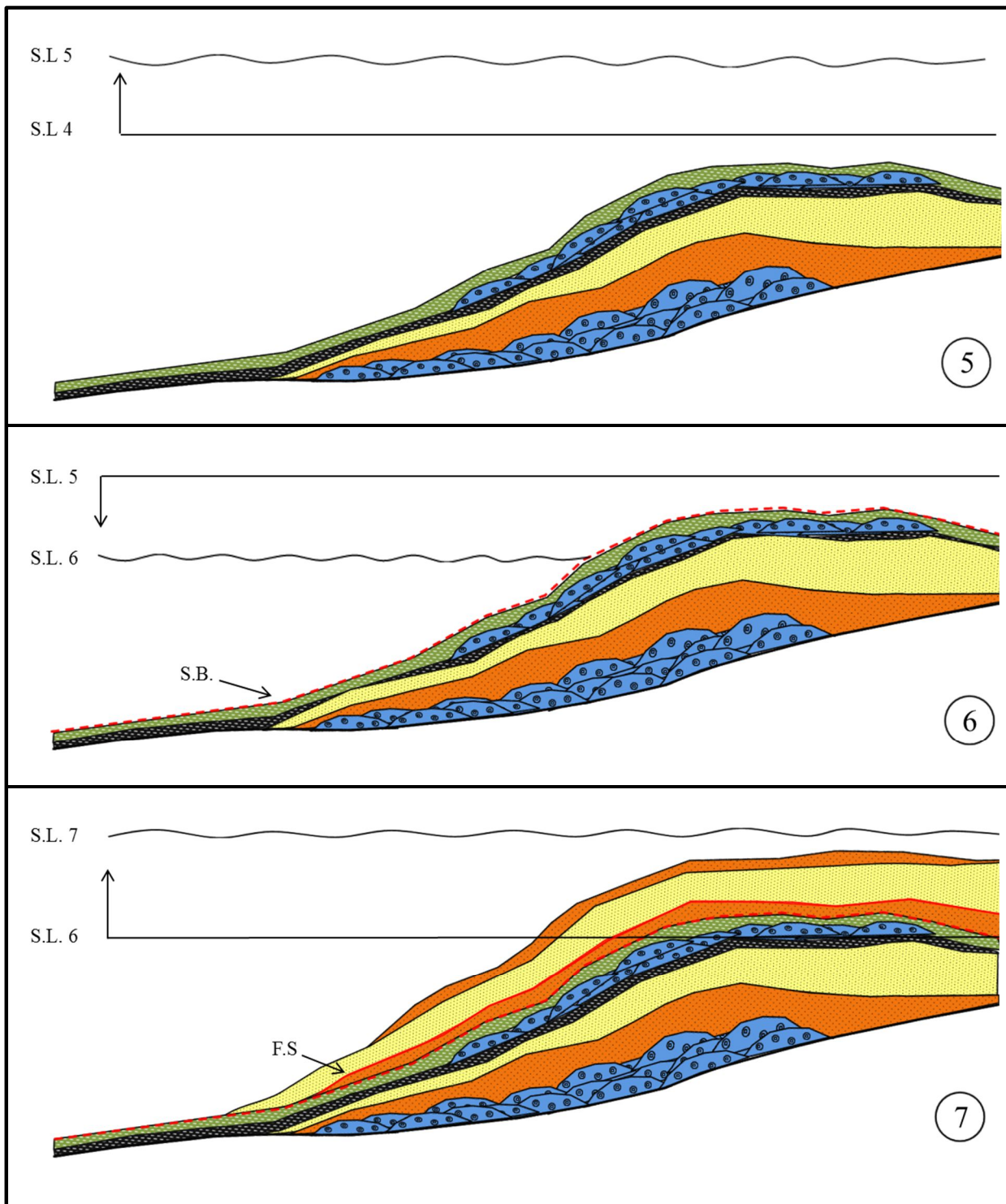


Figure 24: Seven stages of deposition as result of relative sea level rise and fall. 1) formation of an ooid shoal, 2) relative sea level rise, thickening and subsequent drowning of the ooid shoal, 3) relative sea level fall, landward facies prograde seaward, 4) relative sea level rise,

seaward facies retrograde landward, 5) continual sea level rise, deep marine facies blankets the carbonate platform, 6) relative sea level fall, erosional surface due to subaerial exposure, and 7) the carbonate platform is flooded due to a relative sea level rise and supratidal and intertidal facies are deposited.

A schematic interpretation of the environment during the deposition of the St. Louis and Ste. Genevieve limestone is illustrated in Figure 25. This depositional environment reconstruction generated was original created by Handford (1988), and was proven to be analogous within the depositional history of another St. Louis limestone study of western Kansas by Carr and Lianshuang (2003). The reconstruction of the depositional history, gathered from the evaluation of three cored intervals and geophysical well logs, concludes that this schematic interpretation is also analogous within the Kearny County study area.

The landward-most depositional environment is the coastal eolianite, which is represented by lithofacies 3 (quartz-carbonate grainstone). Moving seaward, the lagoon, represented by lithofacies 4 (peloidal grainstone), is restricted by the ooid shoal, represented by lithofacies 1 and 2 (porous and highly-cemented ooid grainstone). Further seaward from the ooid shoal, a transition into an open shelf environment, represent by lithofacies 6 (skeletal wacke/packstone) and a final transition into a relatively deep marine environment, represented lithofacies 5 (clay-rich mudstone), concludes the relative geographic position and the depositional profile of each lithofacies during the time of deposition in the Upper Mississippian.

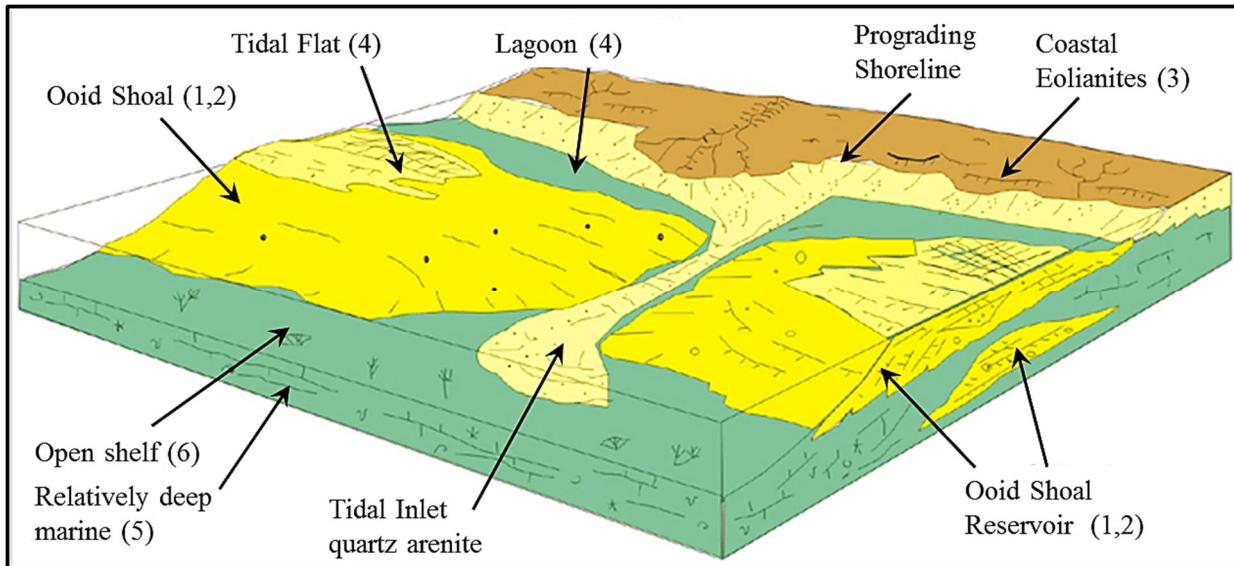


Figure 25: Illustration of the depositional environment of the Upper Mississippian. Image modified from (Qi and Carr, 2003) and (Hardford, 1988).

A cross section of this depositional interpretation (Figure 26) highlights the ooid shoal which is found in St. Louis B and C zones, and the depositional environment which surround it. The cross section illustrates the stacking pattern and typical geometric shape that the ooid shoals are notoriously characterized by highlighting that the thickest portions of the shoal, and potential hydrocarbon reservoir, is located at the apex of the shoal, and thins gradually towards its flanks.

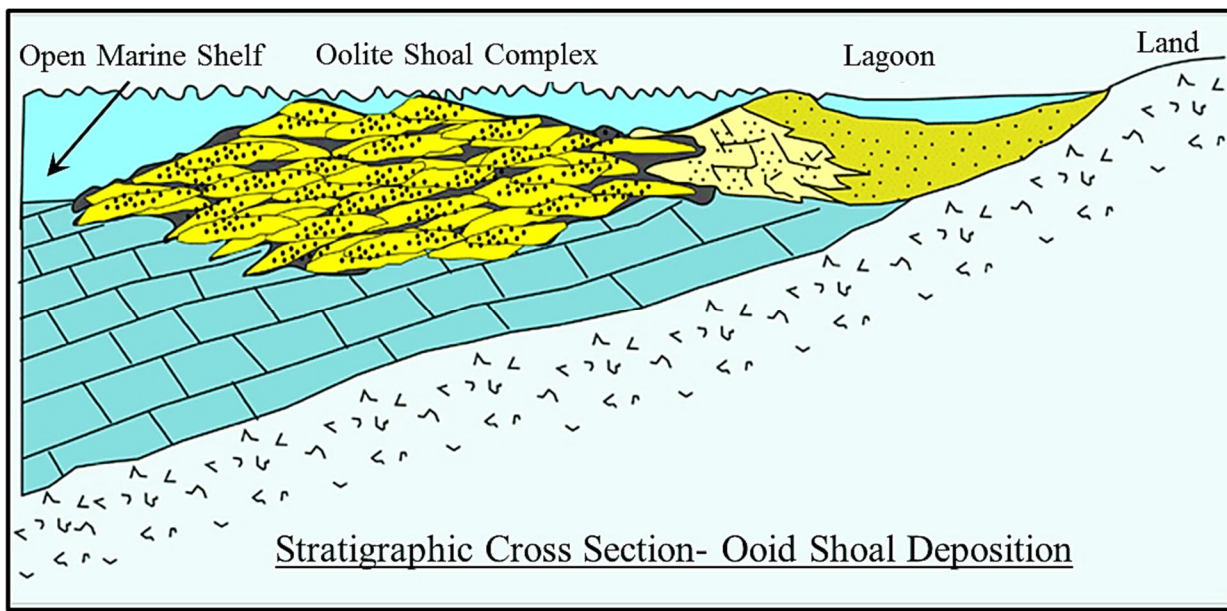


Figure 26: Illustration of a stratigraphic cross section of the ooid shoals. Image modified from Qi and Carr (2003) and Hardford (1988).

### Geologic Controls on Production

All oil production from the Mississippian Limestone within Lakin field is extracted from the St. Louis C pay zone, which is the porous ooid grainstone facies. Reports on production from this pay zone in Lakin field totals over 1.83 million barrels. Production in barrels is posted over each St. Louis C pay zone producing wells in Figure 26. Figure 26 is an isopach map of the porous ooid grainstone from the St. Louis C pay zone. As seen in Figure 26, the thickest portion of the isopach map is conversely related to higher production values. Conversely, as the pay zone thins, cumulative production values diminish. Within the thickest portions of the isopach map, the highest cumulative production values are recorded (412,267 & 345,589 mbl), although significantly smaller values (81,064 & 94,892 mbl) can be seen in the thickest area of the pay zone as well. This is a common occurrence and numerous factors can attribute to this. One conclusion for production variability in an area of the same pay zone

thickness could have to do with which well was completed first. The wells with the highest cumulative production were most likely drilled first, and the remaining wells were drilled after proven production as offset wells. If the wells with higher production were drilled second, it could be due to bad well placement of the original well. The first well drilled could have missed the structural high, hindering the ability to drain any oil that is further up dip. The second well drilled (higher production values) may have been placed further up dip at the apex of the structural high, which would explain higher production values. In this specific situation, the date of the well completion was responsible for production variation. The reservoir had been depleted, or “played out”. This can be expressed by correlating production with the completion year:

<b>Oil Production in barrels</b>	<b>Completion year</b>
412,267	1975
350,399	1975
345,589	1978
94,892	1978
81,064	1978

Directly to the west of Lake NW field, eight dry holes and two gas wells were drilled. These ten wells are located on the west flank of the ooid shoal (Figure 27), where the pay zone thins out to less than six feet. Kearny County’s ooid shoal is naturally a lenticular, elongate body, with the thickest portions being towards the middle of the shoal. Poor placement of eight wells along the western flank of the ooid shoal body resulted in eight dry holes.

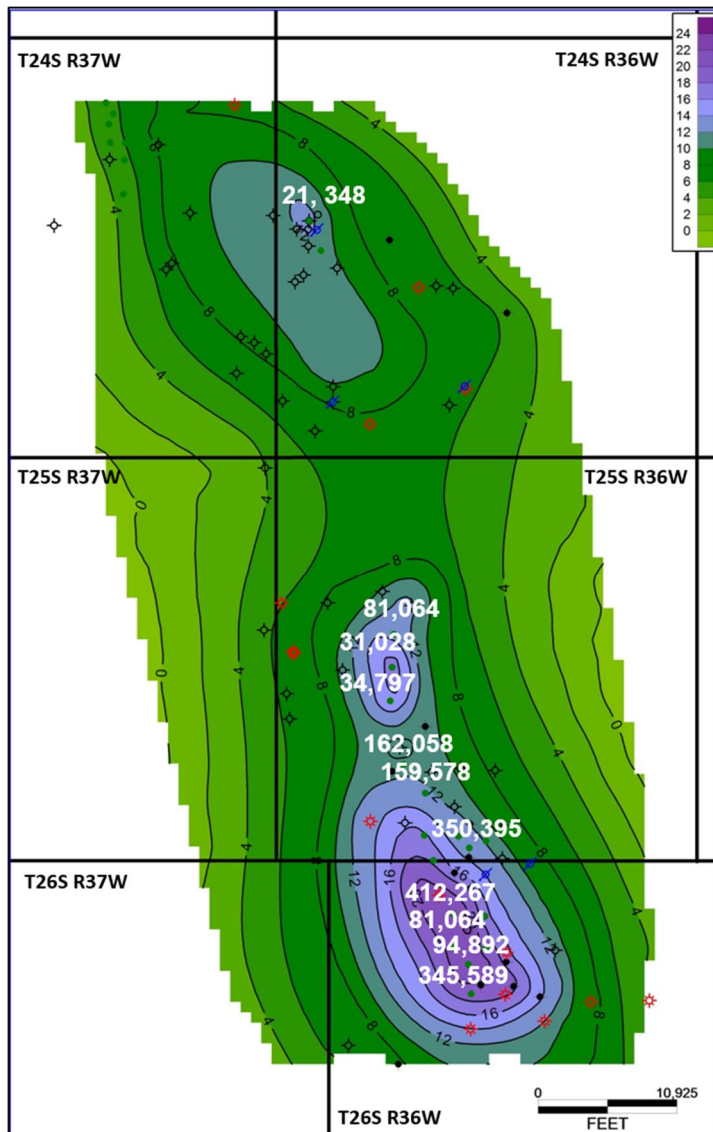


Figure 27: Isopach of the ooid grainstone facies within the St. Louis C zone with production data from this zone posted.

Moving further north, between Lakin NW field to Moser field, 2.9 mi (4.7 km), no wells were drilled deeper than 4,000 feet, ruling out the Mississippian Limestone as a target. With very limited well control across this section, it is difficult to determine lithofacies presence, thickness, and continuity. As seen in the structural map in Figure 28, the unit correlations shows a slight down-dip trend across the section with no evidence of closure. As

shown in the isopach map in Figure 27, starting from Lakin NW and moving towards Moser field, the pay zone gradually thins out to the north to less than six feet. The large area between the two fields has not been drilled because 1) traveling from south to north it is structurally down dip, 2) there is no apparent structural closure of the down dip trend, and 3) the pay zone thins to less than 6 feet across this large area. With these key factors, past exploration geologists may have been discouraged from drilling in this area, although, without further well control, it is difficult to make an interpretation.

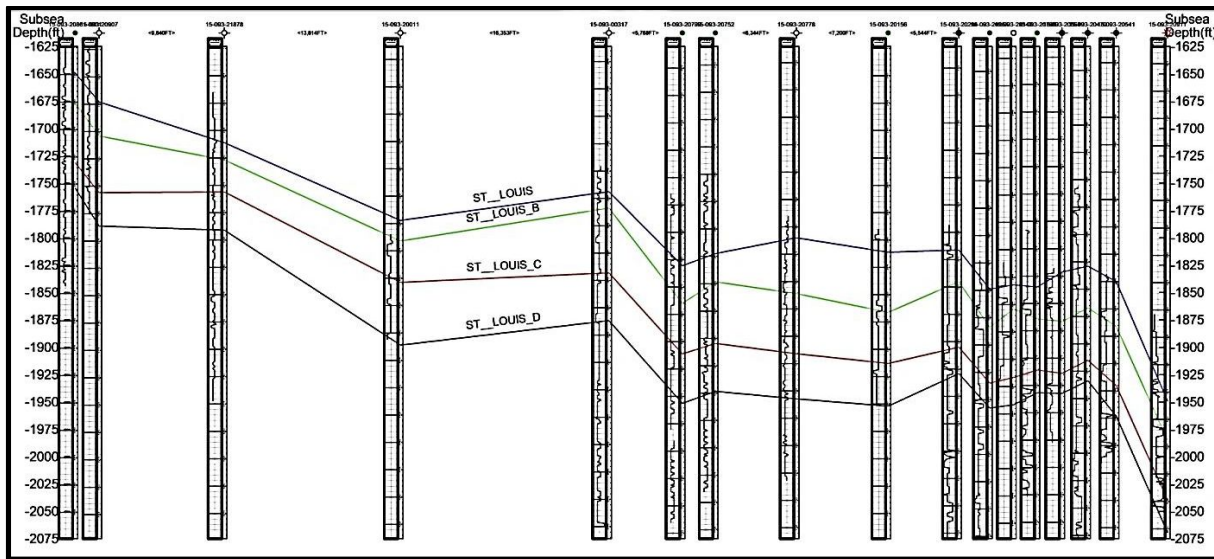


Figure 28: Structural map throughout the entire study area. The boreholes are plotted with a relative to the wells XY or geographic location.

In comparison to the Lakin Field, the Hartland Field, at the very northwest side of the study area (Figure 2), is a prolific oil producing field, with a cumulative production of over 1.3 million barrels. However, the Mississippian is not a producing formation within this field, and other formations such as the Marmaton Group, Upper Kearny County Member, Kansas City Group serve as the chief producing intervals in Hartland field. Structurally, Hartland

Field is significantly higher than Moser and Lakin NW, Lakin, and Lakin S Fields. Being structurally up dip, it is probable that hydrocarbons migrated through the southern fields into Hartland field. As shown previously, the production from the Lakin Fields is predominately from the St. Louis C pay zone. Although local structural highs definitely played a role in high production values, the Lakin Fields are mainly composed of stratigraphic traps. Comparing Lakin Fields with Hartland field, production in the latter comes from many sources (i.e. Marmaton Group, Upper Kearny County Member, Kansas City Group). Being structurally up dip and having various units producing hydrocarbons, Hartland field is interpreted as being composed of structural traps.

As previously illustrated in various forms, the St. Louis C zone has been the targeted pay zone within the study area. Lakin field has been a great oil producing field, although toward the north/northwest , dry holes become more frequent, which can be illustrated in the isopach map in Figure 27. South of Lakin NW field, excluding “unknown” wells, 76.7% of wells drills produced economic quantities of hydrocarbons, while north of Lakin NW field success rate averages only 21.7%. Referring back to the isopach map of the St. Louis C zone, significant thinning takes place from south to north. In the heart of Lakin field, the St. Louis C zone reaches a thickness of 20 feet. North of the Lakin field, gradual thinning begins, resulting in a thickness of 6 ft. or less in the northernmost portion of the study area. The thinning of the pay zone contributed heavily to the decrease in drilling frequency and the increase in dry holes drilled. Another key factor is diagenetic alterations, mainly the infilling of pores with calcite cement. As stated previously, three cored intervals were evaluated within the south, south central, and north portions of the study area. The southernmost and south central core intervals had great porosity shows within the St. Louis C zone. Within the

northernmost core interval, porosity was significantly reduced by the infilling of calcite cement. Two chief factors that contributed significantly to lower success of producing hydrocarbons north of Lakin NW field include: 1) significant thinning of the St. Louis C zone (pay zone), 2) increase in diagenetic alteration (the infilling of pores with calcite cement), and 3) not being located on a structural high and having little structural closer (Hartland field is structurally higher and has produced over 1.3 million barrels of oil).

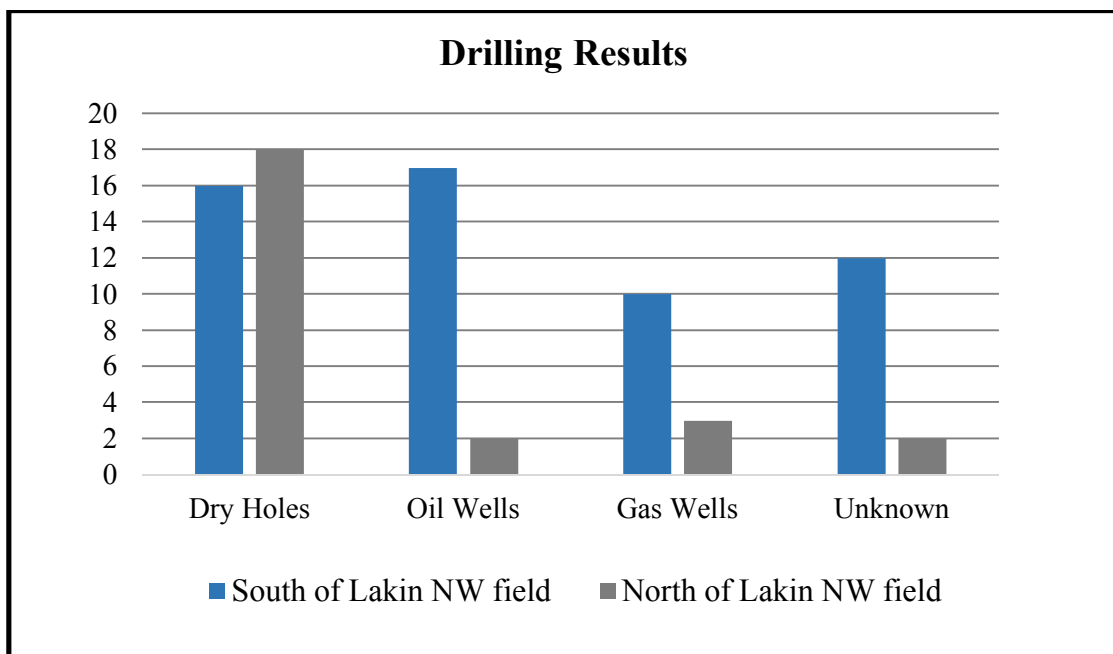


Figure 29: Bar graph which illustrates the drilling results south of Lakin NW field (27.1% success rate) and north of Lake NW field (76.7% success rate) showing the number of dry holes, oil wells, gas wells, and unknown per geographic location.

### **Reservoir Considerations**

Future exploration for ooid shoal reservoirs within Kearny County and other western Kansas counties may prove to be difficult as many fields in this region have been located and “played out”. The limited areal extent and outstretched, lenticular shape of the ooid shoal

complexes within St. Louis B and C zone also places difficulty on predicting new areas of exploration. With ooid shoal reservoir thickness only recording 24 feet at it thickest, the ooid shoals are too thin and lack sufficient velocity contrast for direct seismic mapping (Parkham and Sutterlin, 1993). While there are difficulties when exploring these complexes, positive findings for exploration have been gained through this study, which include the following; 1) all known hydrocarbon-bearing shoals in Kearny County are NW-SE trending, 2) their vertical extent covers up to 16 miles, with economically viable patches covering up to 8 miles in length, with roughly 2 miles of width, 3) the thickest and best reservoir quality is along the center of the shoal, with reservoir quality diminishing along the margins, and 4) the shoal complexes form along the depositional strike of the low angle ramp.

### **Future Study**

For further study, examination of cuttings from wells of the 30 wells that lithofacies were predicted on with the neural networks. A study of this sort would illustrate the accuracy of the predictions outside of the three main study wells. Once the neural network predictions are tested through well cuttings analysis, a 3D geostatistical analysis could be conducted within Petra. For further detail over this process, view the AAPG publication by Lianshuang et al. (2003), “Carbonate Lithofacies Prediction Using Neural Network and Geostatistical 3-D Modeling of Oolite Shoals, St. Louis Limestone, Southwest Kansas”.

Although seismic data have not been reported in the Kearny County study area, future prospecting by oil and gas companies may result in 2D-3D seismic shoots. Conducting a seismic attributes study would contribute significantly to tracking the lateral facies distributions, and could also be compared with the 30 wells of this study for which there are predicted lithofacies. In any other area with available core and reasonable well control, the

workflow from this study could be followed to unlock information on the internal framework of any prospective area.

## CHAPTER IX: CONCLUSION

This study increases the understanding of the internal complexity of the Ste. Genevieve and St. Louis limestone in Kearny County, Kansas, through detailed analysis of three core intervals to determine facies successions, lateral distributions, and continuity. Investigating reservoir quality and potential per lithofacies and analyzing their predictability was concluded by integrating depositional facies and sequence stratigraphy to characterize reservoir potential within the study area. Collectively, this multifaceted study concludes the following:

1. Between the Ste. Genevieve and St. Louis limestone, six lithofacies were identified in the three cored intervals: 1) Lithofacies 1- Porous Ooid Grainstone, 2) Lithofacies 2 - Highly-Cemented Ooid Grainstone, 3) Lithofacies 3 - Quartz-Carbonate Grainstone, 4) Lithofacies 4 - Peloidal Grainstone, 5) Lithofacices 5- Micritic Mudstone, and 6) Lithofacies 6- Skeletal Wackestone/Packstone.
2. The following depositional environments were interpreted from core evaluation and thin section analysis: 1) Lithofacies 1 & 2 – high energy ooid shoal, 2) Lithofacies 3 – Eolianite, 3) Lithofacies 4 – Back barrier restricted lagoon, 4) Lithofacies 5 – Deep marine, and 5) Lithofacies 6 – Open marine.
3. Lithofacies 1 is the only reservoir quality facies, with porosity values up to 16%. The porous ooid grainstone occurs in St. Louis B (up to 10 ft) and C zone (up to 24 ft). The ooid shoal deposits are very difficult to predict, and porosity is often reduced through diagenesis, where calcite cement infills the pore space. The apex

of the shoal contains the highest porosity values, while the back shoal (landward) porosity is of good quality as well. Porosity quality diminished on the foreshoal (seaward) and collectively porosity diminished the further away it is from the apex of the shoal.

- a. Within the St. Louis C zone, the porous ooid grainstone (ooid shoal) is the pay zone within the study area. St. Louis B zone is the chief producer in other counties of western Kansas, but was found to be very thin <10 feet, absent, or highly cemented in this locality.
4. The southeastern side of the study area has achieved the highest hydrocarbon production, producing chiefly out of the porous ooid grainstone in the St. Louis C zone. The following contribute to the success of hydrocarbon production on the southeastern side of the study: 1) the ooid shoal (pay zone) is at its thickest, up to 28 feet, 2) porosity values are high, between 12-18 percent, and 3) local structural highs allows for a combination trap, containing both structure and stratigraphic traps.
5. Predicting ooid shoal subsurface location and geometry is difficult. During exploration, even if an ooid shoal was located in the subsurface, the porosity variability from diagenetic alterations would remain an unknown, and could lead to drilling a dry hole.
6. Using facies prediction software, Kipling2.xla (neural network analysis tool), can provide vital information on the presence of lithofacies in large areas without available core. The proximity of a well to which the neural network model has been applied is key. The further away a well is from wells used to create the neural

network model leads to greater uncertainty in predictions, due to subtle lithofacies changes. More neural network models (more wells with core intervals and the necessary log curves) within close proximity to the wells that the model is applied to, the more effective and accurate the prediction.

7. The use of wire-line log signatures within the St. Louis limestone:
  - a. Lithofacies log signatures were difficult to differentiate, as different lithofacies gave very similar wire-line log readings, especially in the case of Lithofacies 3 and 4, which exhibits a gradational variation. Favorably, the porous ooid grainstone or the “pay zone” gives a distinctive signature, as the neutron/density values increase significantly in its presence.
  - b. The St. Louis sequence boundary can be tracked throughout the study area via log curves, although, other significant sequence stratigraphy surfaces are difficult to correlate. As Carr and Lundgren (2009) found, gamma ray spectral logs can be used to recognize exposure surfaces at reservoir scale within the St. Louis limestone of western Kansas. Gamma ray spectral logs were not available, complicating the correlation of significant surfaces in wells that did not have core available for evaluation.

## REFERENCES

- Ahr, W. M., 1973, The carbonate ramp: an alternative to the shelf model: Gulf Coast Association Geological Societies Transactions, v. 23, p. 221-225.
- Bohling, G., June 2007, Technology to Manage Large Digital Datasets,  
[http://www.kgs.ku.edu/PRS/publication/2007/OFR07\\_06/KGS\\_2007-06-5\\_Chapter05\\_Technology.pdf](http://www.kgs.ku.edu/PRS/publication/2007/OFR07_06/KGS_2007-06-5_Chapter05_Technology.pdf)
- Bohling, G., May 2001, An Excel Add-in for Nonparametric Regression and Classification,  
<http://www.kgs.ku.edu/software/Kipling/Theory.html>
- Burchete, T.P., Wright, V.P., 1992. Carbonate ramp depositional systems. *Sedimentary Geology*, 79, 3-57.
- Cluff, R. M., 1984, Carbonate sand shoals in the Middle Mississippian (Valmeyeran) Salem-St.Louis-Ste. Genevieve Limestones, Illinois basin; in, Carbonate Sands--A Core Workshop, P. M. Harris, ed.: Soc. of Economic Paleontologists and Mineralogists, Core Workshop No. 5, p. 94-135
- Cross, E., 2014, The Mississippian Lime: Not New, But Reinvented,  
<http://oilindependents.org/the-mississippian-lime-not-new-but-reinvented/>
- Enos, P. (1983). Shelf. In Carbonate depositional environments (pp. 267-296). Tulsa, Okla., U.S.A.: American Association of Petroleum Geologists.
- Enos, P., 1977, Holocene Sediment accumulations of the south Florida shelf margin, in P. Enos and R.D. Perkins, eds., Quaternary sedimentation in south Florida: Geol. Soc. American Mem. 147, pt. I, p. 1-130.
- Esan, A. O., 2002. "High resolution sequence stratigraphic and reservoir characterization studies of D-07, D-08 and E-01 sands, Block 2 Meren Field, Offshore, Niger Delta",

Publ. M.S. Geology Thesis, Texas A & M University, Texas, USA, 115 pp.

Evans, P.S., Newell, K.D., March 2013, The Mississippian Limestone Play in Kansas: Oil and Gas in a Complex Geologic Setting,  
<http://www.kgs.ku.edu/Publications/PIC/pic33.html>

Fairbridge, R.W., Johnson D.L., 1978 Eolianite in Fairbridge R W and Bourgeois J., eds., The Encyclopedia of Sedimentology Stroudsburg Pennsylvania, Dowden, Hutchinson & Ross, p. 279-282

Goebel, E.D., December 1968, Stratigraphic Succession in Kansas: Mississippian System,  
[http://www.kgs.ku.edu/Publications/Bulletins/189/06\\_miss.html](http://www.kgs.ku.edu/Publications/Bulletins/189/06_miss.html)

Handford, C.R., 1988, Review of carbonate sand-belt deposition of ooid grainstones and application to Mississippian reservoir, Damme Field, southwestern Kansas: American Association of Petroleum Geologists Bulletin, v. 72, p. 1184-1199.  
Kansas Geologic Survey, May 2014, Kearny County—Oil and Gas Production,  
<http://www.kgs.ku.edu/PRS/County/klm/kearny.html>

Kansas Independent Oil & Gas Association, January 2014, Mississippian Lime Play in Kansas: Not New- Reinvented, <http://www.kioga.org/communications/reports/mississippian-lime-play-in-kansas/view>

Lane, H.R., and T.L. De Keyser, 1980, Paleogeography of the late Early Mississippian (Tournaisian 3) in the central and south-western United States, in T.D. Fouch and E.R. Magathan, eds., Paleozoic Paleogeography of west-central United States: Rocky Mountain Section SEPM, p.149-159.

Lianshuang, Q., Carr, T.R., Goldstein, R.H., December 2004, Carbonate Lithofacies Prediction Using Neural Network and Geostatistical 3-D Modeling of Oolite Shoals, St. Louis Limestone, Southwest Kansas, <http://www.kgs.ku.edu/PRS/publication/2004>

Lianshuang, Q., T.R. Carr., May 2003, Reservoir Characterization of Mississippian St. Louis Carbonate Reservoir Systems in Kansas, Stratigraphic Architecture Modeling,  
<http://www.kgs.ku.edu/PRS/publication/2003/ofr2003-27/index.html>

McKee, D., Ward, W. C., 1983, Eolian environment, in Scholle, P. A., Bebout, D. G., and Moore, C. H., eds., Carbonate Depositional Environments: American Association of Petroleum Geologists Memoir 33, p. 132-170.

Montgomery, S., Frans, E. (2000). Schaben Field, Kansas: Improving Performance in a Mississippian Shallow-Shelf Carbonate (E&P Notes). AAPG Bulletin, 84(8), 1069-1086.

Parham, K.D., and Sutterlin, P.G., 1993, Oolite shoals of the Mississippian St. Louis Formation, Gray County, Kansas; a guide for oil and gas exploration, in Keith, B.D., and Zuppann, C.W., eds., Mississippian oolites and modern analogs: American Association of Petroleum Geologists, Studies in Geology, no. 35, p. 185-197

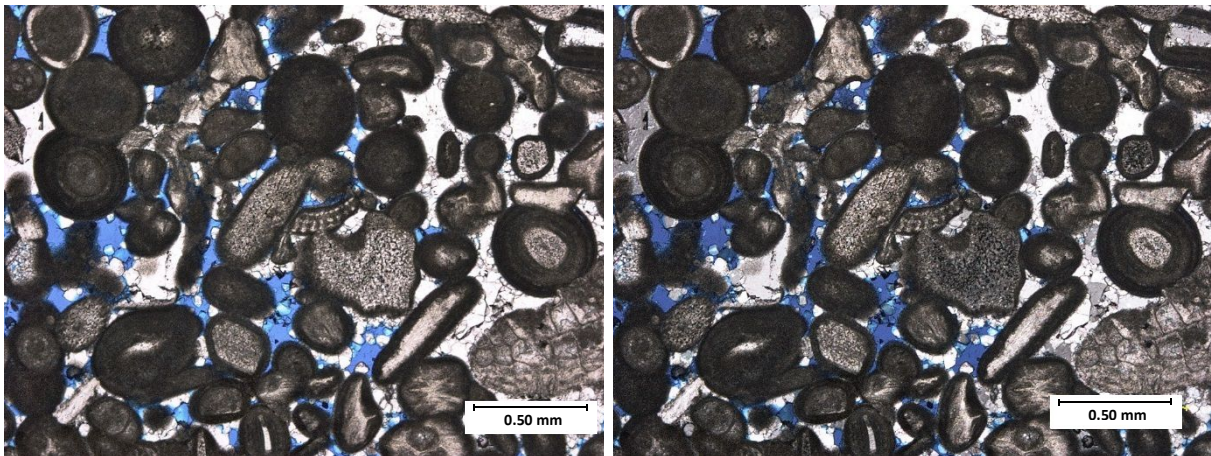
Read, J. F., 1981, Carbonate platforms of passive (extensional) continental margins: types, characteristics and evolution: Tectonophysics, v. 81, p. 195-212.

Scholle, Peter A., Don G. Bebout, and Clyde H. Moore, eds. 1983. AAPG Memoir. Vol. 33, Carbonate Depositional Environments. Tulsa, Okla., U.S.A.: American Association of Petroleum Geologists.

Watney, W.L., E.K. Franseen, J.H. Doveton, T.L. Thompson, D.R. Boardman, E.T. Rasbury, K.D. Newell, J. Victorine, N.H. Suneson, and E. Starbuck, 2008, High-resolution sequence stratigraphic and chronostratigraphic investigations of the lower shelf and basin lithofacies of the Mississippian subsystem in the southern Midcontinent U.S.A.: AAPG National Meeting, San Antonio, TX.

Workman, S.J., 2013. "Integrating Depositional Facies and Sequence Stratigraphy in Characterizing Unconventional Reservoirs: Eagle Ford Shale, South Texas", Publ. M.S. Geology Thesis, Western Michigan University, Michigan, USA, 148 pp.

## APPENDIX A



Well API: 15-093-20147

Depth: 4987 ft.

Lithofacies: Porous ooid grainstone

Depositional Environment: Ooid shoal

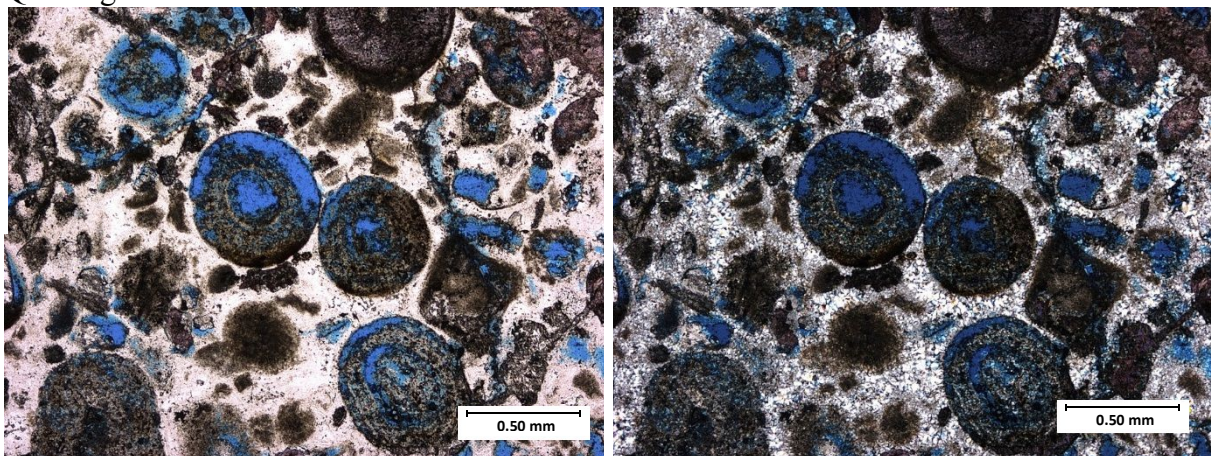
Primary Porosity Type: Interparticle

Porosity %: 11

Cement: Equant calcite cement

Primary Constituents: Ooids, echinoderms

Quartz grain %: -



Well API: 15-093-20147

Depth: 4966 ft.

Lithofacies: porous ooid grainstone

Depositional Environment: Ooid shoal

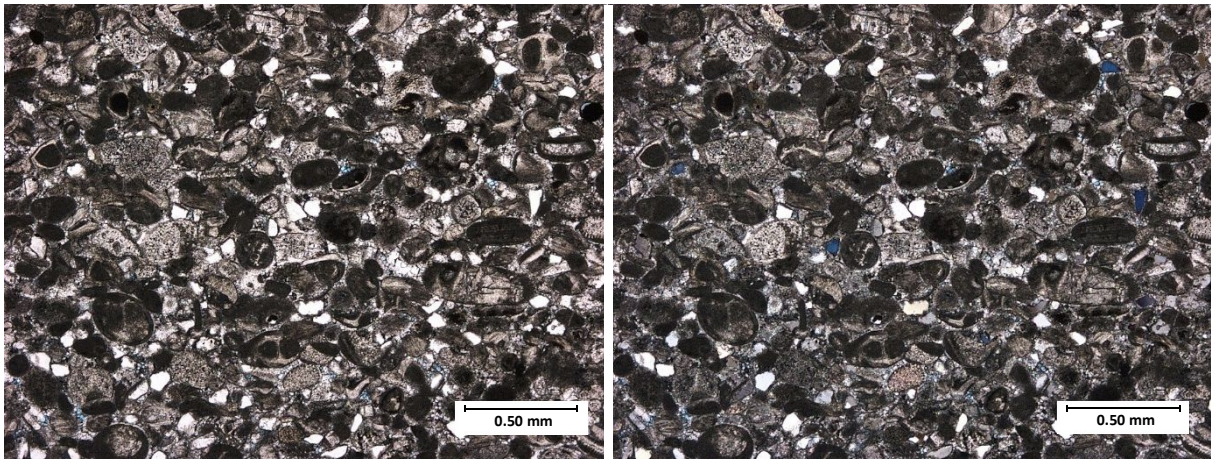
Primary Porosity Type: oomoldic, intraparticle

Porosity %: 5

Cement: equant calcite cement

Primary Constituents: ooid, peloids

Quartz %: 1



Well API: 15-093-20147

Depth: 4954 ft.

Lithofacies: Peloid-rich grainstone

Depositional Environment: Lagoon

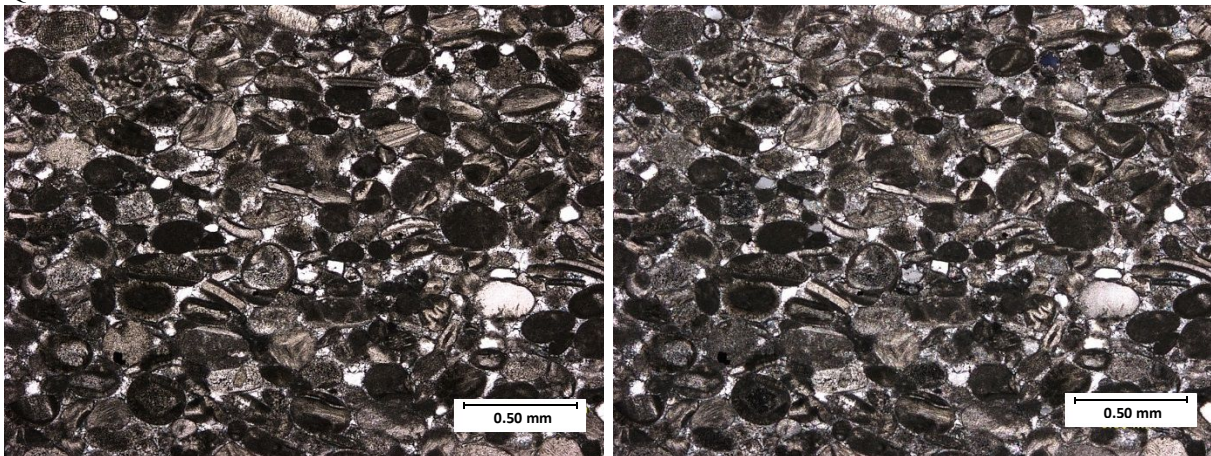
Primary Porosity Type: -

Porosity %: -

Cement: calcite

Primary Constituents: Peloids, quartz grains

Quartz %: 6



Well API: 15-093-20147

Depth: 4939 ft.

Lithofacies: Peloid-rich grainstone

Depositional Environment: Lagoon

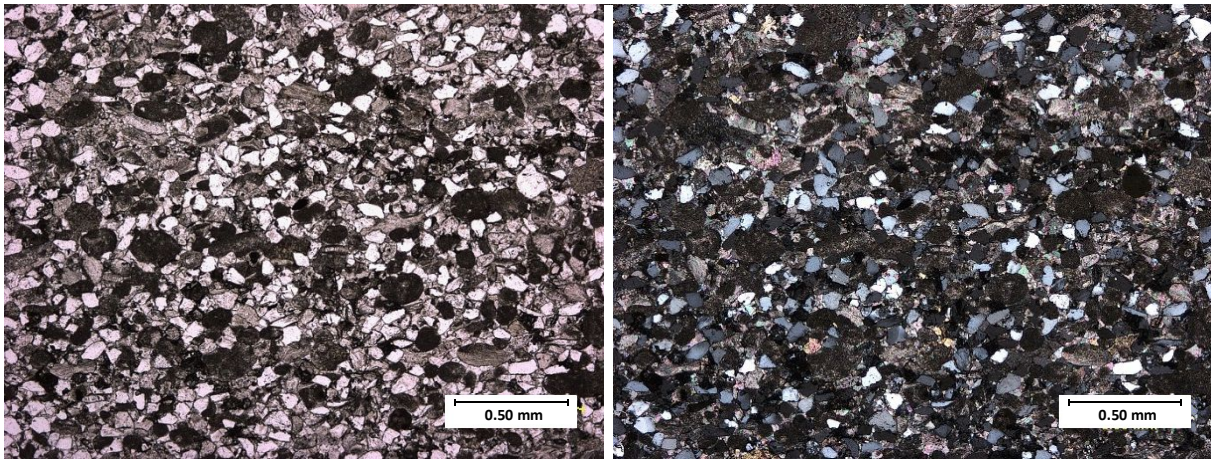
Primary Porosity Type: -

Porosity %: -

Cement: calcite

Primary Constituents: Peloids, ooids, quartz grains

Quartz %: 5



Well API: 15-093-20147

Depth: 4932 ft.

Lithofacies: Quartz-carbonate grainstone

Depositional Environment: Carbonate Eolianite

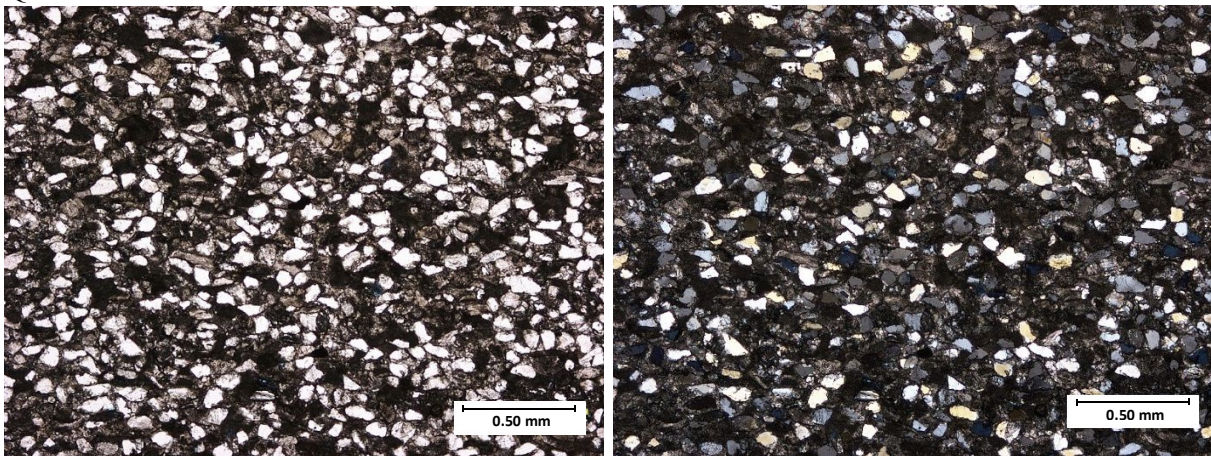
Primary Porosity Type: -

Porosity %: -

Cement: calcite, micrite

Primary Constituents: Quartz, peloids

Quartz %: 21



Well API: 15-093-20147

Depth: 4923 ft.

Lithofacies: Quartz-carbonate grainstone

Depositional Environment: Carbonate Eolianite

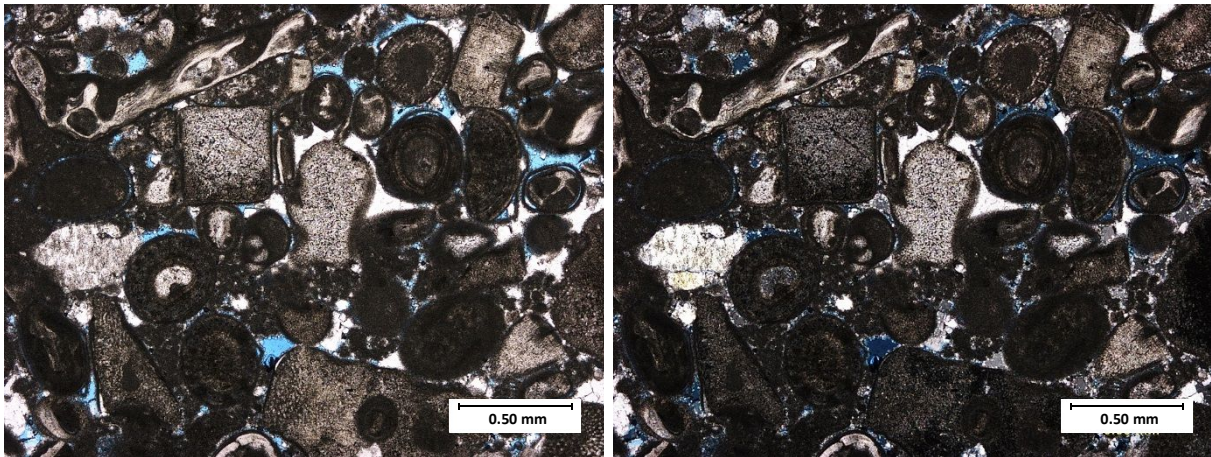
Primary Porosity Type: -

Porosity %: -

Cement: calcite, micrite

Primary Constituents: Quartz, peloids

Quartz %: 23



Well API: 15-093-20147

Depth: 4894 ft.

Lithofacies: Porous ooid grainstone

Depositional Environment: Ooid shoal

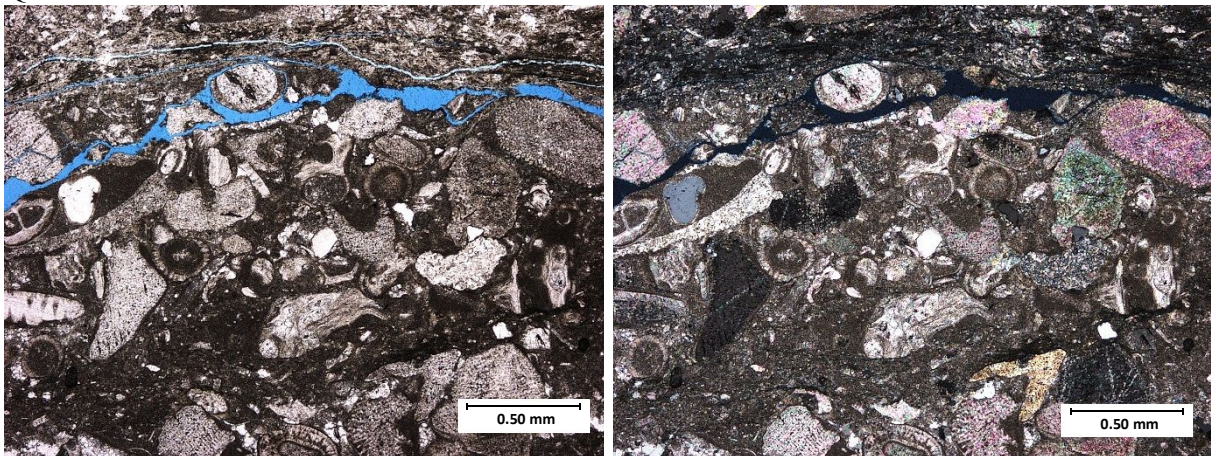
Primary Porosity Type: interparticle

Porosity %: 5

Cement: equant to blocky calcite

Primary Constituents: ooids, large echinoderms (~1.5mm), peloids

Quartz %: <1



Well API: 15-093-20147

Depth: 4886 ft.

Lithofacies: Skeletal wackestone/packstone

Depositional Environment: Open marine

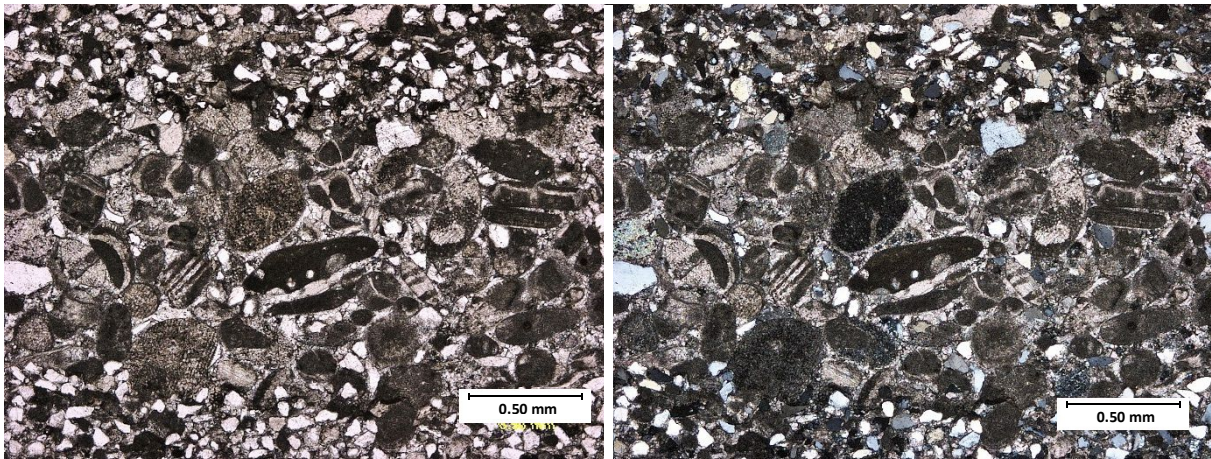
Primary Porosity Type: channel, fracture (?)

Porosity %: <2

Cement: micritic

Primary Constituents: fossil rich, echinoderms, ostracods, gastropods, crinoid stems

Quartz %: <1



Well API: 15-093-20147

Depth: 4861 ft.

Lithofacies: Quartz-carbonate grainstone (gradational- peloid-rich grainstone)

Depositional Environment: Carbonate Eolianite

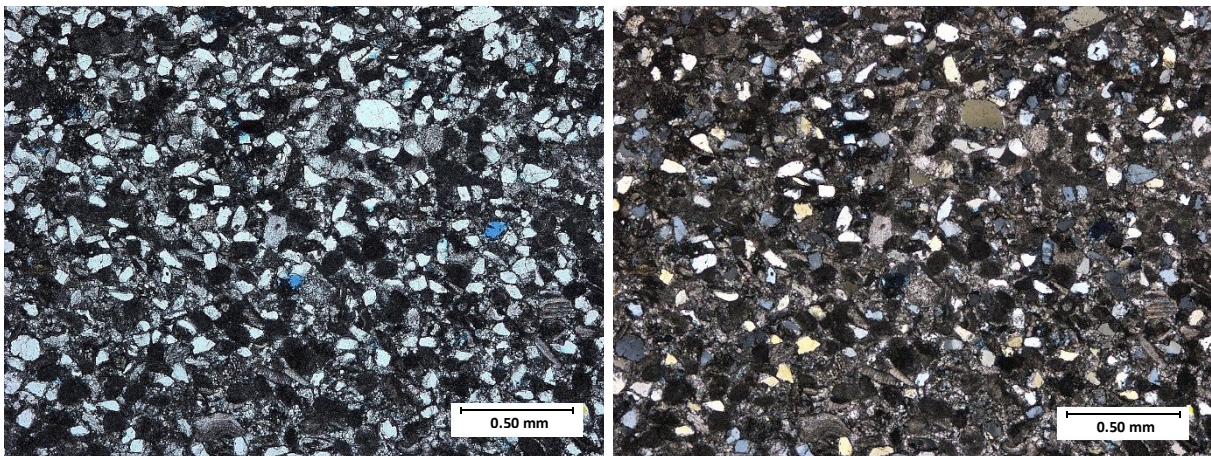
Primary Porosity Type: -

Porosity %: -

Cement: calcite

Primary Constituents: quartz, peloids, very low fossil content

Quartz % (whole-rock volume): 14, numerous 0.4mm quartz laminations



Well API: 15-093-20147

Depth: 4853 ft.

Lithofacies: Quartz-carbonate grainstone

Depositional Environment: Carbonate Eolianite

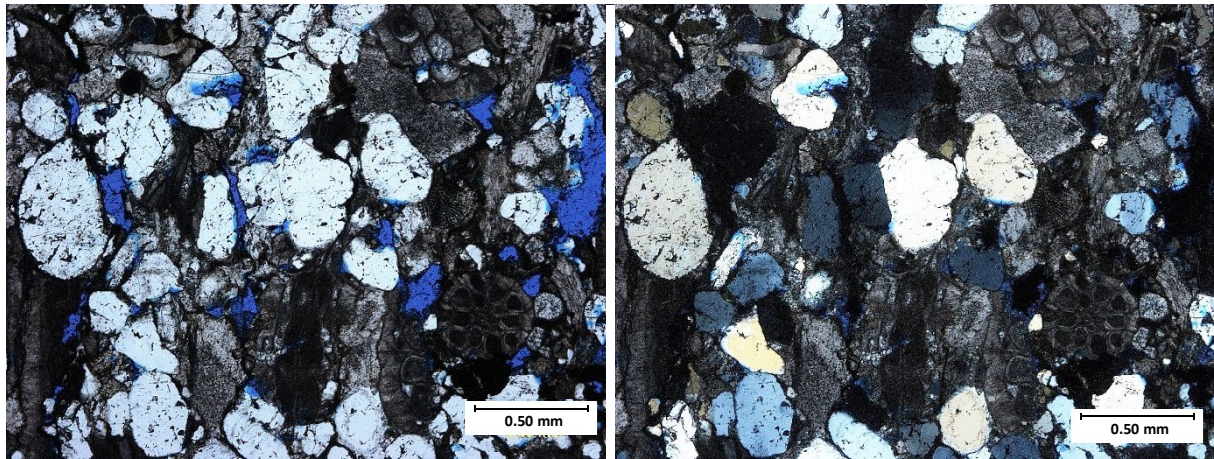
Primary Porosity Type: -

Porosity %: -

Cement: equant calcite cement

Primary Constituents: quartz grains, peloids

Quartz % (whole-rock volume): 23



Well API: 15-093-20147

Depth: 4846 ft.

Lithofacies: Quartz-rich grainstone

Depositional Environment: -

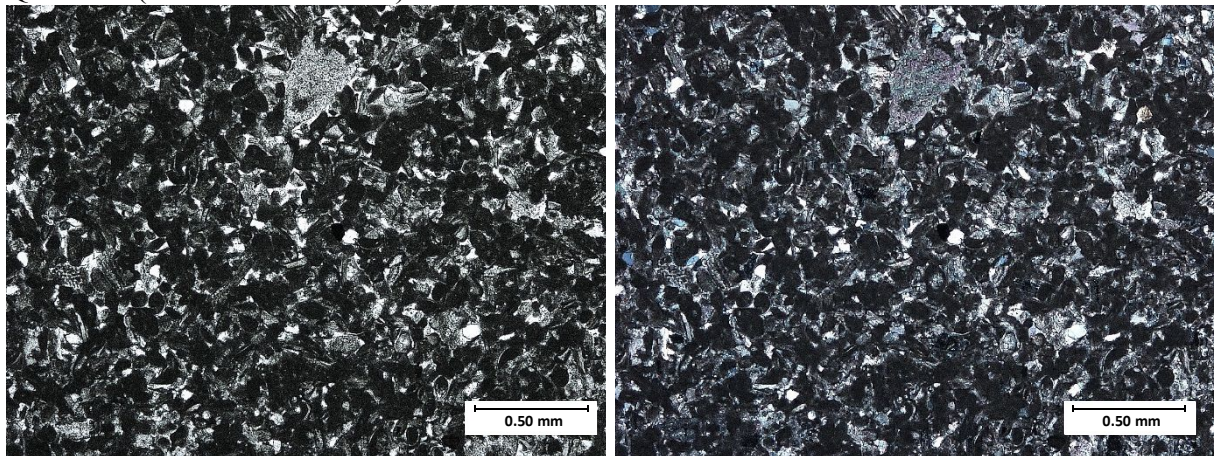
Primary Porosity Type: interparticle

Cement: block calcite

Primary Constituents: large quartz grains (0.6 mm), echinoderm, crinoid stem, brachiopod

Porosity %: 5

Quartz % (whole-rock volume): 23



Well API: 15-093-20147

Depth: 4832 ft.

Lithofacies: Peloid-rich grainstone

Depositional Environment: Lagoon

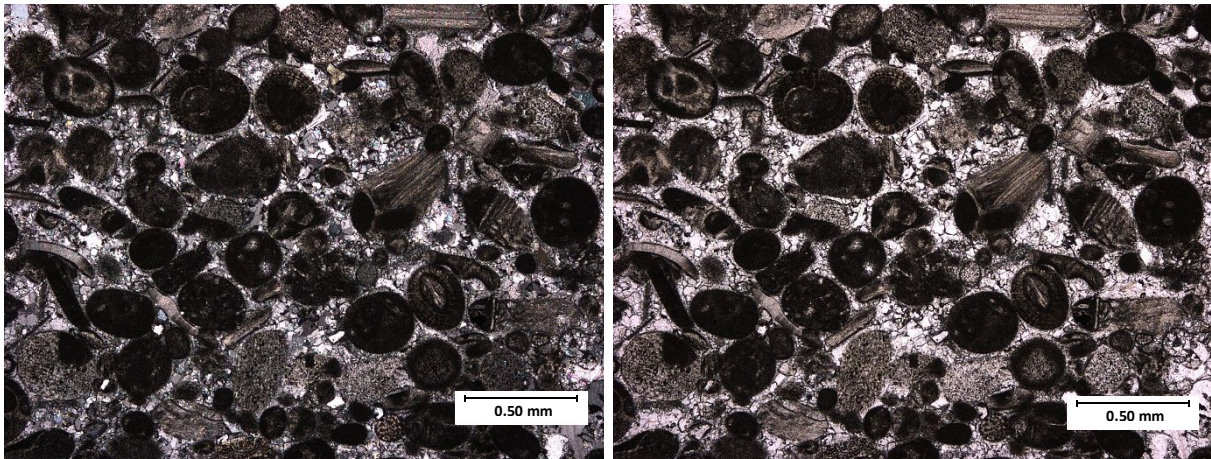
Primary Porosity Type: -

Porosity %: -

Cement: calcite, micrite

Primary Constituents: peloids, quartz grains

Quartz % (whole-rock volume): 3



Well API: 15-093-20011

Depth: 5052.7 ft.

Lithofacies: High-cemented ooid grainstone

Depositional Environment: Ooid shoal

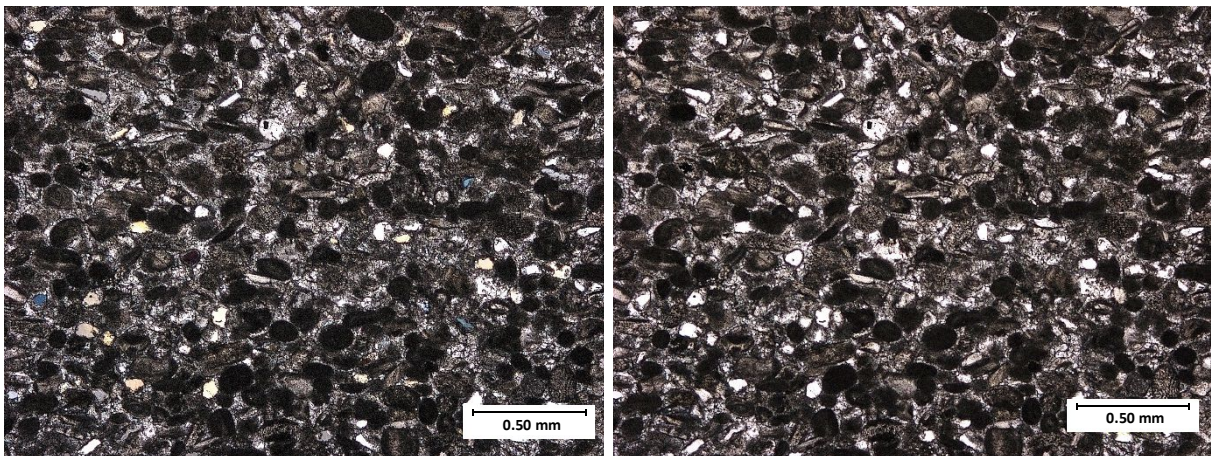
Primary Porosity Type:-

Porosity %: -

Cement: equant calcite cement

Primary Constituents: ooids, peloids, gastropods

Quartz % (whole-rock volume): 4



Well API: 15-093-20011

Depth: 5043.3 ft.

Lithofacies: peloid-rich grainstone

Depositional Environment: Lagoon

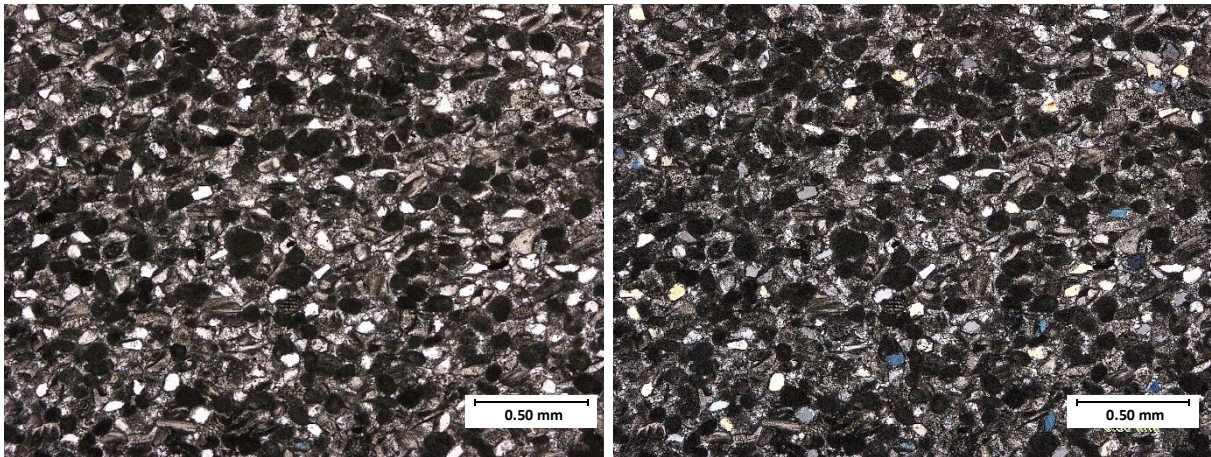
Primary Porosity Type: -

Porosity %: -

Cement: equant and blocky calcite cement

Primary Constituents: peloids, quartz grains

Quartz % (whole-rock volume): 5



Well API: 15-093-20011

Depth: 5027.4 ft.

Lithofacies: peloid-rich grainstone

Depositional Environment: Lagoon

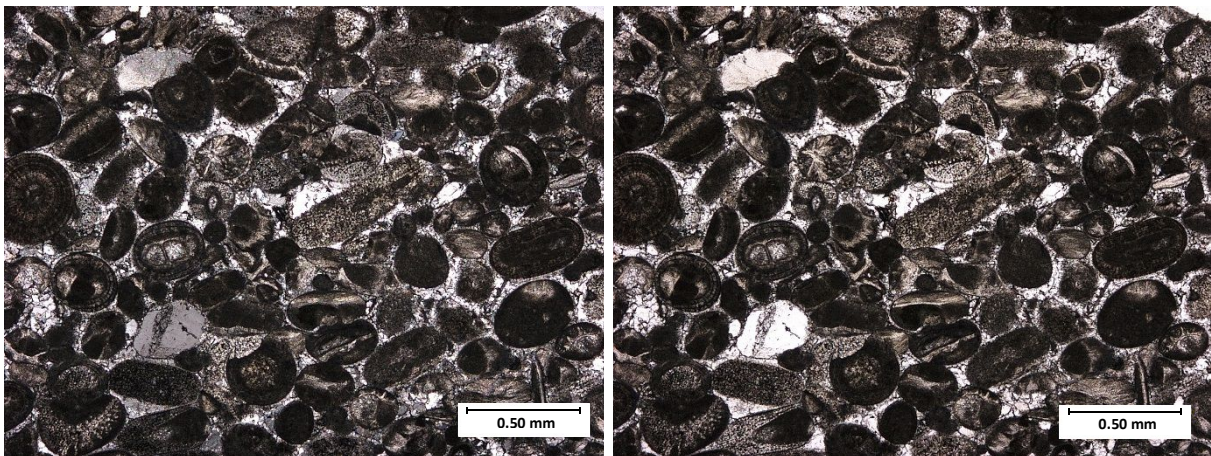
Primary Porosity Type: -

Porosity %: -

Cement: equant and blocky calcite cement

Primary Constituents: peloids, quartz grains

Quartz % (whole-rock volume): 7



Well API: 15-093-20011

Depth: 5018.4 ft.

Lithofacies: Highly-cemented ooid grainstone

Depositional Environment: Ooid shoal

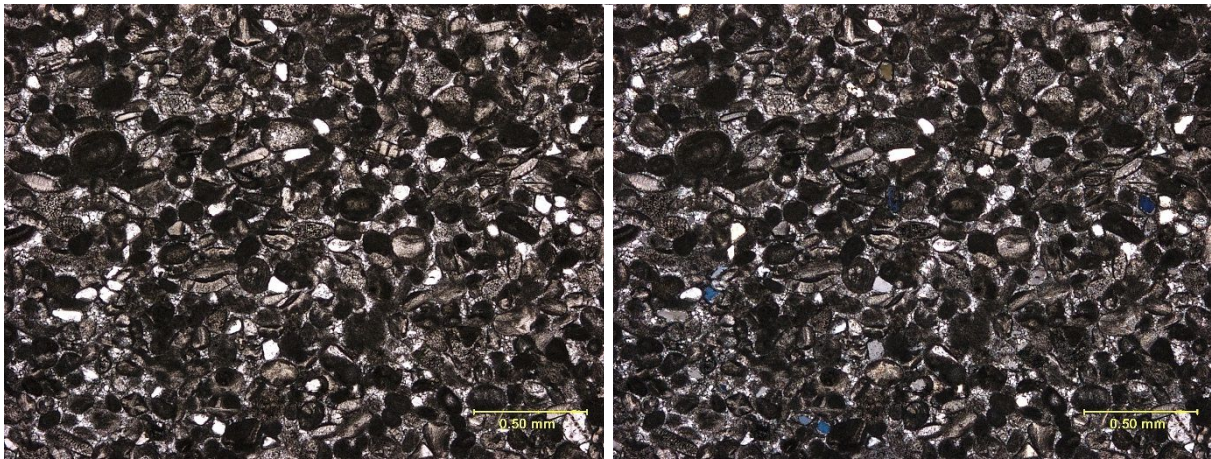
Primary Porosity Type: -

Porosity %: -

Cement: equant calcite cement

Primary Constituents: ooids, echinoderms, gastropods, large quartz grains (0.37mm)

Quartz % (whole-rock volume): 6



Well API: 15-093-20011

Depth: 5007.8 ft.

Lithofacies: peloid-rich grainstone

Depositional Environment: Lagoon

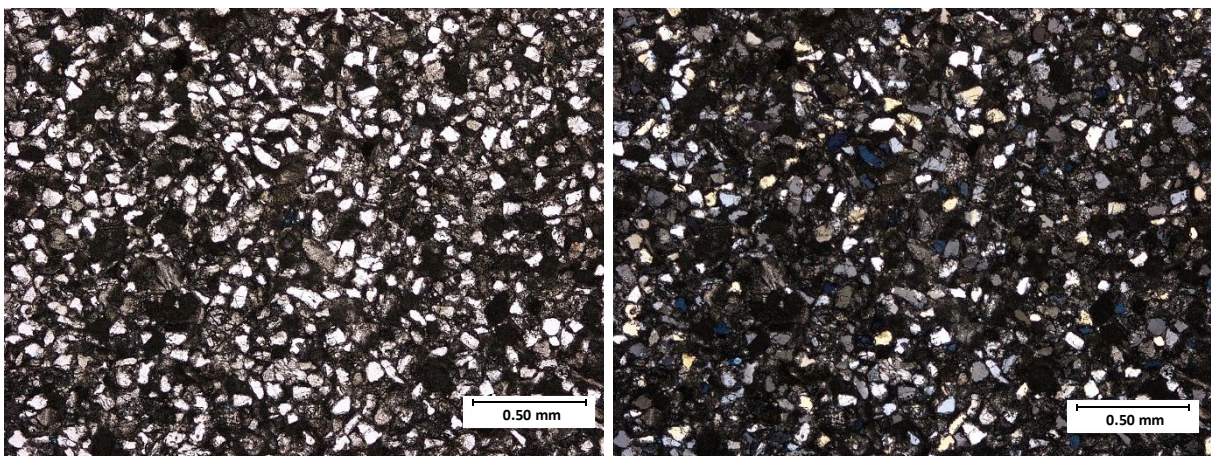
Primary Porosity Type: interparticle

Porosity %: 4

Cement: equant and blocky calcite cement

Primary Constituents: peloids, quartz grains

Quartz % (whole-rock volume): 6



Well API: 15-093-20011

Depth: 5002.3 ft.

Lithofacies: Quartz-carbonate grainstone

Depositional Environment: Carbonate Eolianite

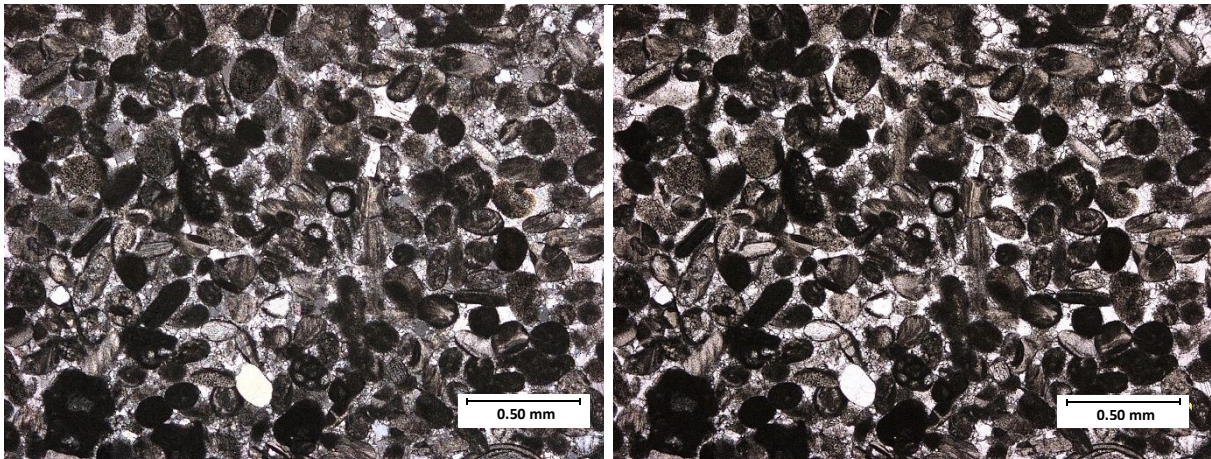
Primary Porosity Type: -

Porosity %: -

Cement: micrite

Primary Constituents: quartz grains, peloidal fabric

Quartz % (whole-rock volume): 32



Well API: 15-093-20011

Depth: 4995.7 ft.

Lithofacies: peloid-rich grainstone

Depositional Environment: Lagoon

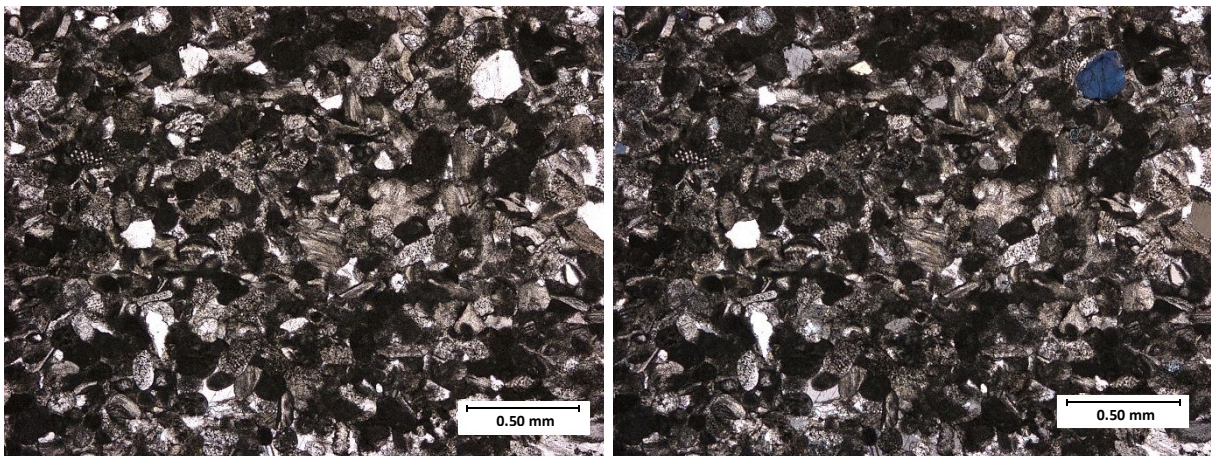
Primary Porosity Type: -

Porosity %: -

Cement: equant and blocky calcite cement

Primary Constituents: peloids, quartz grains, brachiopods, echinoderms, bryozoans, gastropod

Quartz % (whole-rock volume): 3



Well API: 15-093-20011

Depth: 4984.5 ft.

Lithofacies: Quartz-carbonate grainstone (TS not a good representation of entire thin section)

Depositional Environment: Carbonate Eolianite

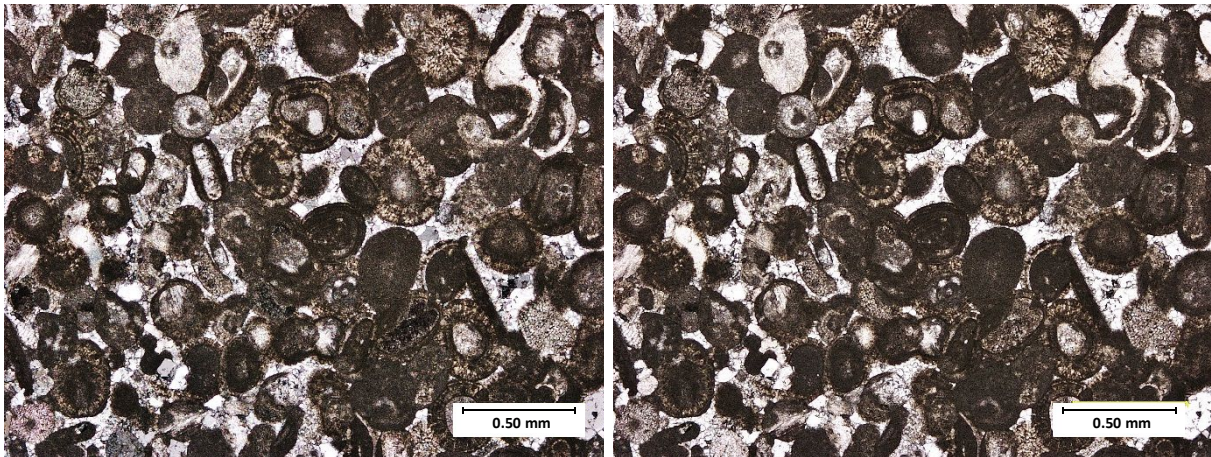
Primary Porosity Type: -

Porosity 5: -

Cement: micrite, calcite

Primary Constituents: quartz grains, peloidal fabric

Quartz % (whole-rock volume): 21



Well API: 15-093-20011

Depth: 4973.3 ft.

Lithofacies: Highly-cemented ooid grainstone

Depositional Environment: Ooid shoal

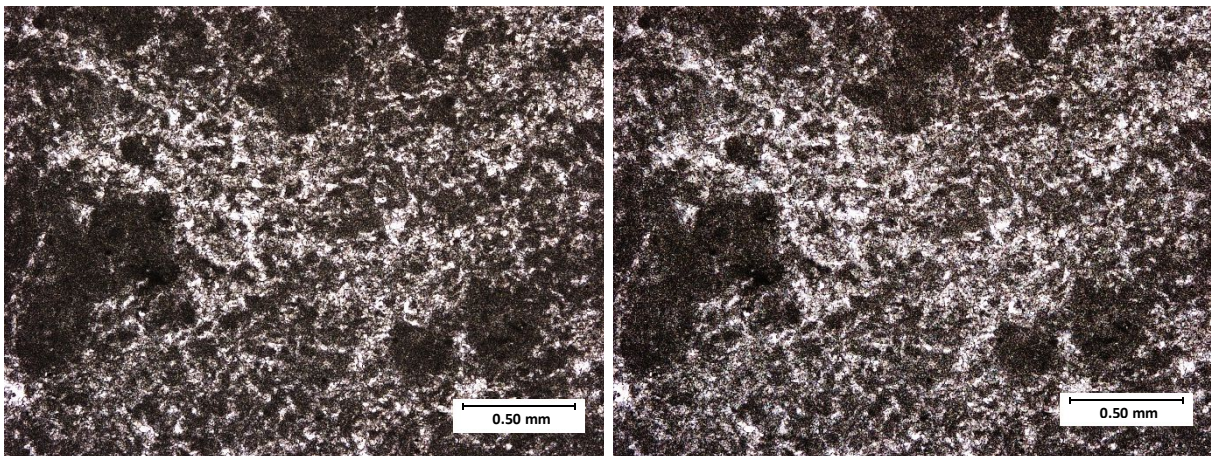
Primary Porosity Type: -

Porosity %: -

Cement: equant calcite cement

Primary Constituents: ooids, echinoderms, gastropods

Quartz % (whole-rock volume): 5



Well API: 15-093-20011

Depth: 4966.5 ft.

Lithofacies: Clay-rich mudstone

Depositional Environment: Deep Marine

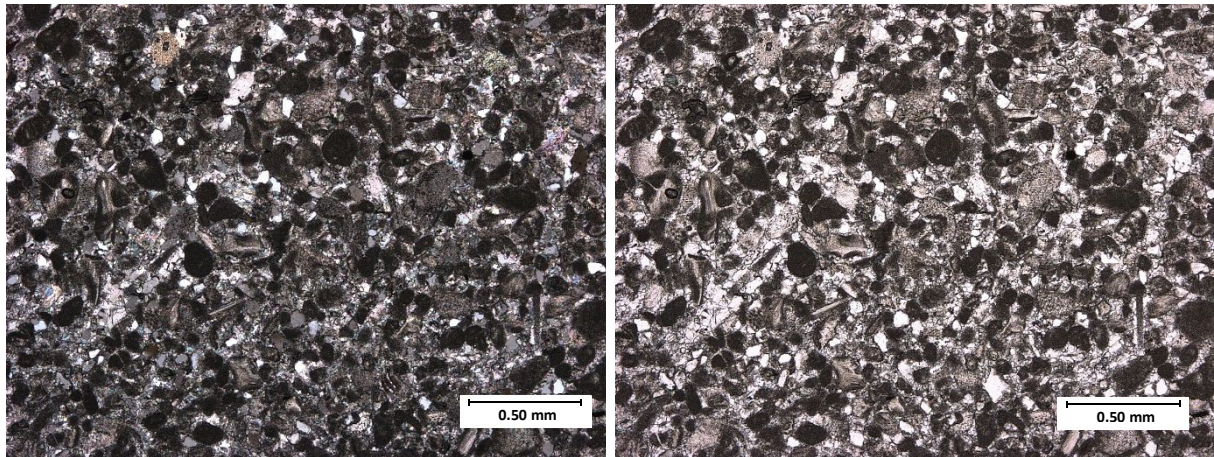
Primary Porosity Type:-

Porosity %: -

Cement: micrite

Primary Constituents: clays, mud, no fossil content

Quartz % (whole-rock volume): -



Well API: 15-093-20011

Depth: 4964.5 ft.

Lithofacies: peloid-rich grainstone

Depositional Environment: Lagoon

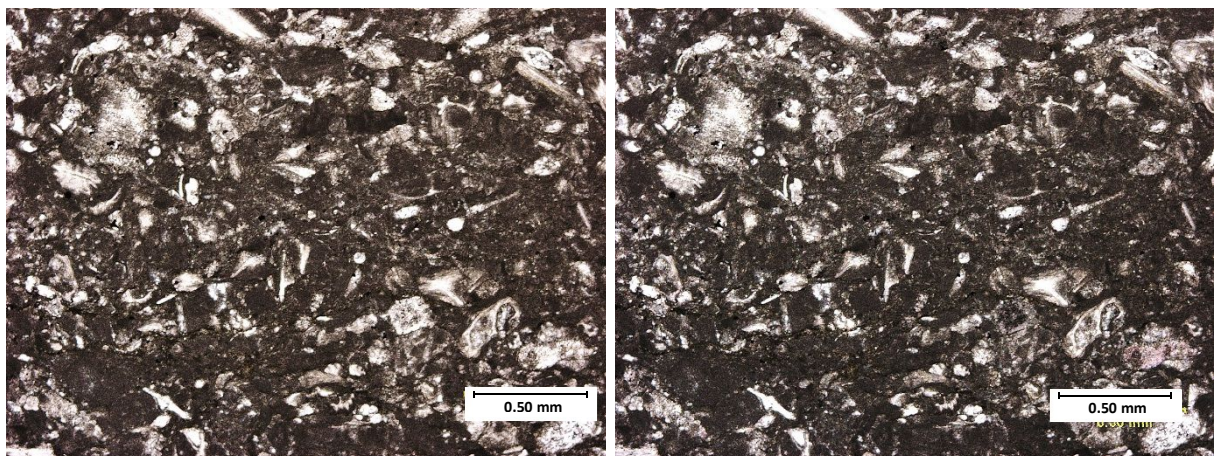
Primary Porosity Type: -

Porosity %: -

Cement: equant and blocky calcite cement

Primary Constituents: peloids, quartz grains, ooids, echinoderms, gastropod

Quartz % (whole-rock volume): 9



Well API: 15-093-00317

Depth: 4974.6

Lithofacies: Skeletal wackestone/packstone

Depositional Environment: Open marine

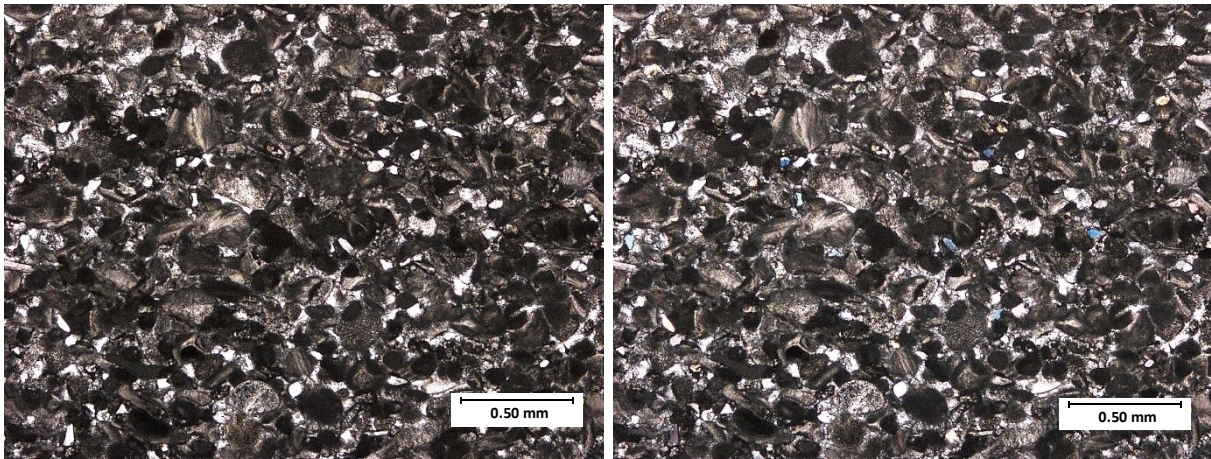
Primary Porosity Type:-

Porosity %: -

Cement: micrite

Primary Constituents: very rich with fossils and fossil fragments

Quartz % (whole-rock volume): -



Well API: 15-093-00317

Depth: 4946.8 ft.

Lithofacies: peloid-rich grainstone

Depositional Environment: Lagoon

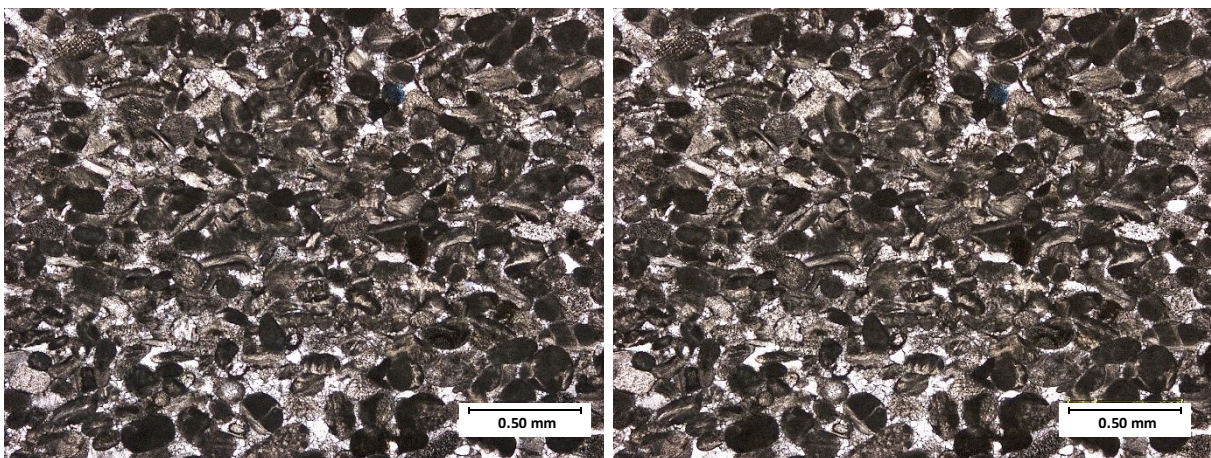
Primary Porosity Type: -

Porosity %: -

Cement: equant and blocky calcite cement

Primary Constituents: peloids, quartz grains, ooids, echinoderms, gastropod

Quartz % (whole-rock volume): 1



Well API: 15-093-00317

Depth: 4963.4 ft.

Lithofacies: peloid-rich grainstone

Depositional Environment: Lagoon

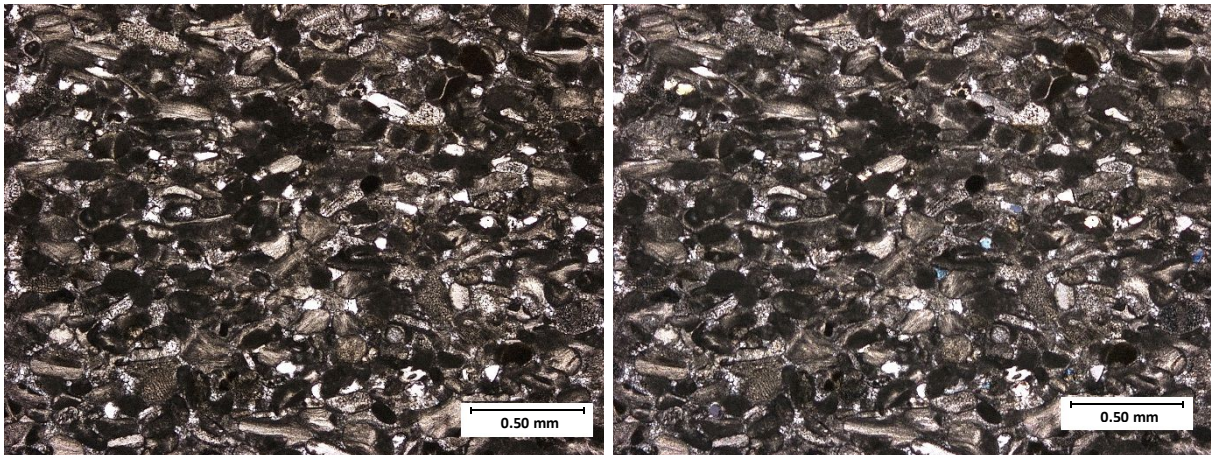
Primary Porosity Type: -

Porosity %: -

Cement: equant and blocky calcite cement

Primary Constituents: peloids, quartz grains, ooids, echinoderms, gastropod

Quartz % (whole-rock volume): 9



Well API: 15-093-00317

Depth: 4942.3 ft.

Lithofacies: peloid-rich grainstone

Depositional Environment: Lagoon

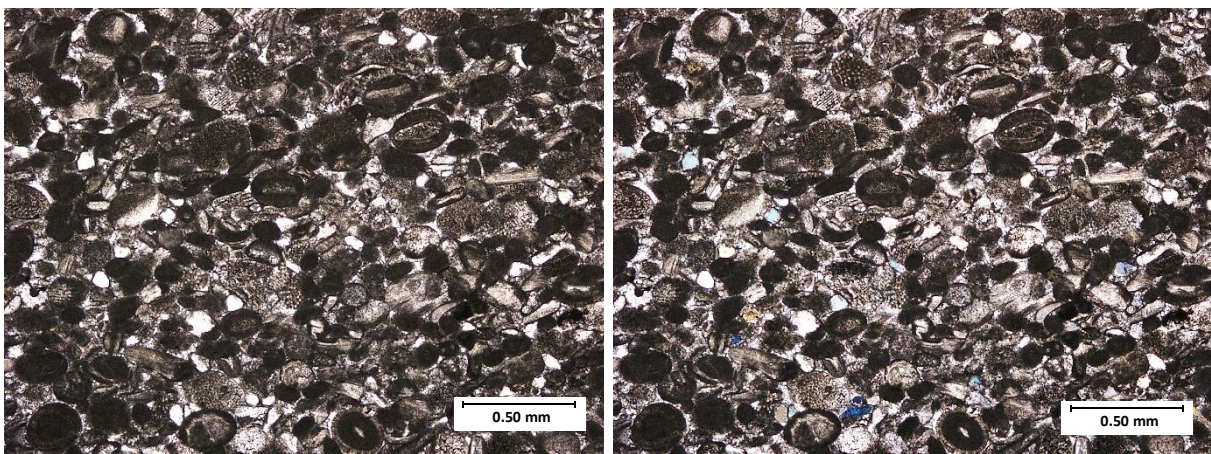
Primary Porosity Type: -

Porosity %: -

Cement: equant and blocky calcite cement

Primary Constituents: peloids, quartz grains, ooids, echinoderms, gastropod

Quartz % (whole-rock volume): 2



Well API: 15-093-00317

Depth: 4932.3 ft.

Lithofacies: peloid-rich grainstone

Depositional Environment: Lagoon

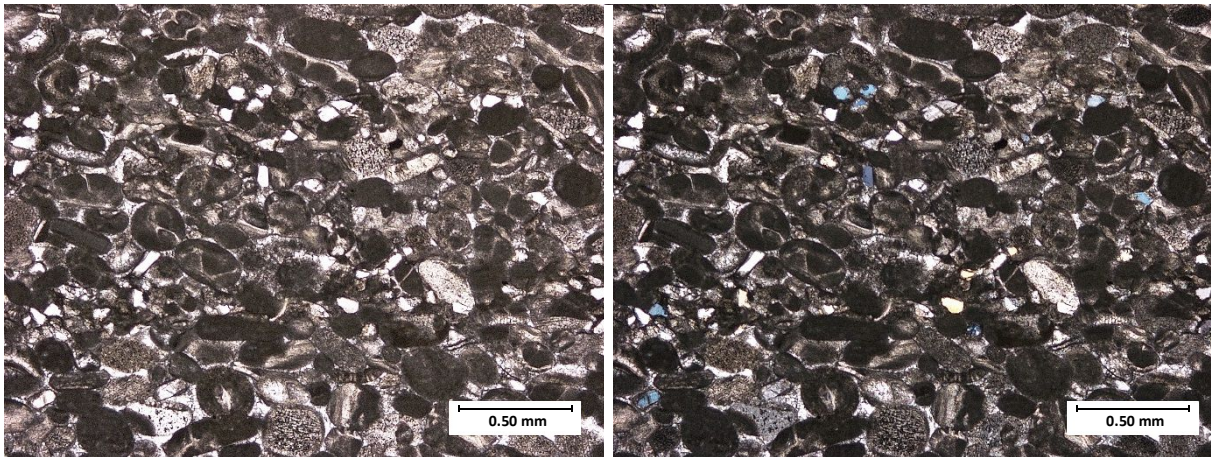
Primary Porosity Type: -

Porosity %: -

Cement: equant and blocky calcite cement

Primary Constituents: peloids, quartz grains, ooids, echinoderms, gastropod

Quartz % (whole-rock volume): 2



Well API: 15-093-00317

Depth: 4914.5 ft.

Lithofacies: peloid-rich grainstone

Depositional Environment: Lagoon

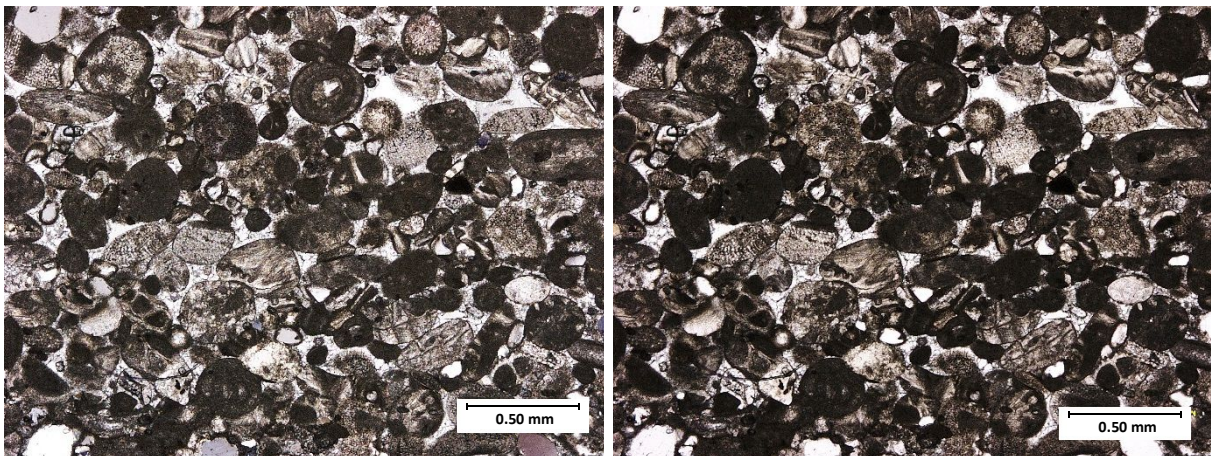
Primary Porosity Type: -

Porosity %: -

Cement: equant and blocky calcite cement

Primary Constituents: peloids, quartz grains, ooids, echinoderms, gastropod

Quartz % (whole-rock volume): 6



Well API: 15-093-00317

Depth: 4907.5 ft.

Lithofacies: Highly-cemented ooid grainstone

Depositional Environment: Ooid shoal

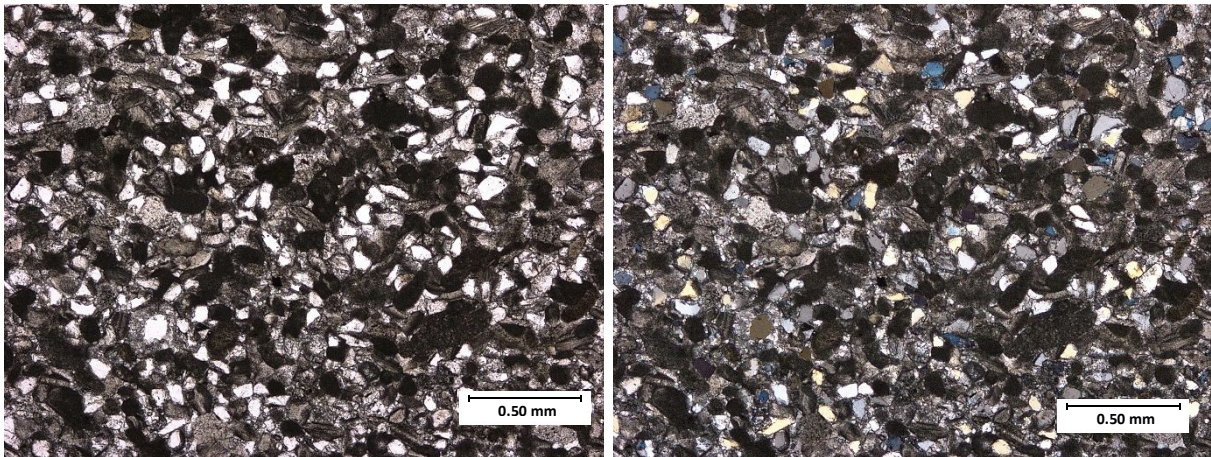
Primary Porosity Type: -

Porosity %: -

Cement: blocky and equant calcite

Primary Constituents: ooids, peloids

Quartz % (whole-rock volume): 3



Well API: 15-093-00317

Depth: 4903.4 ft.

Lithofacies: Quartz-carbonate grainstone

Depositional Environment: Carbonate Eolianite

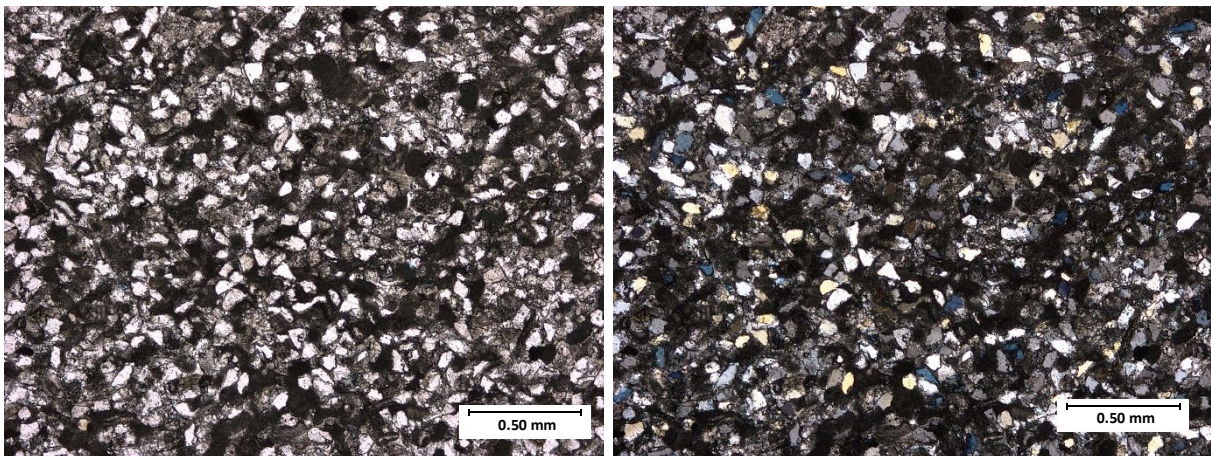
Primary Porosity Type: -

Porosity %: -

Cement: equant calcite

Primary Constituents: quartz grains, peloids, peloidal fabric

Quartz % (whole-rock volume): 23



Well API: 15-093-00317

Depth: 4882.5 ft.

Lithofacies: Quartz-carbonate grainstone

Depositional Environment: Carbonate Eolianite

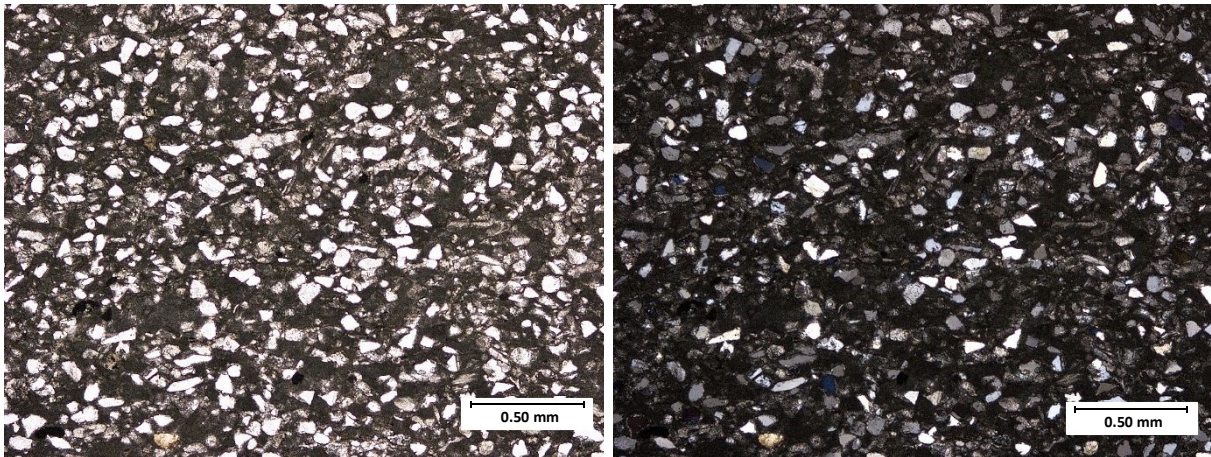
Primary Porosity Type: -

Porosity %: -

Cement: blocky calcite

Primary Constituents: quartz grains, peloidal fabric

Quartz % (whole-rock volume): 33



Well API: 15-093-00317

Depth: 4871.3 ft.

Litho facies: Quartz-carbonate grainstone

Depositional Environment: Carbonate Eolianite

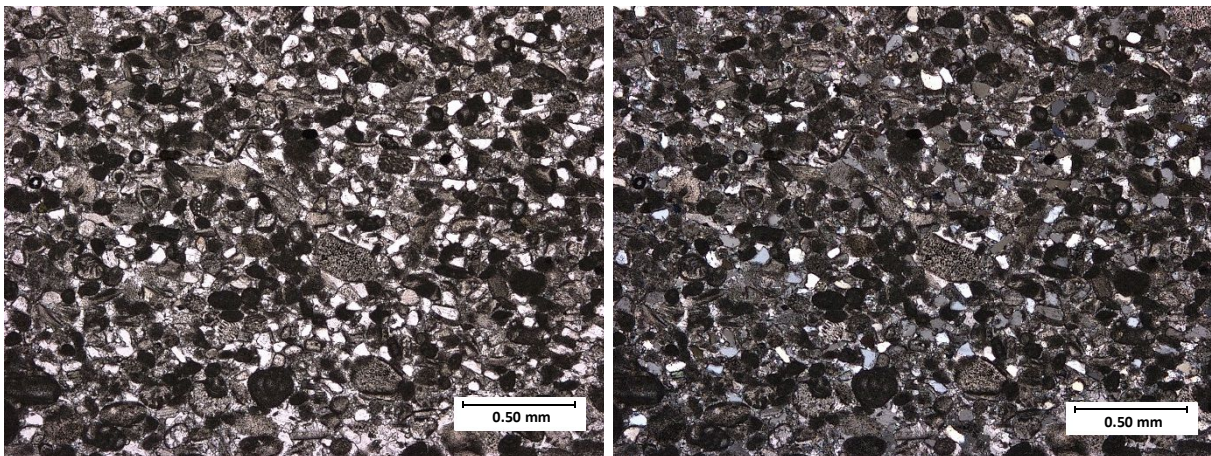
Primary Porosity Type: -

Porosity %: -

Cement: micrite

Primary Constituents: quartz grain

Quartz % (whole-rock volume): 25



Well API: 15-093-00317

Depth: 4859.5 ft.

Litho facies: peloid-rich grainstone

Depositional Environment: Lagoon

Primary Porosity Type: -

Porosity %: -

Cement: equant and blocky calcite cement

Primary Constituents: peloids, quartz grains, ooids, echinoderms, gastropod

Quartz % (whole-rock volume): 9

## APPENDIX B

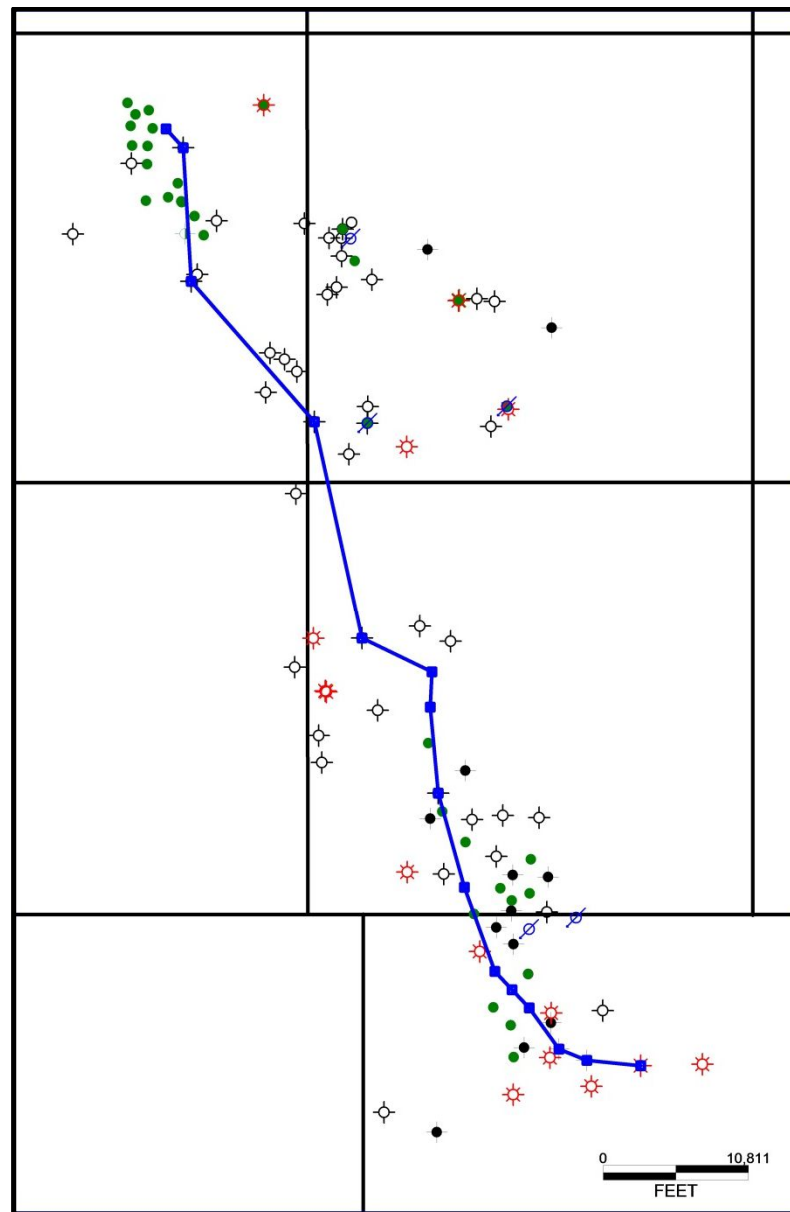


Figure 30: Basemap of the study area with a N-S cross section line.

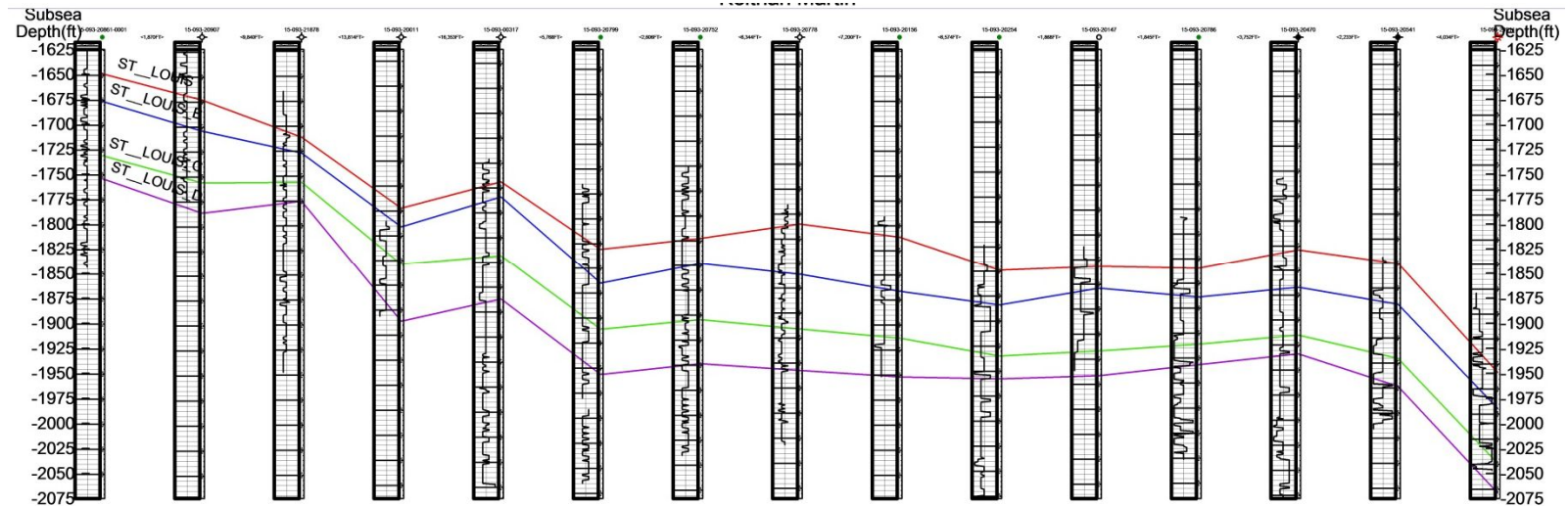


Figure 31: A structural cross section that correlates with cross section line from Figure 30.

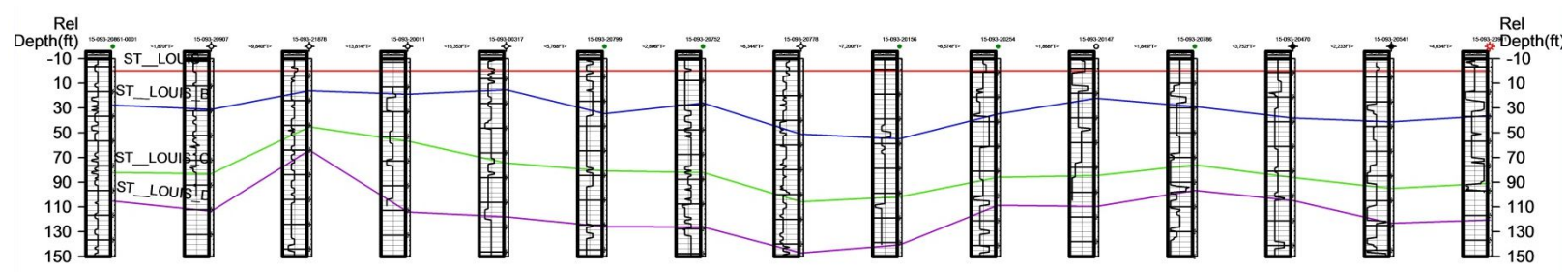


Figure 32: Stratigraphic cross section “hung” on the St. Louis Limestone that correlates with the cross section line from Figure 30.

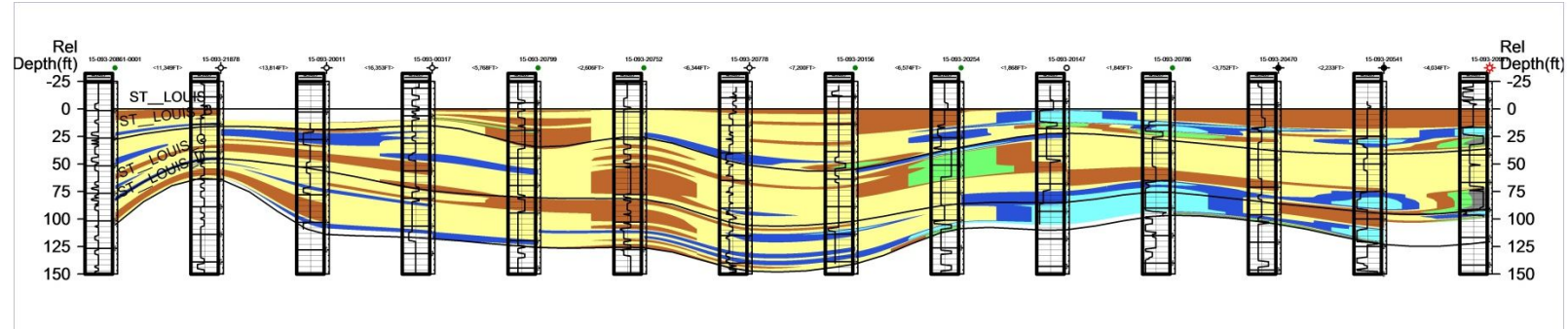


Figure 33: Stratigraphic cross section “hung” on the St. Louis Limestone that correlates with the cross section line from Figure 30 with the color coded facies predictions.

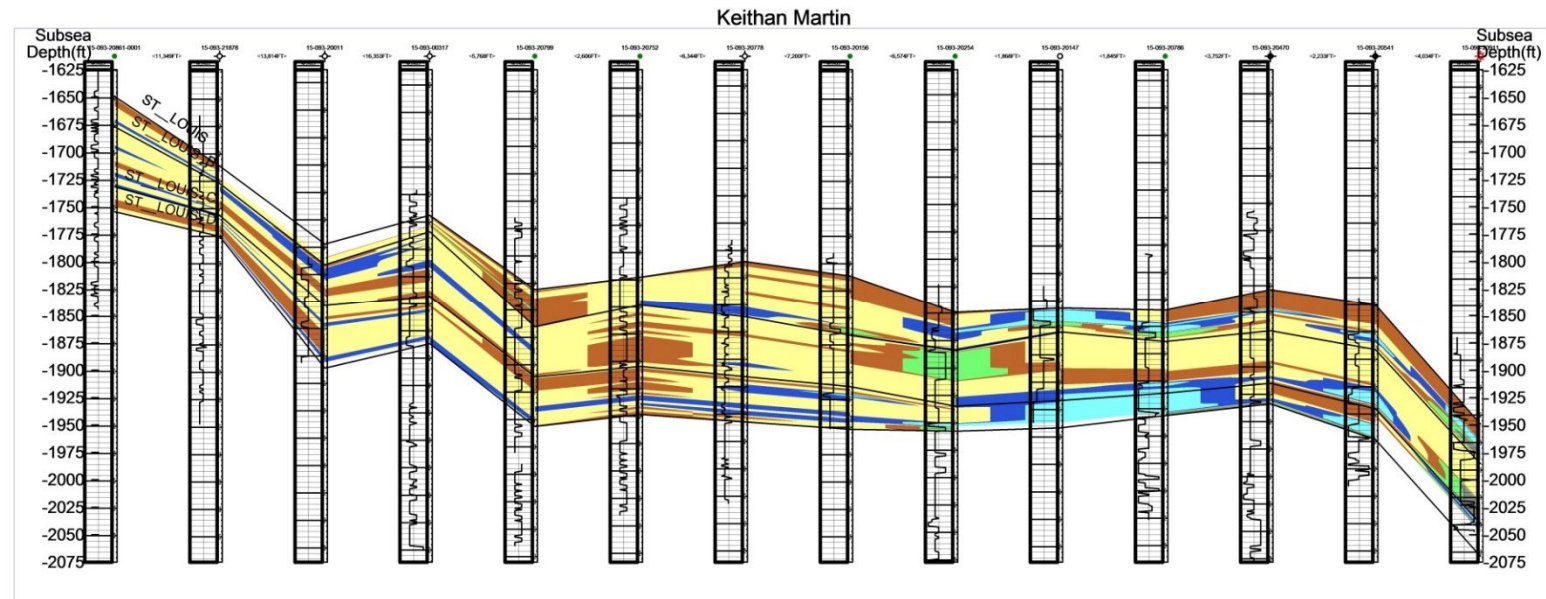


Figure 34: A structural cross section that correlates with cross section line from Figure 30 with color coded facies predictions.

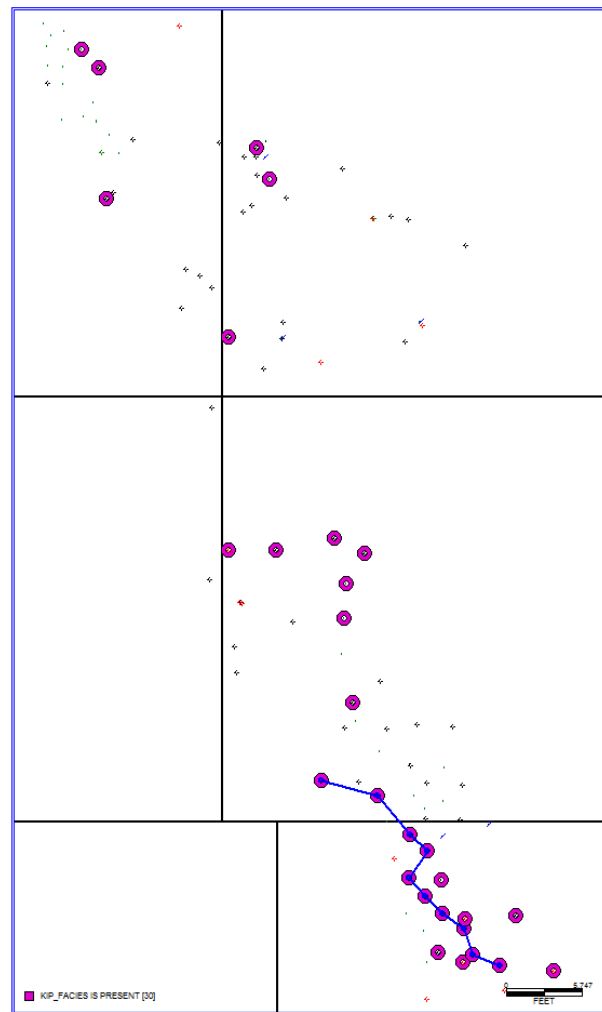


Figure 34: Basemap of the study area with N-S cross section lines in the southern area.

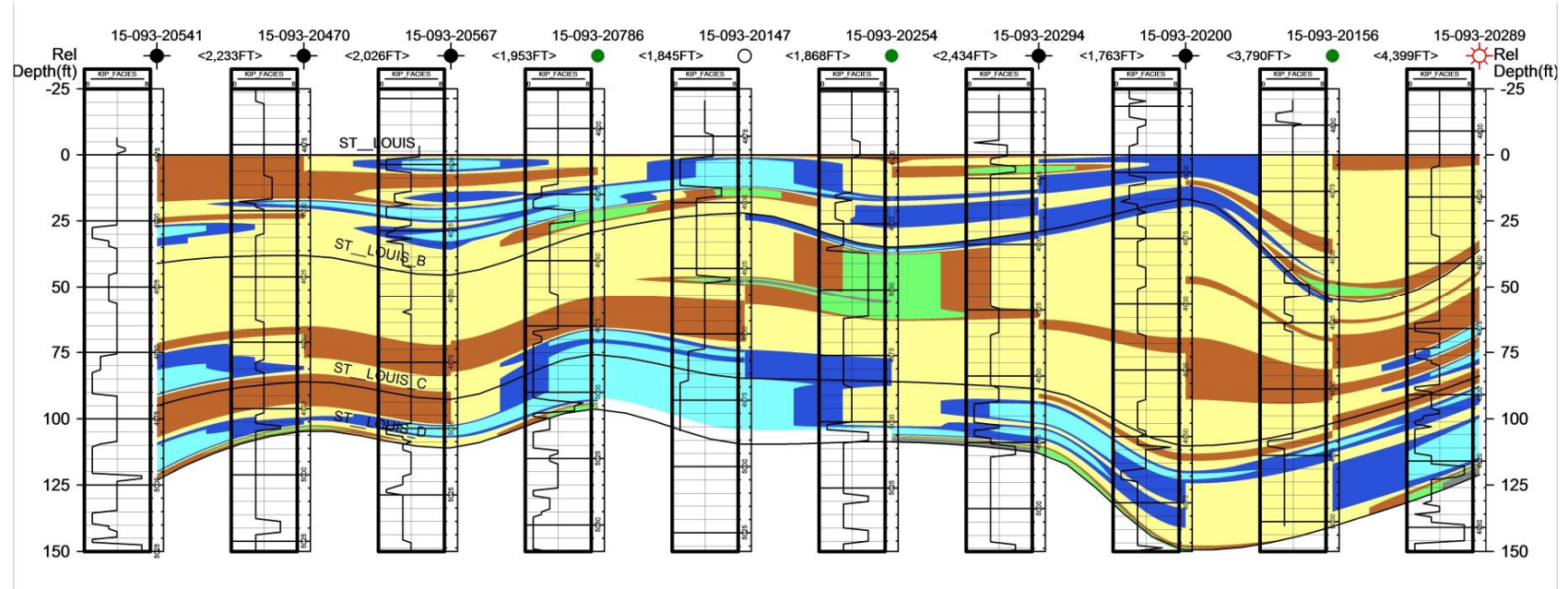
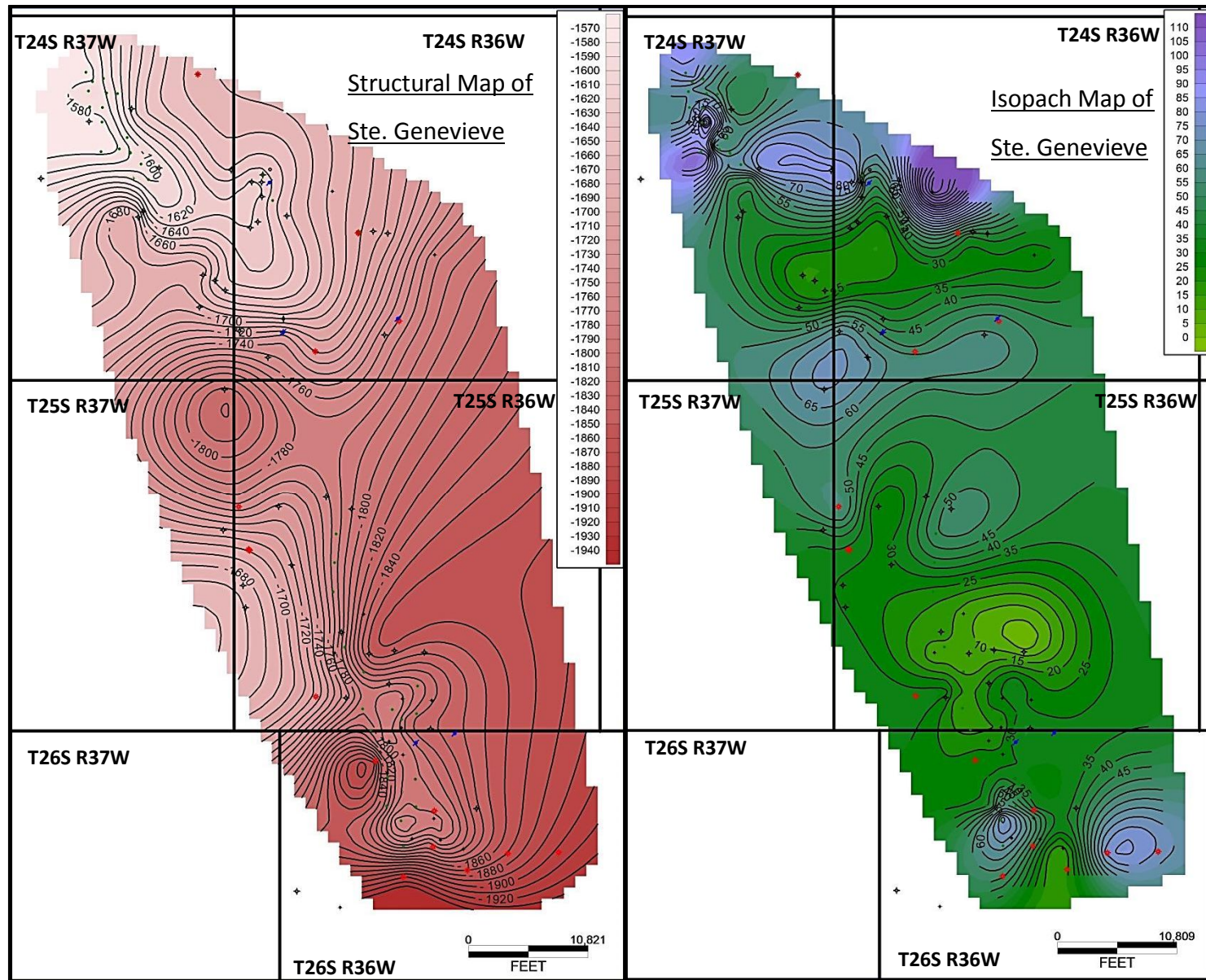
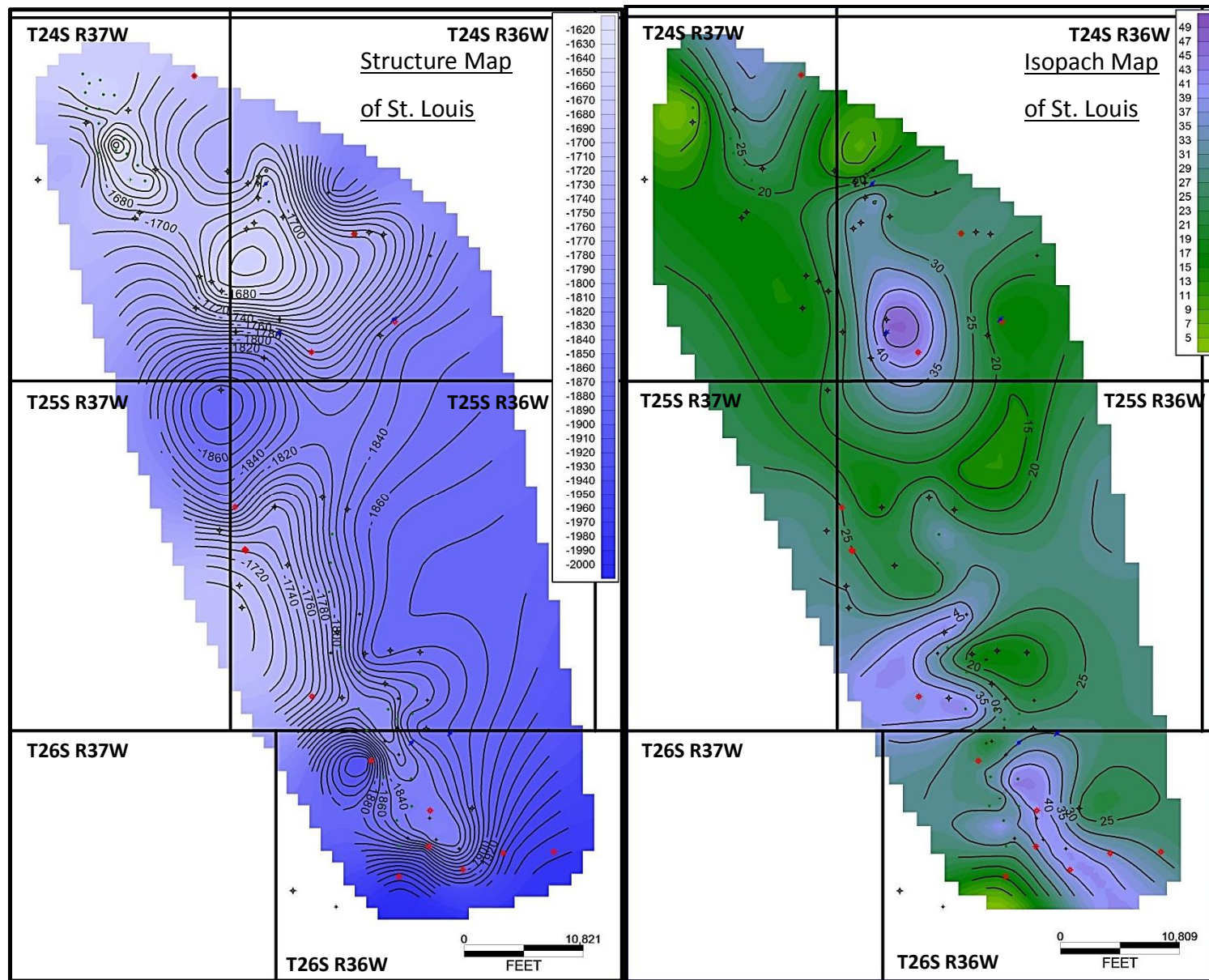
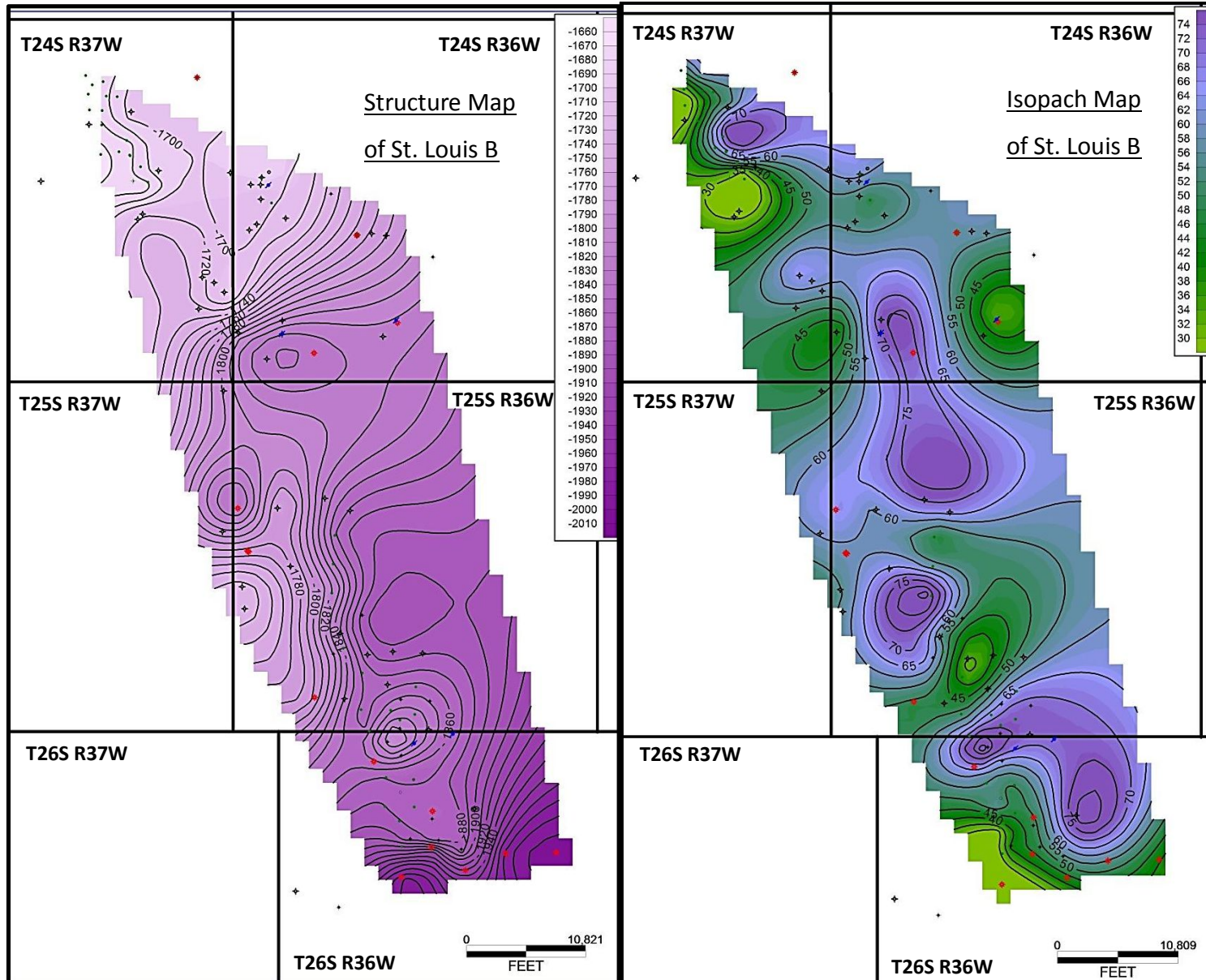
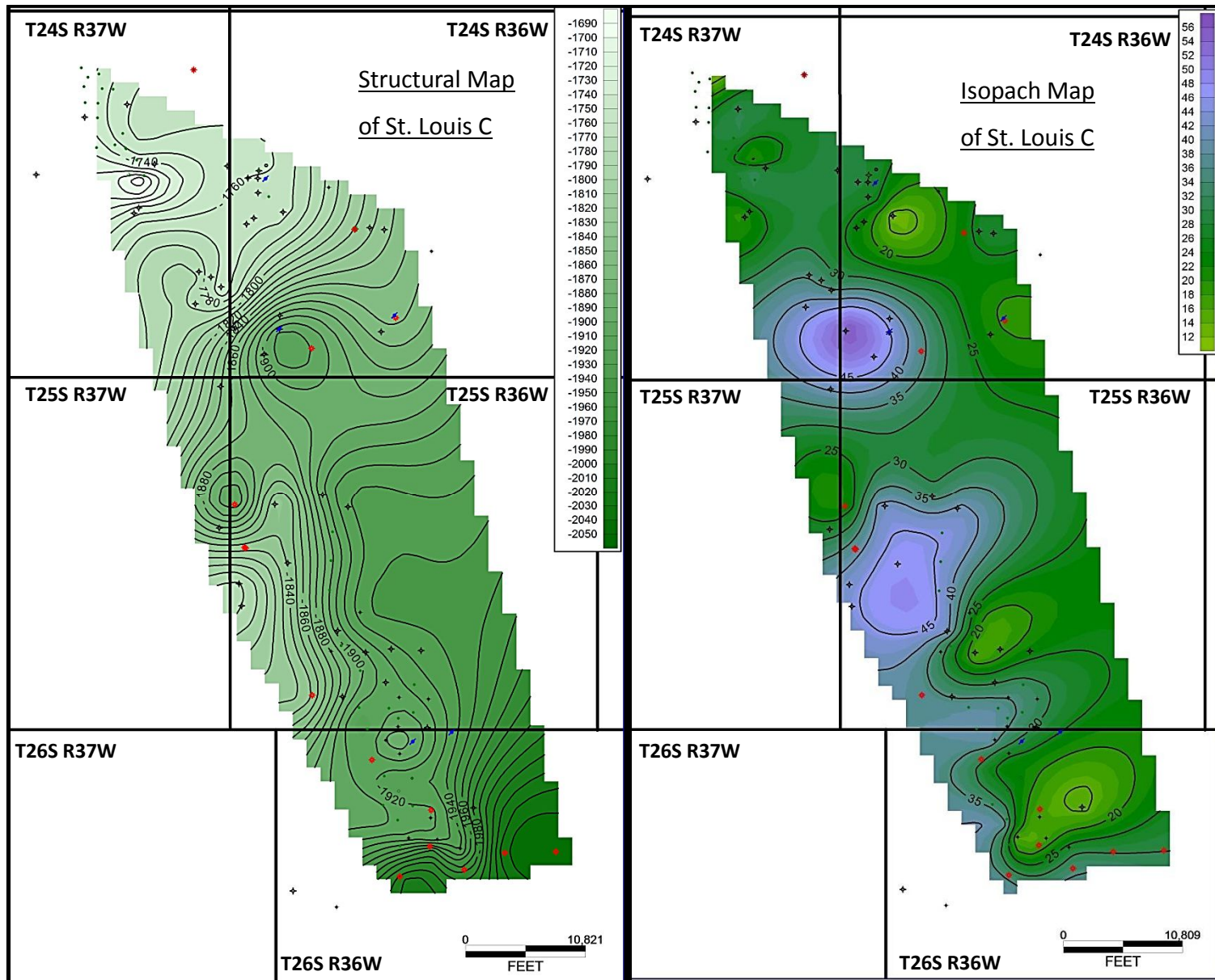


Figure 35: Stratigraphic cross section “hung” on the St. Louis limestone that correlated with the cross section line from Figure 34 with color coded facies predictions.









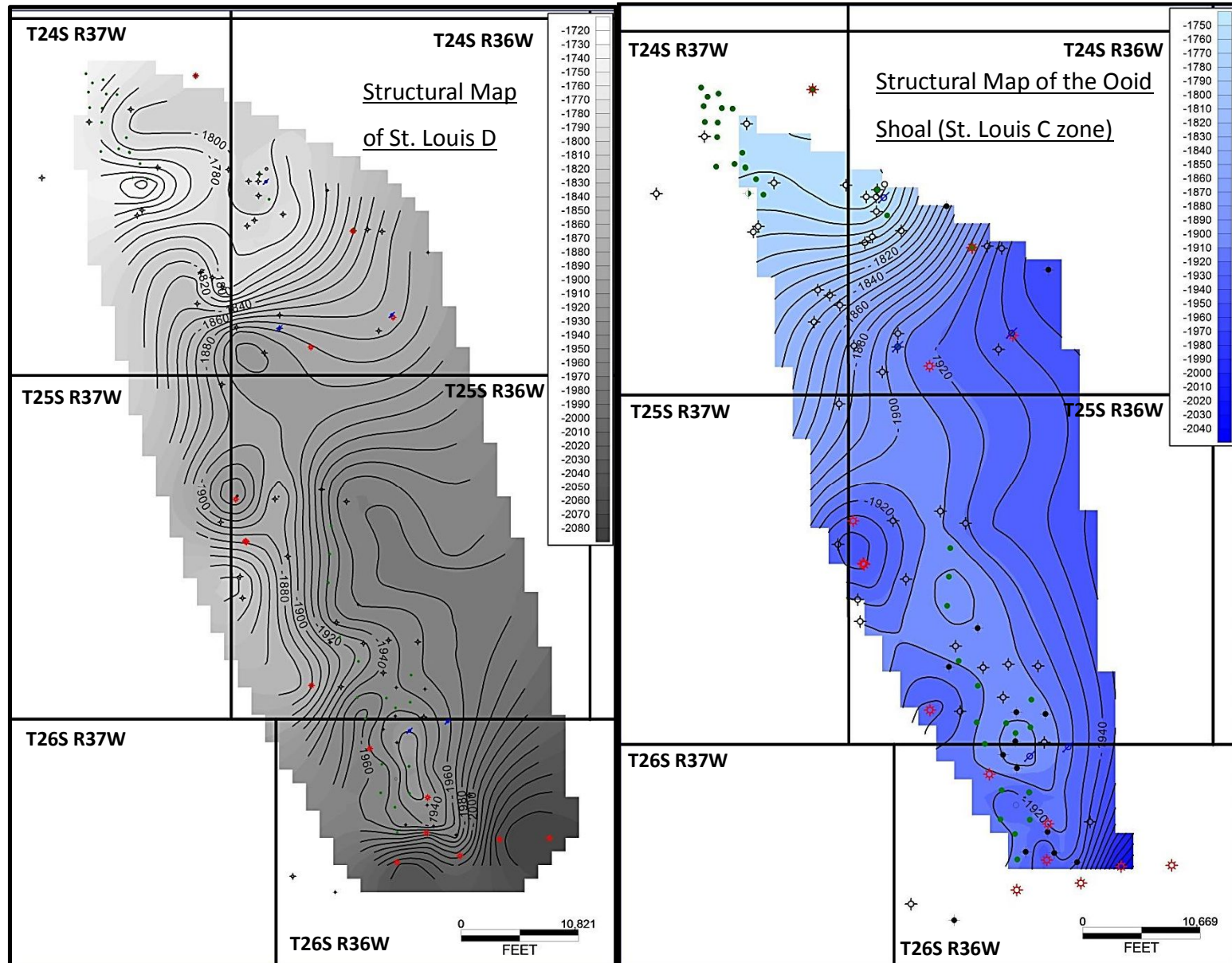


Figure 36-46: Isopach and structural map of the Ste. Genevieve, St. Louis, St. Louis B, C, and D, and ooid shoal from St. Louis C zone.

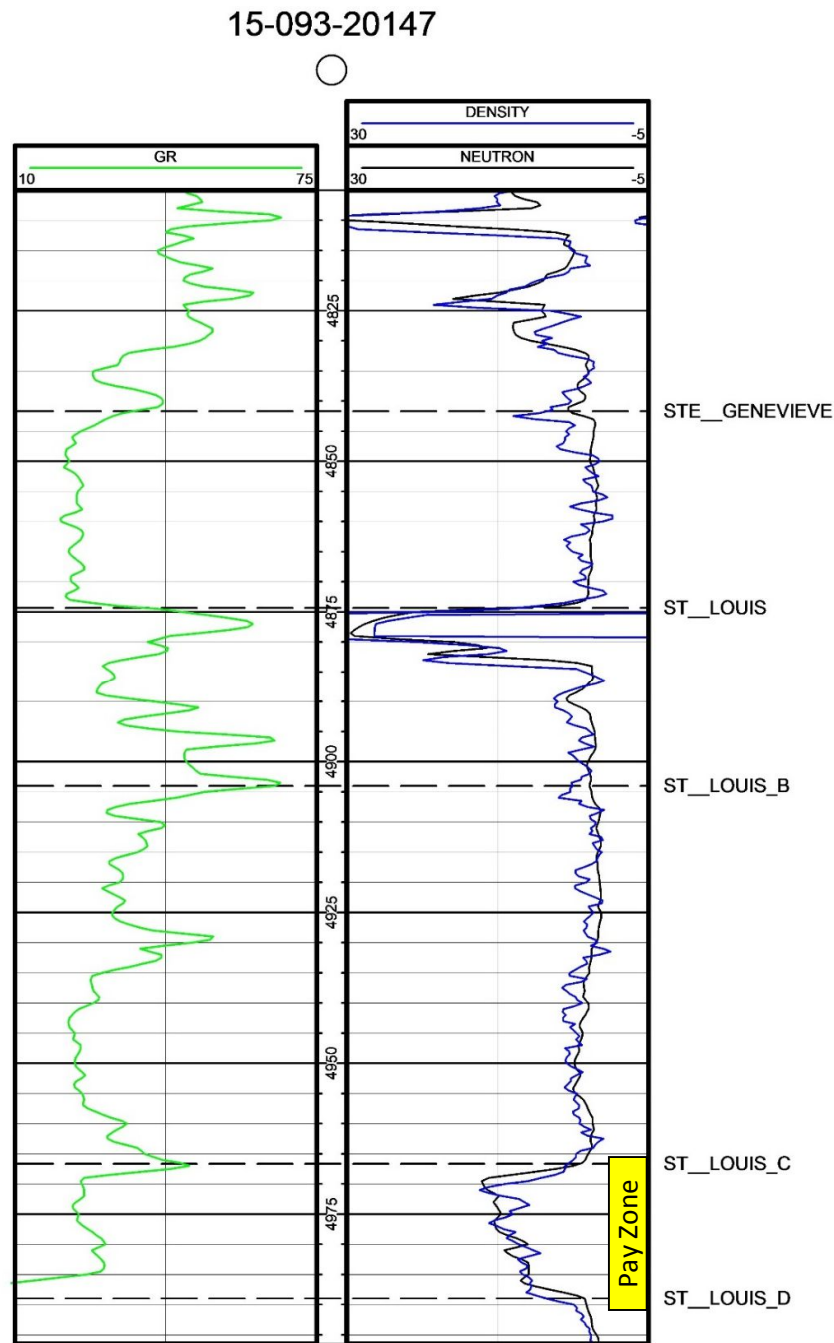


Figure 47: Type log illustrating the log responses from GR and Neu/Den, with the St. Louis C zone highlighted as the pay zone.



34	-0.76816	-0.651514267	0.943925	0.960389	33	1.046508	-1.31409	2.724241	-2.20393	-0.10225	-0.1585	33	73.02771313	109	48.45461
35	-4.48138	-1.718856074	-0.6295	-12.0441	34	-0.35096	-0.87081	-1.2155	0.906699	1.067357	0.483301	34	71.68856724	110	48.37095
36	0.48321	0.225653788	-0.56687	-0.47031	35	8.586942	-5.28557	0.09065	-3.08606	-0.28283	-0.04619	35	70.44799503	111	48.26691
37	1.028375	-0.918888946	-0.62045	-0.08313	36	0.911137	0.375831	0.15128	-0.33006	-0.58813	-0.54792	36	69.85704053	112	48.18123
38	-1.80452	-7.660396599	-1.38228	9.378522	37	0.562751	0.716875	0.190308	0.690711	-1.19545	-0.92677	37	68.96320952	113	48.12624
39	-1.86058	0.677203597	1.324473	-0.22933	38	-0.8686	6.771403	-5.70457	1.852398	-1.90029	-0.19264	38	68.04098647	114	48.02414
40	-1.29649	-0.572266252	-1.41085	0.143617	39	-0.01971	-1.03947	-0.22627	-1.16926	1.186689	1.212999	39	67.25268007	115	48.01287
41	-0.43884	0.042577371	-0.37572	-0.55881	40	0.146137	0.334858	1.304328	-1.40051	-0.22028	-0.20824	40	66.06326492	116	47.91055
42	0.57083	0.26250839	-0.79304	-0.55292	41	0.786242	0.619244	-0.05526	-0.53721	-0.38725	-0.42049	41	65.53082799	117	47.90405
43	0.391714	-0.562413061	-7.9047	-0.90466	42	0.720205	0.033684	0.831171	-0.12639	-0.70404	-0.74187	42	64.52595947	118	47.80308
44	-5.81858	-0.506485277	2.37989	8.390464	43	-0.33508	2.726997	-4.24825	2.162851	-0.08899	-0.24968	43	63.72801721	119	47.77708
45	-0.3045	0.232534681	-0.3706	0.087248	44	0.069805	1.77216	4.33526	-7.0191	2.797418	-2.00427	44	63.22140626	120	47.67343
46	-1.58217	3.155305762	0.690141	-6.99676	45	0.505533	0.318825	-0.04986	0.019083	-0.23183	-0.52129	45	62.69808973	121	47.6327
47	0.530856	2.06311715	-4.74844	3.509088	46	-0.19804	2.748314	0.056355	-3.45809	-3.57964	4.390902	46	61.93784636	122	47.57612
48	-2.0863	0.087645702	-2.6772	0.066854	47	0.379357	-5.02846	2.049239	3.404389	-0.53823	-0.25336	47	61.52327492	123	47.47903
49	-0.91004	-0.008847212	-1.46053	-0.32995	48	0.430281	-0.85209	2.19922	-1.59779	-0.06546	-0.12244	48	60.81432513	124	47.44189
50	-1.60002	-1.633818036	0.684235	2.548421	49	0.612158	-0.80762	1.5097	-0.86041	-0.24081	-0.20417	49	60.36139479	125	47.42976
51	2.21575	-0.607400578	-1.20965	0.676906	50	0.53867	-0.36763	-2.69849	1.865475	1.56666	-0.91149	50	59.50714355		
52	0.408776	0.135193989	-0.66931	-0.46745	51	-0.20929	0.839931	0.86986	1.246584	-1.11971	-1.61744	51	59.12603772		
53	-1.29676	0.395668317	-0.11023	-0.79539	52	0.785618	0.439299	0.375072	-0.38448	-0.60855	-0.5881	52	58.8317726		
54	0.552358	-1.647738528	3.818647	-1.53647	53	1.133149	1.23445	-0.6511	-1.19473	-0.3147	-0.22399	53	58.18761173		
55	-2.83935	-4.612096736	4.178743	4.605408	54	-1.2118	3.524288	-1.89193	-0.57291	0.052901	0.112427	54	57.80725567		
56	0.221446	0.409441295	-0.53629	0.749386	55	2.051801	-1.15733	-5.40751	4.200531	-0.00371	0.345632	55	57.60264631		
57	-4.58168	-0.59970663	-5.95655	-12.0666	56	0.167071	0.097769	0.494645	0.118637	0.110998	-0.97479	56	57.34969538		
58	-0.01718	0.103502394	-0.66003	-0.55998	57	-3.54892	-2.52876	8.054549	-1.7003	-0.08856	-0.21218	57	56.89695178		
59	-0.6514	0.407602803	-0.41591	-0.68182	58	0.817988	0.249181	0.459926	-0.53517	-0.52424	-0.44107	58	56.35766065		
60	-0.62238	0.114313993	0.037745	-0.77589	59	1.165593	0.565706	-0.12649	-0.93805	-0.25112	-0.44524	59	56.13159554		
61	1.912583	-2.108045219	0.053849	-0.93942	60	0.343829	-0.01393	-0.37673	-0.52315	-0.03958	0.609781	60	55.692547		
62	-0.79373	0.125216892	-0.20417	0.173088	61	0.004785	-0.32712	-1.18322	2.461577	-1.25251	0.280949	61	55.34607555		
63	-4.57899	6.651997252	0.233504	-17.3898	62	0.230259	0.202411	-0.07814	0.01097	-0.00745	-0.343	62	55.05861092		
64	0.471632	0.139776179	-1.08784	0.039881	63	-8.83459	7.490944	4.523041	-3.10225	-0.5692	0.543281	63	54.83228745		
65	0.093959	1.12948302	-1.06911	-0.24471	64	0.620568	0.388473	0.334883	0.258379	-0.68904	-0.87417	64	54.41345042		
66	0.107334	-0.265301658	0.578999	0.723842	65	0.993654	-0.07525	0.839895	-0.60879	-0.65397	-0.54921	65	54.22267089		
67	-0.32569	-0.105008841	0.631802	0.18467	66	-0.83541	-0.29229	-0.45869	0.827302	0.671103	0.065369	66	53.93608157		
68	-0.61496	0.376098296	-0.38334	-0.42351	67	0.397213	0.014895	-1.02274	-0.09566	0.411995	0.300724	67	53.6450388		
69	-0.92302	0.318259138	-0.51259	-0.41294	68	0.375089	0.719745	0.473419	-0.78587	-0.419	-0.35261	68	53.32194051		
70	-2.04574	5.429052114	-10.4077	-4.63001	69	0.398649	0.536754	0.40722	-0.80719	-0.09828	-0.3859	69	53.11112459		
71	-5.77	3.180648033	3.45829	-1.63554	70	-3.87217	5.102458	-5.61343	4.490706	-0.02587	-0.10625	70	52.94543598		
72	0.613157	0.246012717	-0.69087	-0.71797	71	0.129735	-5.81342	1.291364	-1.06778	3.834144	1.60499	71	52.84914722		
73	0.174148	-0.411601609	-0.31028	-0.53379	72	0.966356	-0.29651	1.001547	-0.18939	-0.75522	-0.7127	72	52.44626009		
74	0.482715	2.107397684	-3.11691	2.940626	73	0.3779	0.336323	-0.20558	0.185139	-0.61385	-0.09718	73	52.10795594		
75	-0.19694	0.027768204	-0.5301	-0.2589	74	-0.15491	-2.76986	2.21395	2.666094	-1.46676	-0.48856	74	51.95879813		
					75	0.489458	-0.07937	0.662182	-0.16718	-0.61621	-0.30365	75	51.74660854		

Figure 48: Neural network model spread sheet of a cored well (API: 15-093-00317).



34	-4.27503	-1.15236	-1.35742	-3.58424		33	0.765013	-0.14634	-0.55558	-0.10259		33	37.04977		84	25.82459
35	-0.00476	-0.23789	0.113629	-0.10528		34	4.059799	0.002529	-3.883	-0.19315		34	36.16643		85	25.77577
36	1.401396	-0.60545	-1.33213	0.014345		35	0.232307	0.061569	-0.37456	0.082282		35	35.59845		86	25.74536
37	-0.39255	0.418774	0.035645	-0.11214		36	-0.65803	-1.18408	1.381005	0.44538		36	34.66274		87	25.70853
38	-0.20112	-0.80914	0.821106	0.359639		37	-0.21709	0.518426	-0.15896	-0.13603		37	34.36167		88	25.65197
39	0.306752	-0.66332	0.317314	-1.10044		38	0.664155	-0.48436	-0.8511	0.660152		38	33.08129		89	25.62252
40	-2.90507	0.006265	7.622955	-3.26849		39	0.661127	-1.1171	0.136352	0.358037		39	32.04145		90	25.58966
41	-1.86174	3.610208	0.878095	1.057829		40	-5.88611	2.245016	3.700181	-0.05168		40	31.69235		91	25.51058
42	-1.66067	2.844623	-6.25184	-0.04763		41	-1.36921	-2.00169	3.016012	0.331182		41	31.41758		92	25.48491
43	-0.5384	-0.51327	0.275231	-0.69513		42	-0.53642	5.680915	-2.3254	-2.85968		42	30.81802		93	25.42276
44	-0.7526	-0.19677	0.580367	0.469687		43	0.94491	-0.24962	-0.64296	-0.10194		43	30.39143		94	25.36988
45	-0.31436	-0.31376	0.208248	-0.48259		44	0.017212	-0.40054	-0.67838	1.07794		44	30.08377		95	25.31977
46	-2.70241	-8.03911	3.53863	-0.90179		45	0.519718	-0.0879	-0.26173	-0.16702		45	29.4925		96	25.30538
47	-0.81809	-1.14743	-0.55372	-0.07128		46	-5.23832	0.36472	7.046755	-2.20322		46	29.06868		97	25.28485
48	-1.26864	0.681784	1.139099	0.180639		47	0.852914	0.686429	-1.1351	-0.4126		47	28.81431		98	25.2654
49	-2.6582	-4.05517	1.678919	-7.56684		48	0.248428	1.126368	-1.43752	0.072763		48	28.79908		99	25.24534
50	1.708674	1.706987	-0.10528	-1.57422		49	5.615195	-0.08114	-4.99185	-0.51698		49	28.59414		100	25.22594
						50	-0.73636	-1.82272	1.159114	1.395343		50	28.20952			

Figure 49: Neural network model spread sheet of a cored well (API: 15-093-20011).

Number of predictor variables:	4														
Number of hidden-layer nodes	75														
Categorical response variable:	Facies														
Number of categories:	6														
Continuous response variable:	[NONE]														
Predictor	Mean	Standard deviation													
DENSITY	6.465129	10.74541													
GR	33.41137	10.55048													
NEUTRON	4.644883	6.150349													
SONIC	56.3656	6.131595													
Input-to-hidden layer weights															
Node	Constant	DENSITY	GR	NEUTRON	SONIC	Node	1	2	3	4	5	6	Iteration history	Iteration	Objective function
1	-0.19552	-0.15647	0.252433	-0.87133	0.026433	Constant	-0.16522	0.161284	0.083542	-0.04018	-0.06216	0.023001		0	912.0047
2	0.144341	0.039974	-0.37796	0.812315	0.036103	1	-0.28165	-0.04098	0.694394	-0.28459	-0.53307	0.445207		1	753.2121
3	0.287041	0.053813	-0.42482	1.008598	0.043336	2	0.040636	0.229921	-0.54572	0.324691	0.437148	-0.4859		2	691.5016
4	0.036349	0.004614	-0.38632	-0.8017	0.245084	3	0.183169	0.237779	-0.75229	0.404071	0.523449	-0.59603		3	576.6585
5	-0.3157	-0.17274	0.335079	-0.99829	0.009556	4	0.003296	-0.03184	0.806161	0.020209	-0.5873	-0.21021		4	523.7582
6	0.02091	-0.09543	-0.60601	-0.55034	0.115859	5	-0.3505	-0.05319	0.775968	-0.3541	-0.60495	0.58765		5	469.0801
7	0.19167	0.006918	-0.35121	0.796394	0.030539	6	-0.06512	0.106921	0.611238	0.266573	-0.55997	-0.35827		6	416.3124
8	0.291717	0.027959	-0.41032	0.966669	0.02003	7	0.023659	0.237768	-0.52977	0.318763	0.427491	-0.4779		7	276.3732
9	-0.21662	-0.13459	0.393122	-0.92004	-0.02097	8	0.142982	0.242488	-0.71641	0.416826	0.47417	-0.56095		8	241.0309
10	0.026212	-0.09485	-0.40664	-0.80228	0.226163	9	-0.23888	-0.08528	0.693606	-0.3784	-0.53161	0.54034		9	208.7843
11	-0.17986	-0.16903	0.321421	-0.84061	-0.0448	10	-0.18133	0.087937	0.825665	0.064886	-0.61231	-0.18471		10	198.4271
12	0.163535	0.029042	-0.35729	0.879458	0.018057	11	-0.21384	-0.06202	0.588669	-0.27587	-0.53807	0.500111		11	190.3485
13	0.982583	-0.16801	-0.54913	2.212866	-0.00111	12	0.075297	0.227188	-0.62364	0.351335	0.464194	-0.49434		12	180.8281
14	-0.55439	-0.20768	1.139672	0.681024	-0.02502	13	0.391347	0.778549	-1.84486	1.049154	0.530062	-0.90405		13	174.3241
15	0.126685	0.213717	-0.21849	1.059102	0.005864	14	-0.68961	0.129519	-0.72503	-0.20009	0.736727	0.748497		14	164.846
16	0.039541	0.362513	-0.07221	0.601407	0.205525	15	0.306019	0.174798	-0.83716	0.186294	0.639537	-0.47009		15	154.1775
17	-0.1458	-0.15298	0.327813	-0.89109	-0.02349	16	0.320688	0.106302	-0.36016	-0.11668	0.466999	-0.41555		16	147.151
18	-0.02047	2.335562	1.775353	1.162283	2.254586	17	-0.24604	-0.03721	0.658839	-0.34129	-0.54924	0.515634		17	146.3208
19	-0.0621	0.104671	0.557334	0.502662	-0.05258	18	1.600763	0.848479	0.801319	-3.26239	0.472916	-0.46034		18	141.5597
20	0.348254	-0.02373	-0.41034	1.117357	-0.02922	19	-0.0183	0.002764	-0.46714	-0.31487	0.512927	0.284131		19	137.1369
21	0.054877	-0.10441	-0.60463	-0.66335	0.142414	20	0.134023	0.298824	-0.88793	0.462465	0.559211	-0.56801		20	133.9737
22	0.219743	0.010977	-0.40394	0.93424	0.006924	21	-0.07092	0.104229	0.712793	0.240413	-0.63581	-0.35122		21	125.7119
23	-0.255	1.127018	0.448393	0.515499	0.922326	22	0.084843	0.23294	-0.67569	0.398671	0.486648	-0.52863		22	122.1514
24	-0.18874	-0.14995	0.340223	-0.77477	-0.05134	23	0.759351	0.087433	0.291635	-1.09589	0.57524	-0.61674		23	116.6779
25	0.216078	-0.8838	-0.26456	-0.52322	-0.52117	24	-0.18181	-0.05428	0.521279	-0.28801	-0.49805	0.502049		24	113.9059
26	-0.27639	1.563349	0.766265	0.75009	1.521379	25	-0.67498	0.126272	0.090814	0.654367	-0.66478	0.46715		25	111.7928
27	0.230872	0.013011	-0.38962	0.877005	0.015699	26	0.969345	0.267689	0.800573	-1.74418	0.582538	-0.87686		26	110.107
28	0.044197	-0.09905	-0.62624	-0.333378	0.077491	27	0.078678	0.249028	-0.62673	0.384693	0.431115	-0.51626		27	108.6733
29	-0.00457	-0.33636	-0.11116	-0.60567	-0.04222	28	0.046549	0.162672	0.326603	0.305701	-0.43481	-0.40694		28	106.8774
30	0.055693	-0.0619	-0.62245	-0.48168	0.104693	29	-0.25725	-0.00679	0.462278	0.148456	-0.56485	0.21772		29	105.4231
31	0.262089	0.043156	-0.39346	0.958498	0.030229	30	0.054027	0.09209	0.506639	0.285388	-0.54918	-0.38979		30	103.9495
32	-3.731	-0.22267	-1.76615	-4.46291	-2.45872	31	0.152362	0.25683	-0.71846	0.383689	0.488524	-0.56382		31	102.4292
33	0.188278	-0.66823	-0.18514	-0.53294	-0.38342	32	-1.9895	0.95261	4.791097	-3.50285	-0.0915	-0.16066		32	101.6223
														108	91.28639

34	0.285617	-0.05017	-0.40065	0.95027	0.00168		33	-0.52634	0.067704	0.212347	0.478842	-0.62012	0.386603		33	100.8616		109	91.27128
35	0.201704	0.151376	-0.36887	0.9108	0.063372		34	0.024811	0.284633	-0.68976	0.467516	0.452547	-0.53902		34	100.3683		110	91.25816
36	0.277634	-0.04953	-0.41131	1.073471	-0.00975		35	0.261499	0.17033	-0.68772	0.315158	0.502801	-0.56283		35	99.56138		111	91.2527
37	0.024776	0.231688	-0.12403	0.58517	0.152078		36	0.074049	0.300714	-0.79266	0.468938	0.513907	-0.56554		36	99.16173		112	91.24178
38	0.156491	0.196505	-0.27654	0.714758	0.113848		37	0.156078	0.134467	-0.32018	-0.01018	0.428723	-0.38822		37	98.54467		113	91.23593
39	-0.23993	-0.12317	0.414258	-0.96482	-0.03506		38	0.212078	0.167485	-0.46163	0.15754	0.423167	-0.49855		38	97.92447		114	91.22696
40	-0.05883	0.039062	0.103156	-0.87408	0.146539		39	-0.22714	-0.10792	0.701005	-0.38429	-0.55346	0.571012		39	97.52157		115	91.21844
41	1.034918	0.58568	-1.76824	-0.8549	-0.29483		40	-0.00688	-0.11487	0.687035	-0.23556	-0.54063	0.210691		40	97.02346		116	91.21286
42	-2.15552	-1.46643	0.094738	-5.33082	2.578813		41	1.547474	-0.33082	0.798833	0.08665	-1.00415	-1.0967		41	96.63317		117	91.20669
43	2.172565	-1.05396	-0.8474	4.085503	0.732364		42	-3.72749	-1.84042	4.886415	0.185866	-0.37489	0.870487		42	96.37624		118	91.20047
44	-0.25261	0.987208	0.364163	0.483979	0.710271		43	-0.20664	2.366095	-3.34263	2.195458	0.371436	-1.38499		43	96.04342		119	91.19524
45	0.179018	-0.9409	-0.36389	-0.48284	-0.53957		44	0.705732	0.004928	0.115327	-0.88474	0.580413	-0.5225		44	95.95082		120	91.19144
46	0.167431	0.178787	-0.31021	0.813482	0.098079		45	-0.76208	0.154466	0.076268	0.754553	-0.63283	0.409022		45	95.50832		121	91.18655
47	0.08017	0.562676	-2.35712	1.02564	3.862894		46	0.227276	0.161863	-0.55494	0.218195	0.482251	-0.53585		46	95.13099		122	91.18103
48	0.141916	0.137941	-0.28614	0.865175	0.055322		47	1.029714	-2.87257	-0.92431	2.84744	-0.03897	-0.04149		47	94.82736		123	91.17719
49	-0.00927	-0.17366	-0.51314	-0.581	0.109428		48	0.21079	0.155203	-0.63804	0.250252	0.519887	-0.49803		48	94.65401		124	91.17344
50	0.261123	-1.45683	-0.5878	-0.6111	-1.14908		49	-0.17544	0.107458	0.615588	0.238981	-0.5824	-0.20446		49	94.44734		125	91.16938
51	0.280381	0.04964	-0.42339	1.026758	0.010364		50	-1.02712	0.009906	-0.48496	1.389565	-0.64125	0.75517		50	94.22045			
52	-0.23641	-0.02892	0.389109	-1.04308	0.02229		51	0.167415	0.239979	-0.77717	0.413648	0.525916	-0.57146		51	94.09909			
53	0.15824	-0.03736	-0.35146	0.720566	0.015191		52	-0.13894	-0.15212	0.807535	-0.45453	-0.5784	0.516646		52	94.0069			
54	0.074267	0.247362	-0.16384	0.574824	0.160005		53	-0.05809	0.246072	-0.4652	0.351588	0.350756	-0.42487		53	93.89296			
55	-0.19761	-0.1427	0.422048	-0.978	-0.0537		54	0.167304	0.114694	-0.322	0.031158	0.455471	-0.44714		54	93.77786			
56	0.288213	-0.00769	-0.38662	1.048204	-0.00568		55	-0.25144	-0.05886	0.703381	-0.40923	-0.5657	0.580775		55	93.66791			
57	-3.27565	-0.47666	1.849504	2.422413	-6.34235		56	0.11099	0.258565	-0.80895	0.454072	0.520525	-0.53537		56	93.61227			
58	0.022335	0.132578	0.401192	0.269643	0.031084		57	0.02455	-0.058893	-2.02511	4.193777	0.755721	2.140775		57	93.52146			
59	-0.12516	0.256783	0.006722	0.401936	0.214724		58	0.030179	0.016241	-0.21713	-0.31579	0.332105	0.154554		58	93.51663			
60	0.106568	-0.06493	-0.64791	-0.52449	0.105209		59	0.075549	0.101602	0.13044	-0.13158	0.377343	-0.29135		59	93.38705			
61	0.408997	2.832869	-2.94731	1.799127	1.080725		60	0.072897	0.080766	0.557917	0.292989	-0.57989	-0.42572		60	93.33623			
62	-0.0933	-0.14371	-0.40402	-0.80585	0.20211		61	-1.86853	-1.07656	-1.24939	3.471547	0.778472	-0.05469		61	93.26815			
63	-0.17791	-0.04117	0.358408	-0.93727	-0.00733		62	-0.2714	0.092013	0.813836	0.11474	-0.60635	-0.14231		62	93.21763			
64	-0.08963	0.991776	0.090868	4.697717	-6.92654		63	-0.10927	-0.1225	0.674517	-0.37961	-0.54829	0.48451		63	93.11817			
65	-0.17677	0.691613	0.229813	0.417289	0.499461		64	5.657941	0.42704	-4.62755	-3.10684	0.040318	1.609614		64	93.03289			
66	0.031967	-0.10317	-0.59655	-0.6508	0.149575		65	0.462275	0.031332	-0.00091	-0.57969	0.501977	-0.41533		65	92.94656			
67	-0.2733	-0.15747	0.394248	-1.06346	-0.01154		66	-0.07315	0.081931	0.690486	0.246092	-0.61962	-0.32583		66	92.92538			
68	0.026041	0.177361	-0.10841	0.8199	0.017448		67	-0.36296	-0.09263	0.859127	-0.40703	-0.5902	0.594797		67	92.81532			
69	-0.08958	0.558885	0.135758	0.413625	0.410748		68	0.213804	0.138005	-0.63791	0.100393	0.558014	-0.37187		68	92.73765			
70	-0.18384	-0.09054	0.379887	-0.93796	-0.02058		69	0.391662	0.046264	-0.05501	-0.42894	0.463905	-0.41749		69	92.68833			
71	0.029236	-0.11639	-0.53151	-0.70726	0.184377		70	-0.16458	-0.12383	0.686035	-0.37552	-0.54751	0.525111		70	92.57714			
72	0.809546	0.252476	-4.20598	-0.9664	0.744982		71	-0.16206	0.105526	0.760343	0.187657	-0.62355	-0.26665		71	92.49653			
73	0.157342	0.137076	-0.32105	0.745841	0.084404		72	3.563575	-0.29472	0.573152	-2.33823	-1.19022	-0.31269		72	92.4555			
74	-0.32184	0.080197	0.445042	-1.35114	0.063958		73	0.177766	0.18985	-0.49674	0.229318	0.417764	-0.51736		73	92.37096			
75	1.481132	-0.54984	-0.63485	3.102974	0.181651		74	-0.11526	-0.2544	1.088717	-0.62258	-0.69172	0.594424		74	92.31451			
							75	0.24247	1.375286	-2.58971	1.599131	0.458245	-1.08512		75	92.31254			

Figure 50: Neural network model spread sheet of a cored well (API: 15-093-20147).



5	4881	0.002074	0.002833	2.61E-13	0.013506	0.981587	2.69E-12	5 Facies 5	0.9815869	2.11E-10	1.92E-11	1.68E-33	0.000797	0.923667	6.8E-18	2.29E-10	2.07E-11	1.82E-33	0.00086	0.999138	7.36E-18	5 Facies 5	0.999138002
5	4881.5	0.000398	0.000511	2.11E-15	0.003097	0.995994	7.35E-14	5 Facies 5	0.9959937	9.9E-08	4.84E-09	8.49E-37	0.000182	0.937093	7.27E-20	1.06E-07	5.16E-09	9.06E-37	0.00019	0.999805	7.75E-20	5 Facies 5	0.999805333
5	4882	0.000199	0.000197	1.49E-16	0.001241	0.998363	8.4E-15	5 Facies 5	0.9983632	0.000108	2.21E-08	3.18E-36	3.19E-05	0.41947	2.03E-21	0.000257	5.26E-06	7.57E-36	7.6E-05	0.999661	4.83E-21	5 Facies 5	0.999661218
5	4882.5	0.023235	0.003648	3.14E-13	0.010786	0.962332	5.79E-13	5 Facies 5	0.9623318	0.022406	6.4E-05	2.29E-30	7.4E-07	0.017379	1.02E-20	0.562258	0.001606	5.74E-29	1.9E-05	0.436117	2.56E-19	1 Facies 1	0.562257716
1	4883	0.911977	0.017053	5.32E-08	0.025509	0.045462	2.38E-10	1 Facies 1	0.9119769	0.880073	0.000301	4.09E-22	1.2E-06	0.000786	7.71E-17	0.998765	0.000342	4.65E-22	1.4E-06	0.000892	8.75E-17	1 Facies 1	0.998765201
1	4883.5	0.935633	0.014912	0.000105	0.046333	0.003017	4.31E-08	1 Facies 1	0.9356331	0.894689	0.000391	3.83E-15	2.23E-05	5.15E-05	3.75E-14	0.999481	0.000436	4.28E-15	2.5E-05	5.76E-05	4.19E-14	1 Facies 1	0.999481075
1	4884	0.843295	0.129695	0.003874	0.022937	0.000151	4.8E-05	1 Facies 1	0.8432955	0.776863	0.0075	6.86E-12	5.27E-05	2.49E-06	2.64E-10	0.990391	0.009533	8.72E-12	6.7E-05	3.16E-06	3.36E-10	1 Facies 1	0.99039092
1	4884.5	0.666615	0.255672	0.010143	0.046715	7.28E-05	0.000582	1 Facies 1	0.6668153	0.599436	0.027088	1.1E-10	0.000265	1.13E-06	1.2E-08	0.956359	0.043217	1.76E-10	0.00042	1.81E-06	1.92E-08	1 Facies 1	0.956358631
1	4885	0.725244	0.20345	0.011826	0.058104	8.02E-05	0.001296	1 Facies 1	0.7252435	0.513513	0.053667	4.02E-10	0.000898	1.01E-06	6.94E-08	0.903946	0.09447	7.08E-10	0.00158	1.79E-06	1.22E-07	1 Facies 1	0.903946153
1	4885.5	0.577596	0.300722	0.038129	0.081074	9.62E-05	0.002393	1 Facies 1	0.5775957	0.330911	0.118474	1.26E-09	0.00183	9.85E-07	1.69E-07	0.733343	0.262554	2.8E-09	0.0041	2.18E-06	3.75E-07	1 Facies 1	0.73334021
1	4886	0.369055	0.431156	0.092164	0.104885	9.92E-05	0.002641	2 Facies 2	0.4311555	0.226656	0.153174	5.19E-10	0.00208	1.09E-06	1.46E-07	0.593372	0.401176	1.36E-09	0.00545	2.85E-06	3.81E-07	1 Facies 1	0.593371859
1	4886.5	0.188507	0.612341	0.06191	0.13645	7.4E-05	0.000718	2 Facies 2	0.612341	0.156908	0.088831	1.31E-11	0.001046	1.1E-06	1.65E-08	0.635805	0.359591	5.33E-11	0.00424	4.46E-06	6.69E-08	1 Facies 1	0.635805496
1	4887	0.176763	0.593186	0.009706	0.220147	7.5E-05	0.000123	2 Facies 2	0.5931857	0.165731	0.026168	9.72E-14	0.00034	1.26E-06	4.89E-10	0.8621	0.136123	5.06E-13	0.00177	6.53E-06	2.54E-09	1 Facies 1	0.862099776
1	4887.5	0.365727	0.402218	0.000546	0.231379	9.24E-05	3.75E-05	2 Facies 2	0.4022181	0.349926	0.010312	7.34E-16	0.00111	1.58E-06	4.33E-11	0.971073	0.286616	2.04E-15	0.00031	4.38E-06	1.2E-10	1 Facies 1	0.971073143
1	4888	0.540274	0.240581	2.79E-05	0.229011	9.52E-05	1.08E-05	1 Facies 1	0.5402743	0.519888	0.004691	2.54E-18	4.66E-05	1.64E-06	0.990097	0.008941	4.84E-18	8.9E-05	3.12E-06	1.61E-11	1 Facies 1	0.990096728	
1	4888.5	0.572837	0.097635	6.78E-07	0.329419	0.000107	1.43E-06	1 Facies 1	0.5728368	0.55218	0.00183	4.67E-21	3.35E-05	1.84E-06	6.05E-13	0.996633	0.003303	8.43E-21	6.1E-05	3.33E-06	1.09E-12	1 Facies 1	0.996633485
1	4889	0.753494	0.058794	4.3E-08	0.187548	0.000164	5.04E-07	1 Facies 1	0.7534949	0.725551	0.001161	2.69E-22	2.36E-05	2.81E-06	6.01E-14	0.998366	0.001598	3.7E-22	3.3E-05	3.87E-06	8.26E-14	1 Facies 1	0.998365853
1	4889.5	0.844844	0.106405	5.59E-08	0.048078	0.000671	2.46E-06	1 Facies 1	0.8448443	0.812851	0.002177	2.17E-21	4.74E-06	1.16E-05	6.11E-14	0.997306	0.002671	2.67E-21	9.2E-06	1.42E-05	7.5E-14	1 Facies 1	0.997305789
1	4890	0.810678	0.149381	6.08E-07	0.036309	0.003541	9.05E-05	1 Facies 1	0.8106784	0.782011	0.002688	4.21E-17	1.5E-06	6.13E-05	3.65E-13	0.9966494	0.003426	5.37E-17	1.9E-06	7.82E-05	4.66E-13	1 Facies 1	0.996649355
1	4890.5	0.937207	0.041859	2.05E-05	0.012152	0.005263	0.003499	1 Facies 1	0.9372068	0.904531	0.000733	4.29E-13	2.33E-07	9.12E-05	7.48E-10	0.990989	0.00081	4.73E-13	2.6E-07	0.000101	8.26E-10	1 Facies 1	0.990089132
1	4891	0.904303	0.01433	0.000699	0.005884	0.005047	0.0069736	1 Facies 1	0.9043034	0.872323	0.000257	1.89E-10	4.4E-07	8.75E-05	2.17E-07	0.999604	0.000295	2.17E-10	5E-07	0.0001	2.49E-07	1 Facies 1	0.99960415
1	4891.5	0.678717	0.203555	0.006499	0.033949	0.004411	0.025317	1 Facies 1	0.6787169	0.652154	0.0005	3.85E-09	2.32E-05	7.08E-05	2.07E-06	0.999087	0.000766	5.9E-09	3.5E-05	0.000108	3.18E-06	1 Facies 1	0.999086628
1	4892	0.51692	0.066968	0.018452	0.227549	0.002287	0.167825	1 Facies 1	0.5169197	0.491349	0.0021	2.12E-07	0.000246	3.89E-05	1.01E-06	0.995166	0.004254	4.29E-07	0.0005	7.88E-05	2.05E-06	1 Facies 1	0.995165638
1	4892.5	0.502178	0.209829	0.024118	0.232822	0.000885	0.024708	1 Facies 1	0.5021781	0.475721	0.00727	5.63E-06	0.000208	1.05E-05	1.3E-07	0.98448	0.0150455	1.17E-05	0.00043	3.1E-05	2.68E-07	1 Facies 1	0.984479505
1	4893	0.564236	0.34526	0.022272	0.06636	0.000195	0.01677	1 Facies 1	0.5642361	0.5345	0.010099	0.000129	3.88E-05	3.29E-06	0.981147	0.018538	0.000237	7.1E-05	6.04E-06	4.38E-07	1 Facies 1	0.981147092	
1	4893.5	0.609533	0.320255	0.024424	0.044671	0.000128	0.000989	1 Facies 1	0.6095326	0.497104	0.006533	0.002999	1.21E-05	1.86E-06	0.981126	0.012895	0.0059	2.4E-05	3.68E-06	5.25E-05	1 Facies 1	0.98112554	
1	4894	0.527662	0.308641	0.072067	0.085784	0.000219	0.0056228	1 Facies 1	0.5276623	0.097662	0.000713	0.014141	3.87E-07	4.84E-07	0.003456	0.842104	0.006149	0.121936	3.3E-06	4.17E-06	0.029804	1 Facies 1	0.842104013
6	4894.5	0.174458	0.122831	0.169999	0.425501	0.000162	0.106549	4 Facies 4	0.425501	0.015211	1.21E-05	0.016278	3.09E-09	5.64E-08	0.087035	0.128232	0.000102	0.137328	2.6E-08	5.52E-07	0.734246359	6 Facies 6	0.734246359
6	4895	0.040183	0.007854	0.059769	0.160774	0.000533	0.692958	6 Facies 6	0.6929576	0.003361	8.92E-08	0.008415	3.45E-11	6.07E-09	0.575291	0.005726	1.52E-07	0.014333	5.9E-11	1.03E-08	0.979941	6 Facies 6	0.979940868
6	4895.5	0.006312	0.000188	0.029224	0.001103	9.84E-05	0.963075	6 Facies 6	0.963075	0.000528	2.32E-09	0.002541	7.82E-14	1.21E-09	0.798786	0.000658	2.89E-09	0.003169	9.8E-14	1.51E-09	0.996173	6 Facies 6	0.996173171
6	4896	0.066687	4E-05	0.028446	1.71E-05	5.96E-05	0.964567	6 Facies 6	0.9645670	0.000558	4.23E-10	0.003186	6.96E-16	6.3E-10	0.778186	0.000713	5.41E-10	0.004074	8.9E-16	8.06E-10	0.995212664	6 Facies 6	0.995212664
6	4896.5	0.060602	3.6E-05	0.045506	1.25E-05	6.4E-05	0.94833	6 Facies 6	0.9483295	0.000337	1.51E-10	0.017501	3.14E-16	2.69E-10	0.530836	0.000614	2.76E-10	0.031896	5.7E-16	4.9E-10	0.96749	6 Facies 6	0.967490039
6	4897	0.003645	6.54E-05	0.086753	7.62E-05	7.95E-05	0.909382	6 Facies 6	0.9093818	5.24E-05	4.68E-11	0.071883	4.07E-15	5.69E-11	0.142807	0.000244	2.18E-10	0.33474	1.9E-14	2.65E-10	0.665016	6 Facies 6	0.66501626
6	4897.5	0.003727	0.000452	0.14909	0.000504	0.000155	0.841542	6 Facies 6	0.8415424	7.19E-06	1.4E-10	0.143524	3.57E-13	4.78E-11	0.029791	4.15E-05	8.08E-08	0.280705	2.1E-12	2.76E-10	0.171884	3 Facies 3	0.828074688
6	4898	0.021124	0.009572	0.426616	0.059561	0.000657	0.48607	6 Facies 6	0.4860696	7.66E-06	2.67E-10	0.417851	5.1E-13	4.29E-11	0.00811	1.79E-05	1.47E-09	0.077042	1.2E-12	1E-10	0.02294	3 Facies 3	0.9770441848
3	4898.5	0.034525	0.035445	0.72443	0.027668	0.001326	0.176606	3 Facies 3	0.7244301	2.71E-06	1.42E-10	0.711744	3.83E-14	5.26E-12	0.003079	3.79E-06	1.98E-10	0.995689	5.4E-14	7.37E-12	0.004307	3 Facies 3	0.995689178
3	4899	0.009742	0.055676	0.86792	0.018107	0.00																	

3	4906	0.00049	0.024427	0.973558	0.00061	0.000111	0.000805	3 Facies 3	0.9735579	3.07E-10	1.94E-14	0.957325	7.28E-19	8.49E-17	1.34E-05	3.21E-10	2.03E-14	0.999986	7.6E-19	8.87E-17	1.4E-05	3 Facies 3	0.999985988
3	4906.5	0.000256	0.037139	0.951047	0.011096	3.92E-05	0.000422	3 Facies 3	0.9510472	4.16E-11	2.56E-14	0.935195	2.95E-18	2.68E-17	7.04E-06	4.45E-11	2.73E-14	0.999992	3.2E-18	2.87E-17	7.52E-06	3 Facies 3	0.999992477
3	4907	0.000827	0.03167	0.946007	0.021375	1.34E-05	0.000109	3 Facies 3	0.9460067	3.69E-11	4.5E-15	0.930239	5.24E-17	1.5E-18	1.81E-06	3.97E-11	4.84E-15	0.999998	5.6E-17	1.62E-18	1.95E-06	3 Facies 3	0.999998052
3	4907.5	0.000238	0.010187	0.983061	0.006481	1.67E-06	3.11E-05	3 Facies 3	0.9830613	6.3E-12	3.02E-14	0.966677	1.07E-15	3.23E-19	5.18E-07	6.51E-12	3.12E-14	0.999999	1.1E-15	3.34E-19	5.35E-07	3 Facies 3	0.999999465
3	4908	9.22E-05	0.006193	0.991719	0.001976	3.99E-07	1.85E-05	3 Facies 3	0.9917191	1.1E-11	2.82E-12	0.975189	3.91E-14	1.6E-17	3.09E-07	1.12E-11	2.89E-12	1	4E-14	1.65E-17	3.17E-07	3 Facies 3	0.999999683
3	4908.5	0.001061	0.02196	0.97363	0.003266	1.51E-06	8.03E-05	3 Facies 3	0.9736302	2.23E-09	4.16E-10	0.957388	8.81E-13	1.97E-14	1.34E-06	2.33E-09	4.34E-10	0.999999	9.2E-13	2.06E-14	1.4E-06	3 Facies 3	0.999998599
3	4909	0.015814	0.05605	0.921164	0.006087	8E-06	0.000876	3 Facies 3	0.9211643	6.83E-07	5.61E-09	0.905432	1.18E-13	7.97E-13	1.49E-05	7.54E-07	6.2E-09	0.999983	1.3E-13	8.81E-13	1.65E-05	3 Facies 3	0.999982761
3	4909.5	0.01859	0.033486	0.891835	0.035617	4.65E-05	0.020425	3 Facies 3	0.8918352	5.06E-06	3.89E-10	0.874357	1.01E-14	5.4E-13	0.000395	5.78E-06	4.45E-10	0.999543	1.1E-14	6.17E-13	0.000451	3 Facies 3	0.999542966
3	4910	0.006235	0.011839	0.734172	0.112434	0.000118	0.135202	3 Facies 3	0.7341717	4.87E-07	4.6E-12	0.721316	1.79E-15	4.57E-14	0.002357	6.73E-07	6.35E-12	0.996743	2.5E-15	6.32E-14	0.003257	3 Facies 3	0.99674252
3	4910.5	0.001678	0.013047	0.886548	0.068877	9.47E-05	0.047755	3 Facies 3	0.8685477	1.92E-08	3.04E-12	0.853964	2.51E-16	2.22E-15	0.000801	2.25E-08	3.56E-13	0.990663	2.9E-16	2.57E-15	0.000937	3 Facies 3	0.999662548
3	4911	0.000517	0.01738	0.948355	0.026019	4.86E-05	0.007681	3 Facies 3	0.9483552	1.26E-09	7.47E-14	0.932524	1.35E-16	2.03E-16	1.35E-09	8.01E-14	0.999863	1.5E-16	2.18E-16	0.000137	3 Facies 3	0.999862545	
3	4911.5	0.000315	0.018375	0.963727	0.01591	1.59E-05	0.001657	3 Facies 3	0.9637273	2.3E-10	1.13E-12	0.947658	2.8E-17	9.71E-17	2.76E-05	2.43E-10	1.19E-13	0.999971	3E-17	1.02E-16	2.91E-05	3 Facies 3	0.999970853
3	4912	0.000324	0.014389	0.97842	0.006355	5.81E-06	0.000505	3 Facies 3	0.9784203	3.4E-10	3.89E-14	0.962102	1.19E-18	1.57E-17	8.42E-06	3.53E-10	4.04E-14	0.999991	1.2E-18	1.63E-17	8.76E-06	3 Facies 3	0.999991245
3	4912.5	0.000107	0.006573	0.986974	0.005611	3.25E-06	0.000732	3 Facies 3	0.9869742	1.52E-10	4.17E-16	0.970513	1.73E-19	2.06E-18	1.22E-05	1.56E-10	4.29E-15	0.999987	1.8E-19	2.12E-18	1.26E-05	3 Facies 3	0.999987472
3	4913	5.75E-05	0.003266	0.991545	0.004134	2.31E-06	0.000995	3 Facies 3	0.9915455	3.58E-11	6.89E-16	0.975013	4.56E-20	4.86E-19	1.66E-05	3.67E-11	7.06E-16	0.999983	4.7E-20	4.98E-19	1.7E-05	3 Facies 3	0.999982938
3	4913.5	3.15E-05	0.002242	0.995684	0.001598	1.46E-06	0.000443	3 Facies 3	0.9956838	1.2E-11	2.47E-16	0.979085	4.06E-20	1.6E-19	7.38E-06	1.22E-11	2.52E-16	0.999992	4.1E-20	1.64E-19	7.54E-06	3 Facies 3	0.999992459
3	4914	1.6E-05	0.002067	0.996191	0.001458	1.17E-06	0.000267	3 Facies 3	0.9961908	6.23E-12	5.65E-16	0.979583	2.74E-19	3.16E-19	4.46E-06	6.36E-12	5.77E-16	0.999995	2.8E-19	3.23E-19	4.55E-06	3 Facies 3	0.999995449
3	4914.5	3.71E-05	0.004823	0.991581	0.003284	2.14E-06	0.000274	3 Facies 3	0.9915806	1.52E-11	3.99E-15	0.97505	9.73E-18	1.63E-18	4.56E-06	1.09E-15	0.999995	1E-17	1.68E-18	4.68E-06	3 Facies 3	0.999995323	
3	4915	0.000116	0.013334	0.976947	0.009316	3.86E-06	0.000284	3 Facies 3	0.9769466	4.26E-11	6.26E-14	0.96066	1.26E-16	1.7E-17	4.74E-06	4.43E-11	6.51E-14	0.999995	1.3E-16	1.77E-17	4.93E-06	3 Facies 3	0.999995069
3	4915.5	0.000777	0.035869	0.948417	0.014684	6.11E-06	0.000247	3 Facies 3	0.9484169	2.38E-10	2.85E-13	0.932607	2.3E-16	4.65E-17	4.12E-06	2.55E-10	3.06E-13	0.999996	2.5E-16	4.99E-17	4.42E-06	3 Facies 3	0.999995582
3	4916	0.002661	0.070903	0.905656	0.020576	7.94E-06	0.000196	3 Facies 3	0.9056562	3.93E-10	3.15E-13	0.89056	2.89E-16	3.29E-17	3.27E-06	4.42E-10	3.53E-13	0.999996	3.2E-16	3.69E-17	3.67E-06	3 Facies 3	0.999996328
3	4916.5	0.001935	0.058568	0.919148	0.020257	5.57E-06	9.6E-05	3 Facies 3	0.9191477	2.17E-10	2.83E-13	0.903827	3.74E-16	2.47E-17	1.6E-06	2.4E-10	3.13E-13	0.999998	4.1E-16	2.74E-17	1.77E-06	3 Facies 3	0.999998229
3	4917	0.001458	0.041974	0.941377	0.015111	4.46E-06	7.45E-05	3 Facies 3	0.9413774	2.38E-10	3.85E-13	0.925686	3.38E-16	3.88E-17	1.24E-06	2.58E-10	4.16E-13	0.999999	3.6E-16	4.19E-17	1.34E-06	3 Facies 3	0.999998658
3	4917.5	0.001941	0.040395	0.946208	0.011342	5.82E-06	0.000109	3 Facies 3	0.9462078	4.69E-10	4.76E-13	0.930435	1.12E-16	6.73E-17	1.82E-06	5.04E-10	5.11E-13	0.999998	1.2E-16	7.23E-17	1.96E-06	3 Facies 3	0.999998043
3	4918	0.0029	0.041739	0.946178	0.009014	8.35E-06	0.000161	3 Facies 3	0.9461777	6.24E-10	2.1E-13	0.930406	2.76E-17	4.15E-17	2.69E-06	7.6E-10	2.26E-13	0.999997	3E-17	4.46E-17	2.89E-06	3 Facies 3	0.999997107
3	4918.5	0.001463	0.023309	0.970772	0.004303	4.8E-06	0.000148	3 Facies 3	0.9707723	2.75E-10	6.69E-14	0.954591	7E-18	1.36E-17	2.46E-06	2.88E-10	7.01E-14	0.999997	7.3E-18	1.42E-17	2.58E-06	3 Facies 3	0.999997422
3	4919	0.000782	0.014049	0.98266	0.020394	2.69E-06	0.000131	3 Facies 3	0.9826003	1.59E-10	3.59E-14	0.966222	9.87E-18	6.62E-18	2.18E-06	1.65E-10	3.72E-14	0.999998	1E-17	6.85E-18	2.25E-06	3 Facies 3	0.999997748
3	4919.5	0.000553	0.013388	0.982833	0.026032	1.98E-06	0.000141	3 Facies 3	0.9832827	1.38E-10	8.93E-14	0.966892	1.03E-16	1.15E-17	2.36E-06	1.43E-10	9.24E-14	0.999998	1.1E-16	1.19E-17	2.44E-06	3 Facies 3	0.999997563
3	4920	0.002125	0.018549	0.977266	0.002796	2.61E-06	0.000173	3 Facies 3	0.9772655	3.25E-10	8.47E-13	0.960975	6.76E-16	1.05E-16	2.88E-06	3.38E-10	8.81E-13	0.999997	7E-16	1.1E-16	2.99E-06	3 Facies 3	0.999997007
3	4920.5	0.006488	0.043452	0.94517	0.0040708	5.25E-06	0.000177	3 Facies 3	0.9451697	2.18E-09	5.13E-12	0.929413	1.71E-15	5.77E-16	2.96E-06	2.34E-09	5.52E-12	0.999997	1.8E-15	6.21E-16	3.18E-06	3 Facies 3	0.999996816
3	4921	0.013383	0.069945	0.980719	0.007733	7.35E-06	0.000212	3 Facies 3	0.9087193	5.7E-09	7.45E-12	0.89357	1.52E-15	7.51E-16	3.53E-06	6.38E-09	8.34E-12	0.999996	1.7E-15	8.41E-16	3.95E-06	3 Facies 3	0.999996041
3	4921.5	0.00952	0.045044	0.94138	0.003771	4.73E-06	0.00028	3 Facies 3	0.9413802	5.49E-09	4.16E-12	0.925685	6.77E-16	4.18E-16	4.67E-06	5.93E-09	4.52E-12	0.999995	7.3E-16	4.52E-16	5.05E-06	3 Facies 3	0.999994948
3	4922	0.004974	0.024684	0.987625	0.002324	3.01E-06	0.000391	3 Facies 3	0.9676248	4.89E-09	3.9E-12	0.951488	1.34E-15	4.4E-16	6.52E-06	5.13E-09	4.1E-12	0.999993	1.4E-15	4.62E-16	6.86E-06	3 Facies 3	0.999993139
3	4922.5	0.003475	0.018238	0.974932	0.002681	3.01E-06	0.000671	3 Facies 3	0.9749317	8.11E-09	1.2E-11	0.958659	2.97E-14	1.32E-15	1.12E-05	8.46E-09	1.26E-11	0.999988	3.1E-14	1.38E-15	1.17E-05	3 Facies 3	0.999998303
3	4923	0.003277	0.017502	0.972227	0.005046	4.64E-06	0.001583	3 Facies 3	0.9722275	2.44E-08	2.21E-10	0.95595	9.74E-13	4.05E-14	2.65E-05	2.55E-08	2.31E-10	0.999972	1E-12	4.23E-14	2.77E-05	3 Facies 3	0.9999972265
3	4923.5	0.021529	0.049866	0.907201	0.016851	1.61E-05	0.0004417	3 Facies 3	0.9072012	4.51E-10	3.65E-09	0.891911	2.13E-12	1.13E-12	7.43E-05	5.06E-07	4.09E-09	0.999996	2.4E-12	1.26E-12	8.33E-05	3 Facies 3	0.999991642
3	4924	0.225788	0.148474	0.587246	0.03140																		

4	4932	0.041609	0.062395	0.092933	0.661108	0.000729	0.141226	4 Facies 4	0.661108	1.71E-05	5.27E-08	3.83E-05	0.649581	5.73E-10	0.002346	2.63E-05	8.08E-08	5.87E-05	0.99632	8.78E-10	0.003598	4 Facies 4	0.996316852
4	4932.5	0.131558	0.138434	0.127741	0.46125	0.001539	0.139478	4 Facies 4	0.4612497	2.08E-05	2.83E-08	2.02E-05	0.454434	2.33E-10	0.002017	4.55E-05	6.2E-08	4.42E-05	0.99549	5.1E-10	0.004418	4 Facies 4	0.99549216
4	4933	0.105151	0.199222	0.11071	0.515293	0.001177	0.068447	4 Facies 4	0.515293	4.46E-06	2.85E-08	4.37E-06	0.508368	1.03E-10	0.000914	8.76E-06	5.59E-08	8.58E-06	0.99819	2.02E-10	0.001795	4 Facies 4	0.998187563
4	4933.5	0.13408	0.385739	0.064146	0.401775	0.000634	0.013625	4 Facies 4	0.4017751	2.01E-06	2.31E-08	7.92E-07	0.396498	3.28E-11	0.000179	5.07E-06	5.82E-08	2E-06	0.99954	8.26E-11	0.00045	4 Facies 4	0.999542708
4	4934	0.266286	0.531684	0.025152	0.174648	0.000308	0.001924	2 Facies 2	0.5316841	5.17E-07	1.47E-08	4.55E-08	0.172376	8.2E-13	2.5E-05	3E-06	8.51E-09	2.64E-07	0.99985	4.75E-12	0.000145	4 Facies 4	0.999851607
4	4934.5	0.217627	0.577613	0.027519	0.176796	0.000156	0.000289	2 Facies 2	0.5776134	2.71E-08	1.47E-11	3.4E-09	0.1745	3.86E-15	3.75E-06	1.55E-07	8.44E-11	1.95E-08	0.99998	2.21E-14	2.15E-05	4 Facies 4	0.999978323
4	4935	0.091727	0.34426	0.023136	0.540694	0.000123	6.08E-05	4 Facies 4	0.5406937	7.64E-10	4.54E-13	1.91E-10	0.533672	1.59E-16	7.89E-07	1.43E-09	8.5E-13	3.58E-10	1	2.98E-16	1.48E-06	4 Facies 4	0.99999852
4	4935.5	0.029305	0.095843	0.001758	0.873031	5.66E-05	6.57E-06	4 Facies 4	0.8730307	6.52E-11	1.18E-14	3.9E-12	0.861693	6.88E-18	8.53E-08	7.57E-11	1.37E-14	4.53E-12	1	7.98E-18	9.9E-08	4 Facies 4	0.999999901
4	4936	0.008675	0.046329	0.000419	0.944552	2.38E-05	1.91E-06	4 Facies 4	0.9445519	6.57E-12	1.45E-15	3.16E-13	0.932285	7.23E-19	2.48E-08	7.05E-12	1.56E-15	3.39E-13	1	7.76E-19	2.66E-08	4 Facies 4	0.999999973
4	4936.5	0.039321	0.018021	0.000168	0.977876	1.62E-05	6.74E-07	4 Facies 4	0.9778758	1.7E-12	9.59E-16	7.15E-14	0.965176	8.31E-19	8.75E-09	1.76E-12	9.94E-16	7.41E-14	1	8.61E-19	9.07E-09	4 Facies 4	0.999999991
4	4937	0.004058	0.010787	9.62E-05	0.985039	1.94E-05	3.87E-07	4 Facies 4	0.9850393	2.89E-12	2.06E-15	6.75E-14	0.972247	3.56E-17	5.03E-09	2.97E-12	2.12E-15	6.94E-14	1	3.66E-18	5.17E-09	4 Facies 4	0.999999995
4	4937.5	0.007072	0.01594	0.001403	0.976816	2.78E-05	6.25E-07	4 Facies 4	0.9768157	1.03E-11	7.75E-15	2.04E-13	0.96413	1.25E-17	8.11E-09	1.06E-11	8.04E-15	2.12E-13	1	1.3E-17	8.41E-09	4 Facies 4	0.999999992
4	4938	0.016017	0.02773	0.000266	0.961351	3.4E-05	1.25E-06	4 Facies 4	0.9613515	2.48E-11	3.5E-14	6.05E-13	0.948866	4.02E-17	1.62E-08	2.61E-11	3.69E-14	6.37E-13	1	4.23E-17	1.71E-08	4 Facies 4	0.999999983
4	4938.5	0.017718	0.045002	0.000254	0.936979	4.44E-05	1.94E-06	4 Facies 4	0.9369789	6.34E-11	7.75E-14	8.86E-13	0.92481	7.53E-17	6.52E-08	6.85E-11	8.38E-14	9.58E-13	1	8.14E-17	2.72E-08	4 Facies 4	0.999999973
4	4939	0.024733	0.067916	0.000266	0.907029	5.34E-05	2.88E-06	4 Facies 4	0.9072091	8.79E-11	2.72E-14	9.4E-13	0.895249	2.13E-17	3.74E-08	9.82E-11	3.04E-14	1.05E-12	1	2.38E-17	4.18E-08	4 Facies 4	0.999999958
4	4939.5	0.008475	0.043814	0.001215	0.946459	3.4E-05	3.05E-06	4 Facies 4	0.9464592	2.16E-11	2.11E-15	3.1E-12	0.934168	1.62E-18	3.96E-08	2.31E-11	2.26E-15	3.32E-12	1	1.74E-18	4.24E-08	4 Facies 4	0.999999958
4	4940	0.002028	0.020406	0.042028	0.973341	1.53E-05	2.26E-06	4 Facies 4	0.9733409	2.66E-12	3.94E-16	5.52E-12	0.9607	2.92E-19	2.93E-08	2.77E-12	4.1E-16	5.75E-12	1	3.04E-19	3.05E-08	4 Facies 4	0.999999969
4	4940.5	0.00168	0.013945	0.002284	0.982076	1.27E-05	1.17E-06	4 Facies 4	0.9820761	1.07E-12	2.19E-16	1.46E-12	0.969322	1.98E-19	1.52E-08	1.11E-12	2.26E-16	1.5E-12	1	2.04E-19	1.57E-08	4 Facies 4	0.999999984
4	4941	0.00254	0.012007	0.000616	0.984822	1.39E-05	5.73E-07	4 Facies 4	0.9848224	8.8E-13	1.18E-16	2.13E-13	0.972033	1.36E-19	7.44E-09	9.05E-13	1.21E-16	2.19E-13	1	1.4E-19	7.66E-09	4 Facies 4	0.999999992
4	4941.5	0.003261	0.011018	0.000158	0.985549	1.34E-05	3.11E-07	4 Facies 4	0.9855489	5.53E-13	3.78E-17	2.68E-14	0.97275	4.58E-20	4.04E-09	5.68E-13	3.88E-17	2.76E-14	1	4.7E-20	4.15E-09	4 Facies 4	0.999999996
4	4942	0.003006	0.008701	4.16E-05	0.988241	1.09E-05	1.53E-07	4 Facies 4	0.9882412	1.93E-12	1.35E-17	2.67E-15	0.975407	1.68E-20	1.98E-09	1.39E-13	2.74E-15	1	1.72E-20	2.03E-09	4 Facies 4	0.999999998	
4	4942.5	0.002842	0.005759	8.53E-06	0.991381	9.42E-06	5.8E-08	4 Facies 4	0.9913812	8.79E-14	5.67E-16	2.63E-16	0.978506	9.25E-21	7.54E-10	8.98E-14	5.79E-18	2.69E-16	1	9.45E-21	7.7E-10	4 Facies 4	0.999999999
4	4943	0.002669	0.004187	2.27E-06	0.993133	8.27E-06	2.8E-08	4 Facies 4	0.9931328	5.58E-14	2.2E-18	4.74E-17	0.980235	4.33E-21	3.63E-10	5.69E-14	2.25E-18	4.84E-17	1	4.42E-21	3.7E-10	4 Facies 4	1
4	4943.5	0.001475	0.003104	1.32E-06	0.995415	5.36E-06	1.9E-08	4 Facies 4	0.9954146	2.98E-14	2.9E-18	2.66E-17	0.982487	4.99E-21	2.46E-10	3.03E-14	2.95E-18	2.7E-17	1	5.08E-21	2.51E-10	4 Facies 4	1
4	4944	0.00179	0.003078	1.15E-06	0.995124	6.2E-06	1.83E-08	4 Facies 4	0.9951243	5.3E-14	2.35E-18	3.4E-17	0.982201	4.73E-21	2.38E-10	5.4E-14	2.39E-18	3.46E-17	1	4.81E-21	2.42E-10	4 Facies 4	1
4	4944.5	0.000991	0.002817	3.9E-06	0.996183	5.12E-06	2.69E-08	4 Facies 4	0.9961834	4.35E-14	8.63E-16	1.71E-16	0.983249	1.57E-21	3.49E-10	4.42E-14	8.78E-19	1.74E-16	1	1.59E-21	3.55E-10	4 Facies 4	1
4	4945	0.000633	0.002699	1.15E-05	0.996652	4.48E-06	3.99E-08	4 Facies 4	0.9966562	1.75E-14	3.31E-19	3.18E-16	0.983709	5.49E-22	5.18E-10	1.77E-14	3.36E-19	3.23E-16	1	5.58E-22	5.27E-10	4 Facies 4	0.999999999
4	4945.5	0.000424	0.001943	7.08E-06	0.997622	3.47E-06	2.51E-08	4 Facies 4	0.9976224	6.99E-15	1.71E-19	1.17E-16	0.984666	3.04E-22	6.21E-10	1.73E-19	1.18E-16	1	3.09E-22	3.31E-10	4 Facies 4	1	
4	4946	0.000401	0.001489	3.3E-06	0.998103	3.31E-06	1.5E-08	4 Facies 4	0.998103	5.01E-15	7.5E-20	4.13E-17	0.985141	1.66E-22	1.95E-10	5.09E-15	7.62E-20	4.19E-17	1	1.69E-22	1.98E-10	4 Facies 4	1
4	4946.5	0.000304	0.001084	2.16E-06	0.998607	2.93E-06	1.14E-08	4 Facies 4	0.9986069	2.88E-15	2.75E-20	2.05E-17	0.985638	7.41E-23	1.48E-10	2.92E-15	2.79E-20	2.08E-17	1	7.52E-23	1.5E-10	4 Facies 4	1
4	4947	0.000207	0.000754	1.63E-06	0.990934	2.52E-06	8.62E-09	4 Facies 4	0.9990344	1.45E-14	2.4E-20	1.41E-17	0.98606	8.02E-23	1.12E-10	1.47E-15	2.43E-20	1.16E-17	1	8.13E-23	1.14E-10	4 Facies 4	1
4	4947.5	0.000299	0.000666	1.64E-06	0.999036	3.99E-06	6.38E-09	4 Facies 4	0.9990357	1.82E-15	1.01E-20	9.94E-18	0.986061	6.12E-23	8.28E-11	1.84E-15	1.03E-20	1.01E-17	1	6.21E-23	8.4E-11	4 Facies 4	1
4	4948	0.000194	0.000522	1.75E-06	0.999279	3.02E-06	5.54E-09	4 Facies 4	0.9992793	8.78E-16	9.96E-21	7.95E-18	0.986302	5.75E-23	7.19E-11	8.91E-16	1.01E-20	8.06E-18	1	5.83E-23	7.29E-11	4 Facies 4	1
4	4948.5	0.000269	0.000609	6.14E-07	0.999119	3.14E-06	4.13E-09	4 Facies 4	0.9991187	1.09E-15	3.6E-20	2.49E-18	0.986143	1.85E-22	5.37E-11	1.15E-15	3.65E-20	2.52E-18	1	1.87E-22	5.44E-11	4 Facies 4	1
4	4949	0.000626	0.000882	2E-07	0.998487	4.33E-06	3.69E-09	4 Facies 4	0.9984872	3.36E-15	2.62E-19	1.07E-18	0.98552	1.28E-21	4.79E-11	3.41E-15	2.66E-19	1.09E-18	1	1.3E-21	4.86E-11	4 Facies 4	1
4	4949.5	0.001788	0.001949	9.78E-08	0.996715	6.58E-08	4.87E-09	4 Facies 4	0.9967153	1.69E-14	1.01E-18	9.2E-19	0.983771	4.47E-21	6.32E-11	1.72E-14	1.03E-18	9.35E-19	1	4.54E-21	6.43E-11	4 Facies 4	1
4	4950	0.004468	0.002614	7.76E-08	0.992908	9.26E-06	8.52E-09	4 Facies 4	0.9929083	3.86E-14	7.35E-19	6.7E-19	0.980013	2.6E-21	1.11E-10	3.94E-14	7.5E-19	6.83E-19	1	2.66E-21	1.13E-10	4 Facies 4	1
4	4950.5	0.002097	0.001959	1.35E-06	0.995937	5.65E-06	7																

2	4958	0.45783	0.406874	0.002253	0.13288	8.57E-05	7.65E-05	1	Facies 1	0.4578301	6.75E-08	0.385174	1.19E-11	0.007069	2.19E-13	1.02E-08	1.72E-07	0.981977	3.04E-11	0.01802	5.58E-13	2.61E-08	2	Facies 2	0.981977103
2	4958.5	0.445045	0.4556364	0.011384	0.087629	8.97E-05	0.000218	2	Facies 2	0.4556339	6.46E-08	0.432188	3.46E-10	0.0045	2.07E-13	2.37E-08	1.48E-07	0.989696	7.93E-10	0.0103	4.74E-13	5.42E-08	2	Facies 2	0.989695933
2	4959	0.34621	0.514925	0.061927	0.076174	9.67E-05	0.000668	2	Facies 2	0.5149247	6.57E-08	0.487153	7.11E-09	0.004097	1.98E-13	9.54E-08	1.34E-07	0.991659	1.45E-08	0.00834	4.03E-13	1.94E-07	2	Facies 2	0.991658937
2	4959.5	0.31145	0.474833	0.12323	0.088031	0.00015	0.002306	2	Facies 2	0.4748327	5.38E-08	0.448044	1.84E-08	0.004951	1.46E-13	4.08E-07	1.19E-07	0.98907	4.05E-08	0.01093	3.23E-13	9E-07	2	Facies 2	0.989069909
2	4960	0.284782	0.4556369	0.146838	0.108447	0.000215	0.004081	2	Facies 2	0.4556387	2.46E-08	0.430756	1.37E-08	0.005906	9.16E-14	6.19E-07	5.64E-08	0.986474	3.13E-08	0.01352	2.1E-13	1.42E-06	2	Facies 2	0.986473608
2	4960.5	0.149638	0.473906	0.277557	0.096651	0.000126	0.002212	2	Facies 2	0.4739057	1.13E-08	0.447949	1.41E-08	0.005274	1.02E-13	3.4E-07	2.49E-08	0.988362	3.12E-08	0.01164	2.24E-13	7.5E-07	2	Facies 2	0.988362418
2	4961	0.064884	0.418175	0.428324	0.087542	6.6E-05	0.001009	3	Facies 3	0.4283242	1.87E-08	0.395538	8.33E-09	0.004726	3.2E-13	1.46E-07	4.67E-08	0.988192	2.08E-08	0.01181	7.99E-13	3.65E-07	2	Facies 2	0.98819225
2	4961.5	0.188447	0.574189	0.128389	0.108255	0.000101	0.000619	2	Facies 2	0.5741887	1.54E-07	0.541726	1.53E-09	0.006101	1.46E-12	1.1E-07	2.81E-07	0.988863	2.79E-09	0.01114	2.67E-12	2E-07	2	Facies 2	0.988862593
2	4962	0.231935	0.599519	0.03452	0.133599	8.99E-05	0.000336	2	Facies 2	0.599519	4.78E-07	0.564344	1.04E-09	0.007811	3.28E-12	6.95E-08	8.35E-07	0.986348	1.81E-09	0.01365	5.73E-12	1.21E-07	2	Facies 2	0.986347611
2	4962.5	0.187504	0.627666	0.038756	0.145539	7.21E-05	0.000462	2	Facies 2	0.6276663	1.26E-06	0.586643	6.54E-09	0.009468	8.52E-12	1.38E-07	2.11E-06	0.984115	1.1E-08	0.01588	1.43E-11	2.31E-07	2	Facies 2	0.984115166
2	4963	0.303585	0.530089	0.034488	0.130673	0.000101	0.001064	2	Facies 2	0.5300892	3.39E-06	0.483834	3.08E-08	0.011322	1.9E-11	6.39E-07	6.85E-06	0.977126	6.22E-08	0.02287	3.83E-11	1.29E-06	2	Facies 2	0.977125762
2	4963.5	0.237041	0.476145	0.087391	0.195128	0.000186	0.004109	2	Facies 2	0.476145	4.86E-06	0.425899	1.09E-07	0.020421	4.67E-11	3.5E-06	1.09E-05	0.954229	2.43E-07	0.04575	4.54E-10	7.85E-06	2	Facies 2	0.954227849
2	4964	0.087427	0.385714	0.187744	0.327779	0.000331	0.011005	2	Facies 2	0.3857137	7.68E-06	0.356428	6.91E-08	0.024712	5.19E-10	4.87E-06	2.01E-05	0.935131	1.81E-07	0.06484	1.36E-09	1.28E-05	2	Facies 2	0.935130979
2	4964.5	0.105179	0.514065	0.113914	0.259458	0.005506	0.006827	2	Facies 2	0.5140653	4.5E-05	0.480362	1.51E-08	0.16821	4.29E-09	2.02E-06	0.966076	3.04E-08	0.03383	8.63E-09	4.06E-06	2	Facies 2	0.966075794	
2	4965	0.090604	0.618818	0.067071	0.225123	0.000824	0.003931	2	Facies 2	0.6188175	0.00263	0.579887	4.81E-09	0.013446	4.38E-08	8.89E-07	0.000443	0.976904	8.11E-09	0.02265	7.37E-08	1.5E-06	2	Facies 2	0.976903501
2	4965.5	0.06266	0.656248	0.060626	0.21381	0.001433	0.005223	2	Facies 2	0.6562475	0.001854	0.603569	1.6E-09	0.010695	7.96E-07	5.68E-07	0.003009	0.979629	2.59E-09	0.01736	1.29E-06	9.21E-07	2	Facies 2	0.979629489
2	4966	0.056871	0.72423	0.077439	0.131907	0.002672	0.006881	2	Facies 2	0.7242301	0.015798	0.495437	5.24E-10	0.004304	1.46E-05	1.57E-07	0.030643	0.960982	1.02E-09	0.00835	2.84E-10	3.04E-07	2	Facies 2	0.960980394
2	4966.5	0.083698	0.761065	0.091362	0.043216	0.080866	0.012573	2	Facies 2	0.7610647	0.064248	0.158548	3.12E-12	0.000391	0.000121	1.81E-08	0.28771	0.709997	1.4E-11	0.00175	0.000544	8.11E-08	2	Facies 2	0.709997241
2	4967	0.188921	0.775981	0.002381	0.012656	0.017580	0.002475	2	Facies 2	0.7759811	1.74414	0.044636	2.33E-17	4.23E-05	0.000305	8.99E-11	0.795035	0.203463	1.06E-16	0.00011	0.00139	4.1E-10	1	Facies 1	0.795035482
2	4967.5	0.303508	0.672935	2.8E-07	0.005959	0.01579	7.83E-06	2	Facies 2	0.6729353	0.293866	0.013185	7.47E-25	8.59E-07	0.00028	3.61E-14	0.956185	0.042901	2.43E-24	2.8E-06	0.000911	1.18E-13	1	Facies 1	0.956184891
1	4968	0.822507	0.116278	7.05E-11	0.031571	0.027053	2.81E-08	1	Facies 1	0.8250969	0.796516	0.002009	3.65E-32	2.84E-07	0.000469	2.56E-17	0.996988	0.002514	4.57E-32	3.6E-07	0.000588	3.2E-17	1	Facies 1	0.996897726
1	4968.5	0.97794	0.002205	2.77E-14	0.013211	0.006645	3.03E-11	1	Facies 1	0.9779395	0.944135	3.8E-05	6.13E-38	6.61E-08	0.001115	5.88E-21	0.999838	4.03E-05	6.5E-38	7E-08	0.000122	6.22E-21	1	Facies 1	0.999837823
1	4969	0.992357	0.000479	6.21E-16	0.002825	0.004434	5.56E-13	1	Facies 1	0.9923567	0.958054	8.25E-06	8.14E-41	1.43E-08	7.52E-05	2.55E-23	0.999913	8.61E-06	8.49E-41	1.5E-08	7.84E-05	2.66E-23	1	Facies 1	0.999912933
1	4969.5	0.994307	0.000299	2.13E-16	0.000837	0.004558	1.47E-13	1	Facies 1	0.9943066	0.959953	5.15E-06	5E-42	3.39E-09	7.89E-05	1.51E-24	0.999912	5.36E-06	5.2E-42	3.5E-09	8.21E-05	1.57E-24	1	Facies 1	0.999912486
1	4970	0.995914	0.000193	1.46E-16	0.00021	0.003683	5.83E-14	1	Facies 1	0.995914	0.961512	3.33E-06	1.53E-42	7.61E-10	6.37E-05	2.71E-25	0.99993	3.46E-06	1.6E-42	7.9E-10	6.63E-05	2.82E-25	1	Facies 1	0.999930285
1	4970.5	0.996419	0.000149	1.28E-16	0.000109	0.003323	4.12E-14	1	Facies 1	0.9964189	0.962007	2.57E-06	1.81E-42	3.45E-10	5.75E-05	1.22E-25	0.999938	2.67E-06	1.88E-42	3.6E-10	5.97E-05	1.27E-25	1	Facies 1	0.999937604
1	4971	0.996676	0.000135	1.46E-16	8.84E-05	0.002901	4.06E-14	1	Facies 1	0.9966755	0.962459	2.33E-06	9.04E-42	2.19E-10	5.01E-05	1.63E-25	0.999946	2.43E-06	9.39E-42	2.3E-10	5.21E-05	1.69E-25	1	Facies 1	0.999945503
1	4971.5	0.997466	0.000176	3.16E-16	0.00014	0.002218	2.73E-14	1	Facies 1	0.9974662	0.963035	3.03E-06	9.5E-41	2.98E-08	3.83E-05	7.16E-25	0.999957	3.15E-06	9.87E-41	3.1E-10	3.98E-05	7.44E-25	1	Facies 1	0.999957076
1	4972	0.997617	0.000257	7.74E-16	0.000297	0.001828	1.64E-13	1	Facies 1	0.9976175	4.93E-06	3.44E-04	7.21E-10	3.16E-05	3.47E-24	0.999963	4.606E-06	3.57E-06	7.5E-10	3.28E-05	3.61E-24	1	Facies 1	0.9999626	
1	4972.5	0.996992	0.000342	8.58E-16	0.000625	0.002042	2.02E-13	1	Facies 1	0.9969917	0.96257	5.9E-06	4.83E-40	1.57E-09	3.53E-05	5.13E-24	0.999957	6.13E-06	5.02E-40	1.6E-09	3.66E-05	5.33E-24	1	Facies 1	0.99995723
1	4973	0.996735	0.000362	7.33E-16	0.000795	0.002019	1.62E-13	1	Facies 1	0.996735	0.962324	6.24E-06	3.18E-40	1.88E-09	3.64E-05	6.51E-24	0.999956	5.68E-06	3.31E-40	2.0E-09	3.78E-05	6.76E-24	1	Facies 1	0.999955674
1	4973.5	0.99615	0.000441	1.12E-15	0.001499	0.00191	2.32E-13	1	Facies 1	0.9961501	0.961766	7.6E-06	2.07E-04	2.97E-09	3.3E-05	5.01E-24	0.999958	7.9E-06	2.15E-04	3.1E-09	3.43E-05	5.21E-24	1	Facies 1	0.999957802
1	4974	0.997127	0.000372	1.16E-15	0.000902	0.0016	1.77E-13	1	Facies 1	0.9971265	0.962712	6.41E-06	1.97E-40	1.6E-09	2.76E-05	2.13E-24	0.999965	6.65E-06	2.04E-04	1.7E-09	2.87E-05	2.22E-24	1	Facies 1	0.999964464
1	4974.5	0.997758	0.000309	1.14E-15	0.000475	0.001457	1.43E-13	1	Facies 1	0.9977582	0.96332	5.34E-06	1.5E-40	8.96E-10	2.52E-05	1.97E-24	0.999968	5.54E-06	1.56E-09	9.3E-10	2.61E-05	2.04E-24	1	Facies 1	0.999968347
1	4975	0.997585	0.000345	1.5E-15	0.000539	1.94E-13	1	Facies 1	0.997585	0.963153	5.95E-06	5.13E-41	1.02E-09	2.64E-05	1.52E-24	0.999966	6.17E-06	5.33E-41	1.1E-09	2.75E-05	1.58E-24	1	Facies 1	0.99996376	
1	4975.5	0.997827	0.000275	9.03E-16	0.0003	0.001598	1.06E-13																		

Prediction results using data sheet 20011 raw data and neural net sheet NNet01																					
User comment on neural net sheet:																					
Number of predictor variables:		3																			
Predictor variables in NNet01:		GR NEUTRON DENSITY SONIC																			
Predictor variables in 20011 raw data:		GR NEUTRON																			
Categorical response variable:		Facies																			
Number of categories:		4																			
Continuous response variable:		[NONE]																			
Number of variables copied:		1																			
Variables copied from 20011 raw data:		Facies																			
		Probabilities for Facies																			
		Predicted Facies Max. Probab Products of transition and log-based probabilities Modified probabilities Predicted Facies , modifier Maximum pro																			
Facies	DEPTH	Cemented	Quartz-Carl	Peloidal	Micritic Mu	Pred.Categ	Pred.Facies	Prob.max	Cemented	Quartz-Carl	Peloidal	Micritic Mu	Cemented	Quartz-Carl	Peloidal	Micritic Mu	Pred.Categ	Pred.Facies	Prob.Max		
4	4960	0.0037093	0.0012466	0.9950287	1.544E-05	3	Peloidal	0.9950287	6.053E-05	1.015E-05	0.9706889	2.314E-11	6.235E-05	1.046E-05	0.9999272	2.383E-11	3	Peloidal	0.9999272		
4	4960.5	0.003709	0.0016483	0.9946268	1.594E-05	3	Peloidal	0.9946268	6.105E-05	1.343E-05	0.9701447	8.374E-11	6.293E-05	1.384E-05	0.9999232	8.631E-11	3	Peloidal	0.9999232		
4	4961	0.012697	0.0024564	0.9848111	3.557E-05	3	Peloidal	0.9848111	0.000212	1.997E-05	0.9603522	4.054E-10	0.0002207	2.078E-05	0.9997585	4.221E-10	3	Peloidal	0.9997585		
4	4961.5	0.023259	0.0002237	0.9764712	4.614E-05	3	Peloidal	0.9764712	0.0004545	1.812E-06	0.9493958	3.951E-09	0.0004785	1.908E-06	0.9995196	4.159E-09	3	Peloidal	0.9995196		
4	4962	0.1497041	1.817E-05	0.8502078	6.994E-05	3	Peloidal	0.8502078	0.0029824	1.472E-07	0.8263039	6.685E-09	0.0035964	1.775E-07	0.9964034	8.061E-09	3	Peloidal	0.9964034		
4	4962.5	0.1946635	2.14E-05	0.8052332	8.184E-05	3	Peloidal	0.8052332	0.003166	1.74E-07	0.7855902	8.125E-12	0.0040139	2.206E-07	0.9959859	1.03E-11	3	Peloidal	0.9959859		
4	4963	0.0002025	2.336E-05	0.9997112	1.543E-05	3	Peloidal	0.9997112	4.067E-06	1.903E-07	0.9753061	2.946E-12	4.17E-06	1.951E-07	0.999956	3.021E-12	3	Peloidal	0.999956		
4	4963.5	0.0004798	0.0018753	0.9974814	0.0001636	3	Peloidal	0.9974814	7.802E-06	1.525E-05	0.9731511	4.669E-12	8.017E-06	1.567E-05	0.9999763	4.798E-12	3	Peloidal	0.9999763		
4	4964	7.191E-05	4.905E-05	0.9998699	9.093E-06	3	Peloidal	0.9998699	1.176E-06	3.988E-07	0.9754791	8.448E-13	1.199E-06	4.088E-07	0.9999984	8.661E-13	3	Peloidal	0.9999984		
4	4964.5	0.0002326	2.716E-05	0.9997328	7.42E-06	3	Peloidal	0.9997328	3.805E-06	2.208E-07	0.9752478	1.929E-11	3.902E-06	2.264E-07	0.9999959	1.978E-11	3	Peloidal	0.9999959		
4	4965	0.0065055	1.068E-05	0.9934582	2.553E-05	3	Peloidal	0.9934582	0.0001058	8.686E-08	0.969193	9.047E-10	0.0001091	8.957E-08	0.9998908	9.333E-10	3	Peloidal	0.9998908		
4	4965.5	0.0007386	1.096E-06	0.9992488	1.152E-05	3	Peloidal	0.9992488	1.006E-07	7.732E-11	0.2063155	9.137E-06	4.877E-07	3.748E-10	0.9999552	4.428E-05	3	Peloidal	0.9999552		
5	4966	0.0366718	0.3040811	0.0214096	0.6378375	4	Micritic Mud	0.6378375	3.206E-07	1.488E-06	0.0042908	0.5099959	6.233E-07	2.893E-06	0.0083432	0.9916533	4	Micritic Mud	0.9916533		
5	4966.5	0.0013334	0.0775578	0.0019674	0.9191414	4	Micritic Mud	0.9191414	1.406E-08	4.105E-07	0.0003945	0.7348369	1.912E-08	5.583E-07	0.0005365	0.9994629	4	Micritic Mud	0.9994629		
5	4967	0.0003073	0.0049122	0.0025644	0.9921504	4	Micritic Mud	0.9921504	1.267E-08	2.337E-08	0.000514	0.7932519	1.596E-08	2.944E-08	0.0006475	0.9993524	4	Micritic Mud	0.9993524		
5	4967.5	0.0003101	0.0022522	0.0021775	0.9952602	4	Micritic Mud	0.9952602	1.799E-05	1.336E-07	0.000418	0.7406129	2.671E-05	1.803E-07	0.0005641	0.999409	4	Micritic Mud	0.999409		
5	4968	0.0019529	0.0223684	0.0015694	0.9741093	4	Micritic Mud	0.9741093	0.0018013	9.311E-06	0.259E-05	0.0243403	0.0686846	3.555E-05	0.0031492	0.9281308	4	Micritic Mud	0.9281308		
2	4968.5	0.8567806	0.0012951	0.0855956	0.0563283	1	Cemented	Oi	0.8567806	0.7953494	3.127E-09	0.0040996	0.0013408	0.9932062	3.905E-09	0.0051194	0.0016743	1	Cemented	Oi	0.9932062
2	4969	0.09442187	1.476E-06	0.0057591	2.076E-05	1	Cemented	Oi	0.9942187	0.9232004	3.372E-14	0.0002743	4.943E-07	0.9997025	3.651E-14	0.000297	5.352E-07	1	Cemented	Oi	0.9997025
2	4969.5	0.0999399	1.35E-07	5.471E-05	5.247E-06	1	Cemented	Oi	0.9999399	0.928454	7.313E-14	2.608E-06	1.249E-07	0.9999771	7.877E-14	2.809E-06	1.346E-07	1	Cemented	Oi	0.9999771
2	4970	0.9986769	6.221E-07	0.0012894	3.305E-05	1	Cemented	Oi	0.9986769	0.9270585	1.574E-12	6.177E-05	7.866E-07	0.9999325	1.698E-12	6.663E-05	8.484E-07	1	Cemented	Oi	0.9999325
2	4970.5	0.9939414	7.943E-08	0.0060285	3.003E-05	1	Cemented	Oi	0.9939414	0.9228988	3.299E-14	0.0002874	7.149E-07	0.999688	3.574E-14	0.0003113	7.744E-07	1	Cemented	Oi	0.999688
2	4971	0.9989857	2.369E-08	0.0009593	1.906E-05	1	Cemented	Oi	0.9989857	0.927629	9.225E-17	4.739E-05	4.537E-07	0.9999484	9.945E-17	5.109E-05	4.891E-07	1	Cemented	Oi	0.9999484
2	4971.5	0.999988	3.657E-08	9.14E-06	2.792E-06	1	Cemented	Oi	0.999988	0.9275817	3.189E-13	4.443E-07	6.64E-08	0.9999994	3.438E-13	4.79E-07	7.158E-08	1	Cemented	Oi	0.9999994
2	4972	0.979533	1.708E-09	0.0204635	3.492E-06	1	Cemented	Oi	0.979533	0.9094698	1.5E-15	0.0009765	8.314E-08	0.9989274	1.648E-08	0.0010726	9.131E-08	1	Cemented	Oi	0.9989274
2	4972.5	0.9978989	1.637E-09	0.0020996	1.452E-06	1	Cemented	Oi	0.9978989	0.9265598	8.828E-16	0.0001001	3.456E-08	0.9998919	9.527E-16	0.000108	3.73E-08	1	Cemented	Oi	0.9998919
2	4973	0.9987	9.954E-09	0.0012913	8.678E-06	1	Cemented	Oi	0.9987	0.9273342	2.658E-15	6.153E-05	2.066E-07	0.9999334	2.866E-15	6.635E-05	2.228E-07	1	Cemented	Oi	0.9999334
2	4973.5	0.999352	1.29E-08	0.0006393	8.714E-06	1	Cemented	Oi	0.999352	0.9279182	5.896E-15	3.047E-05	2.075E-07	0.9999663	6.354E-15	3.284E-05	2.236E-07	1	Cemented	Oi	0.9999663
2	4974	0.9988965	3.571E-08	0.0010907	1.271E-05	1	Cemented	Oi	0.9988965	0.9273804	5.277E-14	5.212E-05	3.026E-07	0.9999435	5.69E-14	5.62E-05	3.263E-07	1	Cemented	Oi	0.9999435
2	4974.5	0.9965216	1.368E-07	0.0034504	2.787E-05	1	Cemented	Oi	0.9965216	0.9242889	1.285E-12	0.000168	6.629E-07	0.9998175	1.391E-12	0.0001817	7.171E-07	1	Cemented	Oi	0.9998175
2	4975	0.9789873	1.864E-06	0.0209503	6.056E-05	1	Cemented	Oi	0.9789873	0.9066781	4.038E-11	0.0010494	1.438E-06	0.9988423	4.448E-11	0.0011561	1.584E-06	1	Cemented	Oi	0.9988423
2	4975.5	0.9542706	1.72E-05	0.0456497	6.245E-05	1	Cemented	Oi	0.9542706	0.8823335	6.063E-10	0.0023574	1.48E-06	0.9973336	6.853E-10	0.0026647	1.673E-06	1	Cemented	Oi	0.9973336
2	4976	0.9217351	4.282E-05	0.0781787	4.339E-05	1	Cemented	Oi	0.9217351	0.8558582	1.598E-11	0.0037261	1.033E-06	0.995664	1.86E-11	0.0043348	1.202E-06	1	Cemented	Oi	0.995664
2	4976.5	0.9990931	8.964E-06	0.0008945	3.516E-06	1	Cemented	Oi	0.9990931	0.9277284	6.935E-14	4.259E-05	8.371E-08	0.999954	7.475E-14	4.591E-05	9.022E-08	1	Cemented	Oi	0.999954
2	4977	0.9999595	2.113E-05	1.855E-05	8.269E-07	1	Cemented	Oi	0.9999595	0.9285328	1.833E-13	8.836E-07	1.969E-08	0.999999	1.974E-13	9.516E-07	2.126E-08	1	Cemented	Oi	0.999999
2	4977.5	0.9999247	5.346E-05	2.08E-05	9.949E-07	1	Cemented	Oi	0.9999247												

2	4979	0.9195357	0.0010181	0.0789212	0.000525	1 Cemented Or	0.9195357	0.0153182	8.302E-06	0.0769621	5.468E-09	0.1659819	8.996E-05	0.8339281	5.925E-08	3 Peloidal	0.8339281
4	4979.5	0.0253703	0.0033723	0.9689228	0.0023347	3 Peloidal	0.9689228	0.0004136	2.749E-05	0.9452297	2.543E-09	0.0004373	2.906E-05	0.9995336	2.689E-09	3 Peloidal	0.9995336
4	4980	0.0027239	0.0026281	0.9937075	0.0009405	3 Peloidal	0.9937075	4.434E-05	2.139E-05	0.9694462	4.112E-10	4.573E-05	2.206E-05	0.9999322	4.241E-10	3 Peloidal	0.9999322
4	4980.5	0.0010968	0.0009886	0.9976847	0.0002299	3 Peloidal	0.9976847	1.787E-05	8.04E-06	0.9733178	1.784E-10	1.836E-05	8.26E-06	0.9999734	1.833E-10	3 Peloidal	0.9999734
4	4981	0.0019418	0.0003885	0.9975525	0.0001172	3 Peloidal	0.9975525	3.17E-05	3.162E-06	0.9731438	2.039E-10	3.258E-05	3.249E-06	0.9999642	2.095E-10	3 Peloidal	0.9999642
4	4981.5	0.0043563	0.0013642	0.9934881	0.0007915	3 Peloidal	0.9934881	7.084E-05	1.11E-05	0.9692476	2.069E-11	7.308E-05	1.145E-05	0.9999155	2.135E-11	3 Peloidal	0.9999155
4	4982	6.579E-05	0.0010504	0.998495	0.0003887	3 Peloidal	0.998495	1.07E-06	8.541E-06	0.9741408	1.47E-13	1.098E-06	8.767E-06	0.999901	1.509E-13	3 Peloidal	0.999901
4	4982.5	9.528E-07	9.181E-05	0.999892	1.525E-05	3 Peloidal	0.999892	1.549E-08	7.465E-07	0.9755041	2.536E-16	1.588E-08	7.652E-07	0.999992	2.6E-16	3 Peloidal	0.999992
4	4983	4.19E-08	3.884E-05	0.9999593	1.854E-06	3 Peloidal	0.9999593	6.813E-10	3.158E-07	0.9755683	2.998E-17	6.983E-10	3.237E-07	0.999997	3.073E-17	3 Peloidal	0.999997
4	4983.5	4.073E-08	0.0002294	0.9997681	2.464E-06	3 Peloidal	0.9997681	6.622E-10	1.866E-06	0.9753803	3.062E-17	6.789E-10	1.913E-06	0.999981	3.14E-17	3 Peloidal	0.999981
4	4984	3.131E-08	0.0004218	0.9995749	3.336E-06	3 Peloidal	0.9995749	5.091E-10	3.429E-06	0.9751941	3.721E-17	5.221E-10	3.517E-06	0.999965	3.816E-17	3 Peloidal	0.999965
4	4984.5	2.811E-08	0.0001113	0.9998844	2.558E-06	3 Peloidal	0.9998844	4.571E-10	9.188E-07	0.9754968	8.031E-17	4.686E-10	9.418E-07	0.999991	8.232E-17	3 Peloidal	0.999991
4	4985	7.912E-08	3.224E-05	0.9999656	2.104E-06	3 Peloidal	0.9999656	1.287E-09	2.621E-07	0.975576	1.083E-16	1.319E-09	2.687E-07	0.999997	1.11E-16	3 Peloidal	0.999997
4	4985.5	1.297E-07	2.085E-05	0.9999778	1.233E-06	3 Peloidal	0.9999778	2.119E-09	1.695E-07	0.9755877	9.725E-17	2.162E-09	1.738E-07	0.999998	9.969E-17	3 Peloidal	0.999998
4	4986	1.988E-07	5.746E-05	0.9999407	1.598E-06	3 Peloidal	0.9999407	3.232E-09	4.675E-07	0.9755454	3.256E-16	3.313E-09	4.793E-07	0.999995	3.331E-16	3 Peloidal	0.999995
4	4986.5	5.12E-07	0.0008523	0.9991425	4.753E-06	3 Peloidal	0.9991425	8.326E-09	6.935E-06	0.9747663	3.58E-16	8.541E-09	7.114E-06	0.9999929	3.673E-16	3 Peloidal	0.9999929
4	4987	1.896E-07	0.0008828	0.9991127	4.396E-06	3 Peloidal	0.9991127	3.084E-09	7.181E-06	0.9747394	2.468E-16	3.163E-09	7.367E-06	0.9999926	2.532E-16	3 Peloidal	0.9999926
4	4987.5	1.414E-07	0.0006036	0.9993927	3.556E-06	3 Peloidal	0.9993927	2.299E-09	4.91E-06	0.9750125	1.042E-15	2.358E-09	5.036E-06	0.999995	1.069E-15	3 Peloidal	0.999995
4	4988	7.355E-07	0.0006273	0.9993677	4.282E-06	3 Peloidal	0.9993677	1.197E-08	5.109E-06	0.9749688	9.611E-13	1.227E-08	5.24E-06	0.999947	9.858E-13	3 Peloidal	0.999947
4	4988.5	0.0005641	0.0018554	0.9975622	1.826E-05	3 Peloidal	0.9975622	9.174E-06	1.51E-05	0.9732206	1.598E-12	9.427E-06	1.551E-05	0.9999751	1.642E-12	3 Peloidal	0.9999751
4	4989	0.0002204	0.0009651	0.9988035	1.104E-05	3 Peloidal	0.9988035	3.583E-06	7.854E-06	0.9744353	7.216E-15	3.677E-06	8.059E-06	0.999983	7.406E-15	3 Peloidal	0.999983
4	4989.5	1.646E-06	0.0008941	0.9990984	5.865E-06	3 Peloidal	0.9990984	2.675E-08	7.48E-06	0.9744982	1.141E-16	2.745E-08	7.676E-06	0.9999923	1.171E-16	3 Peloidal	0.9999923
4	4990	4.767E-08	0.0280636	0.9718882	4.811E-05	3 Peloidal	0.9718882	7.748E-10	0.0002379	0.9478536	7.22E-16	8.172E-10	0.0002509	0.9997491	7.616E-16	3 Peloidal	0.9997491
4	4990.5	3.633E-08	0.0393765	0.9804633	0.0001602	3 Peloidal	0.9604633	5.903E-10	0.0003437	0.9364722	5.979E-15	6.301E-10	0.0003669	0.9996331	6.382E-15	3 Peloidal	0.9996331
4	4991	8.673E-08	0.0635568	0.9360789	0.0003642	3 Peloidal	0.9360789	1.409E-09	0.0005804	0.9123268	6.691E-13	1.543E-09	0.0006357	0.9993643	7.329E-13	3 Peloidal	0.9993643
4	4991.5	9.619E-07	0.1008431	0.8985761	0.0005799	3 Peloidal	0.8985761	1.572E-08	0.0009317	0.9755868	1.545E-09	1.794E-08	0.0010629	0.9989371	1.762E-09	3 Peloidal	0.9989371
4	4992	0.00057778	0.1229454	0.8685526	0.0027242	3 Peloidal	0.8685526	9.464E-05	0.0009994	0.847263	8.481E-09	0.0001116	0.0011781	0.9987104	9.997E-09	3 Peloidal	0.9987104
4	4992.5	0.0071873	8.673E-06	0.9927633	4.08E-05	3 Peloidal	0.9927633	0.0001264	7.041E-08	0.9672048	1.418E-09	0.0001307	7.279E-08	0.9998692	1.466E-09	3 Peloidal	0.9998692
4	4993	0.0805564	3.269E-05	0.9193	0.0001109	3 Peloidal	0.9193	0.0013108	2.658E-07	0.8968673	3.29E-11	0.0014594	2.959E-07	0.9985403	3.663E-11	3 Peloidal	0.9985403
4	4993.5	0.0007466	1.62E-05	0.99923	7.227E-06	3 Peloidal	0.99923	1.214E-05	1.317E-07	0.9748539	6.324E-13	1.246E-05	1.351E-07	0.9999874	6.487E-13	3 Peloidal	0.9999874
4	4994	0.0002206	5.936E-05	0.9997154	4.665E-06	3 Peloidal	0.9997154	5.358E-06	1.249E-06	0.9626449	2.548E-13	3.676E-06	1.298E-06	0.999995	2.647E-13	3 Peloidal	0.999995
4	4994.5	0.0001501	0.0091112	0.997004	3.828E-05	3 Peloidal	0.997004	9.119E-07	0.0054498	0.9392103	4.861E-13	2.294E-06	0.0137084	0.9862893	1.222E-12	3 Peloidal	0.9862893
4	4995	0.0001893	0.1271699	0.872487	0.0001538	3 Peloidal	0.872487	9.954E-08	0.1169385	0.69737	3.268E-13	5.332E-07	0.6264263	0.3735732	1.751E-12	2 Quartz-Carb	0.6264263
3	4995.5	0.0003716	0.6500801	0.3486482	0.0009001	2 Quartz-Carb	0.6500801	5.641E-08	0.6118599	0.0204452	6.143E-13	8.922E-08	0.9676656	0.0323343	9.715E-13	2 Quartz-Carb	0.9676656
3	4996	0.0015964	0.8043986	0.1417304	0.05022746	2 Quartz-Carb	0.8043986	2.157E-08	0.7635496	0.0071954	1.551E-11	2.799E-08	0.9906643	0.0093357	2.013E-11	2 Quartz-Carb	0.9906643
3	4996.5	0.0028363	0.9092363	0.0142906	0.0736368	2 Quartz-Carb	0.9092363	1.074E-08	0.8635751	0.0007176	9.416E-13	1.243E-08	0.9991697	0.0008303	1.089E-12	2 Quartz-Carb	0.9991697
3	4997	0.0003389	0.9858918	0.0043551	0.0094142	2 Quartz-Carb	0.9858918	5.026E-10	0.9365125	0.0002181	1.293E-14	5.366E-10	0.9997671	0.0002329	1.38E-14	2 Quartz-Carb	0.9997671
3	4997.5	0.0002021	0.9905982	0.0017163	0.0074834	2 Quartz-Carb	0.9905982	5.422E-11	0.9410529	8.584E-05	1.637E-15	5.761E-11	0.9999088	9.121E-05	1.739E-15	2 Quartz-Carb	0.9999088
3	4998	0.0001302	0.9925029	0.0003111	0.0070558	2 Quartz-Carb	0.9925029	8.636E-12	0.942874	1.556E-05	8.017E-16	9.159E-12	0.9999835	1.65E-05	8.502E-16	2 Quartz-Carb	0.9999835
3	4998.5	0.0001448	0.9917691	7.685E-05	0.00080093	2 Quartz-Carb	0.9917691	4.375E-12	0.9421789	3.843E-06	3.615E-15	4.643E-12	0.9999599	4.079E-06	3.837E-15	2 Quartz-Carb	0.9999599
3	4999	0.0001944	0.9888338	3.49E-05	0.0109369	2 Quartz-Carb	0.9888338	1.414E-11	0.939388	1.745E-06	1.093E-13	1.505E-11	0.9999881	1.858E-06	1.163E-13	2 Quartz-Carb	0.9999881
3	4999.5	0.0003445	0.969573	8.21E-05	0.0300004	2 Quartz-Carb	0.969573	2.106E-10	0.9210604	4.108E-06	5.235E-12	2.287E-10	0.999955	4.46E-06	5.683E-12	2 Quartz-Carb	0.999955
3	5000	0.0007012	0.866578	0.0006061	0.1321147	2 Quartz-Carb	0.866578	6.016E-09	0.8228185	3.06E-05	4.313E-13	7.311E-09	0.9999628	3.719E-05	5.241E-13	2 Quartz-Carb	0.9999628
3	5000.5	1.969E-05	0.969827	0.0096523	0.020501	2 Quartz-Carb	0.969827	1.262E-10	0.9209755	0.0004861	3.302E-15	1.37E-10	0.9994724	0.0005276	3.584E-15	2 Quartz-Carb	0.9994724
3	5001	8.751E-06	0.9911811	0.0074223	0.0013879	2 Quartz-Carb	0.9911811	6.373E-12	0.9415802	0.0003714	1.244E-18	6.766E-12	0.9996057	0.0003943	1.321E-18	2 Quartz-Carb	0.9996057
3	5001.5	3.957E-06	0.9991281	0.0008502	1.772E-05	2 Quartz-Carb	0.9991281	3.574E-14	0.9491712	4.251E-05	7.199E-21	3.766E-14	0.9999552	4.479E-05	7.584E-21	2 Quartz-Carb	0.9999552
3	5002	3.493E-06	0.9999834	1.056E-05	2.568E-06	2 Quartz-Carb	0.9999834	1.621E-14	0.9499839	5.278E-07	7.524E-22	1.707E-14	0.999994	5.556E-07			

3	5004	1.199E-06	0.9999492	4.747E-05	2.101E-06	2 Quartz-Carb	0.9999492	3.587E-09	0.7766976	1.046E-05	5.229E-15	4.618E-09	0.9999865	1.346E-05	6.732E-15	2 Quartz-Carb	0.9999865
3	5004.5	8.457E-07	0.9752803	0.0247103	8.515E-06	2 Quartz-Carb	0.9752803	1.242E-08	0.0970941	0.0218874	6.089E-13	1.044E-07	0.8160436	0.1839563	5.117E-12	2 Quartz-Carb	0.8160436
3	5005	1.457E-05	0.9269835	0.0729869	1.504E-05	2 Quartz-Carb	0.9269835	2.368E-07	0.007654	0.0711976	1.282E-13	3.003E-06	0.0970676	0.9029294	1.626E-12	3 Peloidal	0.9029294
4	5005.5	2.114E-05	0.0158424	0.9841327	3.768E-06	3 Peloidal	0.9841327	3.437E-07	0.0001292	0.9601023	4.586E-14	3.58E-07	0.0001346	0.9998651	4.776E-14	3 Peloidal	0.9998651
4	5006	3.052E-05	0.0034901	0.9964773	2.038E-06	3 Peloidal	0.9964773	4.969E-07	2.844E-05	0.9721336	1.131E-12	5.111E-07	2.925E-05	0.9999702	1.163E-12	3 Peloidal	0.9999702
4	5006.5	0.0013824	0.0022791	0.9963327	5.735E-06	3 Peloidal	0.9963327	2.265E-05	1.889E-05	0.9717483	1.881E-11	2.331E-05	1.944E-05	0.9999573	1.936E-11	3 Peloidal	0.9999573
4	5007	0.0080264	0.0195776	0.9723487	4.732E-05	3 Peloidal	0.9723487	0.0001307	0.0001608	0.948524	3.456E-11	0.0001378	0.0001695	0.9996927	3.643E-11	3 Peloidal	0.9996927
4	5007.5	0.0018152	0.0106669	0.9874841	3.373E-05	3 Peloidal	0.9874841	2.955E-05	8.69E-05	0.9633625	1.796E-11	3.067E-05	9.019E-05	0.9998791	1.864E-11	3 Peloidal	0.9998791
4	5008	0.0013327	0.0021188	0.9965326	1.586E-05	3 Peloidal	0.9965326	2.174E-05	1.723E-05	0.9721704	2.229E-11	2.236E-05	1.772E-05	0.9999599	2.293E-11	3 Peloidal	0.9999599
4	5008.5	0.0035121	0.0025457	0.9962217	1.153E-05	3 Peloidal	0.9962217	5.736E-05	2.07E-06	0.9718498	2.189E-11	5.902E-05	2.13E-06	0.9999388	2.253E-11	3 Peloidal	0.9999388
4	5009	0.0042399	1.079E-05	0.9957214	2.793E-05	3 Peloidal	0.9957214	7.728E-05	8.756E-08	0.9694431	1.434E-09	7.971E-05	9.032E-08	0.9999202	1.479E-09	3 Peloidal	0.9999202
4	5009.5	0.1144153	1.071E-05	0.8853467	0.0002272	3 Peloidal	0.8853467	0.0018663	8.705E-08	0.8637065	3.06E-10	0.0021562	1.006E-07	0.978437	3.535E-10	3 Peloidal	0.978437
4	5010	0.0033792	3.753E-07	0.9965936	2.69E-05	3 Peloidal	0.9965936	5.5E-05	3.051E-09	0.9722712	1.053E-11	5.656E-05	3.138E-09	0.9999434	1.083E-11	3 Peloidal	0.9999434
4	5010.5	0.0009855	3.813E-07	0.9990003	1.11E-05	3 Peloidal	0.9990003	1.603E-05	3.1E-09	0.9746357	3.914E-13	1.644E-05	3.181E-09	0.9999836	4.016E-13	3 Peloidal	0.9999836
4	5011	8.883E-05	1.615E-06	0.9999031	6.422E-06	3 Peloidal	0.9999031	1.445E-06	1.313E-08	0.9755135	2.732E-13	1.481E-06	1.346E-08	0.9999885	2.801E-13	3 Peloidal	0.9999885
4	5011.5	0.0001071	1.572E-05	0.9998698	7.45E-06	3 Peloidal	0.9998698	1.743E-06	1.278E-07	0.9754641	3.37E-12	1.787E-06	1.311E-07	0.9999981	3.454E-12	3 Peloidal	0.9999981
4	5012	0.0011378	0.000131	0.9987168	1.433E-05	3 Peloidal	0.9987168	1.851E-05	1.065E-06	0.9743493	2.806E-12	1.9E-05	1.094E-06	0.9999799	2.879E-12	3 Peloidal	0.9999799
4	5012.5	0.0004884	0.0001244	0.9993765	1.03E-05	3 Peloidal	0.9993765	8.013E-06	1.012E-06	0.9748525	4.042E-11	8.22E-06	1.038E-06	0.9999007	4.146E-11	3 Peloidal	0.9999007
4	5013	0.0081867	7.175E-07	0.9917082	3.34E-05	3 Peloidal	0.9917082	0.0001545	5.813E-07	0.9648857	2.277E-09	0.0001601	6.023E-07	0.9998393	2.359E-09	3 Peloidal	0.9998393
4	5013.5	0.1432292	2.469E-05	0.8566655	8.061E-05	3 Peloidal	0.8566655	0.002398	2.006E-07	0.8353508	1.015E-09	0.0028625	2.395E-07	0.9971373	1.212E-09	3 Peloidal	0.9971373
4	5014	0.0291617	1.553E-06	0.9708203	1.652E-05	3 Peloidal	0.9708203	0.0005007	1.262E-08	0.9462427	3.925E-10	0.0005289	1.333E-08	0.9994711	4.146E-10	3 Peloidal	0.9994711
4	5014.5	0.0536712	8.296E-07	0.9462981	2.996E-05	3 Peloidal	0.9462981	0.0009213	6.738E-09	0.9223454	7.085E-10	0.0009979	7.298E-09	0.9990021	7.674E-10	3 Peloidal	0.9990021
4	5015	0.055019	5.237E-07	0.9449377	4.282E-05	3 Peloidal	0.9449377	0.0009162	4.256E-09	0.9215139	4.378E-10	0.0009932	4.614E-09	0.9990068	4.747E-10	3 Peloidal	0.9990068
4	5015.5	0.0249194	2.413E-07	0.9750377	4.275E-05	3 Peloidal	0.9750377	0.0004086	1.961E-09	0.9511204	1.529E-10	0.0004294	2.061E-09	0.9995706	1.606E-10	3 Peloidal	0.9995706
4	5016	0.0088282	1.486E-07	0.9911087	6.293E-05	3 Peloidal	0.9911087	0.0001452	1.208E-09	0.9667477	3.06E-10	0.0001502	1.249E-09	0.9998498	3.165E-10	3 Peloidal	0.9998498
4	5016.5	0.0111993	1.635E-07	0.9886388	0.0001617	3 Peloidal	0.9886388	0.0001966	1.327E-09	0.9632277	5.502E-09	0.0002040	1.378E-09	0.999796	5.711E-09	3 Peloidal	0.999796
4	5017	0.0097504	1.341E-07	0.9901183	0.0001312	3 Peloidal	0.9901183	0.0012139	9.606E-10	0.8569599	3.711E-07	0.0014145	1.119E-09	0.9985851	4.324E-07	3 Peloidal	0.9985851
4	5017.5	0.0235898	4.93E-08	0.9763712	3.887E-05	3 Peloidal	0.9763712	0.0195579	4.371E-11	0.1452976	8.247E-07	0.0186362	2.651E-10	0.8813585	5.002E-06	3 Peloidal	0.8813585
4	5018	0.3370395	4.696E-08	0.6629048	5.562E-05	3 Peloidal	0.6629048	0.0097911	3.941E-10	0.0379165	1.311E-06	0.8890496	1.133E-11	0.1090467	3.769E-06	1 Cemented Oi	0.8909496
2	5018.5	0.8373408	2.679E-08	0.1626129	4.627E-05	1 Cemented Oi	0.8373408	7.757729	5.011E-13	0.0808906	1.0906E-09	0.9896771	6.393E-13	0.0103215	1.402E-06	1 Cemented Oi	0.9896771
2	5019	0.958962	1.317E-08	0.0410161	2.194E-05	1 Cemented Oi	0.958962	0.8882798	2.673E-13	0.0204842	5.212E-07	0.9976898	3.002E-13	0.0023005	5.854E-07	1 Cemented Oi	0.9976898
2	5019.5	0.964435	1.05E-08	0.0355488	1.619E-05	1 Cemented Oi	0.964435	0.8818231	1.331E-12	0.022073	3.795E-07	0.9975027	1.506E-12	0.0024969	4.293E-07	1 Cemented Oi	0.9975027
2	5020	0.8545194	1.839E-08	0.1454438	3.679E-05	1 Cemented Oi	0.8545194	0.7636047	5.73E-12	0.0120981	8.426E-07	0.9844026	7.387E-12	0.0155963	1.086E-06	1 Cemented Oi	0.9844026
2	5020.5	0.7545829	9.581E-08	0.2452812	0.0001358	1 Cemented Oi	0.7545829	0.6568449	4.96E-11	0.0261736	3.029E-06	0.9616753	7.262E-11	0.0383203	4.435E-06	1 Cemented Oi	0.9616753
2	5021	0.853943	5.387E-07	0.1457733	0.0002832	1 Cemented Oi	0.853943	0.5958182	1.093E-09	0.0407015	5.061E-06	0.9363188	1.71E-09	0.0636739	7.918E-06	1 Cemented Oi	0.9363188
2	5021.5	0.6337098	4.306E-07	0.3660907	0.000199	1 Cemented Oi	0.6337098	0.3947219	1.173E-09	0.1312678	3.151E-06	0.7504321	2.23E-09	0.2495619	5.991E-06	1 Cemented Oi	0.7504321
2	5022	0.4946593	2.343E-07	0.5052191	0.0001213	3 Peloidal	0.5052191	0.3248898	5.674E-10	0.1637225	2.029E-06	0.6649208	1.161E-06	0.335075	4.152E-06	1 Cemented Oi	0.6649208
2	5022.5	0.8817952	7.094E-07	0.1179453	0.0002588	1 Cemented Oi	0.8817952	0.2088349	4.373E-09	0.0886063	1.49E-06	0.7021014	1.47E-08	0.2978936	5.009E-06	1 Cemented Oi	0.7021014
2	5023	0.9472984	4.648E-06	0.0507075	0.0019895	1 Cemented Oi	0.9472984	0.0157679	3.777E-08	0.0494509	2.005E-08	0.2417696	5.792E-07	0.7582295	3.074E-07	3 Peloidal	0.7582295
4	5023.5	0.0241589	8.158E-05	0.9580971	0.0176625	3 Peloidal	0.9580971	0.0003946	6.632E-07	0.9346563	3.412E-08	0.0004222	7.093E-07	0.9995772	3.649E-08	3 Peloidal	0.9995772
4	5024	0.0047475	8.529E-05	0.9784029	0.0167643	3 Peloidal	0.9784029	7.726E-05	6.934E-07	0.9545264	5.696E-09	8.093E-05	7.264E-07	0.9999183	5.967E-09	3 Peloidal	0.9999183
4	5024.5	0.0008489	2.002E-05	0.9954819	0.0036491	3 Peloidal	0.9954819	1.382E-05	1.628E-07	0.9711882	1.274E-09	1.423E-05	1.676E-07	0.9999856	3.125E-09	3 Peloidal	0.9999856
4	5025	0.0008731	1.294E-05	0.9970146	0.0020994	3 Peloidal	0.9970146	1.422E-05	1.052E-07	0.9726704	1.448E-09	1.462E-05	1.081E-07	0.9999853	1.488E-09	3 Peloidal	0.9999853
4	5025.5	0.0017299	1.337E-05	0.9960601	0.0021966	3 Peloidal	0.9960601	2.814E-05	1.087E-07	0.9717614	2.591E-10	2.895E-05	1.118E-07	0.9999709	2.666E-10	3 Peloidal	0.9999709
4	5026	0.0002878	1.849E-05	0.9984669	0.0012268	3 Peloidal	0.9984669	4.711E-06	1.503E-07	0.974006	3.417E-09	4.836E-06	1.543E-07	0.999995	3.508E-09	3 Peloidal	0.999995
4	5026.5	0.0067515	8.962E-05	0.9886233	0.0045356	3 Peloidal	0.9886233	0.0001117	7.284E-07	0.9642275	3.33E-08	0.0001158	7.553E-07	0.9998834	3.453E-08	3 Peloidal	0.9998834
4	5027	0.0179766	4.35E-05	0.9806188	0.0013611	3 Peloidal	0.9806188	0.0002948	3.536E-07	0.9656599	5.036E-09	0.0003081	3.696E-07	0.999615	5.263E-09	3 Peloidal	0.999615
4	5027.5	0.0090303	2.027E														

4	5029	0.0187587	1.504E-05	0.9799618	0.0012644	3	Peloidal	0.9799618	0.0003052	1.223E-07	0.956052	2.757E-10	0.0003191	1.279E-07	0.9996808	2.883E-10	3	Peloidal	0.9996808
4	5029.5	0.0005491	5.814E-06	0.9991725	0.0002726	3	Peloidal	0.9991725	8.929E-06	4.727E-08	0.9748023	6.325E-13	9.159E-06	4.849E-08	0.9999908	6.488E-13	3	Peloidal	0.9999908
4	5030	5.846E-06	4.668E-07	0.9999814	1.23E-05	3	Peloidal	0.9999814	9.506E-08	3.795E-09	0.9755916	2.811E-15	9.744E-08	3.89E-09	0.9999999	2.881E-15	3	Peloidal	0.9999999
4	5030.5	5.759E-07	4.025E-08	0.9999977	1.687E-06	3	Peloidal	0.9999977	9.364E-09	3.272E-10	0.9756075	6.714E-16	9.598E-09	3.354E-10	1	6.882E-16	3	Peloidal	1
4	5031	1.003E-06	2.302E-08	0.9999971	1.871E-06	3	Peloidal	0.9999971	1.631E-08	1.872E-10	0.9756069	1.418E-15	1.672E-08	1.919E-10	1	1.454E-15	3	Peloidal	1
4	5031.5	1.91E-06	2.95E-08	0.9999957	2.312E-06	3	Peloidal	0.9999957	3.106E-08	2.399E-10	0.9756056	1.64E-15	3.184E-08	2.459E-10	1	1.681E-15	3	Peloidal	1
4	5032	1.788E-06	3.75E-08	0.9999962	2.016E-06	3	Peloidal	0.9999962	2.907E-08	3.049E-10	0.975606	3.057E-15	2.979E-08	3.125E-10	1	3.134E-15	3	Peloidal	1
4	5032.5	3.821E-06	5.799E-08	0.9999936	2.524E-06	3	Peloidal	0.9999936	6.213E-08	4.714E-10	0.9756032	2.068E-14	6.368E-08	4.832E-10	0.9999999	2.119E-14	3	Peloidal	0.9999999
4	5033	2.065E-05	1.037E-07	0.9999743	4.968E-06	3	Peloidal	0.9999743	3.357E-07	8.432E-10	0.9755842	5.94E-14	3.441E-07	8.643E-10	0.9999997	6.089E-14	3	Peloidal	0.9999997
4	5033.5	3.013E-05	9.643E-08	0.9999649	4.907E-06	3	Peloidal	0.9999649	4.899E-07	7.844E-10	0.9755752	4.009E-14	5.022E-07	8.036E-10	0.9999995	4.11E-14	3	Peloidal	0.9999995
4	5034	2.059E-05	5.295E-08	0.9999765	2.877E-06	3	Peloidal	0.9999765	3.348E-07	4.305E-10	0.9755864	2.943E-14	3.432E-07	4.412E-10	0.9999997	3.017E-14	3	Peloidal	0.9999997
4	5034.5	2.578E-05	2.444E-08	0.9999726	1.637E-06	3	Peloidal	0.9999726	4.192E-07	1.987E-10	0.9755824	2.634E-14	4.297E-07	2.036E-10	0.9999996	2.7E-14	3	Peloidal	0.9999996
4	5035	4.053E-05	1.465E-08	0.9999582	1.228E-06	3	Peloidal	0.9999582	6.592E-07	1.191E-10	0.9755663	8.57E-14	6.757E-07	1.221E-10	0.9999993	8.785E-14	3	Peloidal	0.9999993
4	5035.5	0.0001758	1.932E-08	0.9998218	2.362E-06	3	Peloidal	0.9998218	2.86E-06	1.571E-10	0.9754533	1.793E-13	2.932E-06	1.61E-10	0.999971	1.838E-13	3	Peloidal	0.9999971
4	5036	0.0001912	2.327E-08	0.9998057	3.138E-06	3	Peloidal	0.9998057	3.11E-06	1.892E-10	0.9754129	5.902E-13	3.188E-06	1.939E-10	0.999968	6.051E-13	3	Peloidal	0.999968
4	5036.5	0.0004729	3.889E-08	0.9995218	5.184E-06	3	Peloidal	0.9995218	7.704E-06	3.162E-10	0.9751142	3.876E-12	7.9E-06	3.242E-10	0.9999921	3.975E-12	3	Peloidal	0.9999921
4	5037	0.0018694	6.514E-08	0.9981211	9.434E-06	3	Peloidal	0.9981211	3.058E-05	5.295E-10	0.9736766	2.428E-11	3.141E-05	5.438E-10	0.9999686	2.494E-11	3	Peloidal	0.9999686
4	5037.5	0.0064395	1.305E-07	0.99354	2.03E-05	3	Peloidal	0.99354	0.0001048	1.061E-09	0.9692962	5.847E-12	0.0001081	1.095E-09	0.9998919	6.032E-12	3	Peloidal	0.9998919
4	5038	0.0007252	3.214E-08	0.9992704	4.354E-06	3	Peloidal	0.9992704	1.18E-05	2.613E-10	0.9748911	7.72E-13	1.21E-05	2.68E-10	0.9998979	7.918E-13	3	Peloidal	0.9998979
4	5038.5	0.0004455	1.403E-08	0.9995523	2.14E-06	3	Peloidal	0.9995523	7.262E-06	1.14E-10	0.9751326	2.22E-12	7.447E-06	1.169E-10	0.9999926	2.277E-12	3	Peloidal	0.9999926
4	5039	0.0024306	2.618E-08	0.9975645	4.92E-06	3	Peloidal	0.9975645	4.235E-05	4.235E-10	0.9720508	1.497E-10	4.357E-05	4.287E-10	0.9999564	1.54E-10	3	Peloidal	0.9999564
4	5039.5	0.0493634	2.231E-07	0.9505843	5.21E-05	3	Peloidal	0.9505843	0.0011771	1.798E-09	0.9200638	1.032E-08	0.0012778	1.952E-09	0.9987222	1.12E-08	3	Peloidal	0.9987222
4	5040	0.3178534	1.263E-06	0.6818244	0.000321	3	Peloidal	0.6818244	0.0055705	1.026E-08	0.664317	1.06E-08	0.0083156	1.531E-08	0.9916843	1.582E-08	3	Peloidal	0.9916843
4	5040.5	0.0766389	1.489E-06	0.9230834	0.0002762	3	Peloidal	0.9230834	0.0012507	1.211E-08	0.9005135	4.276E-10	0.001387	1.343E-08	0.998613	4.741E-10	3	Peloidal	0.998613
4	5041	0.0038821	7.351E-07	0.9960336	3.864E-05	3	Peloidal	0.9960336	6.319E-05	5.976E-09	0.9717238	3.504E-11	6.502E-05	6.15E-09	0.999935	3.606E-11	3	Peloidal	0.999935
4	5041.5	0.0010536	1.533E-07	0.998246	2.17E-05	3	Peloidal	0.998246	1.715E-05	1.246E-09	0.9745438	9.365E-12	1.76E-05	1.279E-09	0.999824	9.61E-12	3	Peloidal	0.999824
4	5042	0.0010859	1.142E-07	0.9988924	2.163E-05	3	Peloidal	0.9988924	1.766E-05	9.282E-10	0.9745228	3.533E-12	1.812E-05	9.525E-10	0.9999819	3.625E-12	3	Peloidal	0.9999819
4	5042.5	0.0004113	5.483E-08	0.9957755	1.108E-05	3	Peloidal	0.9957755	6.689E-06	4.458E-10	0.9751947	8.249E-13	6.859E-06	4.571E-10	0.9999931	8.459E-13	3	Peloidal	0.9999931
4	5043	0.0001875	3.771E-08	0.9998076	4.834E-06	3	Peloidal	0.9998076	3.05E-06	3.06E-09	0.9754213	9.36E-14	3.127E-06	3.143E-10	0.999969	9.596E-14	3	Peloidal	0.999969
4	5043.5	4.879E-05	1.672E-08	0.9999495	1.691E-06	3	Peloidal	0.9999495	7.933E-07	1.359E-10	0.9755605	8.509E-16	8.132E-07	1.393E-10	0.9999992	8.722E-16	3	Peloidal	0.9999992
4	5044	1.268E-06	2.463E-09	0.9999985	2.297E-07	3	Peloidal	0.9999985	2.062E-08	2.002E-11	0.9756075	4.676E-15	2.114E-08	2.052E-11	1	4.792E-15	3	Peloidal	1
4	5044.5	5.12E-05	7.839E-09	0.9999473	1.537E-06	3	Peloidal	0.9999473	8.339E-07	6.373E-11	0.97553	1.118E-12	8.548E-07	6.533E-11	0.999991	1.146E-12	3	Peloidal	0.999991
4	5045	0.0018155	6.255E-08	0.9981696	1.483E-05	3	Peloidal	0.9981696	2.975E-05	5.085E-08	0.9736971	4.836E-11	5.055E-05	5.222E-10	0.9999694	4.966E-11	3	Peloidal	0.9999694
4	5045.5	0.0081162	1.439E-07	0.9918462	3.747E-05	3	Peloidal	0.9918462	0.0001326	1.17E-09	0.9675805	7.214E-11	0.000137	1.209E-09	0.999863	7.455E-11	3	Peloidal	0.999863
4	5046	0.0048261	5.569E-08	0.9951562	1.767E-05	3	Peloidal	0.9951562	7.851E-05	4.527E-10	0.970877	3.232E-12	8.086E-05	4.663E-10	0.9999191	3.327E-12	3	Peloidal	0.9999191
4	5046.5	0.0004476	8.088E-09	0.99954	2.405E-06	3	Peloidal	0.99954	7.485E-06	6.575E-11	0.975062	6.119E-12	7.676E-06	6.743E-11	0.9999923	6.275E-12	3	Peloidal	0.9999923
4	5047	0.0024086	1.687E-08	0.9975854	5.972E-06	3	Peloidal	0.9975854	0.0001011	1.333E-09	0.9471711	4.006E-09	0.0001067	1.407E-09	0.9998933	4.229E-09	3	Peloidal	0.9998933
4	5047.5	0.4384813	1.083E-07	0.5614274	9.111E-05	3	Peloidal	0.5614274	0.0155614	8.623E-10	0.5367528	4.572E-08	0.0281749	1.561E-09	0.9718251	8.278E-08	3	Peloidal	0.9718251
4	5048	0.5619755	1.362E-07	0.4379006	0.0001238	1	Cemented Oi	0.5619755	0.0091975	1.107E-09	0.4271728	3.432E-10	0.0210773	2.538E-09	0.9789227	7.865E-10	3	Peloidal	0.9789227
4	5048.5	0.0065132	2.508E-08	0.9934777	9.089E-06	3	Peloidal	0.9934777	0.0001128	2.037E-09	0.9681818	2.5E-10	0.0001165	2.104E-10	0.9998835	2.582E-10	3	Peloidal	0.9998835
4	5049	0.0073697	1.116E-08	0.9926285	1.792E-06	3	Peloidal	0.9926285	0.000983	7.908E-11	0.8501626	5.478E-09	0.0011549	9.291E-11	0.9988451	6.436E-09	3	Peloidal	0.9988451
4	5049.5	0.0411754	2.168E-08	0.9588222	2.368E-06	3	Peloidal	0.9588222	0.0312145	3.294E-11	0.2119311	4.584E-08	0.1283779	1.355E-10	0.8716219	1.885E-07	3	Peloidal	0.8716219
4	5050	0.1859417	2.568E-07	0.81405	8.023E-06	3	Peloidal	0.81405	0.1724646	2.407E-12	0.0396351	1.908E-07	0.8131292	1.135E-11	0.1868699	8.996E-07	1	Cemented Oi	0.8131292
2	5050.5	0.978051	1.273E-06	0.0219381	9.691E-06	1	Cemented Oi	0.978051	0.9080501	1.623E-12	0.0010479	2.307E-07	0.9988471	1.785E-12	0.0011526	2.538E-07	1	Cemented Oi	0.9988471
2	5051	0.9969615	7.871E-07	0.0030311	6.54E-06	1	Cemented Oi	0.9969615	0.9254787	1.907E-12	0.0001452	1.557E-07	0.999843	2.06E-12	0.0001568	1.682E-07	1	Cemented Oi	0.999843
2	5051.5	0.9943677	6.261E-07	0.0056214	1.022E-05	1	Cemented Oi	0.9943677	0.9220944	6.994E-12	0.0002749	2.431E-07	0.9997017	7.583E-12	0.0				

User comment on neural net sheet:																										
Number of predictor variables:		3																								
Predictor variables in 00317- Raw Data:		DENSITY	GR	NEUTRON		SONIC																				
Categorical response variable:		Facies																								
Number of categories:		6																								
Continuous response variable:		[NONE]																								
Number of variables copied:		1																								
Variables copied from 00317- Raw Data:		Facies																								
Probabilities for Facies																										
Facies	DEPTH	Facies 2	Facies 3	Facies 4	Facies 5	Facies 6	Facies 7	Pred.Category	Pred.Faci	Prob.max	Facies 7	Facies 2	Facies 3	Facies 4	Facies 5	Facies 6	Facies 7	Faci	Prob.	Maximum	Pred.Cat	Pred.Faci	Prob.Max			
4	4858	1.59E-08	6.83E-12	1	9.99E-09	9.74407E-20	4.69E-18	3	Facies 4	1	0	1.35E-10	1.84E-23	0.991525	9.47E-34	0	0	1.36E-10	1.85E-23	1	9.55E-34	0	0	3	Facies 4	1
4	4858.5	5.67E-09	1.87E-12	1	2.97E-09	3.02322E-20	1.53E-18	3	Facies 4	1	0	4.8E-11	3.15E-24	0.991525	1.13E-34	0	0	4.85E-11	3.18E-24	1	1.14E-34	0	0	3	Facies 4	1
4	4859	3.55E-09	7.59E-13	1	1.32E-09	1.44073E-20	7.42E-19	3	Facies 4	1	0	3.01E-11	1.27E-24	0.991525	8.99E-35	0	0	3.03E-11	1.28E-24	1	9.07E-35	0	0	3	Facies 4	1
4	4859.5	3.52E-09	7.15E-13	1	1.11E-09	1.18603E-20	6.14E-19	3	Facies 4	1	0	2.98E-11	2.27E-24	0.991525	6.27E-34	0	0	3.01E-11	2.29E-24	1	6.33E-34	0	0	3	Facies 4	1
4	4860	6.69E-09	2.08E-12	1	3.07E-09	3.09727E-20	1.55E-18	3	Facies 4	1	0	5.67E-11	1.87E-23	0.991525	4.28E-32	0	0	5.72E-11	1.89E-23	1	4.32E-32	0	0	3	Facies 4	1
4	4860.5	1.95E-08	1.74E-11	1	2.6E-08	2.22082E-19	1.05E-17	3	Facies 4	1	0	1.61E-10	4.64E-22	0.991525	2.21E-29	0	0	1.62E-10	4.68E-22	1	2.22E-29	0	0	3	Facies 4	1
4	4861	5.61E-08	4.47E-10	0.999999	6.44E-07	4.1926E-18	1.88E-16	3	Facies 4	0.999999	0	4.75E-10	2.52E-21	0.991525	8.84E-22	0	0	4.79E-10	2.54E-21	1	8.92E-22	0	0	3	Facies 4	1
4	4861.5	1.19E-08	2.26E-08	0.999974	2.6E-05	1.12093E-16	4.68E-15	3	Facies 4	0.999974	0	1.01E-10	4.21E-19	0.9915	1.57E-15	0	0	1.01E-10	4.25E-19	1	1.58E-15	0	0	3	Facies 4	1
4	4862	2.95E-08	2.54E-06	0.998871	0.001126	9.2341E-15	3.95E-13	3	Facies 4	0.998871	0	2.46E-10	2.33E-13	0.990406	6.9E-11	0	0	2.48E-10	2.35E-13	1	6.9E-11	0	0	3	Facies 4	1
4	4862.5	3.15E-06	0.000225	0.996421	0.00335	6.87871E-13	3.79E-11	3	Facies 4	0.996421	0	2.67E-08	8.72E-08	0.987564	6.68E-08	0	0	2.7E-08	8.83E-08	1	6.76E-08	0	0	3	Facies 4	1
4	4863	0.001289	0.041807	0.953031	0.003872	7.75385E-11	5.99E-09	3	Facies 4	0.953031	0	1.08E-05	0.000372	0.934428	8.69E-06	0	0	1.16E-05	0.000398	0.999581	9.3E-06	0	0	3	Facies 4	0.999581
4	4863.5	0.000405	0.139355	0.854842	0.005758	4.86975E-10	1.57E-08	3	Facies 4	0.854842	0	2.39E-06	0.005537	0.607597	0.001401	0	0	3.9E-06	0.00901	0.988707	0.00228	0	0	3	Facies 4	0.988707
4	4864	7.22E-05	0.029659	0.939831	0.030438	1.69603E-09	1.91E-08	3	Facies 4	0.939831	0	2.06E-09	0.002035	0.065427	0.02623	0	0	2.2E-08	0.021716	0.698325	0.279959	0	0	3	Facies 4	0.698325
5	4864.5	5.17E-05	0.029132	0.037842	0.932974	6.29219E-08	1.25E-07	4	Facies 5	0.932974	0	2.45E-09	0.001932	0.002718	0.804058	0	0	3.02E-09	0.002388	0.003361	0.994251	0	0	4	Facies 5	0.994251
5	4865	0.000346	0.000107	0.067972	0.931548	2.51359E-05	1.06E-06	4	Facies 5	0.931548	0	7.85E-13	7.16E-06	0.004532	0.807342	0	0	9.67E-13	8.81E-06	0.005581	0.99441	0	0	4	Facies 5	0.99441
5	4865.5	8.76E-11	6.53E-12	3.448E-06	0.999996	2.10184E-07	5.69E-12	4	Facies 5	0.999996	0	5.41E-20	4.36E-13	2.32E-07	0.866663	0	0	6.24E-20	5.03E-13	2.68E-07	1	0	0	4	Facies 5	1
5	4866	2.31E-11	5.91E-12	9.47E-07	0.999999	7.09626E-08	1.32E-12	4	Facies 5	0.999999	0	9.39E-20	3.94E-13	6.31E-08	0.866665	0	0	1.08E-19	4.45E-13	7.28E-08	1	0	0	4	Facies 5	1
5	4866.5	9.3E-11	3.46E-12	6.25E-06	0.999994	3.80102E-07	2.79E-12	4	Facies 5	0.999994	0	7.18E-18	2.3E-13	4.16E-07	0.866663	0	0	8.28E-18	2.66E-13	4.81E-07	1	0	0	4	Facies 5	1
5	4867	8.66E-10	1.34E-11	0.000116	0.998883	2.34205E-07	4.26E-12	4	Facies 5	0.998883	0	7.92E-15	8.91E-13	7.88E-06	0.865622	0	0	9.15E-15	1.03E-12	9.1E-06	0.999991	0	0	4	Facies 5	0.999991
5	4867.5	1.2E-06	0.000133	0.011203	0.988663	5.88956E-09	3.16E-10	4	Facies 5	0.988663	0	1.62E-10	8.69E-06	0.000911	0.843251	0	0	1.92E-10	1.03E-05	0.01079	0.998981	0	0	4	Facies 5	0.998981
5	4868	0.000299	2.18E-05	0.17386	0.826293	1.10489E-12	1.18E-09	4	Facies 5	0.826293	0	1.03E-11	2.43E-06	0.010984	0.68169	0	0	1.49E-11	3.52E-06	0.015858	0.984139	0	0	4	Facies 5	0.984139
5	4868.5	0.00078	0.001434	0.109061	0.888726	7.6944E-13	1.56E-08	4	Facies 5	0.888726	0	2.9E-14	0.001391	1.14E-07	0.026541	0	0	1.04E-12	0.04979	4.07E-06	0.950205	0	0	4	Facies 5	0.950205
3	4869	0.022032	0.965267	0.012212	0.000489	1.65703E-10	3.02E-08	2	Facies 3	0.965267	0	2.52E-14	0.936449	4.11E-09	1.46E-05	0	0	2.69E-14	0.999984	4.38E-09	1.56E-05	0	0	2	Facies 3	0.999984
3	4869.5	0.009425	0.990356	5.74E-05	0.000162	9.33545E-10	2.68E-08	2	Facies 3	0.990356	0	2.98E-15	0.960763	1.29E-10	4.84E-06	0	0	3.1E-15	0.999995	1.34E-10	5.04E-06	0	0	2	Facies 3	0.999995
3	4870	0.025136	0.973702	9.48E-05	0.001067	1.33622E-08	2.83E-07	2	Facies 3	0.973702	0	1.15E-16	0.944631	3.52E-11	3.19E-05	0	0	1.22E-16	0.999966	3.73E-11	3.37E-05	0	0	2	Facies 3	0.999966
3	4870.5	0.001052	0.998765	2.09E-06	0.000181	2.98171E-10	6.09E-09	2	Facies 3	0.998765	0	6.59E-16	0.968948	4.5E-13	5.4E-06	0	0	6.8E-16	0.999994	4.64E-13	5.58E-06	0	0	2	Facies 3	0.999994
3	4871	0.000129	0.999748	1.81E-05	0.000105	1.54556E-11	3.47E-10	2	Facies 3	0.999748	0	2.1E-13	0.969871	4.82E-11	3.13E-06	0	0	2.17E-13	0.999997	4.97E-11	3.22E-06	0	0	2	Facies 3	0.999997
3	4871.5	0.001641	0.974318	0.022872	0.001169	1.1337E-10	3.5E-09	2	Facies 3	0.974318	0	2.83E-12	0.945132	1.81E-07	3.5E-05	0	0	3E-12	0.999963	1.91E-07	3.7E-05	0	0	2	Facies 3	0.999963
3	4872	0.018732	0.701502	0.027756	0.002635	6.54874E-10	3.72E-08	2	Facies 3	0.701502	0	3.54E-13	0.680557	1.39E-07	7.87E-05	0	0	5.2E-13	0.999884	2.04E-07	0.000116	0	0	2	Facies 3	0.999884
3	4872.5	0.019005	0.977113	0.003628	0.000237	1.24659E-09	6.77E-08	2	Facies 3	0.977113	0	1.72E-12	0.947954	1.97E-09	7.07E-06	0	0	1.82E-12	0.999998	2.08E-09	7.46E-06	0	0	2	Facies 3	0.999993
3	4873	0.038518	0.959053	0.002178	0.000205	1.06398E-08	5.31E-07	2	Facies 3	0.959053	0	3.58E-11	0.93039	5.97E-09	4.78E-06	0	0	3.85E-11	0.999992	6.41E-09	8.04E-06	0	0	2	Facies 3	0.999992
3	4873.5	0.017	0.979074	0.002671	0.001025	8.48794E-08	2.69E-06	2	Facies 3	0.979074	0	2.18E-10	0.949469	7.99E-08	3.78E-05	0	0	2.29E-10	0.99996	8.42E-08	3.98E-05	0	0	2	Facies 3	0.999996
3	4874	0.002302	0.988499	0.000935	0.008259	3.69757E-07	5.42E-06	2	Facies 3	0.988499	0	1.7E-10	0.939031	1.4E-06	0.000401	0	0	1.81E-10	0.999972	1.49E-06	0.000427	0	0	2	Facies 3	0.999972
3	4874.5	0.000491	0.963488	0.000185	0.034925																					

5	4877	0.000218	0.043659	1.11E-06	0.946838	0.005470547	0.003813	4 Facies 5	0.946838	0	2.57E-14	0.026808	2.92E-08	0.340572	0	0	7E-14	0.027971	7.94E-08	0.927029	0	0	4 Facies 5	0.927029
5	4877.5	0.000203	0.182565	4.74E-07	0.816861	7.20159E-05	0.000298	4 Facies 5	0.816861	0	7.95E-14	0.158168	3.63E-09	0.102906	0	0	3.05E-13	0.605835	1.39E-08	0.394165	0	0	2 Facies 3	0.605835
5	4878	0.002334	0.533045	3.03E-07	0.464475	9.75616E-06	0.000134	2 Facies 3	0.533045	0	1.39E-12	0.460295	2.39E-08	0.059737	0	0	2.67E-12	0.885128	4.59E-08	0.114872	0	0	2 Facies 3	0.885128
3	4878.5	0.004053	0.456026	5.71E-06	0.538792	2.49174E-05	0.000498	4 Facies 5	0.538792	0	7.51E-14	0.407305	3.24E-08	0.054503	0	0	1.63E-13	0.881979	7.02E-08	0.118021	0	0	2 Facies 3	0.881979
3	4879	0.000657	0.270524	1.91E-06	0.728266	7.10845E-05	0.000481	4 Facies 5	0.728266	0	4.07E-17	0.261402	5.44E-10	0.024349	0	0	1.42E-16	0.914788	1.91E-09	0.085212	0	0	2 Facies 3	0.914788
3	4879.5	3.57E-06	0.87629	1.13E-05	0.12247	0.00115665	6.91E-05	2 Facies 3	0.87629	0	1.3E-18	0.850125	6.24E-12	0.003657	0	0	1.53E-19	0.995717	7.3E-12	0.004283	0	0	2 Facies 3	0.995717
3	4880	2.55E-09	0.996609	5.97E-05	0.000268	0.003061759	1.45E-06	2 Facies 3	0.996609	0	1.18E-19	0.96688	4.16E-11	8.01E-06	0	0	1.22E-19	0.999992	4.31E-11	8.28E-06	0	0	2 Facies 3	0.999992
3	4880.5	1.04E-08	0.984149	0.000131	0.000328	0.015390878	1.69E-06	2 Facies 3	0.984149	0	8.51E-16	0.95436	5.21E-09	9.9E-06	0	0	8.91E-16	0.99999	5.46E-09	1.04E-05	0	0	2 Facies 3	0.99999
3	4881	1.29E-06	0.875423	0.072156	0.012283	0.040128072	8.52E-06	2 Facies 3	0.875423	0	2.05E-14	0.847966	8.18E-06	0.000384	0	0	2.42E-14	0.999538	9.65E-06	0.000452	0	0	2 Facies 3	0.999538
3	4881.5	0.001915	0.912454	0.036743	0.04874	9.99223E-05	4.8E-05	2 Facies 3	0.912455	0	1.97E-14	0.884657	1.66E-06	0.001483	0	0	2.23E-14	0.998325	1.88E-06	0.001673	0	0	2 Facies 3	0.998325
3	4882	0.002476	0.950223	0.026288	0.020977	2.33756E-02	3.45E-05	2 Facies 3	0.950223	0	3.39E-18	0.921858	1.12E-09	0.000626	0	0	3.68E-18	0.999321	1.22E-09	0.000679	0	0	2 Facies 3	0.999321
3	4882.5	3.63E-05	0.996199	0.003744	2.07E-05	2.75488E-12	5.48E-07	2 Facies 3	0.996199	0	4.59E-24	0.966461	1.56E-13	6.18E-07	0	0	4.75E-24	0.999999	1.62E-13	6.4E-07	0	0	2 Facies 3	0.999999
3	4883	3.34E-05	0.999962	4.09E-06	2.03E-08	7.90488E-14	4.79E-08	2 Facies 3	0.999962	0	1.66E-25	0.970113	1.45E-17	6.07E-10	0	0	1.71E-25	1	1.49E-17	6.26E-10	0	0	2 Facies 3	1
3	4883.5	1.7E-05	0.999983	2.6E-07	1.72E-09	1.50128E-13	7.01E-08	2 Facies 3	0.999983	0	1.39E-27	0.970132	5.69E-19	5.15E-11	0	0	1.44E-27	1	5.86E-19	5.31E-11	0	0	2 Facies 3	1
3	4884	6.6E-06	0.999993	8.87E-08	1.07E-09	6.09857E-13	2.17E-07	2 Facies 3	0.999993	0	2.07E-28	0.970143	9.4E-21	3.18E-11	0	0	2.13E-21	0	9.69E-21	3.28E-11	0	0	2 Facies 3	1
3	4884.5	8.61E-06	0.999991	9.12E-08	5.17E-11	4.27103E-13	6.67E-07	2 Facies 3	0.999991	0	9.68E-28	0.970142	3.59E-21	1.54E-12	0	0	9.96E-28	1	3.7E-21	1.59E-12	0	0	2 Facies 3	1
3	4885	0.000121	0.999876	4.98E-07	1.92E-11	7.39276E-13	2.55E-06	2 Facies 3	0.999876	0	1.49E-25	0.970029	1.28E-20	5.73E-13	0	0	1.53E-25	1	1.32E-20	5.91E-13	0	0	2 Facies 3	1
3	4885.5	0.000622	0.999369	5.87E-06	1.25E-11	7.44335E-13	3.18E-06	2 Facies 3	0.999369	0	1.41E-23	0.969537	1.39E-19	3.74E-13	0	0	1.46E-23	1	1.44E-19	3.86E-13	0	0	2 Facies 3	1
3	4886	0.001541	0.998408	4.89E-05	1.16E-11	6.28998E-13	2.62E-06	2 Facies 3	0.998408	0	1.53E-21	0.968605	2.42E-18	3.45E-13	0	0	1.58E-21	1	2.5E-18	3.56E-13	0	0	2 Facies 3	1
3	4886.5	0.002198	0.997563	0.000236	2.4E-11	6.38482E-13	1.23E-06	2 Facies 3	0.997565	0	5.22E-20	0.967787	1.07E-16	7.18E-13	0	0	5.4E-20	1	1.11E-16	7.42E-13	0	0	2 Facies 3	1
3	4887	0.003182	0.995255	0.001563	2.19E-10	1.87424E-12	4.88E-07	2 Facies 3	0.995255	0	7.99E-20	0.965546	2.7E-15	6.55E-12	0	0	8.27E-20	1	2.8E-15	6.79E-12	0	0	2 Facies 3	1
3	4887.5	0.007112	0.992630	0.000249	8.34E-10	1.42338E-11	3.02E-06	2 Facies 3	0.992630	0	3.76E-21	0.963004	2.85E-15	2.49E-11	0	0	3.9E-21	1	2.96E-15	2.59E-11	0	0	2 Facies 3	1
3	4888	0.000775	0.999214	1.2E-06	5.58E-09	3.38376E-11	9.59E-06	2 Facies 3	0.999214	0	3.48E-22	0.969387	6.04E-17	1.66E-10	0	0	3.59E-22	1	6.23E-17	1.72E-10	0	0	2 Facies 3	1
3	4888.5	0.000842	0.999134	5.55E-07	2.45E-08	9.35845E-11	2.37E-05	2 Facies 3	0.999134	0	3E-22	0.969309	5.13E-17	7.32E-10	0	0	3.09E-22	1	5.3E-17	7.55E-10	0	0	2 Facies 3	1
3	4889	0.000861	0.999094	4.06E-07	4.51E-08	1.52387E-10	4.4E-05	2 Facies 3	0.999094	0	1.57E-22	0.969271	4.07E-17	1.34E-09	0	0	1.62E-22	1	4.2E-17	1.39E-09	0	0	2 Facies 3	1
3	4889.5	0.000743	0.9992	2.85E-07	4.88E-08	1.61561E-10	5.68E-05	2 Facies 3	0.9992	0	1.03E-22	0.969373	2.80E-17	1.46E-09	0	0	1.06E-22	1	2.15E-17	1.5E-09	0	0	2 Facies 3	1
3	4890	0.000394	0.999016	5.63E-07	3.57E-08	1.44624E-10	4.99E-05	2 Facies 3	0.999016	0	3.15E-22	0.969195	1.58E-17	1.06E-09	0	0	3.25E-22	1	1.63E-17	1.1E-09	0	0	2 Facies 3	1
3	4890.5	0.002271	0.997693	6.66E-06	1.36E-08	1.14322E-10	2.88E-05	2 Facies 3	0.997693	0	2.14E-21	0.967912	3.83E-17	4.07E-10	0	0	2.21E-21	1	3.95E-17	4.21E-10	0	0	2 Facies 3	1
3	4891	0.006764	0.992993	0.000231	2.78E-09	6.63758E-11	1.24E-05	2 Facies 3	0.992993	0	1.45E-20	0.963531	1.05E-16	8.31E-11	0	0	1.51E-20	1	1.09E-16	8.62E-11	0	0	2 Facies 3	1
3	4891.5	0.0040532	0.995044	0.000422	2.22E-10	3.91774E-12	1.49E-06	2 Facies 3	0.995044	0	7.75E-19	0.965341	1.58E-16	6.62E-12	0	0	8.03E-19	1	1.64E-16	6.86E-12	0	0	2 Facies 3	1
3	4892	0.001566	0.998348	8.57E-05	1.81E-10	1.25188E-13	9.54E-08	2 Facies 3	0.998348	0	1.45E-16	0.968547	3.34E-15	5.41E-12	0	0	1.5E-16	1	3.45E-15	5.58E-12	0	0	2 Facies 3	1
3	4892.5	0.001719	0.997630	0.000642	1.39E-08	1.27229E-13	2.52E-08	2 Facies 3	0.997639	0	4.45E-15	0.967851	1.01E-11	4.15E-10	0	0	4.59E-15	1	1.04E-11	4.29E-10	0	0	2 Facies 3	1
3	4893	0.04248	0.821793	0.135721	6.18E-06	2.03534E-12	4.42E-08	2 Facies 3	0.821793	0	3.55E-15	0.979262	2.43E-10	1.85E-07	0	0	4.45E-15	1	3.05E-10	2.32E-07	0	0	2 Facies 3	1
3	4893.5	0.021891	0.885431	0.092677	7.68E-07	4.65207E-12	3.92E-08	2 Facies 3	0.885431	0	1.55E-16	0.859	8.45E-12	2.29E-08	0	0	1.81E-16	1	9.84E-12	2.67E-08	0	0	2 Facies 3	1
3	4894	0.019644	0.922605	0.057747	4.07E-08	1.40711E-11	1.13E-07	2 Facies 3	0.922609	0	1.87E-18	0.895061	7.49E-13	1.21E-09	0	0	2.08E-18	1	8.36E-13	1.36E-09	0	0	2 Facies 3	1
3	4894.5	0.0040997	0.984430	0.010564	6.22E-09	2.00110E-12	6.71E-08	2 Facies 3	0.984430	0	4.05E-21	0.955033	1.07E-14	1.86E-10	0	0	4.24E-21	1	1.12E-14	1.94E-10	0	0	2 Facies 3	1
3	4895	0.000962	0.998075	0.000963	4.93E-10	2.07488E-13	3.62E-08	2 Facies 3	0.998075	0	3.16E-22	0.968282	9.25E-17	1.47E-11	0	0	3.27E-22	1	9.55E-17	1.52E-11	0	0	2 Facies 3	1
3	4895.5	0.000368	0.999457	0.000175	4.68E-11	4.30012E-14	3.45E-08	2 Facies 3	0.999457	0	2.49E-19	0.969622	9.9E-18	1.4E-12	0	0	2.56E-19	1	1.02E-17	1.44E-12	0	0	2 Facies 3	1
3	4896	0.000332	0.999477	0.000191	1.39E-11	3.70452E-14	5.87E-08	2 Facies 3	0.999477	0	4.48E-16	0.969642	2.74E-14	4.15E-13	0	0	4.62E-16	1	2.82E-14	4.28E-13	0	0	2 Facies 3	1
3	4896.5	0.000867	0.990984	0.008149	4.87E-11	8.45468E-13	3.69E-07	2 Facies 3	0.990984	0	1.27E-13	0.961402	1.39E-10	1.45E-12	0	0	1.33E-13	1	1.44E-10	1.51E-12	0	0	2 Facies 3	1
3	4897	0.004209	0.614162	0.381628	2.13E-06	5.19868E-11	1.																	

3	4902	0.000677	0.998786	0.000538	1.18E-08	2.86923E-14	5.05E-09	2 Facies 3	0.998786	0	4.13E-17	0.968971	1.57E-14	3.53E-10	0	0	0	4.26E-17	1	1.62E-14	3.65E-10	0	0	0	2 Facies 3	1
3	4902.5	0.002523	0.966754	0.030723	1.11E-08	1.70953E-12	2.25E-08	2 Facies 3	0.966754	0	1.14E-14	0.937896	5.48E-12	3.3E-10	0	0	0	1.21E-14	1	5.84E-12	3.52E-10	0	0	0	2 Facies 3	1
3	4903	0.020426	0.694131	0.285443	5.74E-08	5.69887E-11	1.17E-07	2 Facies 3	0.694131	0	3.16E-12	0.673411	5.81E-12	1.71E-09	0	0	0	4.69E-12	1	8.63E-12	2.55E-09	0	0	0	2 Facies 3	1
3	4903.5	0.004427	0.876579	0.118995	8.52E-09	1.04635E-11	7.17E-08	2 Facies 3	0.876579	0	1.39E-10	0.850412	3.68E-13	2.54E-10	0	0	0	1.64E-10	1	4.33E-13	2.99E-10	0	0	0	2 Facies 3	1
3	4904	0.000517	0.991778	0.007075	1.48E-09	3.74867E-13	1.16E-08	2 Facies 3	0.991778	0	3.21E-08	0.962113	3.41E-14	4.41E-11	0	0	0	3.33E-08	1	3.55E-14	4.59E-11	0	0	0	2 Facies 3	1
3	4904.5	0.000247	0.999286	0.000467	2.19E-09	2.5671E-14	1.75E-09	2 Facies 3	0.999286	0	5.06E-05	0.771283	2.31E-15	5.12E-11	0	0	0	6.56E-05	0.999934	2.99E-15	6.64E-11	0	0	0	2 Facies 3	0.999934
3	4905	0.019286	0.978317	0.002396	1.73E-08	2.98693E-14	4.13E-09	2 Facies 3	0.978317	0	0.017998	0.065005	1.21E-16	6.15E-12	0	0	0	0.216833	0.783165	1.46E-15	7.41E-11	0	0	0	2 Facies 3	0.783165
2	4905.5	0.791333	0.161325	0.047342	6.81E-08	2.53854E-14	7.97E-09	1 Facies 2	0.791333	0	0.74716	0.009004	3.15E-17	5.72E-13	0	0	0	0.988092	0.011908	4.17E-17	7.57E-13	0	0	0	1 Facies 2	0.988092
2	4906	0.924495	0.004425	0.07108	2.97E-08	3.16085E-15	1.68E-09	1 Facies 2	0.924495	0	0.873129	0.000246	2.6E-16	4.85E-15	0	0	0	0.999718	0.000282	2.98E-16	5.55E-15	0	0	0	1 Facies 2	0.999718
2	4906.5	0.994413	9.25E-05	0.005495	7.23E-09	1.05127E-16	4.24E-10	1 Facies 2	0.994413	0	0.939167	5.14E-06	3.46E-15	1.58E-16	0	0	0	0.99999	5.47E-06	3.68E-16	1.69E-16	0	0	0	1 Facies 2	0.999995
2	4907	0.991393	1.24E-05	0.008594	9.83E-09	3.62106E-17	3.12E-10	1 Facies 2	0.991393	0	0.936315	6.88E-07	5.94E-13	2.67E-16	0	0	0	0.99999	7.34E-07	6.35E-13	2.86E-16	0	0	0	1 Facies 2	0.999999
2	4907.5	0.958162	1.48E-05	0.041823	4.46E-08	1.3259E-16	5.55E-10	1 Facies 2	0.958162	0	0.90493	8.25E-07	6.31E-11	1.04E-15	0	0	0	0.99999	9.12E-07	6.98E-11	1.15E-15	0	0	0	1 Facies 2	0.999999
2	4908	0.637372	8.47E-06	0.362619	2.69E-07	8.83531E-16	1.74E-10	1 Facies 2	0.637372	0	0.601963	4.71E-07	9.16E-10	2.51E-16	0	0	0	0.99999	7.82E-07	1.52E-07	4.17E-16	0	0	0	1 Facies 2	0.999999
2	4908.5	0.137215	7.29E-08	0.862784	3.27E-07	6.51948E-16	3.13E-12	3 Facies 4	0.862784	0	0.129592	4.05E-09	3.3E-10	4.55E-17	0	0	0	1	3.13E-08	2.55E-09	3.51E-16	0	0	0	1 Facies 2	1
2	4909	0.212832	1.69E-08	0.787166	1.94E-06	9.14289E-16	5.6E-13	3 Facies 4	0.787166	0	0.201008	9.38E-10	7.76E-11	3.58E-15	0	0	0	1	4.67E-09	3.86E-10	1.78E-14	0	0	0	1 Facies 2	1
2	4909.5	0.617737	6.5E-07	0.382225	3.69E-05	1.26511E-14	3.37E-12	1 Facies 2	0.617737	0	0.583417	3.61E-06	5.78E-11	3.74E-12	0	0	0	1	6.19E-08	9.98E-11	6.41E-12	0	0	0	1 Facies 2	1
2	4910	0.927405	5.34E-05	0.072357	0.000184	1.45907E-13	2.38E-11	1 Facies 2	0.927405	0	0.87587	2.97E-06	1.28E-10	7.65E-11	0	0	0	0.999997	3.39E-06	1.47E-10	8.74E-11	0	0	0	1 Facies 2	0.999997
2	4910.5	0.990273	0.000234	0.009387	0.000106	1.77007E-13	1.99E-11	1 Facies 2	0.990273	0	0.935124	1.35E-05	1.64E-09	4.55E-10	0	0	0	0.99986	1.39E-05	1.76E-09	4.87E-10	0	0	0	1 Facies 2	0.99986
2	4911	0.997448	0.001842	0.000686	2.34E-05	3.37469E-13	2.37E-11	1 Facies 2	0.997448	0	0.925108	0.000132	1.62E-07	1.24E-08	0	0	0	0.999857	0.000143	1.76E-07	1.34E-08	0	0	0	1 Facies 2	0.999857
2	4911.5	0.903195	0.065037	0.031714	5.4E-05	1.47045E-11	1.95E-09	1 Facies 2	0.903195	0	0.714792	0.012909	0.000174	2.53E-07	0	0	0	0.98203	0.017732	0.000239	3.47E-07	0	0	0	1 Facies 2	0.98203
2	4912	0.275782	0.437562	0.286653	3.41E-06	1.0278E-10	1.18E-07	2 Facies 3	0.437562	0	0.244937	0.045769	0.001615	5.49E-09	0	0	0	0.837907	0.15657	0.005523	1.88E-08	0	0	0	1 Facies 2	0.837907
2	4912.5	0.483135	0.430541	0.086322	1.92E-06	1.33992E-09	6E-07	1 Facies 2	0.483135	0	0.439859	0.025244	0.002657	3.01E-10	0	0	0	0.940351	0.053968	0.005681	6.43E-10	0	0	0	1 Facies 2	0.940351
2	4913	0.158962	0.076808	0.636492	5.26E-06	9.94202E-08	2.43E-06	1 Facies 2	0.859692	0	0.574175	0.003129	0.018497	2.58E-10	0	0	0	0.963703	0.005252	0.031046	4.33E-10	0	0	0	1 Facies 2	0.963703
2	4913.5	0.191798	0.039287	0.090202	9.86E-06	1.51093E-08	2.83E-06	1 Facies 2	0.919798	0	0.088162	0.002006	0.036767	1.53E-11	0	0	0	0.704536	0.001644	0.29382	1.22E-10	0	0	0	1 Facies 2	0.704536
2	4914	0.860542	0.057759	0.081685	1.12E-05	1.29E-08	2.12E-06	1 Facies 2	0.860542	0	0.008329	4.63E-06	0.080888	3E-12	0	0	0	0.093353	5.19E-06	0.906595	3.37E-11	0	0	0	3 Facies 4	0.906595
4	4914.5	0.114732	0.105411	0.779855	3.97E-07	2.23942E-09	1.3E-06	3 Facies 4	0.779855	0	0.000996	5.69E-06	0.773032	6.55E-13	0	0	0	0.001287	8.98E-06	0.998704	8.46E-13	0	0	0	3 Facies 4	0.998704
4	4915	0.009199	0.633369	0.357431	7.36E-09	4.89278E-11	7.44E-07	2 Facies 3	0.633369	0	7.85E-05	1.96E-05	0.35437	6.24E-15	0	0	0	0.000221	5.53E-05	0.999723	1.76E-14	0	0	0	3 Facies 4	0.999723
4	4915.5	0.005695	0.174856	0.819448	8.48E-09	1.48157E-10	5.53E-07	3 Facies 4	0.819448	0	4.95E-05	2.31E-05	0.812218	3.11E-14	0	0	0	0.609E-05	2.84E-05	0.999911	3.83E-14	0	0	0	3 Facies 4	0.999911
4	4916	0.15918	0.088056	0.896025	4.33E-08	4.32923E-10	5.15E-07	3 Facies 4	0.896025	0	0.000201	0.000109	0.085351	1.31E-12	0	0	0	0.00022	0.000123	0.999649	1.49E-12	0	0	0	3 Facies 4	0.999649
4	4916.5	0.104599	0.455434	0.439966	3.53E-07	5.50218E-10	3.94E-07	2 Facies 3	0.455435	0	0.001942	0.000441	0.431367	4E-12	0	0	0	0.004477	0.001016	0.994507	9.22E-12	0	0	0	3 Facies 4	0.994507
4	4917	0.240322	0.503276	0.2564	1.56E-06	2.14831E-10	1.23E-07	2 Facies 3	0.503276	0	0.002764	9.73E-05	0.253402	6.57E-13	0	0	0	0.010786	0.00038	0.988834	2.56E-12	0	0	0	3 Facies 4	0.988834
4	4917.5	0.15993	0.257294	0.546758	1.45E-05	4.23187E-11	5.94E-08	3 Facies 4	0.546758	0	0.001758	7.65E-05	0.541836	6.6E-14	0	0	0	0.003234	1.41E-05	0.996752	1.21E-13	0	0	0	3 Facies 4	0.996752
4	4918	0.056672	0.011834	0.931328	0.000166	2.79496E-10	9.34E-09	3 Facies 4	0.931328	0	0.000492	1.41E-07	0.923237	1.29E-15	0	0	0	0.000523	1.52E-07	0.999468	1.4E-15	0	0	0	3 Facies 4	0.999468
4	4918.5	0.022804	6.83E-06	0.977102	8.65E-05	8.77418E-14	3.84E-11	3 Facies 4	0.977102	0	0.000207	2.53E-10	0.968177	3.78E-17	0	0	0	0.000214	2.61E-10	0.999786	3.9E-17	0	0	0	3 Facies 4	0.999786
4	4919	0.0652	2.32E-07	0.934759	4E-05	8.11322E-15	1.65E-12	3 Facies 4	0.934759	0	0.000617	1.36E-11	0.925863	4.8E-18	0	0	0	0.000664	1.46E-11	0.999334	5.18E-18	0	0	0	3 Facies 4	0.999334
4	4919.5	0.088743	2.75E-08	0.911248	9.48E-06	1.50088E-12	3.62E-13	3 Facies 4	0.911248	0	0.000949	3.62E-12	0.901382	1.12E-18	0	0	0	0.001957	6.85E-10	0.929948	1.24E-18	0	0	0	3 Facies 4	0.929948
4	4920	0.180091	2.43E-08	0.819903	6.61E-06	1.3673E-15	4.26E-13	3 Facies 4	0.819903	0	0.001928	3.22E-12	0.811015	4.6E-19	0	0	0	0.002372	3.97E-12	0.997628	5.66E-19	0	0	0	3 Facies 4	0.997628
4	4920.5	0.189852	1.94E-08	0.810145	2.37E-06	1.4233E-15	6.79E-13	3 Facies 4	0.810145	0	0.001918	1.87E-12	0.801884	2.42E-19	0	0	0	0.002386	2.							

4	4927	0.008356	5.08E-11	0.991644	3.05E-08	5.71009E-18	3.46E-15	3 Facies 4	0.991644	0	7.26E-05	6.34E-16	0.983019	1.18E-23	0	0	7.38E-05	6.44E-16	0.999926	1.2E-23	0	0
4	4927.5	0.024779	7.24E-10	0.97522	6.6E-07	6.01246E-17	1.66E-14	3 Facies 4	0.97522	0	0.000217	1.25E-14	0.966656	4.27E-21	0	0	0.000225	1.29E-14	0.999775	4.41E-21	0	0
4	4928	0.033573	9.29E-09	0.966422	4.91E-06	3.91928E-16	6.93E-14	3 Facies 4	0.966422	0	0.000297	2.08E-13	0.957846	9.88E-22	0	0	0.00031	2.17E-13	0.99969	1.03E-21	0	0
4	4928.5	0.044499	1.15E-09	0.95555	7.93E-07	1.01917E-16	3.41E-14	3 Facies 4	0.95555	0	0.000381	6.39E-15	0.947308	1.06E-23	0	0	0.000402	6.74E-15	0.999598	1.12E-23	0	0
4	4929	0.01145	1.02E-10	0.988549	2.56E-08	9.19304E-18	8.98E-15	3 Facies 4	0.988549	0	9.79E-05	4.38E-16	0.980096	1.56E-24	0	0	9.98E-05	4.47E-16	0.9999	1.59E-24	0	0
4	4929.5	0.008825	2.67E-10	0.991175	6.05E-09	6.50483E-18	2.46E-14	3 Facies 4	0.991175	0	7.59E-05	2E-15	0.982643	3.11E-24	0	0	7.72E-05	2.04E-15	0.999923	3.17E-24	0	0
4	4930	0.01518	1.33E-09	0.98482	4.53E-09	8.55435E-18	1.07E-13	3 Facies 4	0.98482	0	0.000132	1.68E-14	0.976252	7.04E-24	0	0	0.000135	1.72E-14	0.999865	7.21E-24	0	0
4	4930.5	0.024971	2.47E-09	0.975029	1.19E-08	2.12075E-17	1.94E-13	3 Facies 4	0.975029	0	0.00022	5.03E-14	0.966411	1.35E-23	0	0	0.000228	5.2E-14	0.999772	1.39E-23	0	0
4	4931	0.039888	2.09E-09	0.960112	6.37E-08	6.65237E-17	1.63E-13	3 Facies 4	0.960112	0	0.00035	3.61E-14	0.95168	1.12E-24	0	0	0.000367	3.79E-14	0.999633	1.18E-24	0	0
4	4931.5	0.035007	4.31E-10	0.964993	2.37E-07	4.31255E-17	2.11E-14	3 Facies 4	0.964993	0	0.000297	5.66E-16	0.956792	7.32E-26	0	0	0.000311	5.91E-16	0.999689	7.65E-26	0	0
4	4932	0.002756	4.72E-11	0.997244	7.64E-08	4.48902E-18	1.08E-15	3 Facies 4	0.997244	0	2.34E-05	1.02E-17	0.988789	2.57E-27	0	0	2.36E-05	1.03E-17	0.999976	2.59E-27	0	0
4	4932.5	0.000456	6.9E-12	0.999544	1.34E-08	6.93963E-19	1.56E-16	3 Facies 4	0.999544	0	3.86E-06	1.11E-18	0.991071	2.09E-28	0	0	3.9E-06	1.12E-18	0.999996	2.11E-28	0	0
4	4933	0.00034	2.64E-12	0.999666	4.39E-09	2.93438E-19	8.28E-17	3 Facies 4	0.999666	0	2.88E-06	5.18E-19	0.991185	4.37E-28	0	0	2.91E-06	5.23E-19	0.999997	4.41E-28	0	0
4	4933.5	0.000412	2.37E-12	0.999588	4.27E-10	1.759E-19	2.35E-16	3 Facies 4	0.999588	0	3.5E-06	3.31E-18	0.991092	4.33E-27	0	0	3.53E-06	3.34E-18	0.999996	4.37E-27	0	0
4	4934	0.0029	7.73E-11	0.9971	3.9E-10	5.4148E-19	1.01E-14	3 Facies 4	0.9971	0	2.48E-05	3.35E-16	0.988573	5.17E-26	0	0	2.51E-05	3.39E-16	0.999975	5.23E-26	0	0
4	4934.5	0.008705	2.12E-10	0.991295	6.45E-09	6.33649E-18	3.01E-14	3 Facies 4	0.991295	0	7.68E-05	4.37E-15	0.98253	9.3E-24	0	0	7.82E-05	4.44E-15	0.999922	9.46E-24	0	0
4	4935	0.039319	1.56E-09	0.960681	2.07E-07	1.23167E-16	1.49E-13	3 Facies 4	0.960681	0	0.000353	4.6E-14	0.952033	9.27E-22	0	0	0.00037	4.83E-14	0.99963	9.73E-22	0	0
4	4935.5	0.056432	7.04E-09	0.943566	1.96E-06	6.81084E-16	3.35E-13	3 Facies 4	0.943566	0	0.000497	1.4E-13	0.953234	8.32E-20	0	0	0.000531	1.5E-13	0.999469	8.89E-20	0	0
4	4936	0.038105	4.59E-08	0.961882	1.32E-05	2.7725E-15	6.88E-13	3 Facies 4	0.961882	0	0.000342	1.35E-12	0.953227	2.54E-16	0	0	0.000358	1.41E-12	0.999642	2.66E-16	0	0
4	4936.5	0.056575	2.53E-05	0.94368	0.000619	1.27692E-13	1.37E-11	3 Facies 4	0.94368	0	0.000494	6.01E-10	0.935282	1.28E-13	0	0	0.000528	6.42E-10	0.999472	1.37E-13	0	0
4	4937	0.047179	0.020217	0.947951	0.002853	1.69764E-12	1.07E-10	3 Facies 4	0.947951	0	0.000402	6.53E-09	0.939863	3.67E-15	0	0	0.000428	6.94E-09	0.999572	3.91E-15	0	0
4	4937.5	0.006738	2.16E-05	0.99728	0.00046	1.25297E-13	1.42E-11	3 Facies 4	0.99728	0	5.73E-05	4.25E-11	0.984332	8.61E-17	0	0	5.82E-05	4.31E-11	0.999942	8.74E-17	0	0
4	4938	0.003951	2.94E-07	0.996039	9.4E-06	4.828E-15	8.01E-12	3 Facies 4	0.996039	0	3.49E-05	6.18E-12	0.987225	3.36E-16	0	0	3.53E-05	6.26E-12	0.999965	3.4E-16	0	0
4	4938.5	0.036188	1.29E-05	0.963793	6E-06	6.34619E-15	2.24E-10	3 Facies 4	0.963793	0	0.000361	1.14E-09	0.9541	1.39E-16	0	0	0.000378	1.2E-09	0.999622	1.46E-16	0	0
4	4939	0.157011	0.000393	0.842592	4.72E-06	6.79498E-15	3.63E-09	3 Facies 4	0.842592	0	0.001335	6.49E-10	0.835420	1.38E-20	0	0	0.001595	7.76E-10	0.998405	1.65E-20	0	0
4	4939.5	0.003468	0.000114	0.996415	2.95E-06	1.39443E-15	1.15E-09	3 Facies 4	0.996415	0	2.94E-05	9.69E-14	0.987971	5.28E-23	0	0	2.97E-05	9.81E-14	0.99997	5.35E-23	0	0
4	4940	1.79E-06	5.2E-06	0.999991	2.11E-06	1.34708E-16	3.3E-11	3 Facies 4	0.999991	0	1.51E-08	5.96E-16	0.991516	9.92E-25	0	0	1.53E-08	6.01E-16	1	1E-24	0	0
4	4940.5	2.41E-07	8.04E-08	0.999988	1.96E-05	1.18921E-16	1.54E-12	3 Facies 4	0.999988	0	2.05E-09	1.56E-17	0.991506	4.79E-23	0	0	2.06E-09	1.57E-17	1	4.83E-23	0	0
4	4941	4.08E-07	2.78E-08	0.9999823	0.000176	2.78396E-16	6.26E-13	3 Facies 4	0.9999823	0	3.46E-09	8.03E-17	0.99135	2.07E-20	0	0	3.49E-09	8.1E-17	1	2.09E-20	0	0
4	4941.5	6.06E-06	5.77E-05	0.996873	0.003063	5.55402E-15	3.83E-10	3 Facies 4	0.996873	0	5.13E-08	3.04E-15	0.988425	2.94E-17	0	0	5.19E-08	3.07E-15	1	2.98E-17	0	0
4	4942	1.07E-07	0.025062	0.974627	0.000311	3.2393E-15	5.93E-09	3 Facies 4	0.974627	0	9.1E-10	3.11E-13	0.966367	1.03E-18	0	0	9.42E-10	3.22E-13	1	1.06E-18	0	0
4	4942.5	2.58E-08	0.003779	0.996114	0.000106	6.75186E-16	1.48E-09	3 Facies 4	0.996114	0	2.19E-10	1.09E-13	0.987673	8.32E-20	0	0	2.22E-10	1.11E-13	1	8.42E-20	0	0
4	4943	6.07E-08	0.000503	0.999414	8.28E-05	4.29123E-16	4.88E-10	3 Facies 4	0.999414	0	5.15E-10	2.6E-14	0.990945	1.48E-17	0	0	5.2E-10	2.62E-14	1	1.19E-21	0	0
4	4943.5	1.09E-07	6.55E-05	0.999917	1.78E-05	2.25392E-16	1.43E-10	3 Facies 4	0.999917	0	9.21E-10	4.74E-16	0.991443	1.02E-23	0	0	9.29E-10	4.78E-16	1	1.03E-23	0	0
4	4944	1.53E-08	3.23E-06	0.999967	1.03E-06	4.80952E-17	4.25E-11	3 Facies 4	0.999967	0	1.29E-10	1.9E-17	0.991492	1.01E-25	0	0	1.3E-10	1.92E-17	1	1.02E-25	0	0
4	4944.5	1.24E-09	2.23E-05	0.999978	4.72E-08	6.48349E-18	1.24E-11	3 Facies 4	0.999978	0	1.05E-11	3.25E-18	0.991503	1.92E-26	0	0	1.06E-11	3.27E-18	1	1.94E-26	0	0
4	4945	3.07E-07	7.87E-06	0.999992	3.04E-09	9.23666E-19	3.23E-12	3 Facies 4	0.999992	0	2.6E-12	1.35E-17	0.991516	6.18E-26	0	0	2.62E-12	1.36E-17	1	6.23E-26	0	0
4	4945.5	3.62E-09	3.61E-07	1	9.82E-09	1.06544E-18	5.63E-13	3 Facies 4	1	0	3.07E-11	6.74E-16	0.991525	1.03E-27	0	0	3.09E-11	6.8E-16	1	1.04E-27	0	0
4	4946	3.94E-06	1.38E-08	0.999975	2.09E-05	6.17608E-17	7.25E-13	3 Facies 4	0.999975	0	3.34E-08	3.48E-18	0.991501	1.62E-25	0	0	3.37E-08	3.51E-18	1	1.63E-25	0	0
4	4946.5	5.31E-07	4.13E-09	0.999982	1.78E-05	3.67297E-17	2E-13	3 Facies 4	0.999982	0	4.5E-09	2.57E-19	0.991507	3.88E-26	0	0	4.54E-09	2.59E-19	1	3.92E-26	0	0
4	4947	1.31E-07	5.09E-09	0.999992	8.27E-06	2.45476E-17	2E-13	3 Facies 4	0.999992	0	1.11E-09	7.24E-20	0.991517	2.73E-26	0	0	1.12E-09	7.3E-20	1	2.76E-26	0	0
4	4947.5	2.99E-08	1.2E-07	0.999997	3.16E-06	1.85822E-17	1.44E-12	3 Facies 4	0.999997	0	2.54E-10	8.37E-20	0.991522	8.98E-22	0	0	2.56E-10	8.45E-20	1	9.06E-22	0	0
4	4948	1.45E-09	5.38E-06	0.999994	1.12E-06	1.10128E-17	7.88E-12	3 Facies 4	0.999994	0	1.23E-11	9.39E-15	0.991516	1.56E-18	0	0	1.24E-11	9.47E-15	1	1.57E-18	0	0
4	4948.5	3.57E-06																				

4	4952	6.28E-08	3.27E-09	0.999996	4.24E-06	2.66941E-17	1.23E-15	3 Facies 4	0.999996	0	5.32E-10	3.23E-19	0.991521	6.72E-26	0	0	5.37E-10	3.26E-19	1	6.78E-26	0	0
4	4952.5	2.08E-07	6.42E-09	0.999994	5.89E-06	5.17473E-17	2.61E-15	3 Facies 4	0.999994	0	1.76E-09	5.26E-19	0.991519	9.66E-27	1.2E-292	2.2E-300	1.78E-09	5.31E-19	1	9.74E-27	1.2E-292	2.2E-300
4	4953	1.73E-07	8.69E-09	0.999992	7.66E-06	6.50849E-17	3.25E-15	3 Facies 4	0.999992	0	1.46E-09	5.45E-20	0.991518	3.98E-27	2.7E-276	1.3E-285	1.48E-09	5.49E-20	1	4.02E-27	2.7E-276	1.3E-285
4	4953.5	1.32E-08	9.76E-09	0.999986	1.35E-05	4.10465E-17	1.5E-15	3 Facies 4	0.999986	0	1.12E-10	1.73E-20	0.991512	5.93E-28	4.7E-260	5.8E-271	1.13E-10	1.74E-20	1	5.98E-26	4.7E-260	5.8E-271
4	4954	3.73E-09	2.36E-08	0.999921	7.91E-05	6.26877E-17	1.57E-15	3 Facies 4	0.999921	0	3.16E-11	1.46E-19	0.991447	2.61E-24	1.3E-243	5.7E-256	3.19E-11	1.47E-19	1	2.63E-24	1.3E-243	5.8E-256
4	4954.5	1.3E-08	4.31E-08	0.999646	0.000353	1.22212E-16	2.15E-15	3 Facies 4	0.999646	0	1.1E-10	1.09E-18	0.991175	1.23E-22	2.3E-227	5.4E-241	1.11E-10	1.1E-18	1	1.24E-22	2.3E-227	5.5E-241
4	4955	5.33E-08	8.83E-08	0.998839	0.001161	2.81568E-16	3.66E-15	3 Facies 4	0.998839	0	4.51E-10	4.46E-18	0.990375	2.45E-19	2.2E-211	3.7E-226	4.56E-10	4.5E-18	1	2.47E-19	2.2E-211	3.8E-226
4	4955.5	1.06E-07	3.94E-08	0.998826	0.001174	4.38124E-16	1.07E-14	3 Facies 4	0.998826	0	9E-10	6.96E-15	0.990358	1.1E-18	8.7E-196	1.5E-211	9.09E-10	7.03E-15	1	1.11E-18	8.7E-196	1.5E-211
4	4956	0.000367	3.18E-07	0.988634	0.010999	1.40022E-14	1.41E-11	3 Facies 4	0.988634	0	3.11E-06	3.03E-14	0.980254	1.38E-17	2.2E-180	2.1E-197	3.18E-06	3.09E-14	0.999997	1.41E-17	2.3E-180	2.1E-197
4	4956.5	0.000194	2.06E-06	0.966175	0.003629	6.70139E-13	4.49E-11	3 Facies 4	0.966175	0	1.65E-06	3.07E-14	0.957987	3.28E-16	1.7E-166	2.1E-186	1.72E-06	3.2E-14	0.999998	3.42E-16	1.8E-166	2.2E-186
4	4957	3.08E-05	5.85E-05	0.98266	0.017251	7.56099E-11	6.38E-11	3 Facies 4	0.98266	0	2.61E-07	3.18E-13	0.974332	4.2E-18	2.9E-154	6.9E-176	2.68E-07	3.26E-13	1	4.31E-18	3E-154	7.1E-176
4	4957.5	1.13E-05	7.79E-06	0.983901	0.016079	3.98027E-10	1.53E-10	3 Facies 4	0.983901	0	9.54E-08	7.95E-15	0.975563	3.43E-20	4.2E-144	1.6E-165	9.78E-08	8.15E-15	1	3.51E-20	4.3E-144	1.6E-165
4	4958	2.15E-06	4.93E-08	0.999112	0.000885	6.13047E-10	1.34E-10	3 Facies 4	0.999112	0	1.82E-08	7.06E-17	0.990645	6.63E-21	1.2E-134	1.5E-155	1.84E-08	7.12E-17	1	6.69E-21	1.2E-134	1.6E-155
4	4958.5	3.02E-08	4.16E-08	0.99938	0.000617	6.71032E-10	2.49E-10	3 Facies 4	0.99938	0	2.56E-08	2.33E-16	0.99091	5.47E-19	2.2E-125	1.7E-145	2.58E-08	2.35E-16	1	5.52E-19	2.2E-125	1.7E-145
4	4959	1.17E-05	1.37E-06	0.993524	0.006463	6.21515E-10	6.35E-10	3 Facies 4	0.993524	0	9.92E-08	2.9E-14	0.985103	7.58E-18	3.7E-116	1E-135	1.01E-07	2.95E-14	1	7.7E-18	3.8E-116	1E-135
4	4959.5	4.35E-05	2.82E-06	0.972865	0.027089	2.34324E-10	8.28E-10	3 Facies 4	0.972865	0	3.68E-07	3.79E-14	0.96462	5.96E-19	6.6E-107	2.3E-126	3.82E-07	3.93E-14	1	6.17E-19	6.9E-107	2.4E-126
4	4960	2.79E-05	6.98E-08	0.985722	0.01425	2.66794E-11	1.68E-10	3 Facies 4	0.985722	0	2.36E-07	7.19E-16	0.977368	1.46E-20	3.16E-97	4.1E-117	2.42E-07	7.36E-16	1	1.49E-20	3.23E-97	4.2E-117
4	4960.5	2.17E-05	9.84E-09	0.999713	0.000265	1.35682E-10	2.31E-10	3 Facies 4	0.999713	0	1.84E-07	3.4E-17	0.991241	5.36E-24	1.34E-88	3.6E-107	1.86E-07	3.43E-17	1	5.41E-24	1.35E-88	3.7E-107
4	4961	7.27E-06	1.14E-06	0.999958	3.51E-05	2.36267E-09	7.61E-10	3 Facies 4	0.999958	0	6.16E-08	6.71E-19	0.991483	2.37E-24	1.12E-76	2.34E-97	6.21E-08	6.77E-19	1	2.39E-24	1.13E-76	2.36E-97
4	4961.5	1.24E-05	8.85E-11	0.998848	0.000139	1.67024E-08	2.3E-09	3 Facies 4	0.998848	0	1.05E-07	2.07E-18	0.991375	8.33E-21	5.38E-68	4.57E-88	1.06E-07	2.02E-18	1	8.41E-21	5.42E-68	4.61E-88
4	4962	4.75E-05	5.29E-10	0.997832	0.002121	1.28946E-07	1.28E-08	3 Facies 4	0.997832	0	4.02E-07	4.72E-17	0.989374	6.67E-17	3.64E-60	2.94E-79	4.07E-07	4.78E-17	1	6.75E-17	3.68E-60	2.97E-79
4	4962.5	0.000185	1.88E-08	0.985491	0.014323	2.21771E-07	4.63E-08	3 Facies 4	0.985491	0	1.57E-06	9.79E-15	0.97713	3.51E-14	3.15E-53	3.38E-71	1.61E-06	1E-14	0.999998	3.6E-14	3.23E-53	3.46E-71
4	4963	0.00104	8.26E-06	0.956031	0.042919	7.14414E-07	5.68E-07	3 Facies 4	0.956031	0	8.87E-06	2.43E-11	0.947879	1.85E-12	1.54E-46	1.04E-63	9.35E-06	2.56E-11	0.999991	1.95E-12	1.62E-46	1.09E-63
4	4963.5	0.005984	0.00377	0.968867	0.021309	1.66925E-05	5.22E-05	3 Facies 4	0.968867	0	5.08E-05	1.38E-09	0.96065	1.15E-13	2.37E-40	2.63E-57	5.28E-05	1.44E-09	0.999947	1.2E-13	2.46E-40	2.74E-57
4	4964	0.000767	0.004643	0.993968	6.84E-05	2.32936E-05	0.00053	3 Facies 4	0.993968	0	6.5E-06	1.79E-10	0.985544	1.81E-17	1.6E-35	7.44E-53	6.6E-06	1.81E-10	0.999993	1.84E-17	1.62E-35	7.55E-53
4	4964.5	8.1E-05	0.000421	0.998696	8.61E-07	7.07099E-05	0.00073	3 Facies 4	0.998696	0	6.86E-07	8.81E-12	0.990232	1.56E-23	7.76E-31	2.08E-49	6.93E-07	8.89E-12	0.999999	1.57E-23	7.83E-31	2.11E-49
4	4965	4.39E-05	0.000189	0.996878	3.39E-07	0.000186559	0.002702	3 Facies 4	0.996878	0	3.72E-07	5.99E-16	0.98843	6.85E-26	1.24E-26	4.24E-46	3.76E-07	6.06E-16	1	6.93E-26	1.25E-26	4.29E-46
4	4965.5	6.68E-09	1.56E-05	0.999951	5.57E-11	2.72268E-08	3.34E-05	3 Facies 4	0.999951	0	5.66E-11	6.71E-18	0.991477	6.89E-25	7.53E-23	2.33E-43	5.71E-11	6.77E-18	1	6.95E-25	7.59E-23	2.35E-43
4	4966	6.06E-11	6.64E-06	0.99999	4.29E-11	1.38622E-10	3.16E-06	3 Facies 4	0.99999	0	5.14E-13	4.11E-13	0.991492	1.07E-24	3.13E-15	1.04E-38	5.18E-13	4.15E-13	1	1.08E-24	3.16E-15	1.05E-38
4	4966.5	0.000144	0.000363	0.999143	3.9E-06	3.76849E-05	0.000309	3 Facies 4	0.999143	0	6.58E-07	4.94E-13	0.590355	1.26E-19	1.52E-05	2.91E-33	1.11E-08	8.37E-13	0.999973	2.13E-19	2.58E-05	4.93E-33
4	4967	2.82E-05	0.123862	0.759261	0.007814	0.108960399	7.45E-05	3 Facies 4	0.759261	0	4.95E-09	2.18E-13	0.108555	5.89E-20	0.093363	2.86E-30	2.45E-08	1.08E-12	0.53762	2.92E-19	0.46238	1.41E-29
6	4967.5	3.24E-06	0.011852	0.126677	0.001049	0.860317876	0.000101	5 Facies 6	0.860318	0	2.43E-11	1.94E-16	0.015932	2.35E-22	0.752112	4.41E-26	3.16E-11	2.52E-22	0.020743	3.06E-22	0.979257	5.75E-26
6	4968	2.22E-07	0.001021	0.006148	7.15E-05	0.992716909	4.22E-05	5 Facies 6	0.992717	0	2.56E-13	6.52E-18	0.000769	1.12E-20	0.868509	5.69E-22	2.94E-13	7.5E-18	0.000885	1.26E-22	0.999115	6.54E-22
6	4968.5	2.39E-07	0.002064	0.000948	1.58E-05	0.996862737	0.000109	5 Facies 6	0.996863	0	9.95E-14	4.48E-17	0.000119	1.29E-25	0.872212	1.77E-17	1.14E-13	5.13E-17	0.000136	1.48E-25	0.999864	2.02E-17
6	4969	2.78E-06	0.016738	0.000337	3.43E-05	0.98045829	0.00243	5 Facies 6	0.980458	0	3.35E-13	2.34E-19	4.21E-05	2.68E-23	0.857889	2.08E-13	3.91E-13	2.73E-19	4.9E-05	3.13E-23	0.999951	2.42E-13
6	4969.5	2.7E-07	0.001122	9.95E-05	0.00022	0.998326152	0.000232	5 Facies 6	0.998326	0	1.94E-16	1.44E-18	1.24E-05	7.39E-19	0.873535	1.12E-10	2.22E-16	1.65E-18	1.42E-05	8.46E-19	0.999986	1.28E-10
6	4970	4.7E-06	0.005264	5.85E-07	0.005246	0.988602988	0.000882	5 Facies 6	0.988603	0	7.12E-15	5.05E-16	7.31E-08	3.33E-15	0.864456	6.27E-07	8.23E-15	5.85E-16	8.46E-08	3.85E-15	0.999999	7.26E-07
6	4970.5	1.99E-05	0.000349	1.41E-06	0.002863	0.99239306	0.004373	5 Facies 6	0.992393	0	8.63E-15	3.49E-14	1.3E-07	5.31E-13	0.725494	0.000775	1.19E-14	4.8E-14	1.79E-07	7.31E-13	0.998933	0.001067
6	4971	0.000197	0.001183	2.54E-06	0.010541	0.813643363	0.174434	5 Facies 6	0.813643	0	1.09E-15	3.61E-11	2.09E-08	8.63E-11	0.300187	0.108645	2.66E-15	8.84E-11	5.11E-08	2.11E-10	0.734256	0.265744
7</																						

Sample	NaKa1	MgKa1	AlKa1	SiKa1	P Ka1	S Ka1	K Ka1	CaKa1	BaLa1	TiKa1	V Ka1	CrKa1	MnKa1	FeKa1	CoKa1	NiKa1	CuKa1	ZnKa1
MAJ KM011-4990 15kV	0.424	0.604	1.810	17.437	0.011	0.056	0.947	19.927	-0.004	0.107	0.009041	0.008058	0.023679	0.367766	0.000231	0.005773	0.001053	0.008405
MAJ KM011-5000 15kV	0.448	0.502	1.468	18.018	0.042	0.079	0.956	20.185	0.015	0.107	0.008935	0.007855	0.02536	0.29105	0.000216	0.006399	0.001364	0.007844
MAJ KM011-5002 15kV	0.487	0.365	1.480	18.102	0.002	0.067	0.948	17.439	-0.007	0.113	0.008797	0.008212	0.024318	0.235791	0.000204	0.005761	0.002617	0.007503
MAJ KM011-5003 15kV	0.425	0.674	1.436	17.722	0.033	0.067	0.801	19.994	0.031	0.116	0.006374	0.008714	0.023776	0.274878	0.000204	0.006192	0.000946	0.006764
MAJ KM011-5031 15kV	0.401	0.701	0.319	26.746	0.046	0.201	0.054	12.398	-0.074	0.023	0.018273	0.012075	0.027845	-0.00022	0.00017	0.009139	0.00246	0.008969
MAJ KM011-5032 15kV	0.413	0.468	0.459	34.186	0.032	0.207	-0.049	3.778	-0.068	0.001	0.019929	0.012368	0.031356	-0.20874	0.000144	0.010747	0.006026	0.012569
MAJ KM011-5033 15kV	0.200717	0.980039	0.269449	4.352922	-0.050	-0.012	0.203	36.747	-0.035	0.045	0.004896	0.002289	0.01831	0.447628	0.000186	0.005132	-0.00599	0.007151
MAJ KM011-5056 15kV	0.235375	0.787337	-0.06823	1.995879	-0.06851	0.002724	0.065354	38.1759	-0.04548	0.029099	0.004078	9.21E-05	0.017453	0.476717	0.000186	0.004829	-0.00667	0.008009
MAJ KM011-5059 15kV	0.127235	1.307856	-0.02013	1.832237	-0.16636	0.060948	0.043065	39.87628	-0.06486	0.024522	0.00379	-0.00011	0.017604	0.455483	0.000178	0.005235	-0.0077	0.007044
MAJ KM011-5065 15kV	0.145197	1.071372	-0.17942	1.547244	-0.086	0.181642	0.022446	39.29635	-0.09916	0.026749	0.004091	-0.00044	0.017082	0.478915	0.00018	0.004998	-0.00785	0.007472
MAJ KM011-5068 15kV	0.26567	0.939424	-0.08836	2.017823	-0.09522	0.11253	0.028656	37.51484	-0.08671	0.02076	0.003805	0.000257	0.016801	0.496375	0.000183	0.004235	-0.00699	0.008104
MAJ KM011-4963 15kV	0.373	0.619	0.582	7.022	-0.025	0.051	0.357	30.713	-0.014	0.072	0.006161	0.002621	0.019967	0.548961	0.000235	0.003845	-0.00252	0.007073
MAJ KM011-4965 15kV	0.335	0.566	0.374	2.702	-0.085	0.179	0.199	35.612	-0.066	0.035	0.003952	0.000316	0.017643	0.614574	0.000221	0.003051	-0.00509	0.007712
MAJ KM011-4967 15kV	0.485	0.313	1.442	5.617	-0.049	0.145	0.658	28.029	0.008	0.086	0.001579	0.001833	0.018482	0.907888	0.000341	0.001989	-0.00187	0.008505
MAJ KM011-4968 15kV	0.209	1.104	0.158	2.976	-0.118	0.046	0.107	37.972	-0.052	0.030	0.004947	0.000705	0.018487	0.560368	0.000203	0.004348	-0.00625	0.007409
MAJ KM011-4971 15kV	0.228	0.963	0.008	2.361	-0.108	0.030	0.039	37.498	-0.066	0.019	0.00332	-6.3E-05	0.01749	0.453655	0.000181	0.00448	-0.00686	0.006809
MAJ KM011-4973 15kV	0.378	0.535	0.009	2.513	-0.117	0.117	0.055	34.538	-0.107	0.018	0.002396	-0.00055	0.016121	0.690023	0.000214	0.001943	-0.00613	0.006699
MAJ KM011-4977 15kV	0.230193	0.903476	-0.00707	2.788991	-0.121	0.117	0.054	37.369	-0.046	0.020	0.003928	0.000417	0.017775	0.50864	0.000189	0.004588	-0.00636	0.007934
MAJ KM011-4980 15kV	0.254468	1.127953	0.420823	5.211643	-0.06819	0.131264	0.194864	34.5771	-0.04357	0.044318	0.004828	0.001964	0.018096	0.481404	0.000198	0.004065	-0.00428	0.006396
MAJ KM011-4982 15kV	0.335747	0.69694	0.620695	9.137622	-0.00563	0.111505	0.393872	28.36253	-0.01371	0.073362	0.004777	0.005563	0.019884	0.426615	0.000202	0.003444	-0.00084	0.008177
MAJ KM011-4985 15kV	0.159392	1.120117	0.171995	3.838052	-0.06449	0.087579	0.128477	37.67536	-0.04062	0.030876	0.004064	0.002267	0.018178	0.500653	0.000193	0.004893	-0.00632	0.007155
MAJ KM011-4986 15kV	0.188419	1.033175	0.175386	3.214612	-0.08376	0.07636	0.102433	37.36255	-0.04885	0.026116	0.004842	0.00096	0.017854	0.493964	0.000191	0.004685	-0.00598	0.007032
MAJ KM011-4989 15kV	0.405292	0.569633	0.85757	6.947454	-0.05737	0.076726	0.404535	31.74023	0.008611	0.082508	0.003643	0.003027	0.02361	0.463729	0.000217	0.003613	-0.00254	0.007162
MAJ KM011-4990-1 15kV	0.482024	0.357585	1.267591	14.85012	-0.00018	0.085887	0.706044	20.67673	0.024958	0.105322	0.005256	0.005818	0.023381	0.322733	0.000212	0.004352	0.001205	0.00787
MAJ KM011-4992 15kV	0.267059	0.872905	0.057449	3.022698	-0.10543	0.037696	0.098019	36.34714	-0.05289	0.024936	0.003074	0.001126	0.017766	0.451266	0.000183	0.004483	-0.00635	0.007467
MAJ KM011-4993 15kV	0.302003	0.914193	0.120279	3.86657	-0.07608	0.028363	0.128291	35.77076	-0.05748	0.038612	0.003562	0.001684	0.017804	0.477047	0.000188	0.004092	-0.00558	0.006477
MAJ KM011-4995 15kV	0.121632	1.294078	0.1109	2.857977	-0.06517	0.066181	0.120977	37.86339	-0.05003	0.027616	0.00488	0.001201	0.01777	0.528215	0.000194	0.005009	-0.00696	0.00693
MAJ KM011-4996 15kV	0.240965	1.127903	0.192988	4.076726	-0.05826	0.034493	0.139985	35.32369	-0.04052	0.05142	0.002971	0.000942	0.0186	0.503886	0.000194	0.004008	-0.00495	0.007311
MAJ KM011-5006 15kV	0.289161	0.843604	0.061143	4.868792	-0.05361	0.039704	0.063714	34.61182	-0.04119	0.033343	0.004932	0.001662	0.019101	0.447593	0.000185	0.004077	-0.00309	0.006139
MAJ KM011-5007 15kV	0.216108	1.060367	-0.00694	2.9077	-0.05016	0.084508	0.093386	36.3566	-0.05669	0.03281	0.003934	0.000829	0.01738	0.51205	0.000192	0.004216	-0.00613	0.007609
MAJ KM011-5009 15kV	0.1809	1.046593	0.084711	2.718313	-0.09376	0.122731	0.121628	38.22501	-0.04206	0.02643	0.004032	0.000356	0.017884	0.457945	0.000184	0.004861	-0.00653	0.007393
MAJ KM011-5012 15kV	0.304878	0.738874	0.243972	3.893743	-0.07236	0.064165	0.143106	35.7372	-0.06724	0.033394	0.004291	0.001251	0.017888	0.48964	0.000191	0.00392	-0.00524	0.006729
MAJ KM011-5016 15kV	0.248772	0.895867	0.318966	4.828652	0.006572	0.025717	0.194471	34.71909	-0.03053	0.049602	0.003454	0.001573	0.018087	0.482904	0.000191	0.004211	-0.00533	0.007885
MAJ KM011-5018 15kV	0.29765	0.833958	-0.09078	2.691293	-0.09012	0.03841	0.049208	35.25983	-0.06733	0.021769	0.003939	0.000154	0.01778	0.49779	0.000189	0.003517	-0.00525	0.006962
MAJ KM011-5020 15kV	0.230313	0.891144	-0.13578	3.032058	-0.07058	0.001779	0.090526	36.60943	-0.0497	0.021113	0.003408	0.001779	0.017852	0.480723	0.000185	0.004426	-0.00573	0.006812
MAJ KM011-5022 15kV	0.245433	1.136253	0.177629	3.052073	-0.08462	0.049103	0.164144	37.01051	-0.0633	0.039981	0.00452	0.000545	0.017593	0.524486	0.000199	0.004511	-0.00561	0.006503
MAJ KM011-5025 15kV	0.322613	0.62436	0.189364	3.609556	-0.10207	0.052498	0.171544	35.46315	-0.05955	0.034129	0.004173	0.001133	0.017641	0.491803	0.00019	0.004069	-0.00567	0.007166
MAJ KM011-5027 15kV	0.477817	0.276789	0.21514	4.282005	-0.08557	0.026324	0.190966	28.73231	-0.03304	0.041679	0.002661	0.001446	0.018505	0.432592	0.000188	0.001605	-0.0015	0.007527
MAJ KM011-5035 15kV	0.1342	1.162625	0.225525	4.307294	-0.0342	0.055225	0.192967	37.61729	-0.03698	0.058106	0.003645	0.001945	0.01803	0.45139	0.000188	0.005076	-0.0058	0.006111

<b>MAJ KM011-5038 15kV</b>	0.222009	1.130875	0.187011	3.729091	-0.04964	0.006178	0.166108	36.77008	-0.03057	0.03776	0.004668	0.001008	0.017798	0.479282	0.000189	0.004719	-0.00589	0.007233
<b>MAJ KM011-5040 15kV</b>	0.351458	0.835627	0.156287	4.1245	-0.07132	0.047028	0.19394	34.1423	-0.04395	0.037785	0.004814	0.001589	0.01839	0.463768	0.000191	0.003804	-0.00429	0.007742
<b>MAJ KM011-5043 15kV</b>	0.280162	0.839695	0.363143	4.745264	-0.0406	0.033683	0.237781	35.72428	-0.02815	0.044961	0.0048	0.002289	0.018162	0.436315	0.000187	0.004718	-0.00494	0.006381
<b>MAJ KM011-5046 15kV</b>	0.20384	0.909169	0.21977	3.364621	-0.00379	0.542172	0.156767	37.323	-0.02648	0.026153	0.004422	0.002207	0.016818	0.743619	0.000266	0.004999	-0.00692	0.007222
<b>MAJ KM011-5047 15kV</b>	0.120937	1.147702	0.209024	3.632413	-0.07391	0.014409	0.135101	38.27252	-0.05225	0.036725	0.004816	0.001318	0.018445	0.396697	0.000176	0.005404	-0.00676	0.00667
<b>MAJ KM011-5051 15kV</b>	0.205736	1.025872	-0.09297	1.797937	-0.07	0.006749	0.055405	39.76746	-0.06362	0.027934	0.004287	-4.2E-05	0.01707	0.515164	0.000187	0.005086	-0.0076	0.006463
<b>MAJ KM011-5052 15kV</b>	0.182368	1.066066	-0.01948	2.54902	-0.07075	-0.01113	0.081465	37.52885	-0.04979	0.025268	0.004437	0.000107	0.017142	0.454714	0.000179	0.004562	-0.00616	0.008389
<b>MAJ KM011-5055 15kV</b>	0.249668	0.851053	0.120201	3.142697	-0.06086	-0.00196	0.140987	36.62972	-0.0547	0.037474	0.003385	0.001248	0.017802	0.472554	0.000186	0.003601	-0.00488	0.007746
<b>MAJ KM011-5061 15kV</b>	0.247944	0.839424	-0.03142	2.482975	-0.12696	0.110814	0.065932	37.63359	-0.04653	0.031353	0.004218	-0.00022	0.017426	0.485318	0.000186	0.004654	-0.00617	0.005734

Figure 53: XRF values from a cored well (API: 15-093-20011).

Sample	NaKa1	MgKa1	AlKa1	SiKa1	P Ka1	S Ka1	K Ka1	CaKa1	BaLa1	TiKa1	V Ka1	CrKa1	MnKa1	FeKa1	CoKa1	NiKa1	CuKa1	ZnKa1
<b>MAJ KM317-4865.8 15kV</b>	0.297824	1.094469	1.655053	8.701154	0.048207	0.642687	0.512373	28.31364	0.025426	0.097996	0.003367	0.003886	0.020208	0.753536	0.000283	0.003192	-0.00182	0.008364
<b>MAJ KM317-4867 15kV</b>	0.270104	1.0375	0.813847	12.21306	0.038892	0.518094	0.192065	27.11185	-0.00612	0.03955	0.009756	0.007272	0.022154	0.431831	0.00022	0.005167	-0.00171	0.00728
<b>MAJ KM317-4876 15kV</b>	0.433777	0.44171	0.455976	29.20264	0.042328	0.793347	0.01141	8.524668	-0.04846	0.014326	0.022319	0.011196	0.029704	-0.20866	0.000126	0.011398	0.003706	0.011265
<b>MAJ KM317-4878 15kV</b>	0.521306	0.225835	1.52771	21.4163	0.048376	3.051763	0.807854	7.571058	-0.03761	0.107823	0.006747	0.009075	0.024323	0.607759	0.000332	0.006072	0.005186	0.009026
<b>MAJ KM317-4888 15kV</b>	0.438614	0.587255	1.284335	18.18822	0.036434	0.33718	0.785707	17.93939	0.051313	0.149188	0.005882	0.007896	0.023586	0.442716	0.000268	0.006283	0.002293	0.0084
<b>MAJ KM317-4903 15kV</b>	0.269079	0.988452	0.831138	11.82118	0.02847	0.367063	0.50772	27.36174	-0.01	0.060969	0.009187	0.006013	0.020277	0.371176	0.000207	0.005007	-0.00136	0.007166
<b>MAJ KM317-4907 15kV</b>	0.00899	1.768881	0.116038	3.101035	-0.06728	0.743517	0.094811	38.76285	-0.04847	0.031999	0.005254	0.001255	0.017345	0.54266	0.0002	0.005056	-0.00686	0.007143
<b>MAJ KM317-4911 15kV</b>	0.245338	0.956962	0.066976	3.058546	-0.07059	0.165494	0.105972	36.76307	-0.06029	0.035108	0.003423	0.00117	0.01645	0.737945	0.000242	0.004047	-0.00653	0.006783
<b>MAJ KM317-4929 15kV</b>	0.302734	0.776801	0.164772	3.567108	-0.05381	0.164906	0.134681	35.15317	-0.05981	0.037058	0.004254	0.001345	0.017595	0.511237	0.000199	0.004204	-0.00506	0.007644
<b>MAJ KM317-4932 15kV</b>	0.152813	1.2194	0.080448	3.469712	-0.02893	0.856977	0.110987	35.77077	-0.04321	0.03806	0.002666	0.000908	0.017732	0.473756	0.00019	0.003962	-0.00548	0.007672
<b>MAJ KM317-4942 15kV</b>	-0.31436	2.398918	0.007054	2.966581	0.426763	5.388377	0.108274	36.14466	-0.04324	0.038081	0.004443	0.001458	0.018358	0.517321	0.000199	0.00456	-0.00564	0.007006
<b>MAJ KM317-4968 15kV</b>	0.559296	0.011579	-0.09945	2.621842	-0.02131	0.49954	0.082682	26.2037	-0.0761	0.013786	0.001921	0.000611	0.017583	0.493769	0.00019	-0.00077	0.000197	0.009409
<b>MAJ KM317-4973 15kV</b>	0.445595	0.400224	0.575486	32.62847	0.075603	3.473123	-0.07823	2.603857	-0.09682	0.005711	0.019942	0.012189	0.02948	0.138711	0.000238	0.015016	0.010846	0.00353
<b>MAJ KM317-4974 15kV</b>	0.121311	1.203404	0.295017	2.446002	-0.08945	0.732595	0.164367	39.44125	-0.04521	0.037516	0.003619	0.000264	0.017188	0.520149	0.000202	0.005106	-0.00644	0.006911
<b>MAJ KM317-4859 15kV</b>	0.136324	1.323132	0.372203	6.569913	0.026795	1.563706	0.256138	32.97112	-0.03846	0.043583	0.005901	0.003798	0.01972	0.441867	0.000204	0.00401	-0.00361	0.007994
<b>MAJ KM317-4865 15kV</b>	0.099567	1.455461	1.205083	4.550557	0.007447	1.441158	0.494398	33.4094	-0.00365	0.08618	0.003266	0.002194	0.017111	1.062077	0.000382	0.003389	-0.00349	0.007555
<b>MAJ KM317-4866 15kV</b>	0.146785	0.078487	0.584862	3.656727	-0.01519	0.171867	0.796052	0.982141	-0.11308	0.111435	0.002458	0.002878	0.014846	1.610286	0.000547	-0.00325	0.003882	0.006734
<b>MAJ KM317-4866-5 15kV</b>	0.116356	1.23283	0.465385	4.062754	-0.08191	0.300921	0.126735	37.87486	-0.05835	0.034509	0.005348	0.001869	0.018366	0.554835	0.000208	0.00683	-0.00869	0.005584
<b>MAJ KM317-4868 15kV</b>	0.345419	0.859311	1.451794	9.415738	-0.02145	0.252172	0.600741	27.79151	-0.0044	0.11471	0.002752	0.004839	0.018643	0.822616	0.00032	0.003865	-0.0015	0.008152
<b>MAJ KM317-4870 15kV</b>	0.272056	1.114906	1.382389	10.55232	0.042255	0.385819	0.571648	28.23876	0.042433	0.101451	0.004798	0.005559	0.019495	0.657168	0.000281	0.004559	-0.00172	0.007372
<b>MAJ KM317-4873 15kV</b>	0.409618	0.665707	0.980982	11.36604	-0.02737	0.30596	0.442823	23.35675	-0.03878	0.085717	0.007738	0.005322	0.020792	0.592575	0.000278	0.003634	0.00094	0.006817
<b>MAJ KM317-4875 15kV</b>	0.138261	1.169663	0.809008	4.277431	-0.03409	0.475826	0.290486	36.85625	-0.01045	0.060838	0.003775	0.002124	0.018267	0.700924	0.000256	0.004976	-0.00607	0.006982
<b>MAJ KM317-4878-bottom 15kV</b>	0.432371	0.566056	1.529493	27.5216	0.062393	2.008846	0.828457	8.61529	0.026614	0.082398	0.01183	0.011457	0.028679	0.235852	0.000251	0.009346	0.00454	0.009951
<b>MAJ KM317-4880 15kV</b>	0.333993	0.954942	1.208408	19.23799	0.096336	2.876413	0.702544	17.20849	-0.03006	0.107265	0.009536	0.00818	0.024228	0.25497	0.000218	0.006495	0.001616	0.007369
<b>MAJ KM317-4882 15kV</b>	0.179329	2.206755	1.391408	15.46384	0.064518	2.145535	0.536776	20.07951	0.005057	0.074709	0.009595	0.008835	0.023352	0.506364	0.000259	0.005852	0.000366	0.007051
<b>MAJ KM317-4885 15kV</b>	0.306673	0.895145	1.00414	14.62439	0.03605	0.974927	0.510642	23.88643	0.006877	0.062432	0.008972	0.00708	0.022111	0.342523	0.000207	0.005595	-0.00058	0.007298
<b>MAJ KM317-4890 15kV</b>	0.308408	0.880419	0.757306	10.64131	0.109814	3.89525	0.380703	20.33651	-0.08036	0.061507	0.007561	0.039857	0.018889	2.966864	0.000941	0.001478	0.000429	0.006804
<b>MAJ KM317-4892 15kV</b>	0.170548	1.099239	0.358072	5.629448	-0.05065	0.209936	0.200552	35.16042	-0.01676	0.048386	0.00651	0.003314	0.018617	0.437158	0.000198	0.004751	-0.0052	0.006832
<b>MAJ KM317-4895 15kV</b>	0.345939	0.759116	0.958391	11.81034	0.008437	0.223201	0.487046	26.03843	0.046155	0.094438	0.005081	0.005548	0.021257	0.468077	0.000229	0.004961	-0.00068	0.007023
<b>MAJ KM317-4897 15kV</b>	0.274284	1.060017	0.770342	12.3129	0.032692	0.321528	0.424747	26.6567	0.022966	0.085256	0.007121	0.006274	0.020569	0.424896	0.000221	0.005151	-0.00085	0.007279
<b>MAJ KM317-4899 15kV</b>	0.256691	1.059591	0.830244	12.44913	0.016725	0.352287	0.483568	27.21651	0.006438	0.046356	0.009916	0.006343	0.021169	0.396285	0.000208	0.005468	-0.00085	0.007583
<b>MAJ KM317-4901 15kV</b>	0.246807	1.191706	0.718775	9.767401	0.01079	0.477933	0.390756	28.7584	0.021208	0.066754	0.006577	0.004521	0.020486	0.439552	0.000212	0.004736	-0.00192	0.006826
<b>MAJ KM317-4905 15kV</b>	0.074638	1.665578	0.555504	4.206629	-0.04034	0.721212	0.145532	36.38882	-0.04449	0.052244	0.003481	0.001425	0.017265	0.644713	0.000231	0.004378	-0.00586	0.007124
<b>MAJ KM317-4913 15kV</b>	0.087625	1.62321	0.405774	4.814332	1.67E-05	0.862659	0.196985	36.23638	-0.02701	0.04132	0.005255	0.002532	0.018066	0.500898	0.000202	0.004999	-0.00572	0.006224
<b>MAJ KM317-4915 15kV</b>	0.068262	1.563875	0.124834	5.274994	0.039985	2.352093	0.14109	33.53801	-0.03404	0.049083	0.005084	0.005329	0.017333	0.873117	0.0003	0.004249	-0.00522	0.007594
<b>MAJ KM317-4917 15kV</b>	0.230478	0.991133	0.211074	4.018503	-0.04338	0.754958	0.133287	35.38911	-0.07405	0.042287	0.003377	0.00142	0.017024	0.547778	0.000201	0.003507	-0.00509	0.008132
<b>MAJ KM317-4918 15kV</b>	0.173106	1.0691	0.248287	3.717367	-0.04153	0.852595	0.139271	36.41674	-0.04668	0.02882	0.00474	0.001353	0.017647	0.53519	0.000204	0.004511	-0.00605	0.007168
<b>MAJ KM317-4920 15kV</b>	0.033859	1.579508	0.357699	3.83524	-0.04797	1.040798	0.14002	37.01286	-0.04192	0.034855	0.005079	0.001638	0.017239	0.586752	0.000212	0.004288	-0.00624	0.007083
<b>MAJ KM317-4922 15kV</b>	0.168669	1.124751	0.219975	6.243936	-9.8E-06	1.891749	0.14814	32.18275	-0.05472	0.044718	0.006421	0.002427	0.018929	0.382086	0.000184	0.004989	-0.00428	0.008943

<b>MAJ KM317-4924 15kV</b>	0.105385	1.249948	0.15834	3.738331	0.040285	2.393744	0.129698	35.22663	-0.05212	0.0358	0.004305	0.001328	0.018117	0.473303	0.000192	0.003757	-0.00511	0.007304
<b>MAJ KM317-4926 15kV</b>	0.108387	1.407695	0.110895	3.678968	0.004839	1.71599	0.125665	35.96094	-0.06857	0.035006	0.003343	0.001662	0.0175	0.520573	0.000201	0.004163	-0.00583	0.006322
<b>MAJ KM317-4934 15kV</b>	0.065184	1.335559	0.05665	2.472671	0.005499	1.700652	0.091571	38.34847	-0.08852	0.031942	0.005257	0.000687	0.017819	0.481322	0.000188	0.004552	-0.00645	0.00762
<b>MAJ KM317-4937 15kV</b>	0.048379	1.402377	0.105068	2.87522	-0.07146	0.236302	0.103265	38.83407	-0.04505	0.040341	0.004514	0.000795	0.017344	0.53903	0.0002	0.005126	-0.00743	0.007516
<b>MAJ KM317-4943 15kV</b>	0.134781	1.266924	0.295267	3.373069	0.037825	1.213385	0.144163	35.89786	-0.03847	0.059158	0.00368	0.001447	0.017888	0.558141	0.00021	0.004524	-0.00563	0.007415
<b>MAJ KM317-4945 15kV</b>	0.043092	1.355651	-0.13841	2.343818	0.291445	1.203043	0.091403	37.433	-0.05636	0.037571	0.003883	0.001525	0.017341	0.568275	0.000207	0.004626	-0.00676	0.007439
<b>MAJ KM317-4947 15kV</b>	-0.02823	1.618734	0.046312	2.779228	0.152426	1.033614	0.091085	39.88367	-0.03554	0.032542	0.004066	0.00168	0.017727	0.526148	0.000198	0.005597	-0.00695	0.006457
<b>MAJ KM317-4949 15kV</b>	0.12898	1.443325	0.173249	4.228981	0.222302	1.46133	0.175784	36.32442	-0.04803	0.05313	0.004198	0.001773	0.017757	0.546457	0.000206	0.004649	-0.00544	0.006525
<b>MAJ KM317-4951 15kV</b>	0.096357	1.241196	-0.01196	2.855798	0.169407	1.399075	0.122871	36.97978	-0.02869	0.030612	0.002556	0.000996	0.017183	0.54865	0.0002	0.00457	-0.0066	0.007643
<b>MAJ KM317-4953 15kV</b>	0.393702	0.495367	-0.09303	2.670561	0.048355	1.103488	0.071326	31.82528	-0.08372	0.013636	0.001488	-0.00103	0.015676	0.690407	0.000213	0.001092	-0.00549	0.007131
<b>MAJ KM317-4956 15kV</b>	0.050197	1.659653	0.069022	3.27599	0.066168	1.312827	0.120059	37.43513	-0.05023	0.041488	0.004306	0.001281	0.017704	0.534835	0.000199	0.004856	-0.0065	0.007416
<b>MAJ KM317-4959 15kV</b>	-0.02201	1.840509	0.149814	3.061317	0.160963	1.849645	0.117838	36.45374	-0.04207	0.056525	0.002702	0.001801	0.017459	0.596687	0.000213	0.004529	-0.00574	0.007587
<b>MAJ KM317-4966 15kV</b>	0.125492	1.366995	0.00509	2.55434	-0.05492	0.768533	0.077341	38.15054	-0.05215	0.027249	0.004227	0.000495	0.017826	0.537643	0.000197	0.005134	-0.00694	0.007511
<b>MAJ KM317-4970 15kV</b>	0.127207	1.527942	0.159473	4.058099	0.002314	1.07922	0.152625	36.9655	-0.05027	0.043466	0.003757	0.002426	0.018101	0.547559	0.000207	0.005255	-0.00655	0.007533

Figure 54: XRF values from a cored well (API: 15-093-00317).

Sample	NaKa1	MgKa1	AlKa1	SiKa1	P Ka1	S Ka1	K Ka1	CaKa1	BaLa1	TiKa1	V Ka1	CrKa1	MnKa1	FeKa1	CoKa1	NiKa1	CuKa1	ZnKa1
MAJ KM147-4831 15 KV	0.187	1.201	0.039	1.995	-0.088	0.136	0.063	37.584	-0.081	0.034	0.00083	-0.00076	0.029313	0.368269	0.000209	0.002528	-0.0044	0.007545
MAJ KM147-4834 15 KV	0.271	0.759	0.016	2.845	-0.062	0.543	0.101	35.575	-0.064	0.030	0.007117	-0.0006	0.031597	0.813352	0.000308	0.003475	-0.00459	0.007579
MAJ KM147-4837 15 KV	0.225	0.928	0.011	2.208	-0.073	0.172	0.076	37.409	-0.061	0.028	0.00427	-0.00039	0.025239	0.562089	0.000216	0.004223	-0.00635	0.0074
MAJ KM147-4840 15 KV	0.364	0.615	0.042	4.324	0.175	0.052	0.114	32.679	-0.053	0.038	0.004342	0.001447	0.024616	0.72957	0.000266	0.002747	-0.00358	0.008163
MAJ KM147-4843 15 KV	0.383	0.608	0.145	3.450	-0.061	0.002	0.136	33.104	-0.092	0.028	0.003307	-0.00066	0.032213	0.711217	0.000249	0.001901	-0.00411	0.00772
MAJ KM147-4845 15 KV	0.420	0.626	0.170	9.361	0.133	0.576	0.128	25.881	0.002	0.064	0.00455	0.00387	0.02669	0.941893	0.000369	0.0042	-0.00125	0.0089
MAJ KM147-4847 15 KV	0.329379	0.94104	1.054718	10.60901	-0.036	0.153	0.330	27.928	-0.018	0.079	0.005836	0.005884	0.028727	0.44504	0.000245	0.005112	-0.0012	0.0062
MAJ KM147-4849 15 KV	0.362297	0.990804	0.790795	14.56551	0.013897	0.066435	0.359652	23.90475	0.019128	0.124344	0.004865	0.00588	0.024256	0.412858	0.000241	0.005704	-0.0005	0.006817
MAJ KM147-4852 15 KV	0.396886	0.490729	0.297056	7.489849	-0.0818	0.059595	0.156194	29.74818	-0.07152	0.031765	0.004536	0.00228	0.019137	0.538735	0.000212	0.003079	-0.00347	0.007966
MAJ KM147-4855 15 KV	0.57763	-0.23983	0.185166	7.9934	-0.07643	-0.0085	0.064508	18.30653	-0.14056	0.004527	0.000646	-0.00092	0.015691	0.93096	0.000261	-0.00365	-0.00057	0.008703
MAJ KM147-4858 15 KV	0.408828	0.759623	0.805911	15.48779	0.022396	0.121478	0.391474	21.72875	0.028977	0.114356	0.007243	0.007351	0.023681	0.439352	0.000255	0.004992	0.002154	0.008866
MAJ KM147-4861 15 KV	0.340803	0.807045	0.730156	9.801948	0.019848	0.103592	0.336181	28.67799	-0.00868	0.071815	0.006423	0.004426	0.020087	0.503908	0.00024	0.00411	-0.00139	0.008715
MAJ KM147-4864 15 KV	0.295895	0.881957	0.597955	10.60652	0.008389	0.104114	0.292535	27.9741	-0.01339	0.07797	0.006207	0.005014	0.021109	0.441942	0.000215	0.004584	-0.00199	0.007038
MAJ KM147-4867 15 KV	0.514502	0.258185	0.181049	4.641807	-0.0987	0.00954	0.126601	30.20784	-0.08662	0.023714	0.002433	0.000316	0.017129	0.64009	0.000219	0.001384	-0.00423	0.007684
MAJ KM147-4870 15 KV	0.255287	-0.08726	-0.14202	3.734413	-0.08426	-0.05519	-0.11364	9.92261	-0.24211	-0.00765	-0.00697	-0.00624	0.012272	1.335324	0.000292	-0.01208	0.000691	0.011708
MAJ KM147-4873 15 KV	0.370728	0.60477	0.214889	5.089471	-0.04561	-0.00982	0.168749	32.26369	-0.03602	0.052694	0.002877	0.001957	0.018377	0.583711	0.000216	0.003039	-0.00409	0.007198
MAJ KM147-4875 15 KV	0.560076	0.038639	0.267173	5.335963	-0.09058	-0.0143	0.135758	26.1329	-0.05798	0.051066	-0.00079	-0.00027	0.016563	0.736864	0.00023	-0.00039	-0.0032	0.009021
MAJ KM147-4878 15 KV	0.477226	0.409791	0.201193	3.270651	-0.10284	-0.01556	0.099261	32.24263	-0.07576	0.027779	0.002013	-0.0007	0.016938	0.66714	0.000217	0.001715	-0.00529	0.007716
MAJ KM147-4881 15 KV	0.290896	0.99079	0.557404	6.785001	-0.05092	0.056145	0.259868	32.19593	-0.03976	0.066888	0.007244	0.004113	0.020288	0.450824	0.000211	0.004395	-0.00307	0.006913
MAJ KM147-4881-9 15 KV	0.264076	1.055256	0.169872	30.12884	0.080369	0.18761	-0.01001	9.81874	-0.03707	0.009618	0.021205	0.013484	0.032982	-0.26849	0.00013	0.012291	0.004705	0.010693
MAJ KM147-4885 15 KV	0.18043	1.325797	2.153634	6.086299	-0.05018	0.109669	0.616282	33.90779	-0.03308	0.077283	0.003017	0.001847	0.020521	0.842679	0.000305	0.003674	-0.00502	0.006304
MAJ KM147-4887 15 KV	0.238734	1.005729	0.846447	4.024682	-0.07494	0.390852	0.430664	35.14482	-0.05315	0.059292	0.002788	0.001305	0.019653	0.68225	0.000256	0.003654	-0.00445	0.006367
AJ KM147-4888 spot 1 15 k	0.290043	0.964312	0.114757	32.73969	0.06494	0.191112	-0.10445	6.999842	-0.06614	0.012454	0.022112	0.01396	0.03336	-0.40994	0.000102	0.013303	0.005035	0.013948
AJ KM147-4888 spot 2 15 k	0.342797	0.751122	0.227401	33.81732	0.057242	0.544286	-0.09287	5.844897	-0.07289	0.011362	0.023002	0.014529	0.034699	-0.25844	0.000148	0.013745	0.005932	0.012971
MAJ KM147-4890 15 KV	0.163959	1.17557	0.32333	2.907353	-0.10111	0.043464	0.145892	38.51512	-0.0415	0.032266	0.005321	0.000516	0.018325	0.542856	0.000203	0.004774	-0.00662	0.007344
MAJ KM147-4892 15 KV	0.205035	0.99692	0.227976	2.702718	-0.12683	0.343076	0.105593	37.36429	-0.05276	0.029425	0.003582	0.000869	0.018054	0.551141	0.000205	0.004019	-0.00535	0.007801
MAJ KM147-4894 15 KV	0.507749	0.223771	-0.01279	2.460095	-0.08704	0.909201	0.028161	29.12181	-0.11299	0.016422	0.000148	-0.00182	0.016191	0.800285	0.000236	0.001184	-0.00579	0.0103
MAJ KM147-4897 15 KV	0.20414	0.900109	-0.16346	2.378857	-0.10834	0.012255	0.038896	38.60167	-0.06849	0.02254	0.005392	0.000381	0.017741	0.58783	0.000206	0.005603	-0.00716	0.004941
MAJ KM147-4900 15 KV	0.317659	0.979373	0.721429	9.850155	0.016746	0.053926	0.390786	28.93308	-0.0059	0.073282	0.006511	0.004701	0.020646	0.36969	0.000195	0.004597	-0.0016	0.007185
MAJ KM147-4902 15 KV	0.222835	0.881669	-0.00204	2.340164	-0.12281	0.048985	0.084319	38.32103	-0.05792	0.027369	0.003364	0.000101	0.018245	0.514994	0.000195	0.004433	-0.00671	0.007411
MAJ KM147-4904 15 KV	0.420051	0.571297	1.717728	9.340633	-0.03567	0.307178	0.875315	27.11334	0.031931	0.125358	0.002163	0.004392	0.01855	0.855283	0.000347	0.00377	-0.0017	0.006912
MAJ KM147-4907 15 KV	0.39114	0.719987	1.22406	15.45265	0.030399	0.082716	0.676365	22.49065	0.060125	0.122984	0.004315	0.006547	0.022513	0.42394	0.000243	0.005039	0.000722	0.007721
MAJ KM147-4910 15 KV	0.417045	0.529496	1.681358	17.07181	0.019688	0.083492	0.91342	20.34401	0.073182	0.116935	0.006407	0.007491	0.02296	0.553537	0.000286	0.005821	0.001375	0.008126
MAJ KM147-4913 15 KV	0.21085	1.223932	0.529378	9.205817	0.001362	0.069829	0.339683	31.14709	0.003096	0.062941	0.0071	0.004199	0.020085	0.368221	0.000194	0.005486	-0.00313	0.007696
MAJ KM147-4916 15 KV	0.265374	0.766775	0.325678	4.275444	-0.07532	0.139406	0.216481	34.689	-0.02028	0.061416	0.003968	0.000856	0.018302	0.548151	0.000222	0.004097	-0.00431	0.007246
J KM147-4916 dark spot 15	0.481229	0.498478	2.232169	22.3914	0.027336	0.270764	1.262803	12.57348	0.038353	0.171524	0.005825	0.008089	0.02438	0.723913	0.000387	0.007252	0.003306	0.008384
MAJ KM147-4919 15 KV	0.310983	0.883947	0.698379	11.33573	0.011502	0.065908	0.439212	28.12378	0.012576	0.092913	0.006857	0.005208	0.021599	0.361826	0.000201	0.005926	-0.00174	0.00693
MAJ KM147-4922 15 KV	0.378851	0.637226	0.934666	13.64422	0.018501	0.367202	0.62379	24.03329	-0.02131	0.064553	0.009493	0.006201	0.02161	0.3356	0.000205	0.004795	0.001003	0.008503

MAJ KM147-4925 15 kV	0.296293	0.8766	0.737384	9.82203	-0.01279	0.038428	0.415407	30.29373	0.027385	0.102573	0.005294	0.005202	0.020793	0.354978	0.000198	0.005145	-0.00207	0.006744
MAJ KM147-4928 15 kV	0.372128	0.634509	0.552236	9.024582	0.001353	0.030907	0.390306	29.53232	0.010128	0.080023	0.005196	0.004622	0.019665	0.37453	0.000193	0.004536	-0.00227	0.007541
MAJ KM147-4930 15 kV	0.338907	0.703054	0.844142	11.93477	-0.0045	0.052681	0.535126	27.91575	0.011402	0.079072	0.007502	0.005201	0.021328	0.334059	0.000193	0.005663	-0.00118	0.00628
MAJ KM147-4932 15 kV	0.434568	0.475152	1.258936	14.03312	0.012069	0.415502	0.704583	22.30643	0.014657	0.086392	0.007297	0.005649	0.021866	0.35398	0.000206	0.004372	0.001465	0.007772
MAJ KM147-4935 15 kV	0.588002	-0.08098	0.017239	3.1982	-0.09528	0.109092	0.082308	26.4648	-0.12622	0.016392	-0.00042	-0.00193	0.015212	0.79544	0.000224	-0.00174	-0.00366	0.00895
J KM147-4935 dark spot 15	0.347387	0.762374	0.182629	39.2012	0.043483	0.316453	-0.18462	0.799636	-0.08356	-0.00553	0.025869	0.014633	0.035154	-0.54373	8.34E-05	0.015978	0.006259	0.013355
J KM147-4938 dark lam 15	0.466746	0.3041	0.429346	25.94701	0.021184	0.215129	-0.02671	10.38207	-0.09445	0.014874	0.017527	0.009107	0.025104	0.292895	0.000222	0.006866	0.003335	0.008878
MAJ KM147-4939 15 kV	0.411042	0.550062	0.18371	3.928452	-0.11035	0.14852	0.150569	32.48992	-0.07805	0.031079	0.003159	0.00045	0.01666	0.709579	0.000235	0.002182	-0.00453	0.007609
MAJ KM147-4942 15 kV	0.484635	0.257657	0.088852	3.174387	-0.06447	0.039207	0.130446	30.16995	-0.06274	0.03727	0.001858	3.45E-05	0.017414	0.488843	0.00019	0.00172	-0.00297	0.008254
MAJ KM147-4945 15 kV	0.519527	0.203091	0.338775	5.33407	-0.07532	0.719738	0.201997	27.82557	-0.09434	0.033123	0.001678	0.000923	0.016979	0.63392	0.000212	0.000587	-0.00235	0.007958
MAJ KM147-4948 15 kV	0.392578	0.630408	0.197545	3.641258	-0.08924	0.066534	0.138393	33.0951	-0.09216	0.030436	0.003148	0.000328	0.016651	0.609866	0.000203	0.002575	-0.00519	0.007423
MAJ KM147-4951 15 kV	0.530105	-0.35436	-0.04316	3.266095	-0.10362	0.143365	0.001544	15.93871	-0.21788	-0.02625	-0.00461	-0.00511	0.013063	1.150671	0.000264	-0.00854	-0.00086	0.010085
MAJ KM147-4953 15 kV	0.518621	0.205334	0.218422	4.249896	-0.03158	0.786535	0.163476	28.3515	-0.09773	0.026262	0.001172	-0.00048	0.016164	0.689334	0.000218	-0.00011	-0.00339	0.007722
MAJ KM147-4955 15 kV	0.389495	0.554338	-0.03426	2.455481	-0.08802	0.15061	0.070819	34.11962	-0.09607	0.018798	0.001807	-0.00054	0.016337	0.68098	0.000214	0.002131	-0.00563	0.008013
MAJ KM147-4957 15 kV	0.560403	0.034611	-0.04863	2.389969	-0.11425	0.005032	0.084681	29.65495	-0.12369	0.007736	0.000628	-0.0017	0.015402	0.758677	0.000216	-0.0002	-0.00477	0.008352
MAJ KM147-4958 15 kV	0.397097	0.56566	0.029509	3.509962	-0.03968	0.020058	0.116707	32.44537	-0.10866	0.022885	0.003824	0.00048	0.016851	0.5895	0.000199	0.002549	-0.0046	0.008042
MAJ KM147-4960 15 kV	0.501312	0.141401	-0.11049	2.080015	-0.13801	0.10863	0.033314	31.82921	-0.1225	0.01185	0.002975	-0.0017	0.015697	0.716027	0.000216	0.000259	-0.00511	0.008341
MAJ KM147-4963 15 kV	0.218135	1.095127	-0.05141	2.154612	-0.08475	0.008721	0.071132	38.34317	-0.06992	0.030351	0.004159	0.000165	0.017949	0.535424	0.000194	0.004573	-0.00683	0.007297
MAJ KM147-4964 15 kV	0.289118	0.904675	0.529238	2.700763	-0.05927	0.342717	0.208407	36.39795	-0.06789	0.032418	0.003527	-0.00022	0.017259	0.540612	0.000197	0.003911	-0.00583	0.007206
MAJ KM147-4966 15 kV	0.287376	0.862999	0.077792	3.282079	0.006834	0.444774	0.137016	35.73058	-0.04048	0.030979	0.003165	0.000865	0.017039	0.620924	0.000215	0.003905	-0.0057	0.007351
MAJ KM147-4968 15 kV	0.113215	1.369924	0.199394	3.972878	0.016572	1.597164	0.204928	35.77305	-0.06075	0.042488	0.004209	0.002966	0.018483	0.468116	0.000192	0.004249	-0.00543	0.006441
MAJ KM147-4971 15 kV	0.360601	0.946276	1.137295	11.24425	0.011251	0.090109	0.626139	27.07558	0.035611	0.133101	0.003819	0.004173	0.020812	0.429957	0.000215	0.004446	-0.00104	0.007457
MAJ KM147-4973 15 kV	0.377133	0.682821	0.084953	2.76423	-0.09408	0.033701	0.100281	34.35547	-0.09866	0.023166	0.002755	-0.00035	0.016592	0.578626	0.000195	0.002606	-0.006	0.007559
MAJ KM147-4975 15 kV	0.291167	0.897396	0.036558	1.868627	-0.09644	0.38655	0.046701	35.94813	-0.06651	0.01881	0.002697	-0.00026	0.016695	0.567384	0.000195	0.002959	-0.00532	0.007646
MAJ KM147-4980 15 kV	0.531399	0.165617	-0.23444	1.495819	-0.07907	0.126933	0.006814	30.33358	-0.09784	0.005239	0.001784	-0.00143	0.015796	0.65714	0.0002	0.000622	-0.00517	0.007961
MAJ KM147-4984 15 kV	0.260072	0.793016	-0.2504	1.618019	-0.01804	0.104086	0.031767	37.338	-0.04572	0.017325	0.001405	-0.00056	0.017246	0.503256	0.000184	0.004931	-0.00669	0.008501
MAJ KM147-4987 15 kV	0.399229	0.511947	-0.13681	1.722828	-0.15564	0.048319	0.011692	33.54709	-0.08279	0.008392	0.00132	-0.00143	0.015885	0.673869	0.000203	0.001268	-0.00563	0.008066
MAJ KM147-4990 15 kV	0.203364	1.027457	-0.03367	1.454396	-0.13336	0.072095	0.022691	38.39682	-0.07691	0.018415	0.004061	-0.00015	0.017264	0.510739	0.000184	0.004276	-0.007	0.007393
MAJ KM147-4992 15 kV	0.539693	0.114633	-0.17485	1.681086	-0.1257	0.010595	0.014963	30.96452	-0.12034	0.007684	-0.00016	-0.00213	0.015667	0.754801	0.000215	0.000768	-0.00603	0.007172
MAJ KM147-4995 15 kV	0.304893	0.803734	0.024483	3.041035	-0.09251	0.007262	0.109995	36.14575	-0.04919	0.035862	0.00353	0.000773	0.017669	0.459705	0.000183	0.004026	-0.00563	0.007519
MAJ KM147-4998 15 kV	0.314408	0.850457	0.104365	39.55621	0.038179	0.170612	-0.20143	0.275083	-0.10797	0.001524	0.025578	0.015669	0.036894	-0.70764	4.31E-05	0.016293	0.005991	0.016686
MAJ KM147-4999Kem 15 kV	0.317607	0.864866	0.095557	38.88991	0.044709	0.138792	-0.18737	0.884079	-0.08446	-0.00281	0.025723	0.015482	0.036587	-0.65595	5.34E-05	0.015726	0.006252	0.01428
MAJ KM147-5000 15 kV	0.051136	1.541756	0.14235	3.165003	-0.06918	0.064112	0.132319	38.60746	0.020978	0.029106	0.001209	0.000794	0.017516	0.600568	0.000211	0.005418	-0.00635	0.005772
MAJ KM147-5002 15 kV	0.311802	0.763592	0.055918	2.001577	-0.12111	0.058792	0.090958	36.9527	-0.05604	0.025863	0.003381	-0.00018	0.017028	0.532168	0.000197	0.004033	-0.00639	0.007392
MAJ KM147-5002Kem 15 kV	0.295507	0.812951	0.297708	2.311204	-0.11771	0.048666	0.185423	36.9726	-0.0511	0.038791	0.002429	0.000547	0.017305	0.513854	0.000197	0.004749	-0.00655	0.007029
MAJ KM147-5005 15 kV	0.170687	1.298651	-0.04822	1.784858	-0.17063	0.013586	0.0504099	39.70839	-0.05244	0.020244	0.003128	0.000705	0.017079	0.503073	0.000185	0.004979	-0.00725	0.00642
MAJ KM147-5007 15 kV	0.317426	0.626129	-0.06691	2.651073	-0.14268	0.102317	0.01856	34.76784	-0.07348	0.010713	0.002371	6E-05	0.017044	0.558547	0.000192	0.003023	-0.00566	0.006889

Figure 55: XRF values from a cored well (API: 15-093-20147).